

**Rheological properties
of olefinic
thermoplastic elastomer blends**

Rheological properties of olefinic thermoplastic elastomer blends

Proefschrift

ter verkrijging van de graad van doctor
aan de Technische Universiteit Delft,
op gezag van de Rector Magnificus Prof.dr.ir. J.T. Fokkema,
voorzitter van het College voor Promoties,
in het openbaar te verdedigen op maandag 10 oktober 2005 om 13:00 uur
door:

Willem Gerard Frans SENGERS

ingenieur in de scheikundige technologie
Geboren te Nijmegen

Dit proefschrift is goedgekeurd door de promotor:

Prof. dr. S.J. Picken

Samenstelling promotiecommissie:

Rector Magnificus

Prof. dr. S.J. Picken

Prof. dr. ir. A. Posthuma de Boer

Prof. dr. ir. J.W.M. Noordermeer

Prof. dr. ir. L.P.B.M. Janssen

Prof. dr. ir. P. Moldenaers

Dr. A.D. Gotsis

Dr. ir W. Zoetelief

Prof. Dr. G.J. Kearley

Voorzitter

Technische Universiteit Delft, promotor

Technische Universiteit Delft

Universiteit Twente

Rijksuniversiteit Groningen

Katholieke Universiteit Leuven

Technical University of Crete

DSM Research

Technische Universiteit Delft, reservelid

Dr. A.D. Gotsis heeft als begeleider in belangrijke mate aan de totstandkoming van het proefschrift bijgedragen.



Het onderzoek beschreven in dit proefschrift is onderdeel van het onderzoeksprogramma van het Dutch Polymer Institute (DPI), project nr. 252.

ISBN-10: 9090198121

ISBN-13: 9789090198125

Keywords: polymer blend, thermoplastic elastomer, rheology, morphology

Cover design: Wilco Sengers.

Cover: TEM images of a PP/SEBS/oil blend (red/yellow) and a TPV blend (blue).

The images were made by Pratip Sengupta

© Copyright 2005 by Wilco Sengers

All rights reserved. Save exceptions stated by the law, no part of this publication may be reproduced, stored in a retrieval system of any nature, or transmitted in any form or by any means, electronic, mechanical, photocopying, recording or otherwise, included a complete or partial transcription, without the prior written permission of the authors, application for which should be addressed to author.

Index

1. General Introduction.....	9
1.1 Introduction	10
Classification.....	11
1.2 Olefinic thermoplastic elastomer blends	11
1.2.1 Thermoplastic Vulcanisates.....	12
1.2.2 PP/SEBS blends	12
1.3 Motivation	13
1.4 Scope of the thesis.....	14
1.5 References	15
2. Olefinic thermoplastic elastomer blends	17
2.1 Introduction	18
2.2 Thermoplastic Vulcanisates.....	19
2.2.1 Dynamic Vulcanisation	20
2.2.2 Morphology.....	21
2.2.3 Oil distribution	22
2.2.4 Deformation mechanism	22
2.2.4 Rheological properties	24
2.3 PP/SEBS blends.....	24
2.3.1 Morphology and properties of SEBS triblock copolymer.....	25
2.3.2 Morphology of PP/SEBS blends.....	27
2.3.3 Oil distribution in PP/SEBS blends	27
2.3.4 Mechanical properties.....	28
2.3.5 Rheology	28
2.4 Applications of OTPEs.....	29
2.5 Composition and preparation of OTPE blends	30
2.5.1 Materials	30
2.5.2 Compositions and preparation.....	31
2.6 References	32
3. Dielectric spectroscopy using dielectric probes	35
3.1 Introduction	36
3.2 Experimental.....	37
3.2.1 Materials	37
3.2.2 Sample preparation.....	37
3.2.3 Scanning Electron Microscopy.....	37
3.2.4 Dielectric relaxation spectroscopy	38
3.2.5 Differential scanning calorimetry	38
3.2.6 Dynamic mechanical analysis.....	38
3.3 Results and Discussion	39
3.3.1 Morphology.....	39
3.3.2 DSC and DMA.....	40
3.3.3 Dielectric Relaxation Spectroscopy.....	43
3.3.3.1 Identification of relaxation peaks.....	44
3.3.3.2. Mapping of the relaxation times.....	46
PS-PE blends.....	47
PS-PP blends.....	48
PP-PE blends	49

3.3.3.3 Relaxation strength.....	51
3.4 Conclusions	52
3.5 References	52
4. Distribution of oil in olefinic thermoplastic elastomer blends.....	55
4.1 Introduction	56
4.2 Experimental.....	57
4.2.1 Materials	57
4.2.2 Sample preparation	58
4.2.3 Dynamic mechanical analysis	59
4.2.4 Differential scanning calorimetry	59
4.2.5 Dielectric relaxation spectroscopy	59
4.3 Results	60
4.3.1 DMA and DSC	60
4.3.2 Dielectric Relaxation Spectroscopy.....	63
4.3.2.1 Binary mixtures	65
4.3.2.2 OTPE blends	67
4.3.3 Determination of the oil distribution coefficient.....	68
4.4 Discussion	72
4.5 Conclusions	73
4.6 References	73
5. Linear viscoelastic properties of olefinic thermoplastic elastomer blends.	75
5.1 Introduction	76
5.2 Experimental.....	77
5.2.1 Materials	77
5.2.2 Sample preparation	78
5.2.3 Morphology.....	78
5.2.4 Rheological measurements	79
5.2.5 Gel measurements on TPVs.....	79
5.3 Results and discussion.....	80
5.3.1 Morphology.....	80
5.3.2 Melt state properties	81
5.3.2.1 Binary mixtures: concentration–time superposition.....	81
5.3.2.2 TPE blends	84
5.3.2.3 Summary.....	88
5.3.3 Solid-state properties	89
5.3.3.1 Binary mixtures	89
5.3.3.2 OTPE blends	90
5.3.3.3 Summary.....	90
5.3.4 Micromechanical model description.....	91
5.3.4.1 Micromechanical models.....	92
5.3.4.2 Evaluation of the Coran-Patel model.....	93
5.3.4.3 Evaluation of Veenstra model D.....	94
5.3.4.4 Distribution of oil	96
5.4 Conclusions	97
5.5 References	97

6. Melt creep behaviour of elastomer-polymer blends	99
6.1 Introduction	100
6.2 Experimental.....	102
6.2.1 Materials	102
6.2.2 Sample preparation	102
6.2.3 Morphology.....	103
6.2.4 Rheological measurements	103
6.3 Results	104
6.3.1 Morphology.....	104
6.3.2 Melt creep.....	105
6.3.2.1 Binary mixtures	106
6.3.2.2 PP-SEBS blends	107
6.3.2.3 Thermoplastic vulcanisates	110
6.3.3 Recovery from creep	112
6.3.3.1 PP-SEBS blends	112
6.3.3.4 Thermoplastic Vulcanisates.....	114
6.4 Discussion.....	116
6.4.1 PP-SEBS blends.....	117
6.4.2 Thermoplastic Vulcanisates.....	117
6.5 Conclusion.....	118
6.6 References	119
 7. Capillary rheology of Olefinic Thermoplastic Elastomer blends.....	 121
7.1 Introduction	122
7.2 Experimental.....	123
7.2.1 Materials	123
7.2.2 Sample preparation	124
7.2.3 Morphology.....	124
7.2.4 Rheology	124
7.2.5 Extrudate swell and surface appearance.....	125
7.3 Results and discussion.....	126
7.3.1 Binary mixtures	126
7.3.2 PP/SEBS blends	128
7.3.2.1 Morphology	128
7.3.2.2 Viscosity	128
7.3.2.3 Extrudate swell and surface appearance.....	130
7.3.3 Thermoplastic Vulcanisates.....	132
7.3.3.1 Morphology	132
7.3.3.2 Viscosity	133
7.3.3.3 Extrudate swell and surface appearance.....	137
7.4 Discussion.....	139
7.4.1 Summary of the rheological behaviour of the OTPE blends at high strains/rates	139
7.4.1.1 PP/SEBS blends.....	139
7.3.3.4 TPVs	139
7.4.1 The viscosity.....	140
7.4.2 Processability	141
7.5 Conclusions	142
7.6 Appendix	142
7.7 References	145

8. General overview	147
8.1 Rheological properties of PP-oil and elastomer-oil binary mixtures	147
8.1.1 PP-oil	147
8.1.2 SEBS-oil	147
8.1.3 EPDM-oil.....	148
8.2 Distribution of oil in OTPE blends.	148
8.3 Effect of morphology on rheology	149
8.3.1 Linear viscoelastic properties	149
8.3.2 Transient properties.....	150
8.3.4 Capillary rheology	151
8.3.5 Summary	152
8.4 Rheology of PP/SEBS blends.....	152
8.5 Rheology of TPVs	155
8.6 References	156
List of Symbols.....	157
List of Abbreviations	159
Summary	161
Samenvatting.....	163
Curriculum Vitae.....	167
List of Publications	169
Dankwoord	171

Chapter 1

General Introduction

1.1 Introduction

Thermoplastic elastomers (TPE) are a class of polymers or polymer blends that have rubber-like behaviour but can be melt processed like thermoplastic polymers [1,2]. The combination of these properties is obtained by the two-phase structure of the materials: the soft phase, an elastomer, gives the material the rubber-like properties in the solid state whereas the hard phase, a thermoplastic polymer with a high glass-rubber transition temperature or a semi-crystalline polymer, gives strength to the blend. At the temperature of utilisation, this is the stiffer phase that acts as physical cross-linker for the elastomer phase. At elevated temperatures (above the glass transition temperature or above the melting point), the hard phase softens and the TPE becomes processable. In contrast, the cross-links in thermoset rubbers are chemical in nature: the curing step is irreversible and once the rubber is moulded and cured, the material cannot be (re)processed anymore. Another advantage to use TPEs instead of conventional rubbers or elastomers is the ease of tailoring the properties by adjusting the hard/soft ratio and by the addition of processing oil and/or solid fillers. This compounding can be included in the preparation process of the TPE.

There is a growing interest for TPEs. They are not only good substitutes for thermoset rubbers in many existing applications but also new applications are emerging. The thermoplastic processing allows the preparation of complex shapes and multi component injection moulding. In this way, articles with integrated soft grip/soft touch/sealant parts or damping spots in housings can be made in a single injection moulding step. The advantages and disadvantages of TPE compared thermoset rubbers are listed in Table 1.1.

Table 1.1: Advantages and disadvantages of TPEs compared to thermoset rubber [2]

Advantages	Disadvantage
-No curing step during processing	-Elastomeric recovery may not be as good as thermoset rubber
-Little or no compounding necessary	
-Simple and fast processing	-Limited number of low hardness products
-Fast moulding cycle times	
-Low energy consumption	-Softens at elevated temperatures
-Recycle of scrap and off-spec parts	-Drying prior to processing
-Better quality control	
-Good colourability	

The flexible properties of the TPE are sufficient for many applications, but the thermoset rubbers will not be replaced completely. Because the cross-links in the TPEs are physical in nature, the temperature range of application is limited.

The presence of the hard phase also limits the production of compounds with very low modulus (or low hardness). Finally, their elastic recovery is not as good as that of thermoset rubbers: the tension set or compression set (fraction of plastic deformation after unloading) is high due to plastic deformation.

Classification

The TPE can be divided into three categories, depending on the connection of the soft and the hard phases [1], namely block copolymers, polymer-elastomer blends and ionomers.

In co-polymers, two types of monomer are present on the same polymer chain. The largest group of this type of TPE is the **block copolymers**. The polymer chain contains large segments of alternating hard and soft phases. The formation of the two-phase structure occurs by the lack of miscibility of the hard and soft segments or by crystallisation of the hard segments. The properties of these TPEs can be tailored by the choice of monomer types, the hard/soft ratio and the positions of the hard and soft segments within the polymer chain. The phase-separated block copolymers are mainly based on polystyrene-elastomer copolymers, like the diblock copolymer *polystyrene-co-polybutadiene* (SB), and the triblock copolymers *polystyrene-block-polybutadiene-block-polystyrene* (SBS), *polystyrene-block-polyisobutene-block-polystyrene* (SIS) or *polystyrene-block-polyethylene-co-butene-block-polystyrene* (SEBS). Examples of multi-block copolymers with crystalline segments are thermoplastic polyurethanes (TPU), co-polyesters (COPE) and co-polyamides (COPA).

TPEs can also be made by melt mixing of an elastomer with a thermoplastic polymer. In these **TPE blends**, the two-phase structure is obtained by the lack of miscibility of the polymer and the elastomer phase. A prerequisite for these blends is that the thermoplastic polymer is continuous. Examples are blends of *polypropylene* (PP) with *ethylene-propylene-diene* termer (EPDM), *polyamide-6* (PA6) with *nitril-butyl rubber* (NBR).

The newest class of TPEs are the **ionomers**. The physical cross-links in these materials are realised by complex formation. Anionic side groups are grafted on the elastomeric backbone and they form complexes with metallic cations. Examples are EPM rubber grafted with *maleic anhydride*, sulfonated EPDM rubber or *ethylene-methacrylic acid* copolymer.

1.2 Olefinic thermoplastic elastomer blends

After the polystyrene based block copolymers, the olefinic thermoplastic elastomer blends (OPTe) are the second largest group of TPE. They have good chemical and weathering resistance and, the mechanical properties meet the requirements of the product designers for many applications. OPTes are replacing EPDM vulcanisates in a growing number of applications. In this thesis, we will focus on the investigation of two types of PP-elastomer blends. Both elastomers are olefinic in nature but the type of cross-links differs.

1.2.1 Thermoplastic Vulcanisates

Thermoplastic vulcanisates (TPV) are polymer-elastomer blends in which the elastomer phase is cross-linked. In the preparation process, called *dynamic vulcanisation*, the elastomer phase is cured during continuing mixing with the polymer [4]. The final blend morphology always consists of cross-linked, micron-sized elastomer particles dispersed in a polymer matrix (Fig 1.1). This morphology is permanent and does not change upon (re)processing of the TPV. In the present study, the TPVs consist of blends of PP and the copolymer *ethylene propylene diene termer* (EPDM).

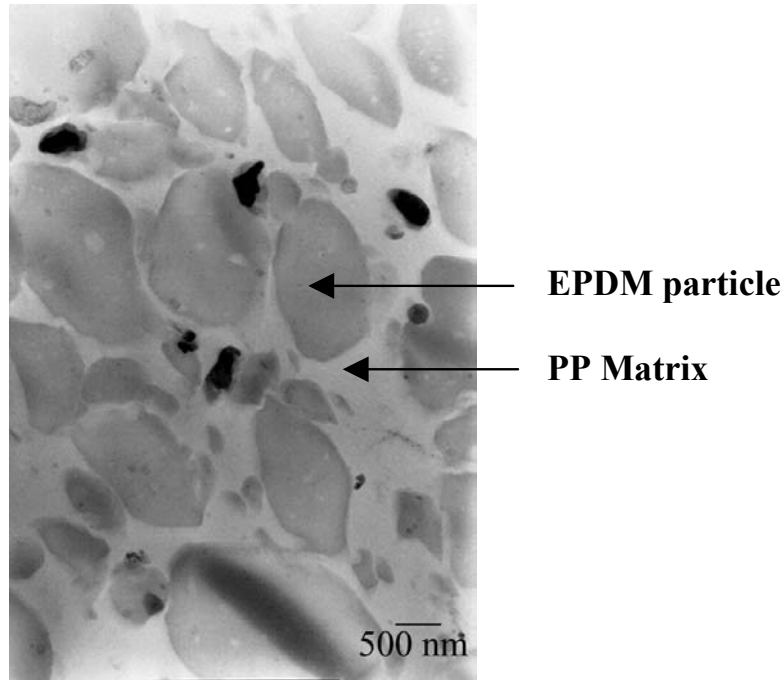


Figure 1.1: TEM image of a TPV [5].

1.2.2 PP/SEBS blends

The second type of OTPE studied in this work contains the triblock copolymer *polystyrene-block-poly(ethylene-co-butylene)-block-polystyrene* (SEBS) as the elastomer. SEBS is a triblock copolymer with an elastomeric middle-block of *poly(ethylene-co-butylene)* (EB) between two *polystyrene* (PS) end-blocks. The PS end-blocks form separate domains and act as physical cross-links for the EB phase [3] (see left side Fig 1.2). Above the glass transition temperature of the PS blocks, they are able to break-up and rearrange and the material becomes processable; SEBS itself is already a TPE.

SEBS is blended with PP to improve the processability and to make compounds with a higher modulus. Depending on the SEBS and the PP type used and the processing conditions, PP/SEBS blends show co-continuous structures (right side of Fig 1.2) over a broad concentration range [6,7]. The PS domains have a stabilising effect on the formation of this morphology.

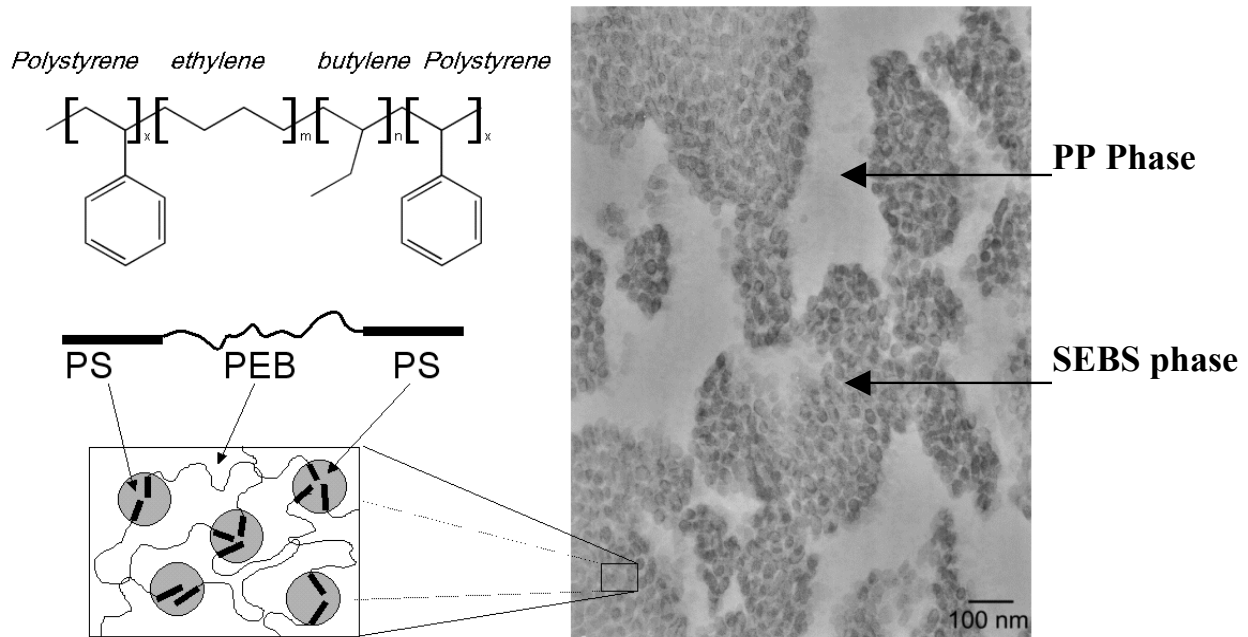


Figure 1.2: Chemical structure and morphology of SEBS (left) and TEM image of SEBS blended with PP (right). TEM image obtained from [5]

1.3 Motivation

Thermoplastic vulcanisates (TPVs) have been commercially applied for about 25 years and are widely used as replacement for EPDM vulcanisates. Blends of PP/SEBS are relatively new and are found to be good alternatives for TPVs. These two OTPE blends differ in morphology, but they have comparable properties. In the TPVs the elastomer phase is dispersed in the PP phase and in the PP/SEBS blends the elastomer phase and the PP phase are both continuous. Therefore, it is remarkable that the properties of these materials are so similar.

As illustrated in Fig 1.3, the morphology plays a key role in the mechanical and rheological properties of polymer blends. Rheology can help to gain insight in the interrelationship between blend morphology and properties. In this way, the empirical route (i.e. correlate mechanical properties directly to processing condition, compositions and components) can be avoided and problems concerning processability or mechanical properties can be solved from a more fundamental point of view. In this study, rheology will be used in order to understand the effect of morphology on the properties and processability of TPVs and PP/SEBS blends.

The present study of the properties of OTPEs was conducted within the framework of the Dutch Polymer Institute in the form of a larger research project (DPI #252). The project involved the group of Rubber Technology of the University of Twente and the Polymer Materials and Engineering group of Delft University of Technology. In Twente, Sengupta [5] studied the morphology, morphology development and mechanical properties of TPVs and PP/SEBS blends (the left half of Fig. 1.3). In Delft, in the present part of the project, the rheological properties are related to the morphology of the blend in order to understand the (differences in) processing characteristics (the right half of Fig. 1.3).

The focus lies here on the identification and quantification of the morphology by rheological measurements: What are the differences in flow and dynamic mechanical properties between OTPE blends with dispersed and co-continuous morphologies? What happens to the mechanical properties after processing?

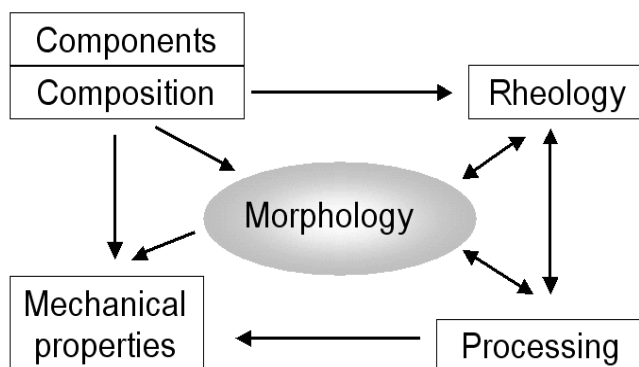


Figure 1.3: Interrelationship between morphology, rheology and mechanical properties for polymer blends.

It should be realised that the two studied OTPE blends contain considerable amounts of oil. This oil is added in the commercial TPEs to make softer compounds and to increase the processability. The oil, being paraffinic in nature, is present in the elastomer and in the PP phase and affects the rheological and mechanical properties of both phases. In order to model the blend properties, the oil concentration in both phases is needed.

The chemical similarity of the PP, elastomer and oil, however, makes the determination of the oil concentration very difficult. In this thesis the role of oil will be studied in detail.

1.4 Scope of the thesis

Chapter 2 is a general overview of TPVs and PP/SEBS blends. The preparation process, properties and applications of OTPE blends are discussed. The first question asked in this thesis concerns the distribution of oil over the two phases. For this purpose, a new technique was developed. This method enables the study of glass transition dynamics of apolar media using dielectric spectroscopy. The principle and validation of this method is explained in **Chapter 3** by the application of dielectric spectroscopy on apolar polymer blends. The distribution of oil over the two phases of the OTPE blends is discussed in **Chapter 4**.

In **Chapter 5** the linear viscoelastic properties of the two OTPE blends are discussed both in the solid state (30 °C) and in melt state (190 °C). Mixing rules based on micromechanical models are used to quantify the correlation between morphology and the behaviour of the dynamic moduli. The distribution of oil is introduced in the models as an additional parameter. In this way, the oil distribution in the melt state can be estimated. **Chapter 6** describes the deformation mechanism of the blends in the melt state. Melt creep experiments were performed to elucidate the yield behaviour of OTPE blends. The recovered strain after creep can be related to changes of the blend structure. The steady state viscosity and processability of the blends is discussed in **Chapter 7**.

In the final, **Chapter 8**, a general overview is given on the effect of morphology on the rheological properties of these blends. The deformation mechanism is schematically shown by combining the findings of the different rheological measurements.

1.5 References

- [1] Holden G, Legge, N eds. Thermoplastic elastomers, New York, 1996: Hanser
- [2] Bohmick AK, Stephens HL, eds, Handbook of Elastomers, New York, 2001: Marcel Dekker
- [3] Holden G, Milkovich R, US Patent 3.265.765, 1962
- [4] Coran AY, Patel R. Rubber Chem Technol 1980;53:141
- [5] Sengupta P, PhD Thesis, Twente University, Enschede 2004
- [6] Ohlsson B, Hassander H, Tornell B, Polymer Engineering and Science 1996; 36:501
- [7] Veenstra H, PhD Thesis, Delft University of Technology, Delft 1999

Chapter 2

Olefinic thermoplastic elastomer blends

2.1 Introduction

Melt mixing of two polymers in most cases results in two-phase materials. Due to the small positive entropy of mixing, the polymers do not mix easily on a molecular scale and they remain present in the mixture as separate phases [1]. Typically, polymer blends form two-phase structures on a micrometer scale. The morphology of the phases depends on the polymer concentration and the rheological properties of each polymer. At low concentrations (0 - 30 wt%) the polymer blends show *particle in matrix* structures, while at intermediate concentrations (40-60 wt%) structures can occur in which both phases are continuous. These *co-continuous* structures are present in the range where phase inversion takes place: the initially dispersed phase becomes continuous and the matrix phase becomes dispersed. Other possible morphologies are *fibre in matrix* or layered (*stratified*) structures.

The morphology has an effect on the mechanical and the rheological properties of the blend. In a dispersed system the properties of the matrix phase are dominant, while in co-continuous morphologies both phases contribute in a balanced way to the overall properties. The morphology is not only a function of blend composition; the processing conditions also affect the blend structure. In this way, the mechanical properties of polymer blends can be optimised by choosing the right blend composition and processing conditions.

Blending an elastomer with a thermoplastic polymer can result in materials called *thermoplastic elastomers* (TPE) [2,3]. They combine the elastic properties of rubbers with the processability of thermoplastic polymers. The elastomer phase gives the materials the rubber-like properties and the thermoplastic polymer gives strength to the blend. A prerequisite for the hard phase is that this phase is continuous and that the polymer is semi-crystalline or has a high glass-rubber transition temperature. This phase melts at elevated temperatures and the material becomes processable.

After the polystyrene based block-copolymers, polymer-elastomer blends are the second most important group of TPE. The advantage of melt mixing is that existing polymers and elastomers can be compounded in a single process to obtain blends with TPE-like properties. Blends of olefinic rubbers and olefinic thermoplastic polymers (OTPEs) are widely used as replacements for EPDM rubbers. In most cases, they are based on blends of dynamically cured EPDM and polypropylene (PP). These blends are also called *thermoplastic vulcanisates* (TPV) [4]. An alternative for these TPVs consist of PP blended with the triblock copolymer *polystyrene-block-poly-ethylene-butylene-block-polystyrene* SEBS [5]. The two blend types have comparable properties but the morphology is different: in the TPVs the elastomer phase is present as dispersed particles in the PP matrix and in PP/SEBS blends, the PP and elastomer phase mostly form co-continuous structures.

This chapter describes the formation of the different morphologies in these blends and the mechanical and rheological properties. This forms the basis for the research strategy in order to understand the correlation between the morphology and the rheological and mechanical properties. This review on OTPEs is partially based also on the part of the research project conducted by Sengupta [6].

2.2 Thermoplastic Vulcanisates

Thermoplastic vulcanisates (TPV) are elastomer-polymer blends in which the elastomer phase is cured. The name comes from the blending process, called *dynamic vulcanisation*. In this process, the elastomer phase is cured during continuing mixing of the components [4]. The resulting blend morphology always consists of elastomer particles dispersed in a thermoplastic matrix. Ideally, the elastomer should be present as finely dispersed particles in a small amount of polymer. The cross-linked elastomer particles promote the blend elasticity and they prevent coalescence: the blend morphology does not change during fabrication and use. The list of the benefits of the TPVs as compared to uncured OTPEs is [2]:

- Reduced compression and tension set
- Improved ultimate properties (e.g. elongation and stress at break)
- Improved fatigue resistance
- Greater resistance to fluids (e.g. hot oils, solvents, fuels and coolants)
- Better utilisation at higher temperatures
- Greater melt strength (higher elasticity of the melt)

Many combinations of elastomer and polymer have been screened for the preparation of TPEs, but only a limited number is suitable for commercial use. Coran and Patel [7] have given some criteria to judge the choice of components and processing conditions:

- The elastomer in the molten blend should be selectively cross-linked at a high enough shear rate to allow the production of discrete thermoset particles (5-10 μm) in a continuous thermoplastic polymer matrix
- The elastomer should have a high entanglement density.
- The thermoplastic polymer should have a high degree of crystallinity, which should be maintained after the dynamic vulcanisation process.
- The elastomer should be nearly 100 % cross-linked, which is achieved by the addition of curatives to the molten blend during continuing shearing.
- The cross-linking process should not affect the thermoplastic matrix phase.
- Plastification of the elastomer-polymer blend can be used to control blend morphology, viscosity and elastomeric properties.
- For good low temperature and compression properties, both the thermoplastic matrix and the elastomer phase should have a T_g below room temperature.
- The matrix phase should be at least 15 wt% crystalline.
- Low interfacial energy difference between the elastomer and the thermoplastic polymer

The first TPVs were commercialised in the beginning of the '80s and were based on blends of PP/EPDM. This polymer/elastomer combination fulfils most of the above stated requirements and it is still the most widely used TPV, especially in the automotive industry. Other combinations used are PE/EPDM [8] and Nylon-6/NBR [9]. The latter has good resistance against hot oils and higher range of service temperature [9].

The principle of dynamic vulcanisation has gained interest in reactive processing of polymer blends. Other combinations of polymer/elastomer with larger polarity differences can be made by (reactive) compatibilisation of the two phases, e.g. by addition of block copolymers (e.g. Ref [10, 11]) or by *in-situ* graft formation (e.g. Ref [12, 13]). Other areas of development on TPVs focus on the improvement of the curing systems of the TPVs [14].

2.2.1 Dynamic Vulcanisation

The dynamic vulcanisation process was developed by Gessler [15]. In his experiment, the minor elastomer phase was cross-linked with peroxide. Fisher [16, 17] used this method to prepare TPVs with different compositions. In this work, however, much of the PP was damaged by degradation. Coran et al. [18] found that it is important that the elastomer phase is well mixed before the onset of the vulcanisation reaction and that the mixing should continue until the dynamic vulcanisation is completed. If the cured elastomer phase is continuous, the resulting compound cannot be processed. The curing technique was improved by Abdou-Sabet et al.. Using a phenolic curing agent the elastomer could be cured completely [19].

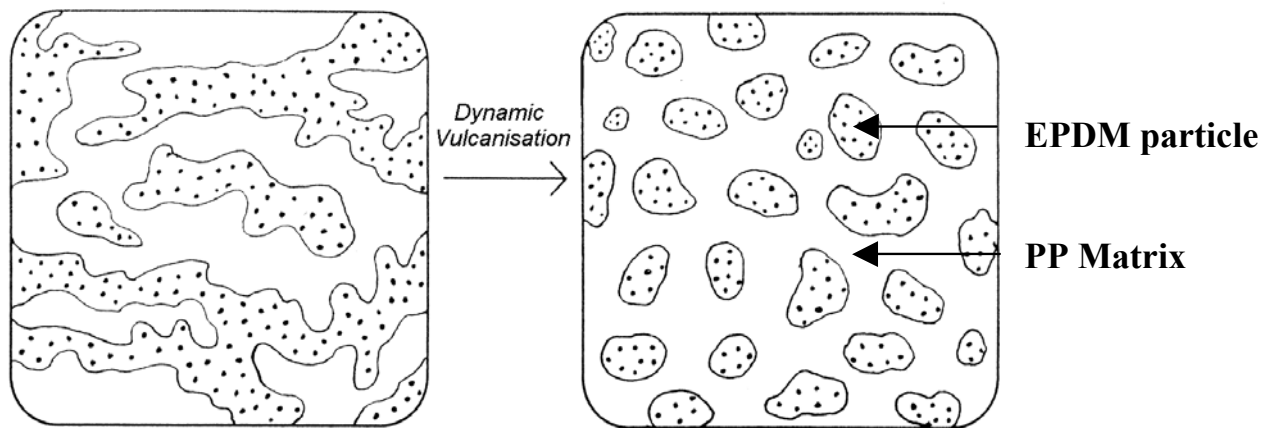


Figure 2.1: Schematic representation of morphology change during dynamic vulcanisation [20].

In dynamic vulcanisation, the elastomer phase changes from a viscous fluid to an elastic solid. The elastomer becomes rigid and cannot adapt to the applied stress. As a result, this phase breaks up into micron-sized elastomer particles [20] (Fig 2.1). Because in most TPVs the elastomer phase is the major component, this phase is continuous in the initial state. Due to the continuing curing and mixing, phase inversion takes place and the elastomer becomes dispersed, even when its volume fraction is very high ($\phi_{EI} = 0.80$).

In principle, any curing agent could be used for the crosslinking of the elastomer phase. Curing systems based on peroxides [21,22], sulphur [4] or phenolic resins [19] are widely used to make TPVs based on PP/EPDM. Another curing technique is based on silane grafting [23]. The advantages and disadvantages of these curing agents are extensively discussed in e.g. Chapter 2 in Ref [14].

The typical particle-in-matrix morphology depends both on mixing speed and curing rate. Because the curing process is very fast, the mixing speed should be high to obtain small rubber particles. These conditions can be reached in a twin screw extrusion process. Abdou-Sabet stated that the dynamic vulcanisation must be carried out at high shear rates to prepare a TPV with a fine structure [24]. The maximum shear rate should be higher than 2000 s^{-1} and the length of the extruder should be larger than 42 L/D. The curing process takes less than a minute.

2.2.2 Morphology

During the dynamic vulcanisation of PP/EPDM blends, the morphology rapidly changes from a co-continuous structure of PP and elastomer into a morphology of dispersed, cured elastomer particles in a PP matrix. Coalescence of the elastomer phase is restricted and the morphology does not change upon (re)processing of the TPV. The morphology has a large effect on the mechanical properties and it has been the subject of many studies (e.g. Ref [4,6,7,25-27]).

In the final morphology of the TPVs the elastomer phase is always dispersed, even at an elastomer fraction of $\phi_{El} = 0.8$. This volume fraction is higher than hexagonal closest packing of spheres ($\phi=0.61$). The high volume fraction is possible due to the elliptical shape of the particles and the distribution of particles sizes. Typically, the particle size varies from 0.5 - 5 μm and depends on the processing conditions, the curing system [25], the content of the curing agent [26] and the interfacial tension [27].

Sengupta [6] studied the morphology of oil-extended PP/EPDM TPVs by several microscopic techniques, i.e. scanning electron microscopy (SEM), transmitting electron microscopy (TEM) and atomic force microscopy (AFM). The most suitable techniques to study oil-extended TPVs were found to be the TEM and the low voltage SEM (LVSEM). The presence of oil lowers the resolution of the images in the other techniques. In TEM analysis, the morphology becomes visible after selective staining of the elastomer phase with *ruthenium tetroxide*. The high volume fraction of the elastomer phase can cause interpretation problems. The particles partially overlap and appear as a continuous phase in the TEM images. The presence of separate particles has been confirmed with LVSEM.

The effect of processing conditions has been intensively studied by Coran and coworkers [28] and Sengupta [6]. The change in morphology is fast and occurs in the first stage of the mixing process. The polymer and elastomer, therefore, have to be mixed well before the curatives are added [28]. Upon increasing the total deformation (the shear rate multiplied by the mixing time), the particle size slightly decreases and the particle size distribution becomes narrower [6].

Sengupta [6] studied the effect of composition on the morphology. Increasing the PP content results in a decrease of the elastomer particle size and the particles become more separated. Increasing the oil content in the TPVs results in an increase of the particle size due to the swelling of the elastomer phase. The inter-particle distance increases with increasing the PP and/or oil content.

2.2.3 Oil distribution

Processing oil is a well-known additive for rubbers and it is commonly used in TPVs [2,3]. It lowers the hardness and improves the processability. The oil, in most cases paraffinic oil, can be considered as low molecular weight olefins. The difference in polarity between the three components is small and the oil is present in both the PP and in the elastomer phases [29-31]. In order to understand the mechanical and the rheological properties of OTPEs, the concentration of oil in each phase must be known.

Several methods have been proposed to estimate the oil distribution, such as the integration of surface area of TEM images [30] and quantitative NMR analysis [31]. In the latter method, however, about 30 wt% of the oil could be traced neither in the PP nor in the elastomer phase. The integration of the surface area in TEM images can be misleading in some cases. At high elastomer content, the overlapping elastomer particles can give an impression that the content of the elastomer phase is higher.

The oil distribution coefficient, K , is the ratio of the oil concentration in the PP phase over the oil concentration in the elastomer phase. In general, K is lower than 1, indicating that the oil prefers to be in the elastomer phase. The effect of the composition or the temperature on the value of K is unknown. It has been stated that the oil migrates to the PP phase upon melting of this phase and acts there as a processing agent [6]. At crystallisation of the PP phase, it is pushed out of the PP phase and absorbed by the elastomer phase. This mechanism, however, has never been proven.

2.2.4 Deformation mechanism

The cross-linking of the elastomer phase in PP/EPDM blends results in better rubber-like properties. The modulus increases and the permanent deformation after unloading (tension or compression set) decreases. The TPVs also have better resistance to oils and high temperatures and improved fatigue resistance compared to their uncured analogues.

The morphology of the TPV plays a key role in the mechanical properties but its effect is still not well understood. Soft TPVs (Shore A values lower than 80) have high volume fraction of elastomer phase ($\phi_{EI} > 0.7$). These blends show rubber-like properties although the stiffer PP phase is still continuous. This phase is present as thin films between the elastomer particles. The deformation mechanism models are based on the deformation of these PP films.

Analysis during tensile testing of the TPV [32-34] and Finite Element Modelling (FEM) [34-36] showed that during deformation in the solid state the PP phase only yields partially. The PP films yield in the equatorial region of the elastomer particles and the rest of the PP phase remains unaffected. Based on these results, Soliman [34] proposed a model (Fig 2.2) that captures this behaviour assuming that the interfacial adhesion between the PP and elastomer phase is good. Upon unloading, the elastomer phase retracts but the stiff PP lamellae cannot deform elastically: they *buckle* (Fig 2.2). This buckling mechanism has been confirmed by AFM studies during deformation of nylon-6/EPDM TPVs [37].

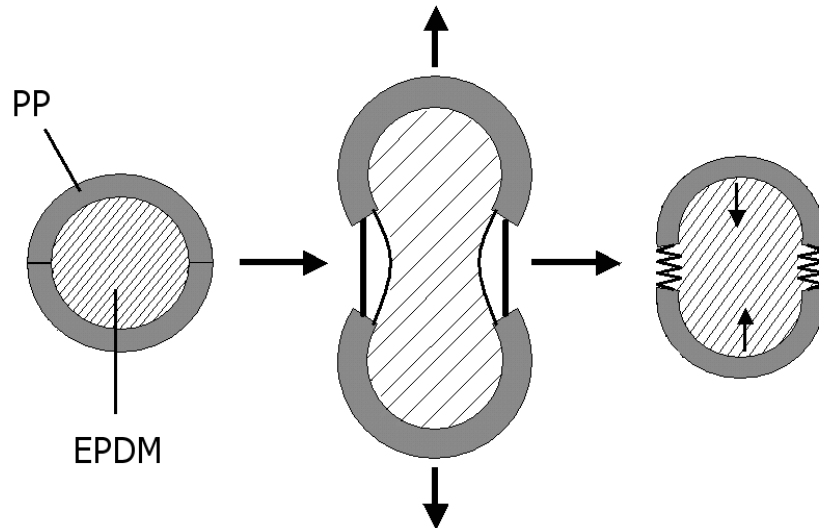


Figure 2.2: Schematic representation of deformation mechanism in TPVs according to Soliman [34]

Boyce et al. modelled the uniaxial compression properties by micromechanical models [35] and FEM analysis [36]. The effect of the thin films is that the elastomer phase can be considered as a pseudo-continuous phase after yielding of the ligaments. Most of the matrix phase undergoes *rigid body motion* as the pseudo-continuous phase gets sheared and stretched around the matrix phase (Fig 2.3).

Another model has been proposed recently by Wright [38]. The microcellular model can predict the mechanical response quit well in terms of critical stress, stiffness and tension set. However, the model includes the mechanical properties of the two phases and does not take in account the effect of the morphology.

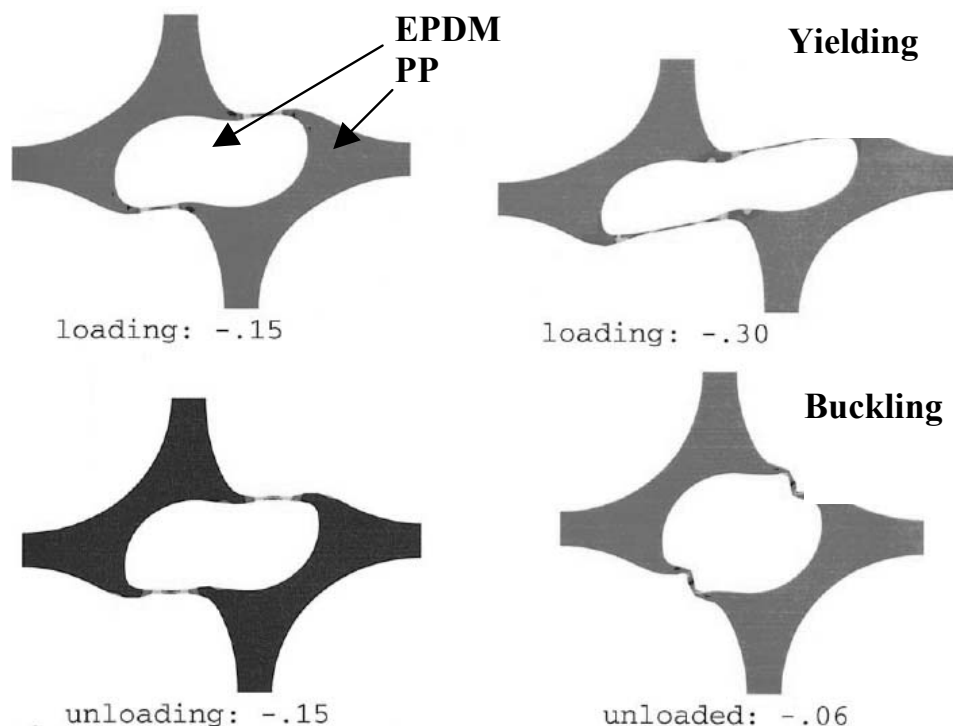


Figure 2.3: Results of FEM analysis for uniaxial compression of a TPV [35].

2.2.4 Rheological properties

The rheological properties of TPVs can be compared with those of highly filled polymers [39]. They have a yield stress for flow and the empirical Cox-Merz relation does not hold: the dynamic viscosity is always higher than the shear viscosity. The flow behaviour depends more on the applied stress and strain than on the temperature.

The dynamic rheological properties differ from common polymer blends. In polymer blends, the storage modulus may show a shoulder at low frequencies [40,41]. This shoulder is due to the interfacial tension between the two phases and can be related to the particle size of the dispersed phase. As the frequency goes to zero, the blends reach the terminal flow regime and the storage modulus decreases with a logarithmic slope of 2. When the elastomer phase in PP/EPDM blends has been cured, the behaviour deviated from this description: the storage modulus becomes always higher than the loss modulus and it tends to reach a constant value as the frequency goes to zero. The plateau value of the storage modulus at low frequencies indicates that these materials have a rest state structure [42]. Indeed, the volume fraction of elastomer particles is so high that they form agglomerates. This network-like structure has to be broken to let the TPV flow, resulting in a solid to liquid transition. The existence of a yield stress was proven by melt creep measurements [43,44]. The value of the yield stress lies in the order of 10-20 kPa and increases with increasing elastomer content.

Once the elastomeric network structure is broken, the viscosity shows a power-law shear thinning behaviour [39,42,44-46]. The value of the power law exponent is close to the one of the PP, indicating that the flow properties in steady shear flow are dominated by this phase.

To summarise, the TPVs have a rest state structure that has to be broken in order to let the material flow. The strength of this network depends on the volume fraction of the elastomer phase. Once the network is broken, the flow properties are dominated by the matrix phase.

It is not clear how the rheological properties are related to the morphology of these materials, especially at high elastomer content. No quantification of the network-like structure and how its properties affect the processability have been reported yet. In this thesis, we will try to find the relation between the deformation mechanism and the morphology. This will help to understand the processability of soft TPV compounds.

2.3 PP/SEBS blends

The formation of block copolymers of styrene and butadiene (SB) was introduced in the late '50s by anionic polymerisation [2,3]. Because the end groups of the polymer chains are still active after the addition of the last monomers, this synthesis route is also called 'living polymerisation'. The chain architecture can be controlled using this method of synthesis. Block copolymers are created by sequentially changing the type of monomer, and the block length can be controlled by the reaction kinetics.

The triblock copolymer *polystyrene-block-polyethylenebutylene-block-polystyrene* (SEBS) is formed by hydrogenation of the triblock copolymer *polystyrene-block-polybutadiene-block-polystyrene* (SBS). Depending on the isomers of *butadiene* used, the monomer becomes either two *ethylene* units or one *butylene* unit. The advantage of a saturated backbone is the increased temperature and UV stability. The SEBS triblock copolymer is never used in its pure form because its processability is poor and the total product cost becomes too high. The final product contains at maximum about 50 wt% copolymer. At low content (1-20 wt%) the copolymer acts as an impact modifier for apolar polymers, like PE, PP and PS. In polymer blends of apolar polymers with other polymers, the addition of SEBS (1-10 wt%) improves the compatibility of the two phases and the obtained blend morphology is more stable. Thermoplastic elastomer gels (TPE-G) are made by the addition of SEBS (5-20 wt%) to mineral oils or waxes. These materials have a very low hardness.

Table 2.1: Effect of oil, PP and fillers on properties of SEBS [2].

	Oil	PP	Solid filler
Modulus	decreases	increases	increases
Processability	improves	improves	-
Solvent resistance	-	improves	-
High temperature resistance	-	improves	-
Service temperature	decreases	increases	-
Cost	decreases	decreases	decreases

A higher SEBS content (20-40 wt%) is used to make TPEs. The elastomer is blended with polyolefins, like PP and PE, to increase the processability and to increase the modulus of the blend. The addition of mineral oil leads to softer blends and better processability. The role of each component is listed in Table 2.1.

2.3.1 Morphology and properties of SEBS triblock copolymer

The triblock copolymers of *polystyrene-block polybutadiene-polystyrene* first demonstrated the properties of thermoplastic elastomers [47]. The reason for this behaviour of SBS can be found in the morphology of triblock copolymers. Because of the lack of miscibility between the block types, the morphology consists of a two-phase system. Since the two polymers are chemically bound together, the dimensions of the phase-separated morphology are limited. For typical compositions of the copolymer the polystyrene is the minor component and, therefore, it is dispersed in small domains (typically 10-50 nm). The morphology changes from spherical domains via cylindrical rods to lamellar sheets with increasing content of the minor phase (from left to right in Fig 2.4). Further increase leads to phase inversion.

Because of the large difference in glass transition temperatures the PS domains are in the glassy state while the EB is in the rubbery state at room temperature. The PS domains act as physical cross-linker for the continuous elastomer phase. By elevating the temperature above the T_g of the PS (the T_g of PS in SEBS is about 80-90 °C), the triblock copolymer becomes melt processable.

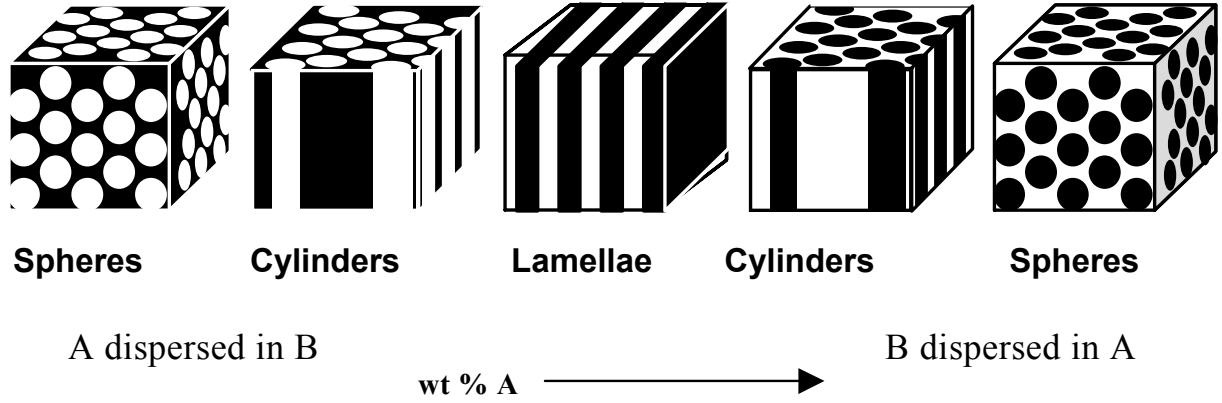


Figure 2.4: Schematic morphology change with composition for block copolymers.

The SEBS used in this work contains 32 wt% PS and the morphology of the triblock copolymer consists of spherical PS domains in a continuous EB matrix (first figure in Fig 2.4). The elastomeric properties are obtained by the large difference in the glass transition between the PS ($T_g = 87^\circ\text{C}$) and the elastomer ($T_g = -53^\circ\text{C}$). Fig 2.5 shows the modulus of this SEBS as a function of temperature. The SEBS has a broad rubber plateau that starts at -20°C and lasts up to the T_g of the PS phase. At higher temperatures, the modulus decreases rapidly and the material becomes processable.

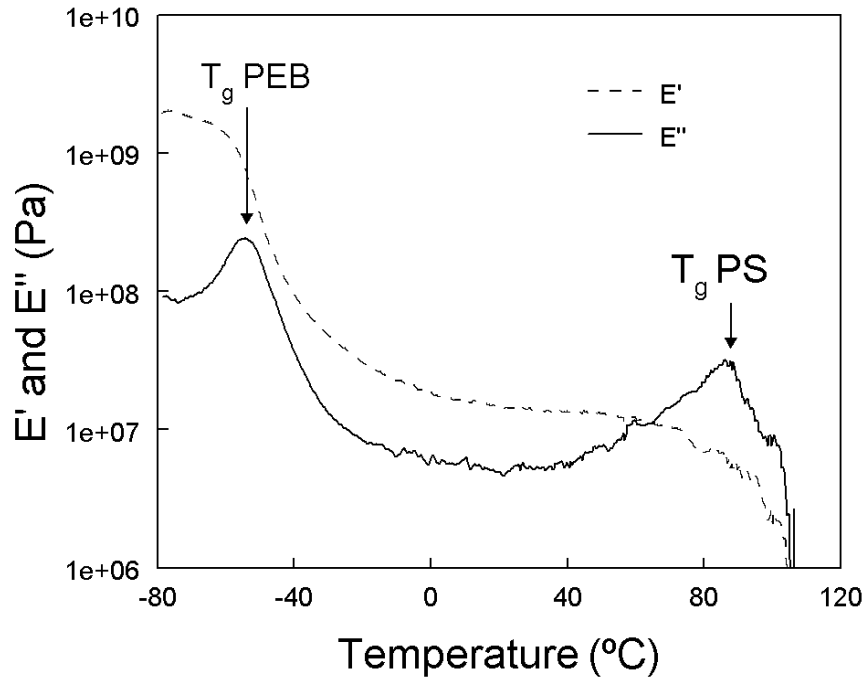


Figure 2.5: Dynamic moduli of SEBS (Kraton G 1651) measured by DMA at 1 Hz and heating at $5^\circ\text{C}/\text{min}$.

The two-phase structure of a block copolymer becomes thermodynamically unfavourable at high temperatures and it can transform into single-phase system: it becomes a (viscoelastic) liquid [48]. The temperature at which this occurs is the order-disorder temperature (ODT). The SEBS used in this work has an ODT that is higher than the degradation temperature [49]. The two-phase structure, and thus the rubber-like behaviour is always present. At temperatures higher than the T_g of the PS

domains the PS end-blocks are able to migrate to other domains by diffusion. Because the system is phase separated, a yield stress for flow is expected. The SEBS can be processed below its ODT if the applied force is high enough to pull the PS end-blocks out of the PS domains.

2.3.2 Morphology of PP/SEBS blends

The morphology of polymer blends depends on the composition, the rheological properties of the components, the interfacial tension between the phases and the processing conditions [50-52]. In studies of PP/SEBS blends with TPE properties it was found that these blends have a broad range at which stable co-continuous structures occur, i.e., both phases are continuous [5,6,52,53]. Veenstra [52] suggested that these structures are stable due to the low interfacial tension and the presence of physical cross-links in the form of the PS domains. The volume fraction interval at which the co-continuous structures are formed depends on the polymer types used and the processing conditions.

Sengupta [6] studied the phase morphology of oil-extended PP/SEBS blends by TEM on samples stained with *ruthenium tetroxide*. The domain size, or the *striation thickness*, of the elastomer phase varies between 0.5 and 2 μm . Increasing the PP content in the blend results in a decrease of the domain size of the SEBS phase and a decrease of the interconnection of this phase. The addition of oil results in a swelling of the SEBS phase. The compositions used in this study are listed in section 2.5.

Veenstra [52] and Sengupta [6] studied the effect of the processing conditions on the formation of co-continuous structures. If the SEBS is above its ODT (in the absence of physical cross-links), the concentration interval at which co-continuous structures are formed becomes smaller [52]. The increase of the temperature in an internal batch mixer resulted in a decrease of interconnectivity of the SEBS phase [6]. By the choice of the type of mixing elements one can control the shear and elongation conditions in a twin-screw extruder [6]. Kneading blocks cause high deformation rates and elongation, leading to the break-up of the elastomer phase. In the transport elements, where the shear stress is lower, the elastomer domains coalesce resulting in larger domain sizes and higher interconnectivity.

2.3.3 Oil distribution in PP/SEBS blends

PP/SEBS blends can contain considerable amounts of processing oil in order to lower the compound modulus and to increase the processability. Being paraffinic, the oil has affinity for both the PP and the EB part of the SEBS. Ohlsson et al. [5] determined the oil concentration in the PP phase using dynamic mechanical thermal analysis (DMTA).

The oil has a plasticizing effect on the amorphous parts of the PP and lowers the glass transition temperature. The position of the glass transition of the blend, therefore, can be considered as a measure for the oil concentration in the PP phase. The average value of the oil distribution coefficient, K , was 0.35, an indication that the oil prefers the elastomer phase. It is unclear how K depends on the composition.

2.3.4 Mechanical properties

Veenstra [52] showed that the morphology of PP/SEBS blends has influence on the value of the dynamic moduli. He prepared blends at similar composition that differed in morphology. The blends with co-continuous morphology had a higher value of the modulus than the blend with dispersed morphology (Fig 2.6). Because both phases contributed to the modulus, Veenstra developed various mechanical models that reflected the blend morphology.

Ohlsson [5] and Sengupta [6] studied the tensile properties of oil-extended PP/SEBS blends. As long as the SEBS phase is continuous, the blends have rubber-like properties [5]. If the elastomer phase is partially or completely discontinuous, the stress-strain curves show a yield stress, caused by the PP phase. The Young's modulus of these blends appeared to be controlled by the elastomeric network and the crystallinity of the PP phase [6]. The stress-strain curves were independent of the blend preparation process. Compared to TPVs, in which the elastomer phase is dispersed, the ultimate tensile stress and elongation at break are higher.

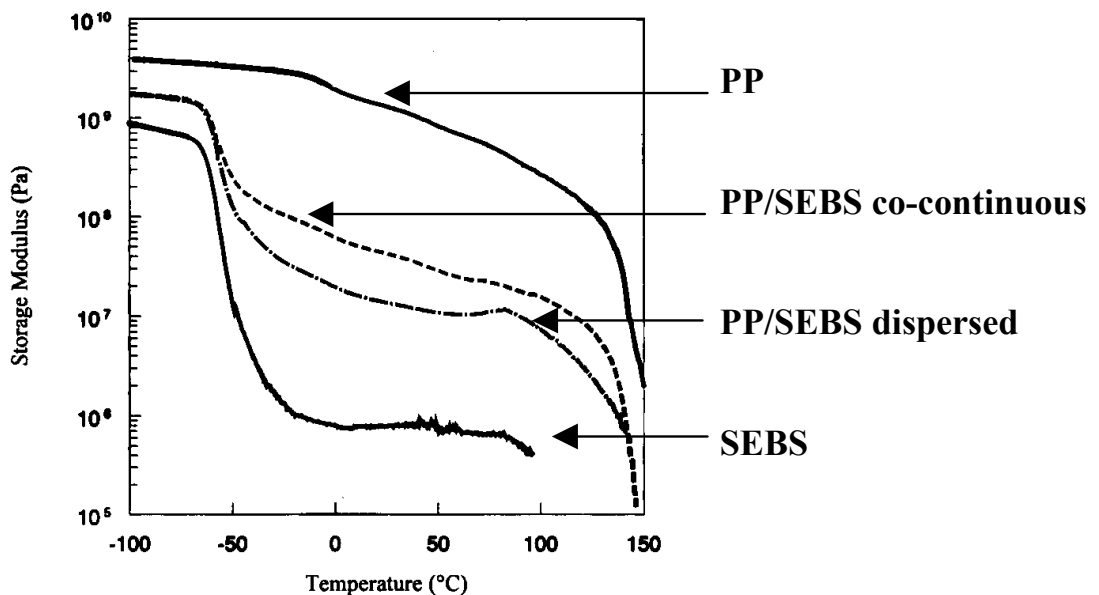


Figure 2.6: Storage modulus of PP/SEBS blends [52].

2.3.5 Rheology

The open literature about the rheological properties of PP/SEBS is limited to the work of Ohlsson et al. [54] and a few others. The melt consist of two liquid phases: the elastomer phase and a low-viscous PP phase. The storage modulus of PP/SEBS blends at low frequencies shows power-law like dependence with a slope much smaller than 2, the normal value for terminal flow behaviour. At these frequencies, the polymer blends show a shoulder in the storage modulus corresponding to the relaxation of the interface [40]. In blends with co-continuous structures, the minimalisation of surface area is a complex process, resulting in a broad relaxation time distribution [55,56]. As a result, the storage modulus shows a power-law like behaviour. The effect of the elasticity of the elastomer phase on these results is not clear.

The shear viscosity of the PP/SEBS melts shows power-law like shear thinning behaviour at high shear rates [54]. The value of the power-law index is close to the one of the (oil free) PP, indicating that the shear flow properties are dominated by the PP phase. The capillary extrudates have a PP rich skin layer. Co-continuous structures are equilibrium structures and they are sensitive to the applied deformation. The skin layer indicates possible phase migration of the low viscosity PP phase toward the high shear stress regions at the wall of the capillary.

2.4 Applications of OTPEs

The use of OTPEs has large advantages compared to the use of thermoset rubbers. Using thermoplastic processing equipment, elastomer parts can be produced in a more economical way than via thermoset processing [58]. No curing step is involved, resulting in short process cycles and high-speed production. The properties of OTPEs can be tailored easily by adjusting the composition.

OTPEs are rapidly replacing EPDM vulcanisates and they are utilised in a growing number of applications related to styling and ergonomic design. The largest market for these OTPE blends is in the automotive industry. They have good resistance to weathering and attack by fluids and have a low permanent set, which makes them ideal for use in gaskets and sealing application. Other applications are related to the soft touch properties or the insulating properties of the OTPEs. Examples of application per category are [2,3,57]:

Automotive industry

- Interior parts

Air bag covers, horn covers, connector strips, seals, bushings, seat belt housings and decorative parts.

- Exterior parts

Weather seals, Body and bumper strips and trunk gaskets.

- Under-the-hood applications

Steering gear boots, protective sealings, gaskets, vacuum tubings, vacuum connectors, air ducts, protective sleeves and shock isolators.

Consumer goods

Soft touch/grip applications on e.g. power tools, vibration damping parts in housings, liners for food and beverage closures, bumpers, and caster wheels.

Industrial hoses and tubes

Agriculture spray, paint spray, industrial tubings and mine hoses.

Electrical applications

Plugs, wire and cable jacketing, housings, bushings and enclosures.

2.5 Composition and preparation of OTPE blends

Pure OTPEs have already good properties by themselves. However, for commercial use they are compounded with fillers and oil. The main reasons for this are to lower the cost price and improve the processability. It also allows preparing TPEs with enhanced properties, like better flexibility or sound/shock damping. The compounding step is often integrated in the blending process.

The study of commercial OTPE blends is far too complex. Because of the large number of ingredients, the relation between morphology and mechanical or rheological properties is too difficult to study. To reduce this complexity, we limited the composition to the components elastomer, PP and processing oil.

2.5.1 Materials

To have a direct comparison between the PP/EPDM TPVs and the PP/SEBS blends, we used similar composition and the same PP and oil grade in all OTPE blends. Thus, all the differences are due to the type of the elastomer. The components are listed in Tables 2.2 and 2.3

Table 2.2: Materials used to prepare TPVs.

PP/EPDM Thermoplastic vulcanisates	
Elastomer	EPDM: Keltan P 597 (DSM Elastomers) (<i>This EPDM contains 50 wt% oil</i>)
PP	iPP: Stamylan P11E10 (DSM Polypropylenes) (<i>New name: Sabic PP 531 P</i>)
Oil	Paraffinic oil: Sunpar 150 (Sun Oil Company)
Curatives	Phenolic resin : SP 1045 (Schenectady) Stannous Chloride dihydrate (Merckx) Zinc Oxide
Stabiliser	Irganox1076 and Irgafos 168 (Ciba Specialty Chemicals)

Table 2.3: Materials used to prepare PP/SEBS blends.

PP/SEBS blends	
Elastomer	SEBS: Kraton G 1651 (Kraton Polymer)
PP	iPP: Stamylan 11E10 (DSM Polypropylenes) (<i>New name: Sabic PP 531 P</i>)
Oil	Paraffinic oil: Sunpar 150 (Sun Oil Company)
Stabiliser	Irganox1076 and Irgafos 168 (Ciba Specialty Chemicals)

2.5.2 Compositions and preparation

The OTPE blends were formulated in such a way that extrusion grade TPEs was obtained in a hardness range of Shore A 50-70. Together with Sengupta [6] an experimental design was used to study the effect of PP and oil content on the morphology and properties. The PP/SEBS blend and TPVs have similar composition in order to make a direct comparison between the two blend types. Three levels of PP and oil contents are used, as can be seen in Figure 2.7 and Table 2.4 and 2.5.

The blends were made either in an internal batch mixer or in a twin-screw extruder. In the internal batch mixer (Brabender Plasticorder 350S (390 cc) with Haake mixing elements), the blends were prepared at a temperature of 180 °C and rotor speed of 80 rpm [6]. The oil was preblended with the SEBS (at room temperature) or the EPDM (at room temperature in a two-roller mill). For both blend types the PP and stabiliser were added first and after 1 minute the elastomer was added. To prepare the TPVs the curatives were added simultaneously with the elastomer. The total mixing time was 10 minutes for the TPVs and 30 minutes for the PP/SEBS blends.

A Werner and Pfeiderer ZSK-40 co-rotating twin-screw extruder was also used for the preparation of the TPVs. The rotor speed was 350 rpm and the temperature profile varied from 180 °C at the hopper to 210 °C at the die. The average residence time was less than 1 minute [59]. All the ingredients were added together in the hopper.

The extruded PP/SEBS blends were prepared in a ZSK type co-rotation twin-screw extruder, operating at 250 rpm [60]. The temperature profile varied from 180 °C at the hopper to 210 °C at the die. The oil and stabiliser were preblended at room temperature and they were fed together with the PP in the hopper at a rate of 5 - 10 kg/h.

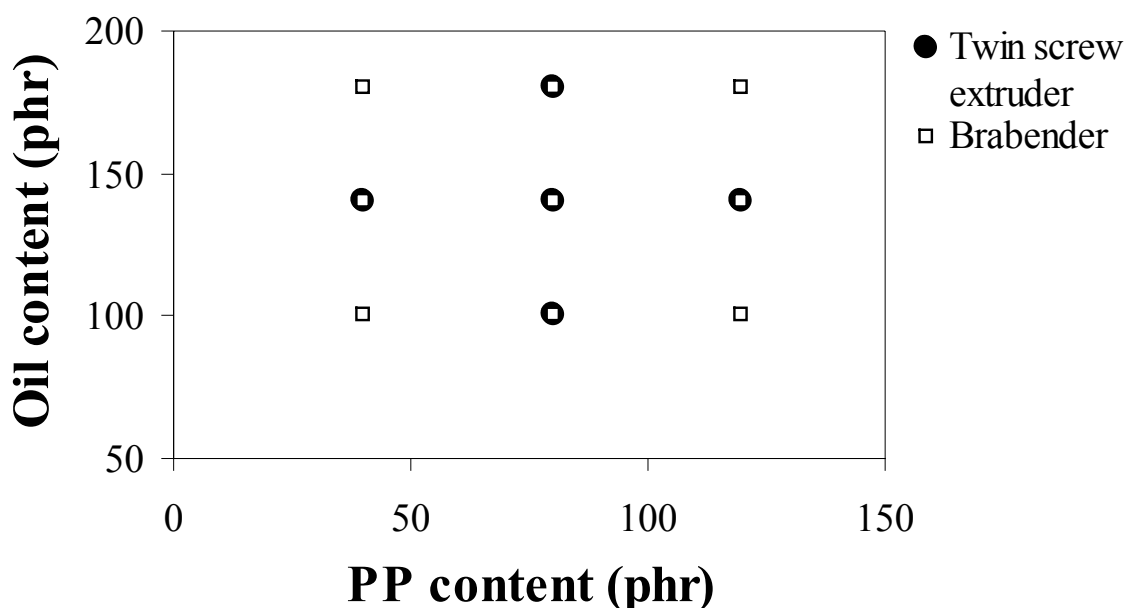


Figure 2.7: Composition of OTPE blends used in this thesis. Amounts are in parts per hundred parts of elastomer (phr).

Table 2.4: Compositions of TPVs

	EPDM -oil	PP	Oil	ZnO	Resin	SnCl ₂	Stabi- lizer	PP	EPDM	Oil
Code	(phr)	(phr)	(phr)	(phr)	(phr)	(phr)	(phr)	(wt%)	(wt%)	(wt%)
E0.4/1.0	200	40	0	2.5	5	1	1	17	42	42
E0.4/1.4	200	40	40	2.5	5	1	1	14	36	50
E0.4/1.8	200	40	80	2.5	5	1	1	13	31	56
E0.8/1.0	200	80	0	2.5	5	1	1	29	36	36
E0.8/1.4	200	80	40	2.5	5	1	1	25	31	44
E0.8/1.8	200	80	80	2.5	5	1	1	22	28	50
E1.2/1.0	200	120	0	2.5	5	1	1	38	31	31
E1.2/1.4	200	120	40	2.5	5	1	1	33	28	39
E1.2/1.8	200	120	80	2.5	5	1	1	30	25	45

Table 2.5: Compositions of PP/SEBS blends

	SEBS	PP	Oil	Stabi- lizer	PP	SEBS	Oil
Code	(phr)	(phr)	(phr)	(phr)	(wt%)	(wt%)	(wt%)
S0.4/1.0	100	40	100	1	17	42	42
S0.4/1.4	100	40	140	1	14	36	50
S0.4/1.8	100	40	180	1	13	31	56
S0.8/1.0	100	80	100	1	29	36	36
S0.8/1.4	100	80	140	1	25	31	44
S0.8/1.8	100	180	180	1	22	28	50
S1.2/1.0	100	120	100	1	38	31	31
S1.2/1.4	100	120	140	1	33	28	39
S1.2/1.8	100	120	180	1	30	25	45

2.6 References

- [1] Paul DR, Sperling LH, eds, Adv. Chem. Ser. No. 211: Multicomponent Polymer Materials, Washington DC, 1986; Am Chem Soc
- [2] Holden G, Legge N, eds. Thermoplastic elastomers, New York, 1996; Hanser
- [3] Coran AY, Patel RP. In: Holden G., Thermoplastic elastomers. New York, 1996; Hanser:153.
- [4] Coran AY, Patel R. Rubber Chem Technol 1980;53:141.
- [5] Ohlsson B, Hassander H, Tornell B. Polym Eng Sci 1996;36:501.
- [6] Sengupta P, PhD thesis, Twente University, Enschede 2004
- [7] Coran AY, Rub. Chem. Techn. 1995;68:369
- [8] John B, Varughese KT, Oommen Z, Potschke P, Thomas S, J. Appl. Pol. Sci.2003;87:2083
- [9] Coran AY, Patel R, Rub Chem. Techn 1980;53:781
- [10] Coran AY, Patel R, Williamsheadd D, Rub Chem. Techn. 1985;58:1014
- [11] Joseph S, Oommen Z, Thomas S, Mat Letters 2002;53:268
- [12] Thomas S, Groeninckx G, Polymer 1999;40:5799
- [13] Corley BE, Radusch HJ, J. Macromolec. Sci.-Phys B 1998;B37:265

- [14] Naskar K, PhD Thesis, Twente University, Enschede 2004
- [15] Gessler AM, US patent 3,037,954, (1962)
- [16] W. K. Fisher, US Patent 3,806,558, 1974
- [17] W. K. Fisher, US Patent 3,758,634, 1973
- [18] Coran AY, Das B, US patent 4,130,535, 1978
- [19] Abdou-Sabet S, Fath MA, US patent 4,311,628, 1982
- [20] Radusch HJ, Pham T, Kautsch. Gummi Kunstst. 1996;49:249
- [21] Hofmann W, Kautsch. Gummi Kunstst. 1978;40:308
- [22] van Duin M, Kautsch. Gummi Kunstst., 2002;55:150
- [23] Fritz HG, Bolz U, Polym. Eng. Sci 1999;39:1087
- [24] Abdou-Sabet S, Shen KS, EP Patent 0,107,635 A1, 1983
- [25] Abdou-Sabet S, Patel RP. Rubber Chem Technol 1991;64:769
- [26] Ellul MD, Patel J, Tinker AJ, Rubber Chemistry and Technology 1995; 68:573.
- [27] Coran AY, Patel R Rub. Chem. Techn. 1981;54:892
- [28] Laokijcharoen P, Coran AY, Rubber Chem. Technol. 1996;71:966
- [29] Ellul MD. Rubber Chem Technol 1998;71:244
- [30] Jayaraman K, Kolli VG, Kang SY, Kumar S, Ellul MD. J Appl Polym Sci 2004;93:113
- [31] Winters R, Lugtenburg J, Litvinov VM, van Duin M, de Groot HJM, Polymer 2001; 42:9745
- [32] Kikuchi Y, Fukui T, Okada T, Inoue T, Pol. Eng. Sci. 1991; 31:1029
- [33] Yang Y, Chiba T, Saito H, Inoue T, Polymer 1998; 39:3365
- [34] Soliman M, van Dijk M, van Es M, Shulmeiste V, ANTEC 1999:1051
- [35] Boyce MC, Socrate S, Kear K, Yeh O, Shaw K, J. Mech. Phys. Solids 2001;49:1323
- [36] Boyce MC, Yeh O, Socrate S, Kear K, Shaw K, J. Mech. Phys. Solids 2001;49:1343.
- [37] Oderkerk J, de Schaetzen G, Goderis B, Hellemans L, Groeninckx G, Macromolecules 2002; 35:6623.
- [38] Wright KJ, Indukuri K, Lesser AJ, Pol Eng Sci. 2003;43:531
- [39] Goettler LA, Richwine FJ. Rubber Chem Technol 1981;55:1448.
- [40] Graebbling D, Muller R. J Rheol 1990;34:193.
- [41] Tucker CL, Moldenaers P, Ann. Rev Fluid Mech 2002;34:177
- [42] Han PK, White JL. Rubber Chem Technol 1995;68:729.
- [43] Araki T, White JL. Polym Eng Sci 1998;38:590.
- [44] Steeman P, Zoetelief W. SPE Tech Papers 2000;46:3297
- [45] Jain AK, Gupta NK, Nagpal AK, J. Appl. Pol. Sci. 2000;77:1488
- [46] Kumar CR, Nair SV, George KE, Oommen Z, Thomas S, Pol. Eng. Sci. 2003;43:1555
- [47] Holden G, Milkovich R, US Patent 3.265.765, 1962
- [48] Leibler L, Macromolecules 1980;15:1602
- [49] information obtain from Kraton Polymers b.v.
- [50] Scott CE, Macosko CW, Polymer 1995;36:461
- [51] Willemse RC, PhD thesis, Delft University of Technology, Delft 1998
- [52] Veenstra H, PhD thesis, Delft University of Technology, Delft 1999
- [53] Setz S, Stricker F, Kressler J, Duschek T, Mulhaupt R, J. Appl. Pol. Sci 1996;59:1117

- [54] Ohlsson B, Tornell B. Polymer Eng Sci 1998;38:108
- [55] Steinmann S, Gronski W, Friedrich C. Polymer 2001;42:6619
- [56] Weis C, Leukel J, Borkenstein K, Maier D, Gronski W, Friedrich C, Polym Bull 1998;40:235
- [57] Dufton P, Thermoplastic elastomers, RAPRA Techn. Ltd, Shawbury, 2002
- [58] O'conner GE, Fath MA, Rubber world, december 1981
- [59] Information obtained from DSM Research b.v.
- [60] Information obtained from Kraton Polymers b.v.

Chapter 3

Dielectric spectroscopy using dielectric probes

A new approach to study glass transition dynamics in immiscible apolar polymer blends

Abstract

In Chapter 4, a new method is used in order to obtain the distribution coefficient of oil in PP/SEBS and in PP/EPDM blends. In this method, dielectric relaxation spectroscopy (DRS) is applied on olefinic polymer blends using *dielectric probes*. Because this method is new, the applicability on complex apolar polymer systems will be demonstrated in this chapter.

Binary blends of isotactic PP, PS and LDPE were doped with 0.5 wt% rigid rod molecule, *4,4'-(N,N-dibutylamino)-(E)-nitrostilbene (DBANS)*. The orientation dynamics of this dielectric probe molecule depend on the viscosity of its surrounding. This way, the dielectric loss is selectively amplified in the region of the glass transition dynamics. Accurate relaxation data were obtained for the dynamic glass transition, β_{PE} , β_{PP} and α_{PS} , even for the minor phase. No substantial influence of the blend composition and the blend morphology on the glass transition dynamics was found, indicating that both blend constituents behave like homogeneous bulk materials. The normalised relaxation strength of glass transition processes remained constant, regardless of the blend type and blend composition. This indicates that the probe molecule, DBANS, was equally distributed over the two blend components in all three polymer combinations PE-PP, PE-PS and PP-PS.

Based on:

W.G.F. Sengers, O. van den Berg, M. Wübbenhorst, A.D. Gotsis and S.J. Picken: Polymer 46 (16) 6064-6074

3.1 Introduction

Broadband dielectric relaxation spectroscopy (DRS) is one of the most suitable and versatile techniques to assess the dynamics of polymer materials in a wide dynamic range, which typically covers 10 decades in frequency or time [1-4]. By virtue of probing orientational fluctuations that involve molecular (permanent) dipoles, DRS is able to provide detailed insight in the molecular and cooperative dynamics on various time and length scales. Depending on the particular polymer system, ranging from "simple" amorphous or semi-crystalline polymers [4-6] to more complex systems like polymer blends, liquid-crystalline polymers [7,8], supramolecular polymers [9] and nano-composites, one or more characteristic dielectric relaxation processes are detected, which can be assigned to e.g. the primary relaxation (usually the α -process) associated with the dynamic glass transition, or local relaxations involving simple bond rotation processes (β , γ , δ – relaxation).

A prerequisite for DRS measurements is the presence of molecular dipoles in the polymer structure. Non-polar polymers like polyethylene and polypropylene do not have appreciable molecular dipoles and are thus not dielectrically active, at least in their pure form. However, these materials can be made accessible to dielectric spectroscopy by introducing polar groups in the structure, which allows the dynamics of the polymer molecules to be detected [10,11].

There are two main routes to achieve this: 1) by chemical modification (*labelling*) of the polymer structure, e.g. by means of partial oxidation [10,11], chlorination or attachment of pendant groups, or 2) by dissolving of suitable polar probe molecules [12] which act as *dielectric probes* in the polymer matrix. Polyethylene can be made dielectrically active by partially oxidation in the presence of air [10] or catalysed by TiO_2 [11] during melt mixing. These methods, however, are unsuitable for isotactic PP as the oxidation of PP leads to chain scission [13].

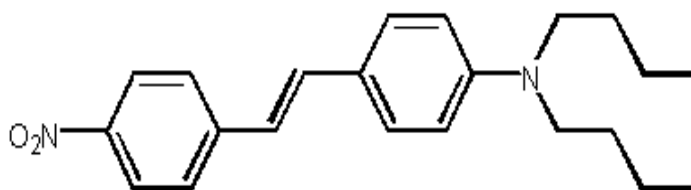


Figure 3.1: Chemical structure of 4,4'-(N,N)-(dibutylamino)-(E)-nitrostilbene (DBANS)

In [12] we have discussed an alternative approach to 'sensibilise' apolar polymers for studying them by dielectric relaxation spectroscopy, namely by using a dielectric probe at low concentrations. Fig. 3.1 shows the chemical structure of the dielectric probe molecule used, 4,4'-(N,N-dibutylamino)-(E)-nitrostilbene (DBANS). This molecule was designed to combine a rigid rod-type aromatic core, facilitating a strong dipole moment of $\mu = 9$ D [14] with an aliphatic tail that ensures good solubility in aliphatic matrices and prevents crystallisation of the probe. The high dipole moment allows the doping level to be kept as low as 0.1 – 0.5 wt%, while maintaining a sufficient dielectric probe response ($\propto \mu^2$). The crucial question of any (rotator) probe technique is the coupling of the probe fluctuations with molecular motions in its environment. For the case of DBANS, dispersed in polystyrene (PS), polypropylene

(PP) and low-density polyethylene (LDPE), it was shown in [12] that large angular fluctuations of the probe DBANS exclusively couple to the primary relaxation, i.e. the cooperative dynamic glass transition. In other words, the dielectric probe senses the microviscosity in its close vicinity in a correct way.

The present chapter aims to extend the *dielectric probe technique* to the case of binary polymer blends, consisting of two apolar polymers. Starting from the previous results obtained from the homopolymers PS, PP and LDPE, we have investigated three binary blends: PS-PP, PS-PE and PE-PP. As the polarity difference between the two polymer fractions is rather small for all the three blend compositions, it is expected that the probe molecule cannot distinguish between two phases and will thus be present in both phases. The relaxation behaviour of all three blend types will be studied as a function of the blend-type and the blend composition.

3.2 Experimental

3.2.1 Materials

The polymers used were polystyrene (PS, Shell N7000), low-density polyethylene (PE, Sabic LDPE 2100TN00) with a melt flow index (MFI) of 0.3 dg/min at 190 °C and 2.16 kg and isotactic polypropylene (PP, DSM Polypropylenes Stamylan 11E10) with a MFI of 0.3 dg/min at 230 °C and 2.16 kg. PS was purified by triple precipitation from dichloromethane/methanol, whereas the PP and PE grades were used as received. Details about the synthesis of the dielectric probe, 4,4'-(*N,N*-dibutylamino)-(E)-nitrostilbene (DBANS) can be found in [12].

3.2.2 Sample preparation

The blends were prepared by melt mixing in an internal batch mixer at 200°C (Brabender plasticorder 20 cc). The polymers were preblended at 100 rpm for 8 min before DBANS was added. After 2 minutes of continuous mixing, the samples were compression moulded at 200 °C into sheets with a thickness of 0.3 mm. For each blend type, three different blend compositions were made with 75, 50 or 25 wt% of each polymer. The sample coding consists of the polymer abbreviations and their weight percentages, like PS25PE75. All samples contain 0.5 wt% DBANS.

3.2.3 Scanning Electron Microscopy

The morphology of the blends was studied with scanning electron microscopy (SEM, Philips XL20). All samples were fractured in liquid nitrogen and sputtered with gold. The acceleration voltage was 15 kV and magnifications from 264x to 2000x were used to observe the blend morphology.

3.2.4 Dielectric relaxation spectroscopy

To obtain samples with well-defined geometry for DRS experiments, sheets of about 0.3 mm in thickness were heated to 180 °C and pressed together with 100 µm glass fibre between circular brass electrodes ($\varnothing = 2$ cm) followed by rapid cooling under a light pressure ($\sim 10^4$ Pa). Dielectric measurements were performed using a high precision dielectric analyser (ALPHA analyzer, Novocontrol Technologies) in combination with a Novocontrol Quatro temperature system providing control of the sample temperature with high accuracy (uncertainty < 0.05 K). Temperature dependent experiments were prepared by consecutive isothermal frequency sweeps ($10^{-1} - 10^7$ Hz) in the temperature range from +200°C to -120°C in steps of 5K, which resulted in an effective cooling rate of about 0.5 K/min. For quantitative evaluation of the relaxation time $\tau(T)$ and other relaxation parameters we fitted the dielectric loss spectra $\varepsilon''(\omega)$ to the empirical Havriliak-Negami (HN) relaxation function (Eq. 3.1):

$$\varepsilon'' = -\text{Im} \left\{ \frac{\Delta\varepsilon}{\left(1 + (i\omega\tau)^a\right)^b} \right\} + \frac{\sigma}{\varepsilon_v \omega} \quad (3.1)$$

where $\Delta\varepsilon$ and τ correspond to the relaxation strength and the mean relaxation time of the relaxation process. The two shape parameters a and b , which give the logarithmic slope of the low frequency loss tail (a) and the high frequency loss tail ($-a \cdot b$), are determined by the underlying distribution in relaxation times. The second term in Eq. 3.1 accounts for Ohmic conduction. A comprehensive description of analysis methods for dielectric data can be found in [15,16].

3.2.5 Differential scanning calorimetry

DSC heat flow curves were recorded with a Perkin Elmer DSC 7. Indium was used for temperature calibration. All samples were annealed for 10 minutes at 200 °C and subsequently cooled at a rate of 10 K/min to -125 °C. The glass transition temperatures were determined from half ΔC_p values and the crystallisation temperatures from the onset of the crystallisation peak. The degree of crystallinity, X_p , was calculated from the heat of crystallisation of the blend using a linear relation:

$$X_p = \frac{\Delta H_b}{w_p \Delta H_p} \quad (3.2)$$

where ΔH_b is the heat of crystallisation in the blend and w_p the mass fraction of polymer p . ΔH_p is the heat of crystallisation for polymer p and amounts to 209 J/g for PP and 290 J/g for PE [17].

3.2.6 Dynamic mechanical analysis

The glass transition temperatures in the pure polymer and their blends were determined by dynamic mechanical analysis (DMA). A Perkin Elmer DMA 7 was used in tensile mode at a frequency of 1 Hz. The samples were heated from -150 to

200 °C at a rate of 5 °C/min. The mechanical T_g was defined as the maximum in the loss modulus.

3.3 Results and Discussion

3.3.1 Morphology

The phases in the binary blends show typical length scales in the order of 1-30 μm . As expected, the morphology in the binary blends changes with the composition and the polymers used. Because the polymers have comparable viscosities during mixing (similar melt flow indices), the phase inversion point is expected to be around 50 wt% in all blends. Fig. 3.2 shows SEM images of the three 50/50 blends. In all the three blend types the two phases show layered structures in which the two phases appear to be continuous. Apart from the 50/50 blends, different structure evolution was found upon changing the composition in the blends. The final morphology depends also on the interfacial tension and the processing conditions [18-20].

The blend PS25PP75, in which PS is the minor phase, shows a droplet in matrix morphology with PS domains of about 4 μm . At 50 wt% PS (Fig 3.2a), both phases seem to be continuous with an average striation size of 5 μm , while for the blend containing 75 wt% PS the morphology reveals a combination of oriented PP sheets (ca. 10 x 30 μm) and smaller PP droplets (1 – 3 μm).

The blends of PE and PS show a structural evolution from sheets of PS (5 x 20 μm) in a PE matrix for PS25PE75 to a co-continuous layered structure of the two phases for PS50PE50 (Fig 3.2b), to sheet morphology of PE in a PS matrix for PS75PE25.

For the PP-PE blends, the morphology of PP25PE75 consists of a fine dispersion of rod like PP particles of 0.5 by 2 μm . At 50 wt% PP co-continuous structures are present (Fig 3.2c) with striation sizes of 3 μm , this changes into dispersed micron-sized spherical PE domains for composition PP75PE25.

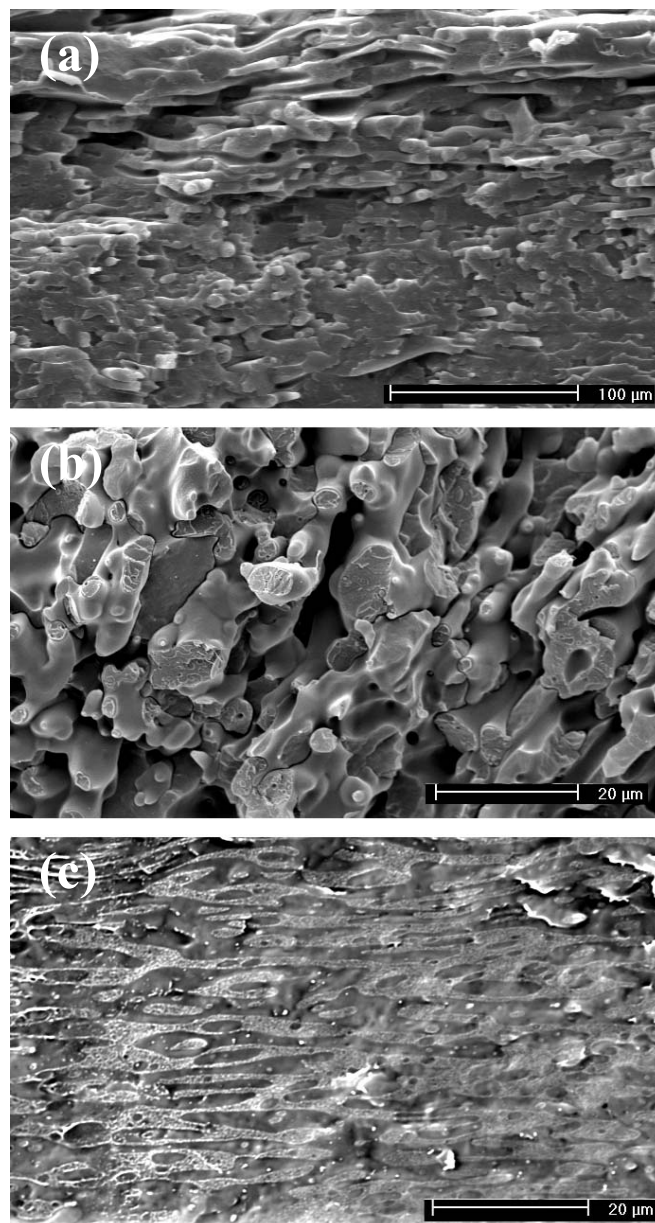


Figure 3.2: SEM images of blends at 50-50 compositions. (a) PS50PP50, (b) PS50PE50 and (c) PP50PE50

3.3.2 DSC and DMA

Differential scanning calorimetry (DSC) and dynamic mechanical analysis (DMA) are well-established techniques for the measurement of thermal transitions including the glass transition, and served in this study as reference techniques. A calorimetric glass transition temperature was obtained from the half ΔC_p values of the DSC heat flow curves upon cooling, this yields a T_g value corresponding to a characteristic frequency between 10^{-4} and 10^{-2} Hz, depending on the cooling rate of the experiment and the local activation energy of the structural relaxation. In contrast to DSC, the “mechanical” glass transition temperature was evaluated from the position of the maximum in the loss modulus, $E''(T)$, at 1 Hz. Due to this difference in the effective measurement frequency, a systematic difference in the T_g s is expected. The results for the glass transition temperatures and crystallisation characteristics are listed in Table 3.1 (DSC) and Table 3.2 (DMA). It was not possible to determine meaningful T_g -values in blends in some cases. For PS-PE blends, for example, the glass transition

region of the PS phase interferes with the crystallisation temperature window of the PE phase. In the case of PP-PE blends, the changes in the heat capacity were too small to determine the glass transition temperatures of the two phases unambiguously.

Table 3.1: Glass transition temperatures and crystallisation characteristics measured by DSC.

	Glass transition			PP crystallisation			PE crystallisation		
	T_g^{PS} (°C)	T_g^{PP} (°C)	T_g^{PE} (°C)	Tc^a (°C)	ΔH (J/g)	X_{PE}^b	Tc^a (°C)	ΔH (J/g)	X_{PE}^c
PS	96.3								
PP		-8.8		112.7	-91.6	0.44			
PE			-31.1				97.9	-77.0	0.27
PS25PP75	e	e		114.1	-71.8	0.46			
PS50PP50	96.5	e		115.6	-46.9	0.45			
PS75PP25	96.4	e		114.0	-18.6	0.36			
PS25PE75	d		e				96.6	-57.5	0.26
PS50PE50	d		e				96.4	-38.3	0.26
PS75PE25	d		e				97.6	-15.5	0.21
PP25PE75		e	e	110.2	-6.2	0.11	99.5	-58.9	0.27
PP50PE50		e	e	118.7	-43.7	0.42	97.6	-28.0	0.19
PP75PE25		-10.1	e	117.6	-68.2	0.44	96.8	-12.7	0.17

a: onset of crystallisation

b: crystallinity calculated using $\Delta H_{PP} = 209$ J/g [14]

c: crystallinity calculated using $\Delta H_{PE} = 290$ J/g [17]

d: overlap with crystallisation of PE

e: T_g not observed

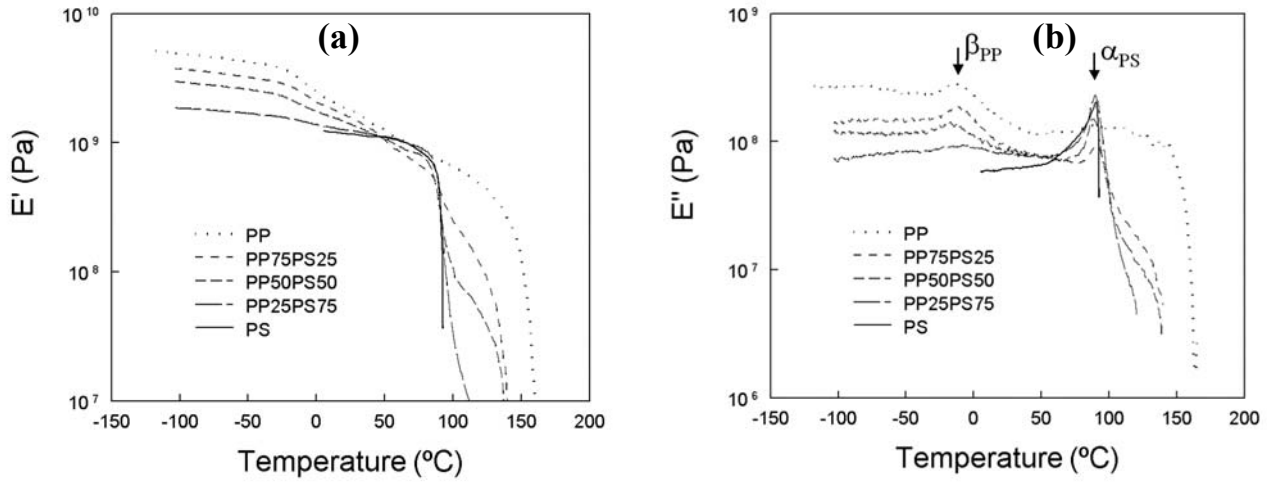


Figure 3.3: Storage (a) and loss (b) modulus of PS-PE blends

The temperature dependent elastic moduli $E'(T)$ and $E''(T)$ of all PS-PP blends and PP-PE blends are summarised in Figs. 3.3 and 3.4. Here, Fig 3.3b reveals two loss maxima corresponding to the glass transition of the PP fraction, $T(\beta_{PP})$, between -11 and -8 °C, and the glass transition of the PS phase, $T(\alpha_{PS})$, around 93 °C.

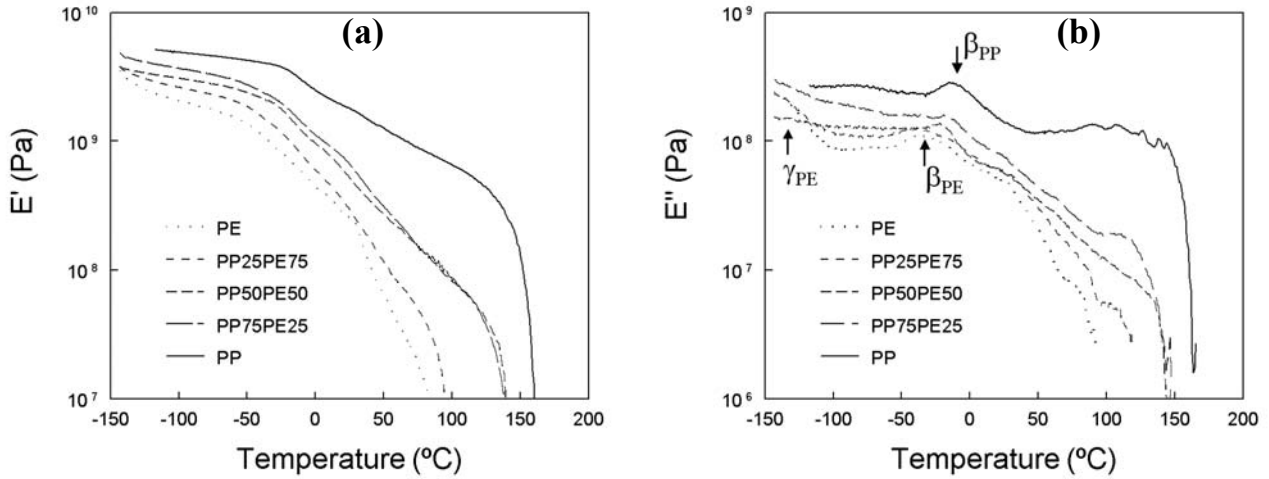


Figure 3.4: Storage (a) and loss (b) modulus of PP-PE blends

With increasing PS content, the PP loss peak decreases and it is broadened in the case where the PP phase is dispersed (blend PS75PP25). In the case of PP-PE blends, the two peaks in the loss modulus partially overlap (Fig 3.4b). The glass transition dynamics of the PP and PE phases, $T(\beta_{PP})$ and $T(\beta_{PE})$ fall within the range of -40 to 30 °C [17]. In the low temperature range, the sub-glass transition process of PE, γ_{PE} , is present. Its maximum however, falls outside the temperature range of the experiment. The maxima in $E''(T)$ of the PP phase corresponding to $T(\beta_{PP})$ are located around -10 °C. In the case of the β_{PE} peak in the blends, the maximum in loss modulus (-33 °C) is only observed in the blend containing 75 wt% PE. The curves of the other blends do not show clear maxima, because the β_{PE} peak overlaps strongly with the peak of the PP phase.

Table 3.2: Glass transition temperatures measured by DMA and by DRS.

	DMA			DRS ^a		
	T_g PS (°C)	T_g PP (°C)	T_g PE (°C)	T_g PS (°C)	T_g PP (°C)	T_g PE (°C)
PS	93			98.4		
PP		-9			-9.1	
PE			-31			-31.9
PS25PP75	91.2	-9.9		100.3	-14.3	
PS50PP50	88.9	-11.0		101.7	-13.0	
PS75PP25	91.8	-9.3		100.9	-10.0	
PS25PE75	b		-35.5	100.4		-33.0
PS50PE50	96.5		-33	100.2		-32.3
PS75PE25	94		-36	99.4		-34.1
PP25PE75		-11.5	-33		-6.0	-32.9
PP50PE50		-9	b		-8.1	-34.5
PP75PE25		-12.3	b		-11.2	-36.4

a: $\tau=1$ s

b: T_g not observed

3.3.3 Dielectric Relaxation Spectroscopy

The two previous sections were aimed to verify the morphology and the fact, that in all cases each polymer phase basically shows its unperturbed bulk behaviour for all blend compositions. This observation is important since we have to realise that all blends contained a mass fraction of 0.5 wt% of the dielectric probe DBANS without showing any substantial effect on the glass transition (DSC, DMA) and the crystallisation behaviour.

We will now focus on the dielectric relaxations of the various blends containing equal amounts of DBANS in order to see in how far the incorporation of dielectric probe molecules helps to study the complex relaxation behaviour of apolar blends in more detail. In a previous paper [12], we demonstrated that addition of DBANS specifically enhances the dielectric relaxation processes associated with the dynamic glass transition, while other processes, viz. local processes in the glassy state and intra-crystalline relaxations are not affected. This specific selectivity for cooperative (segmental) motions in the polymer matrix indicates that there is a good match of the probe length (~ 1.3 nm) with the characteristic length scale of the segmental motions ($2 - 5$ nm [21]), which results in large angular fluctuations of the stiff probe molecule on the time scale of the dynamic glass transition. Local relaxation processes, in contrast, exhibit typical length scales much shorter than the dynamic glass transition and, hence, do not give room for large angular rotational diffusion of the probe molecules around their short axis.

From the addition of dielectric probes to *binary blends* of glassforming polymers we expect, to first approximation, a simple additive behaviour of the two polymer fractions with respect to their dielectric response. However, due to the (electrically) inhomogeneous nature of polymer blends and the introduction of an additional superstructure (morphology) on a μm scale, one has to consider the following:

- (1) The probe molecules might show a different affinity to the two blend constituents, which will result in a preferential location in one of the polymer fractions or at interfaces.
- (2) The proper analysis of dielectric spectra of electrically heterogeneous systems requires the application of mixing rules [22], which account for the shape and interconnectivity of the two-phase system.
- (3) Molecular relaxations might exhibit deviations with respect to their bulk response that originate from the large internal blend interfaces, as well as, from size effects (confinement), particularly if the blend dimensions are far below $1\ \mu\text{m}$.

As already pointed out in the introduction, we do not expect strong preferential dissolution of the probe in the blends under investigation. The solubility parameters of the polymers are close to each other and the probe should thus be present in both phases of the blend. Due to the aromatic nature of the probe, a slightly higher affinity towards the PS fraction compared to PP or PE is to be expected.

Concerning the dielectric heterogeneity, which in principal could affect the apparent intensity of the dielectric response originating from the two different polymer fractions, we are in the fortunate situation that the relative dielectric permittivity, ϵ' ,

of the polymers varies only marginally, i.e. $\epsilon'(\text{PS}) \sim \epsilon'(\text{PP}) \sim \epsilon'(\text{PE}) \sim 2.5$. Hence, no morphology dependent mixing rules are required for quantitative data analysis. However, remaining differences in the conductivity might give rise to interfacial relaxations that will be discussed below.

Possible size effects on the molecular relaxations are not substantial, since the blend dimensions (1 – 20 μm) are still far above typical length scales (~ 100 nm) for which chain confinement or finite size effects have been reported [23-25].

3.3.3.1 Identification of relaxation peaks

An overview of the various dielectric relaxation processes is given by Fig. 3.5, for the dielectric loss, ϵ'' , as a function of temperature and frequency for two blends types. Five relaxation processes can be identified in the blend PS25PE75 (Fig 3.5a). Two processes originate from the PS fraction: the α process of PS (between 100 and 160 $^{\circ}\text{C}$) and the secondary β_{PS} process (around -100 $^{\circ}\text{C}$ at $f \sim 1\text{kHz}$). The other three peaks originate from the PE fraction: the intra crystalline α_{PE} process (high temperature shoulder), the glass transition (β_{PE}) process (the lower and more pronounced peak) in the range -30 to 50 $^{\circ}\text{C}$, and the γ_{PE} process at around -100 $^{\circ}\text{C}$. The latter process strongly interferes with the β_{PS} peak.

To confirm this peak assignment, isochronal loss curves $\epsilon''(T, f=1\text{ kHz})$ for different PS-PE blend compositions, including the pure blend components, are shown in Fig 3.6. With increasing PS content, the relaxation strength of the β_{PE} process decreases gradually, while the relaxation strength of the α_{PS} process shows the reverse trend. In contrast, no shifts in the *loss peak maxima* related to the dynamic glass transition (i.e. α_{PS} and β_{PE}) are observed, indicating that the two phases retain the glass transition dynamics of the corresponding pure polymers. The glass transition dynamics, thus, is not affected by the blend composition or morphology.

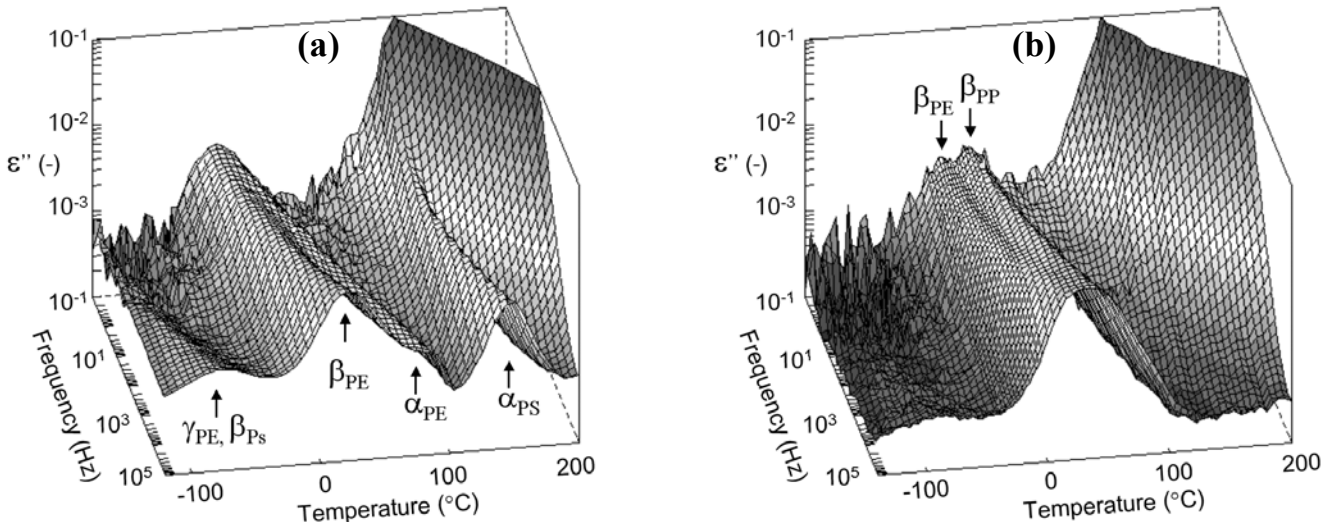


Figure 3.5: Dielectric loss as a function of temperature and frequency.
(a) PS25PE75 (b) PP50PE50

The effect of the blend composition and morphology on the intra crystalline α_{PE} process and the local relaxations γ_{PE} and β_{PS} is less obvious, since these processes do not benefit from the addition of dielectric probes. We believe that the presence of these relaxation peaks in the dielectric loss is due to slight oxidation of the polymers. Their weak intensities, however, do not allow to judge possible effects of the morphology since this relaxation behaviour might arise from e.g. residual stresses or changes in the crystal dimensions [26].

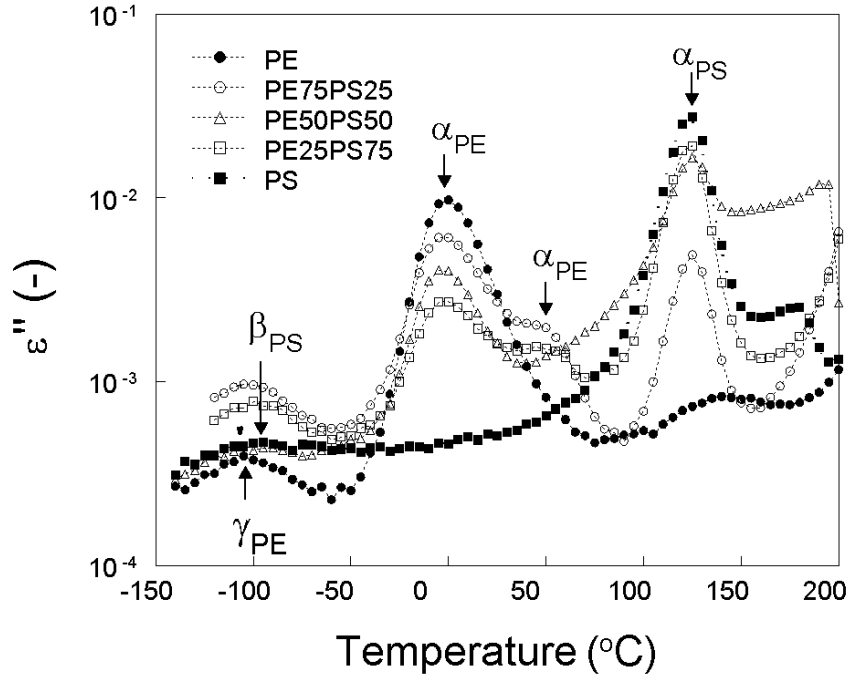


Figure 3.6: Temperature dependence of the dielectric loss at 1 kHz for PS-PE blends

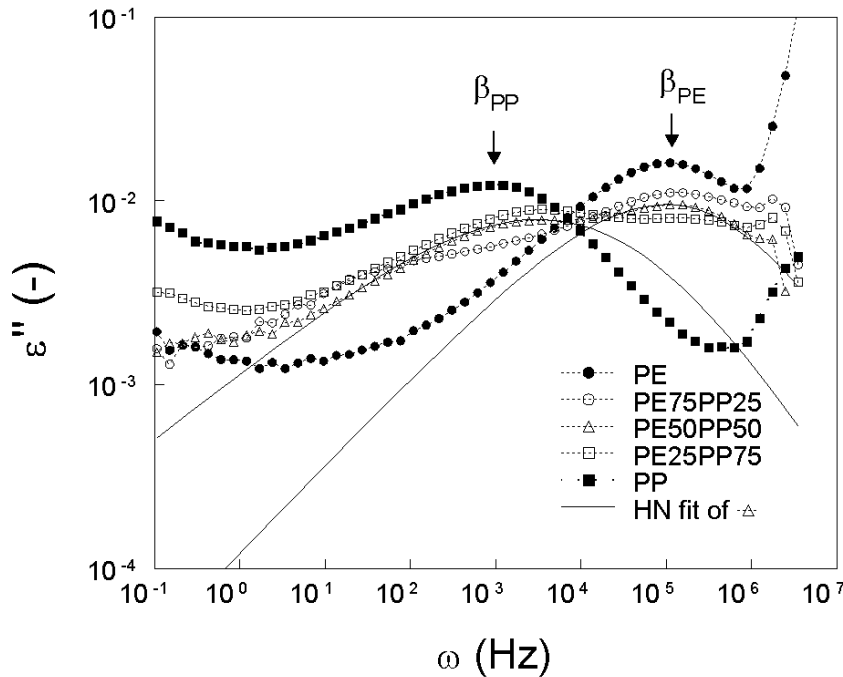


Figure 3.7: Frequency dependence of the dielectric loss at 10 °C for PP-PE blends. The lines represent the Havriliak-Negami relations for the PP and PE phases in the blends

While the glass transitions of PS and PE phases are well separated, the glass transition regions of the two phases in PP-PE blends strongly overlap. Fig 3.5b shows the corresponding 3D representation of the dielectric loss of the blend PP50PE50. Between -30 and 65 °C the two β processes of both polymers can be resolved as partially overlapping peaks. The two intra-crystalline processes α_{PE} and α_{PP} , originating from the crystalline PE and PP fractions, are not discernible for any blend composition. The same holds for the local γ -relaxations of the two polymers, which are generally hardly detectable by DRS, and which do not gain intensity upon the addition of DBANS.

A close-up of the overlapping glass transition region of the PP-PE blend is shown in Fig. 3.7, which shows the β processes of the two polymers in the frequency domain at $T=10$ °C. With increasing PP content, the intensity of the low-frequency (PE) peak decreases, while the high-frequency (PP) peak becomes stronger. In addition a small shift in the PP relaxation time is observed in all of the blends compared to that of the pure PP.

3.3.3.2. Mapping of the relaxation times

The relaxation strength and relaxation times were evaluated from the frequency spectra of the dielectric loss using the HN equation (Eq 3.1). To enhance the stability of the fit-procedure, we have set the shape parameter b_{HN} , which accounts for the asymmetry of the loss peak, to a fixed value based on data obtained from the pure polymers. The relaxation time data (corresponding to peak maxima) for the three blend types are given in an Arrhenius representation in Figures 3.8 to 3.10.

Clearly, all relaxation time data associated with the dynamic glass transition (α_{PS} , β_{PP} and β_{PE}) obey the typical signature of the Vogel-Fulcher-Tammann (VFT) behaviour (Eq. 3.3),

$$\tau(T) = \tau_{\infty} \exp\left(\frac{E_v}{R(T - T_v)}\right) \quad (3.3)$$

here τ_{∞} is the pre-exponential factor, E_v is the “Vogel” energy in kJ/mol, R is the gas constant and T_v is the reference temperature. In contrast, the intra-crystalline α process of PE and the sub T_g processes in PS and PE follow Arrhenius type behaviour:

$$\tau(T) = \tau_{\infty} \exp\left(\frac{E_a}{RT}\right) \quad (3.4)$$

where E_a denotes a "true" Arrhenius activation energy. The experimental findings will now be discussed in detail.

PS-PE blends

The Arrhenius diagram (Fig 3.8) shows all relaxation processes found for various PS-PE blends, which can clearly be assigned to either the PS or the PE fraction. The two glass transition processes β_{PE} and α_{PS} , which can be fitted to the VFT relation (cf. Tables 3.3 and 3.5) turn out to be insensitive to variations in the blend composition and thus the blend morphology. Interestingly, the α_{PE} relaxation, being located between the two glass transition processes, shows a similar robustness to variations of the blend composition. This is demonstrated by the marginal variations in the activation energy $E_a(\alpha_{PE})$ between 106 and 120 kJ/mol, which is in agreement with earlier observations from DRS studies [11] and NMR measurements [27]. Such insensitivity of the intra crystalline α_{PE} relaxation to morphological changes indicates that the thickness of PE lamellae is insensitive to the blend composition and morphology. Besides the α_{PE} process, another slower relaxation process can be seen in the temperature range from 0.0027 to 0.0033 K⁻¹ (90 to 30 °C). This process exhibits a clear dependence on the blend composition, which is a strong indication for assigning it to interfacial polarisation (IFP). Such process originates predominantly from differences in the electrical conductivity of the two polymer fractions that lead to charge accumulation and thus charge polarisation at the blend interfaces. For a given morphology, the temperature dependence of the relaxation time $\tau_{IF}(T)$ basically reflects the temperature dependence of the conductivity of the mobile (conductive) fraction (here PE), which typically follows the VFT relation of the structural relaxation time $\tau_{\beta_{PE}}(T)$. Vertical shifting of the IF relaxation data to the VFT fit line of the β_{PE} process, indeed, confirms the common molecular mechanism for the $\tau_{IF}(T)$ and $\tau_{\beta_{PE}}(T)$ data.

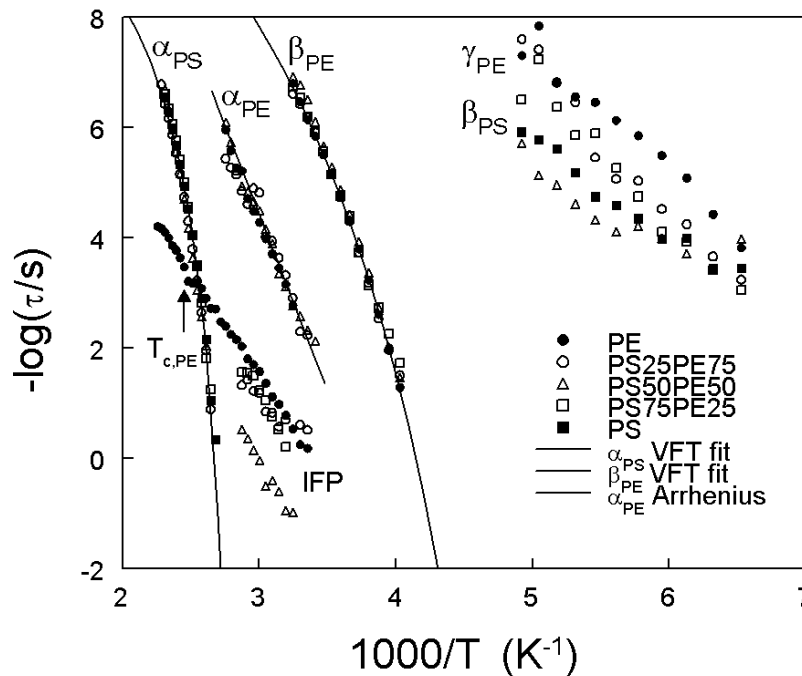


Figure 3.8: Relaxation map of PS-PE blends in Arrhenius representation. The lines represent the Arrhenius fit of the α_{PE} process and the VFT fits of the glass transition processes (α_{PS} and β_{PE}) of the pure polymers.

Table 3.3: VFT fit results for PS and its blends.

	α_{PS}		
	$T_v(K)$	$E_v(kJ/mol)$	$Log(\tau_{\infty})$
PS	317.3	12.7	-12.2
PS25PP75	327.6	9.9	-11.3
PS50PP50	329.8	9.9	-11.5
PS75PP25	324.8	11.2	-11.9
PS25PE75	321.8	11.8	-12.0
PS50PE50	317.3	13.5	-12.6
PS75PE25	319.1	12.7	-12.4

At 0.0049 K^{-1} or higher (lower than $-70\text{ }^{\circ}\text{C}$), the secondary β_{PS} and γ_{PE} relaxations are visible. For the pure polymers, these processes were found to have different activation energies of 34.1 kJ/mol (β_{PS}) and 43.2 kJ/mol (γ_{PE}), respectively. For the blends, however, these individual processes overlapped strongly, resulting in the observation of a single relaxation maximum. Accordingly, the effective activation energies of this "mixed" process fall in between those of the β_{PS} and γ_{PE} process. The intensity of these broad relaxation peaks is low, resulting in large scatter of the data points.

PS-PP blends

Fig 3.9 shows activation plot for the PS-PP blends. The sub glass transition processes and the intra-crystalline α_{PP} process are not observed in PP and its blends. Similar to the PS-PE blends, there is virtually no effect of the blend composition on the glass transition dynamics of PS. The values of the VFT fit results are listed in Table 3.3.

In contrast, for all blend samples, the β_{PP} process reveals a slight, nevertheless significant speed-up of the relaxation times by a factor of two compared to pure PP. The VFT parameters and other details are listed in Table 3.4. In addition, the β_{PP} peak becomes broader with increasing PS content. This indicates an increase in mobility of the amorphous PP parts. The PP in the blends may become more heterogeneous than the pure PP.

The intermediate process, which is visible in the temperature range between 0.0022 and 0.0033 K^{-1} (190 and $30\text{ }^{\circ}\text{C}$), can again be related to the interfacial relaxation provoked by the electrical heterogeneity of the blend. Further inspection of the data reveals that the IFP process changes its temperature dependence upon crystallisation of PP: Between 0.0022 K^{-1} ($190\text{ }^{\circ}\text{C}$) and the crystallisation temperature of PP (0.0024 K^{-1} or $140\text{ }^{\circ}\text{C}$) the IFP relaxation obeys VFT behaviour that is likely governed by the mobility of the PP melt. Upon crystallisation of the PP phase, the effective conductivity of the PP fraction drops due to the formation of PP lamellae, which hamper ionic charge transport. As an indirect effect of crystallisation there might be additional changes in the conductivity of the remaining (intercrystalline) amorphous PP phase due to constraints and confinement effects that affect the segmental mobility.

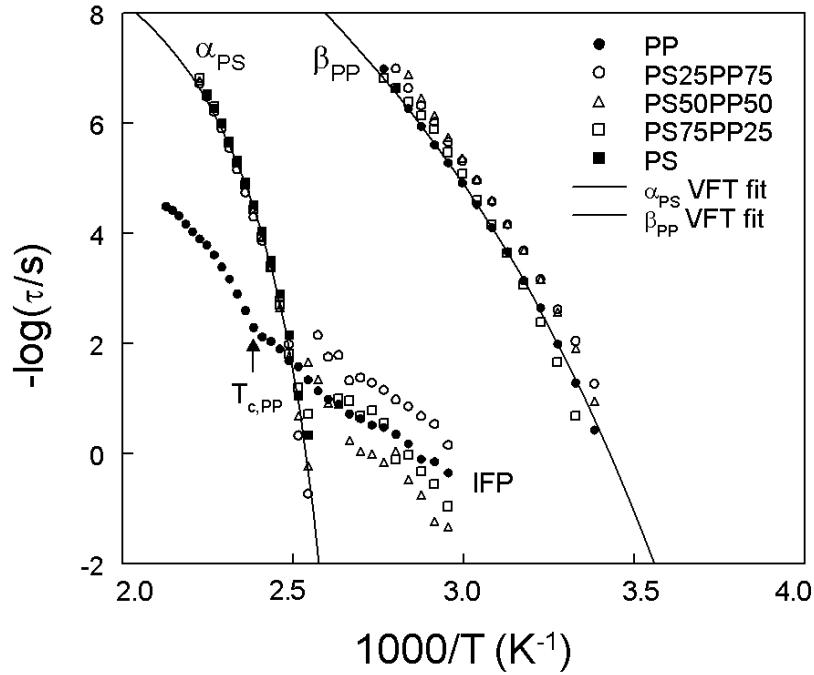


Figure 3.9: Relaxation map of PS-PP blends in Arrhenius representation. The lines represent the VFT fit of the glass transition processes (α_{PS} and β_{PP}) of the pure polymers.

Table 3.4: VFT fit results for PP and its blends.

	β_{PP}		
	T_v (K)	E_v (kJ/mol)	$\text{Log}(\tau_\infty)$
PP	168.3	28.6	-15.6
PS25PP75	162.6	29.0	-15.7
PS50PP50	163.5	30.1	-16.3
PS75PP25	184.6	22.5	-15.0
PP25PE75	164.7	31.6	-16.1
PP50PE50	183.9	24.4	-15.9
PP75PE25	178.9	25.4	-16.0

PP-PE blends

The cooperative β -relaxations of the two phases strongly overlap (cf. Figs 3.4b, 3.5b and 3.7) in the PP-PE blends. To evaluate the relaxation time and strength of the two phases in this case we applied the following two-step fit procedure:

In the first step, the two peaks are fitted separately, using the a and b parameters of the pure polymers. In a next step, the two computed HN-functions were added and the parameters $\Delta\epsilon$, τ and a were adjusted to optimise the fit of the experimental spectrum. Here, the values of the parameter b were kept unchanged.

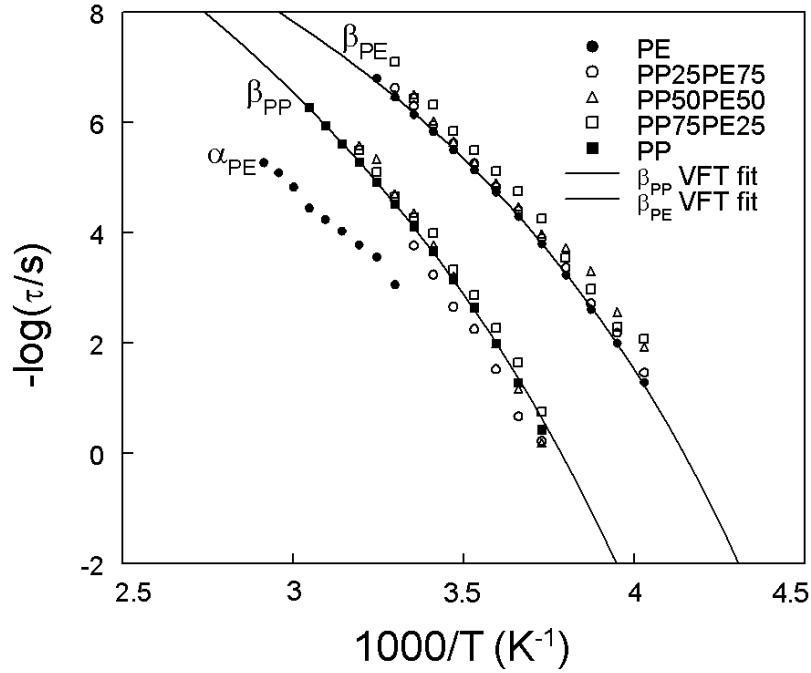


Figure 3.10: Relaxation map of PP-PE blends in Arrhenius representation. The lines represent the VFT fit of the glass transition processes (β_{PP} and β_{PE}) of the pure polymers.

The efficiency of the multi-step fit procedure is demonstrated in Fig. 3.10, which shows two well-separated glass transition processes referring to the PP and PE blend fractions. Both processes reveal again only weak, if any, effects of the blend composition on the structural relaxation time. The VFT fit results of the PP and PE relaxation times are listed in Tables 3.4 and 3.5 respectively.

The intensities of the α_{PE} and γ_{PE} processes in the blends were too low for quantitative analysis and, therefore, they are not shown in Fig. 3.10. The relaxation times for the α process in pure PE are shown as a reference.

Table 3.5: Arrhenius and VFT fit results for PE and its blends

	α_{PE}		T_v (K)	β_{PE}		γ_{PE}	
	E_a (kJ/mol)	$\text{Log}(\tau_\infty)$		E_v (kJ/mol)	$\text{Log}(\tau_\infty)$	E_a (kJ/mol)	$\text{Log}(\tau_\infty)$
PE	119.6	-23.7	169.5	19.1	-13.9	43.2	-18.8
PS25PE75	119.2	-23.0	167.7	19.1	-13.8	39.5	-16.8
PS50PE50	106.5	-21.1	170.6	19.1	-14.2	42.4	-16.4
PS75PE25	119.3	-23.0	165.7	19.2	-13.7	48.5	-19.5
PP25PE75			167.5	19.1	-13.7		
PP50PE50			164.3	19.4	-13.7		
PP75PE25			163.2	18.2	-12.9		

3.3.3.3 Relaxation strength

An essential outcome of previous work [12] was to show the *linearity* between the relaxation strength, $\Delta\epsilon$, of the (amplified) glass transition process and the probe concentration, w_{probe} , in the concentration range from 0.1 to 1 wt%. Moreover, the normalised dielectric response $\Delta\epsilon/w_{probe}$ turned out to be *identical* for all three different polymers (PE, PP and PS), indicating that *all* dissolved probe molecules contribute to the dielectric response in the specific concentration range.

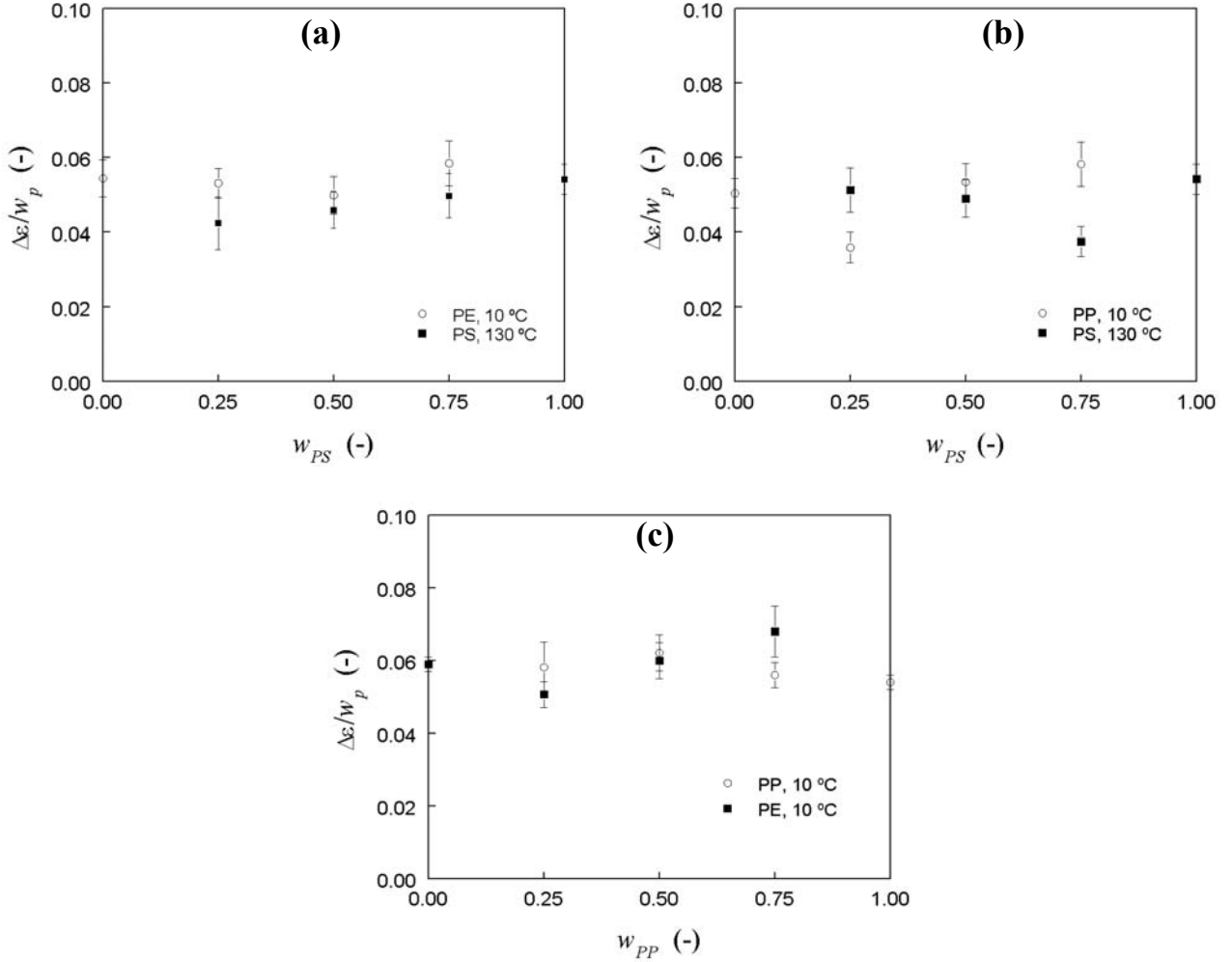


Figure 3.11: Dielectric relaxation strength in the blends as a function of the composition. (a) PS-PE blends, (b) PS-PP blends and (c) PP-PE blends.

Using this finding, we are now in the position to determine the distribution of DBANS molecules over the two blend components from the relaxation strength of the individual glass transition processes. Fig 3.11 shows the normalised relaxation strength of the two glass transition processes, i.e. $\Delta\epsilon$ divided by the mass fraction of the polymer w_p , for each blend type and blend composition. Since PS has an *intrinsic* α -process of substantial intensity ($\Delta\epsilon \sim 0.4$), we had to correct the experimental $\Delta\epsilon$ -values accordingly. As a result, all three blend types reveal nearly concentration independent $\Delta\epsilon/w_p$ values within the experimental error, which is naturally higher for the data corresponding to the minor phase ($w_p = 0.25$). Furthermore, the $\Delta\epsilon/w_p$ curves are not sensitive to the type of polymer, which proves that DBANS shows no preference to one of the blend components.

3.4 Conclusions

Dielectric relaxation spectroscopy using *dielectric probes* has been applied to study the (glass transition) dynamics in apolar polymers blends. By virtue of selective amplification of the cooperative relaxations related to the dynamic glass transition, we were able to obtain accurate relaxation data on the β_{PE} , β_{PP} and α_{PS} processes for three binary blend types and for a wide range of blend compositions.

No substantial influence of the blend composition and thus blend morphology on the glass transition dynamics was found, indicating that the blend constituents behave like homogeneous bulk materials. In other words, the relaxation times of the two phases and their temperature dependence correspond well to those of the pure polymers; a result that is to be expected for immiscible blends with structural dimensions on the micrometer scale.

The relaxation strength of the β_{PE} , β_{PP} and α_{PS} processes, normalised by the weight fraction of the respective polymer phase, revealed a constant value, regardless of the blend type and blend composition. This proves that the probe molecule, DBANS, is equally distributed in both components of all three blends of PE-PP, PE-PS and PP-PS.

These findings were tested using blends with partially overlapping relaxation dynamics. The behaviour of the two individual phases in PP-PE blends could be extracted by the summation of the two HN equations of the pure polymers.

This technique, therefore, allows quantitative analysis of complex systems, e.g. blends with overlapping glass transition dynamics or blends with simultaneous crystallisation and glass transition. In particular this is due to the easy measurement of the dynamics over large frequency and temperature range, which provides the identification of the various relaxation processes.

3.5 References

- [1] Kremer F. editor, Broadband Dielectric Spectroscopy, Berlin Heidelberg New-York: Springer-Verlag, 2002.
- [2] Bottcher CJF, Bordewijk P. eds., Theory of Electric Polarization, New York: Elsevier Scientific Pub. Co., 1978.
- [3] Hill NE, Vaughan WE, Price AH, Davies M. eds., Dielectric Properties and Molecular Behaviour, London: Van Nostrand Reinhold, 1969.
- [4] Runt JP, Fitzgerald JJ. eds., Dielectric Spectroscopy of Polymeric Materials: Fundamentals and Applications, Washington: 1997.
- [5] McCrum NG, Read BE, Williams G. eds., Anelastic and Dielectric Effects in Polymeric Solids, New York: Dover Publications, 1967.
- [6] Wübbenhorst M, de Rooij AL, van Turnhout J, Tacx J, Mathot V, Coll. Polym. Sci. 2001; 279:525.
- [7] Simon GP, Runt JP, ACS WDU, Vol 1, 329 - 378, 1997., in Fitzgerald J.J. editor., Dielectric Spectroscopy of Polymeric Materials: Fundamentals and Applications. Washington: ACS Books, 1997.
- [8] Boersma A, van Turnhout J, Wübbenhorst M, Macromolecules 1998;31:7453.

- [9] Wübbenhorst M, Folmer BJB, van Turnhout J, Sijbesma RP, Meijer EW, IEEE Transactions on Dielectrics and Electrical Insulation 2001; 8:365.
- [10] Ashcraft CR, R.H. B, J. Polym. Sci.: Polym. Phys. Ed. 1976; 14:2153.
- [11] Frübing P, Blischke D, Gerhard-Multhaupt R, Khalil MS, Journal of Physics D-Applied Physics 2001; 34:3051.
- [12] van den Berg O, Sengers WGF, Jager WF, Picken SJ, Wübbenhorst M, Macromolecules 2004; 37:2460.
- [13] Livanova NM, Zaikov GE, Polymer Degradation and Stability 1997; 57:1.
- [14] This dipole moment was calculated with the Chem3D software package from Cambridge Software using the AM1 method in combination with a closed cell wave function and Mulliken charges.
- [15] Wübbenhorst M, van Turnhout J, J. Non-Cryst. Solids 2002; 305:40.
- [16] van Turnhout J, Wübbenhorst M, J. Non-Cryst. Solids 2002; 305:50.
- [17] Brandrup J, Immergut EH, Grulke EA. eds., Polymer Handbook, 5th edition, London: Wiley, 1999.
- [18] Scott CE, Macosko CW, Polymer 1994; 35:5422.
- [19] Willemse RC, Posthuma de Boer A, van Dam J, Gotsis AD, Polymer 1998; 39:5879.
- [20] Sundararaj U, Macromolecular Symposia 1996; 112:85.
- [21] Donth E. editor, The Glass Transition. Relaxation Dynamics in Liquids and Disordered Materials, Berlin Heidelberg: Springer, 2001.
- [22] Steeman P, van Turnhout J, in Kremer F., Schönhals A. eds., Broadband Dielectric Spectroscopy. Springer, 2002.
- [23] Ngai KL, Rzos AK, Plazek DJ, Journal of Non-Crystalline Solids 1998; 235:435.
- [24] Forrest JA, DalnokiVeress K, Dutcher JR, Physical Review E 1997; 56:5705.
- [25] Wübbenhorst M, Murray CA, Dutcher JR, Eur. Phys. J. E direct 2003; 12:S109.
- [26] Boyd RH, Polymer 1985; 26:323.
- [27] Schmidt-Rohr K, Spieß HW, Macromolecules 1991; 24:5288.

Chapter 4

Distribution of oil in olefinic thermoplastic elastomer blends

Abstract

The distribution of processing oil in two olefinic thermoplastic elastomer (OTPE) blends was determined using dielectric spectroscopy. The OPTE blends are blends of dynamically vulcanised EPDM with polypropylene (PP), TPVs, and blends of PP with SEBS. Both blend types contain paraffinic oil, which is present in both the PP and in the elastomer phase. The determination of the actual oil concentration by measuring the reduction in the glass transition temperatures (T_g) is inaccurate using DSC or DMA, because the glass transition dynamics of the two phases overlap. The blends were made sensible for dielectric spectroscopy by the addition of a probe molecule. The oil distribution was determined by modelling of the dielectric loss of the OPTE blends in the T_g regime from the ones of the binary mixtures. The mean value for the oil distribution coefficient was found to be 0.6 for PP/SEBS blends and 0.63 for TPVs.

Based on:

W.G.F. Sengers, M. Wübbenhorst, S.J. Picken and A.D.Gotsis: Polymer 46(17) 6391-6401 (2005)

4.1 Introduction

Thermoplastic elastomers (TPEs) combine the elastic properties of rubbers with the processability of thermoplastic polymers [1]. An important class in these materials are the Olefinic Thermoplastic Elastomers (OTPEs). The most widely used OTPEs are blends of isotactic polypropylene (PP) with cured ethylene-propylene-diene-terpolymer (EPDM) rubber, also called thermoplastic vulcanisates (TPV) [2]. They are prepared by simultaneously curing and mixing of the EPDM with the PP. The resulting blend consists of 0.5-5 μm elastomer particles dispersed in a PP matrix. An alternative material is a blend of polystyrene-block-poly(ethylene-co-butylene)-block-polystyrene triblock copolymer (SEBS) with PP [3,4]. The triblock copolymer is by itself a thermoplastic elastomer: the PS end-blocks cluster together and form separate domains that act as physical cross-links for the elastomeric middle segment. The SEBS is blended with PP to make stiffer compounds and to improve the processability.

Commercial OTPEs often contain various additives in order to tailor the properties. Processing oil is a well-known additive that lowers the hardness and improves the processability. PP/EPDM TPVs and PP/SEBS blends can be largely extended with paraffinic oils. Due to the small polarity differences between the three components, the oil can be present in both the PP and in the elastomer phases. In order to understand the mechanical and rheological properties of OTPEs, the concentration of oil in each phase must be known. Being a low molecular weight additive, the oil plasticizes both the PP and the elastomer phases [3-5]. Its concentration in the two phases can be estimated from the reduction of the glass transition temperature (T_g). Ohlsson et al. [3] defined the distribution coefficient K as the ratio of the oil concentration in the PP phase over the concentration of oil in the elastomer phase. Values of K between 0.33 and 0.47 were found in that article using the depression of the T_g in the PP phase, measured with dynamic mechanical analysis. This indicates that the oil prefers the elastomer phase. Other methods used to estimate the oil distribution were the integration of surface area of TEM images [6] and quantitative NMR analysis [7]. In the latter method, however, about 30 wt% of the oil could not be traced either in the PP or in the elastomer phase.

Sengers et al. determined the value of K of two OTPE blends in the melt state by micromechanical modelling of the frequency dependent dynamic shear moduli [8]. The frequency dependent moduli of the two phases were interpolated from a series of binary PP-oil and elastomer-oil mixtures. The distribution coefficient K was introduced as an additional parameter in the mechanical models to estimate the oil concentrations in the PP and the elastomer phases. The obtained values for K varied between 0.04 and 1.1 and depended on the composition. In both the OTPE blend types, K decreased with increasing PP content. In the PP/SEBS blends, the total oil content did not have a significant effect on K , while K increased with increasing oil content in TPVs.

All the above methods have some shortcomings for the present blends, especially in their utility to determine the oil distribution in the solid state. The glass transition dynamics of the PP and elastomer phases overlap in the present cases. Therefore, it is

inaccurate to make use of the shift in glass transition temperatures determined by dynamic mechanical analysis or differential scanning calorimetry. In addition, the dynamic moduli may depend on the morphology of the blends. Finally, the integration of the surface area in TEM images can be misleading in some cases. At high elastomer content, the overlapping elastomer particles can give an impression that the content of the elastomer phase is higher.

Broadband dielectric relaxation spectroscopy (DRS) is used in the present chapter for the determination of the oil distribution in OTPE blends. This method also uses the frequency or temperature shifts of specific relaxations in each phase to determine the effect of oil. Due to its broad dynamic range, DRS enables the accurate detection of peak shifts in both the frequency domain (isothermal spectra) or in isochronal data (temperature shift), which gives more accurate results than the ones mentioned above. Peaks that may overlap in the temperature domain may be separated in the frequency domain and vice versa. Further, the measurement of the relaxation strength and relaxation time has led to a well established method to separate overlapping peaks by the use of the Havriliak-Negami equation [9].

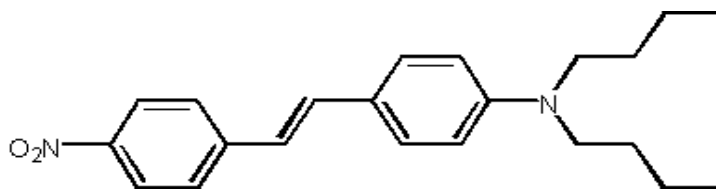


Figure 4.1: Chemical structure of 4,4'-(*N,N*)-(dibutylamino)-(*E*)-nitrostilbene, (DBANS).

Since the polymer blends consist of (almost) apolar components, showing no substantial dielectric relaxation processes, we have applied a recently developed technique based on a dielectric probe molecules [10]. Addition of small quantities of probe molecules (see Fig. 4.1) was shown to specifically enhance the dielectric relaxations related to the dynamic glass transition. The applicability of this method for heterogeneous non-polar materials has also been demonstrated by detecting and separating the dynamics of polyolefin phases in immiscible blends [11]. The phases were shown to retain their intrinsic (bulk) behaviour in dielectric spectroscopy. That is, the relaxation time of the two phases corresponds to those of the pure polymers. Furthermore, in cases of overlapping relaxations, the relaxation strength of the two components in the blend were found to be additive according to their volume fractions. In the present article, these features will enable the reconstruction of the dielectric spectra of the ternary blends from the ones of the PP and the elastomer phases. The latter are interpolated from their corresponding binary oil mixtures. In this way the oil distribution coefficient is obtained.

4.2 Experimental

4.2.1 Materials

In this study, two types of OPTE blends are used. To make a direct comparison, the blends contain the same PP matrix (PP homopolymer with a MFI of 0.3 dg/min at 230 °C and 2.16 kg, DSM Polypropylenes) and paraffinic oil (Sunpar[®] 150, Sun Oil

Company). The elastomer in the TPVs was EPDM (63 wt % C2, 4.5 wt% ENB, extended with 50 wt% of paraffinic oil, DSM Elastomers). The PP/SEBS blends contained SEBS (KRATON[®] G 1651, KRATON Polymers) as the elastomer. The EPDM in the TPVs was dynamically vulcanised using 5 phr phenolic curing agent (SP[®] 1045, Schenectady) in combination with 1 phr Stannous Chloride and Zinc Oxide (Merck). All materials contained antioxidants (0.5 wt% Irganox[®] 1076 and 0.5 wt% Irgafos[®] 168, Ciba Specialty Chemicals). For the dielectric measurements we doped the materials with the dielectric probe molecule, 4,4'-(*N,N*)-(dibutylamino)-(E)-nitrostilbene or DBANS (Fig 4.1). The preparation of the probe is described in [10].

Table 4.1: Composition and crystallinity of TPE blends

Code	PP (wt%)	EPDM (wt%)	SEBS (wt%)	Oil (wt%)	X _{PP} (-)
S0.4/1.0	17		42	42	0.47
S0.4/1.4	14		36	50	0.49
S0.4/1.8	13		31	56	0.50
S0.8/1.0	29		36	36	0.48
S0.8/1.4	25		31	44	0.47
S0.8/1.8	22		28	50	0.49
S1.2/1.0	38		31	31	0.46
S1.2/1.4	33		28	39	0.47
S1.2/1.8	30		25	45	0.49
E0.4/1.0	17	42		42	0.45
E0.4/1.4	14	36		50	0.46
E0.4/1.8	13	31		56	0.48
E0.8/1.0	29	36		36	0.44
E0.8/1.4	25	31		44	0.46
E0.8/1.8	22	28		50	0.46
E1.2/1.0	38	31		31	0.48
E1.2/1.4	33	28		39	0.45
E1.2/1.8	30	25		45	0.47

4.2.2 Sample preparation

The OTPE blends were prepared in an internal batch mixer (Brabender Plasticorder with Banbury rotors, 390 cc) at 180 °C and 80 rpm. The blend composition was varied in order to study the influence of the contents of PP and oil. Similar compositions were used for the PP/SEBS and TPV blends (Table 4.1). The symbol ‘S’ in the coding in Table 1 designates the PP/SEBS blends and ‘E’ the TPV blends. The numbers x/y stand for the PP-elastomer and the oil-elastomer ratio respectively. For the DSC and DMA measurements, samples were compression moulded into sheets of 0.3 mm at 200 °C directly after the blending process.

Binary PP-oil mixtures were made in another internal batch mixer (Brabender Plasticorder with Banbury rotors, 20 cc) at 180 °C and 100 rpm. The total mixing time was 8 minutes. After the mixing step, sheets (0.3 mm) were made by compression moulding at 200 °C. The SEBS-oil mixtures were prepared by dry blending the SEBS

pellets with oil at room temperature followed by compression moulding at 150 °C to make sheets of 0.3 mm. The EPDM-oil vulcanisates with different oil concentration were prepared by preblending the EPDM with curatives (same amount as in the TPVs) on a two-roll mill, followed by curing in compression moulding at 200 °C. An additional sample containing 60 wt% vulcanised EPDM was prepared by extracting first the oil from the EPDM-oil batch using n-hexane, precipitating the EPDM in acetone and adding the appropriate amount of oil and curatives for the vulcanisation. The extracted pure EPDM was also used in DSC and DRS measurements. The sample coding of the binary mixtures consists of the component and its weight fraction, e.g. PP80/Oil20.

4.2.3 Dynamic mechanical analysis

The glass transition temperatures of the binary mixtures and the OTPE blends were determined by dynamic mechanical analysis (DMA). Experiments were performed in a Perkin Elmer DMA 7, in tensile mode, at a frequency of 1 Hz. Samples were heated from -80 to 0 °C at a rate of 2 K/min. The peak temperatures in the loss modulus were taken to define operational 'mechanical' glass transition temperatures.

4.2.4 Differential scanning calorimetry

DSC heat flow curves were recorded with a Perkin Elmer DSC 7. Indium was used for the temperature calibration. All samples were annealed for 10 minutes at 200°C to erase their thermal history, and subsequently cooled at a rate of 10 K/min. to -100 °C. The glass transition temperatures were determined at the half ΔC_p values. The degree of crystallinity of the PP, X_{PP} , was calculated from the heat of crystallisation of the blend, ΔH_{TPE} , the heat of crystallisation of PP, ΔH_{PP} (=209 J/g [12]) and its mass fraction, w_{PP} :

$$X_{PP} = \frac{\Delta H_{TPE}}{w_{PP} \Delta H_{PP}} \quad (4.1)$$

4.2.5 Dielectric relaxation spectroscopy

Samples for dielectric measurements were prepared by melt mixing the blends or the binary mixtures with 0.5 wt% of the probe, DBANS, in the internal batch mixer. In these samples, the EPDM in the TPVs and in the binary mixtures was not cured to avoid interference of the curatives with the probe molecule in the dielectric measurements. We should refer to these blends as PP/EPDM blends instead of TPVs. The DBANS was added after premixing the ternary blends for 8 min at 100 rpm. The blends were mixed for 2 minutes to ensure a homogenise probe distribution. The samples were subsequently compression moulded into sheets of 0.3 mm thickness at 200 °C. The same procedure was used for the PP-oil mixtures. The elastomer-oil mixtures were mixed and compression moulded at 150 °C. For the dielectric measurements, the materials were hot pressed between circular brass electrodes ($\varnothing = 2\text{cm}$) together with 100 μm glass fibre spacers.

Dielectric measurements were performed using a high precision dielectric analyzer (ALPHA analyzer, Novocontrol Technologies) in combination with a Novocontrol Quatro temperature control system. Isothermal frequency sweeps (10^{-1} to 10^7 Hz) were taken in the temperature range of +200°C to -120°C in steps of -5K. This way,

thermal and mechanical history is removed, and the measurement starts from an isotropic sample. A comprehensive description of the analysis methods for dielectric data can be found in [13,14].

4.3 Results

4.3.1 DMA and DSC

Fig 4.2a shows the loss modulus of SEBS-oil binary mixtures as a function of temperature. The oil is present in the olefinic EB blocks and it plasticizes that phase: increasing the oil content results in a gradual decrease of the glass transition temperature, indicated by the position of the maximum in E'' , and the peak becomes narrower. Similar trends are found for the EPDM-oil vulcanisates. The effect of oil on the loss moduli of PP is shown in Fig. 4.2b. Addition of oil results in a drastic decrease of the glass transition temperature. PP is semi-crystalline and only the amorphous parts are accessible for the oil. Therefore, the local concentration of oil in the amorphous parts increases faster than the overall oil concentration. Moreover, even for low oil concentrations, two additional local maxima can be observed in the ranges from -20 to -30 °C and from -50 to -70 °C, which point to phase-separation in the PP-oil system. The higher temperature relaxation in Fig. 4.2b diminishes with increasing oil content and is absent above 30 wt% oil. In the range of the concentrations that should correspond to the oil in the phases of the ternary blends (25 - 40 wt%) only the lower temperature transition can be observed. The presence of separate oil domains in the binary mixtures or in the blends, however, could not be proven by morphology studies on these OTPE blends [15].

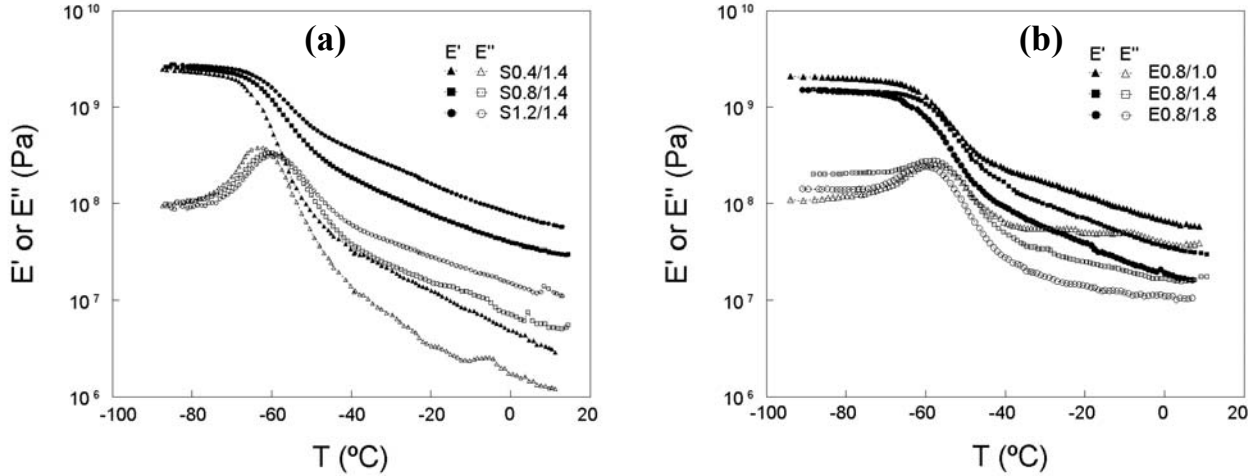


Figure 4.2: Temperature dependence of the loss modulus of the binary mixtures (a) SEBS-oil (b) PP-oil.

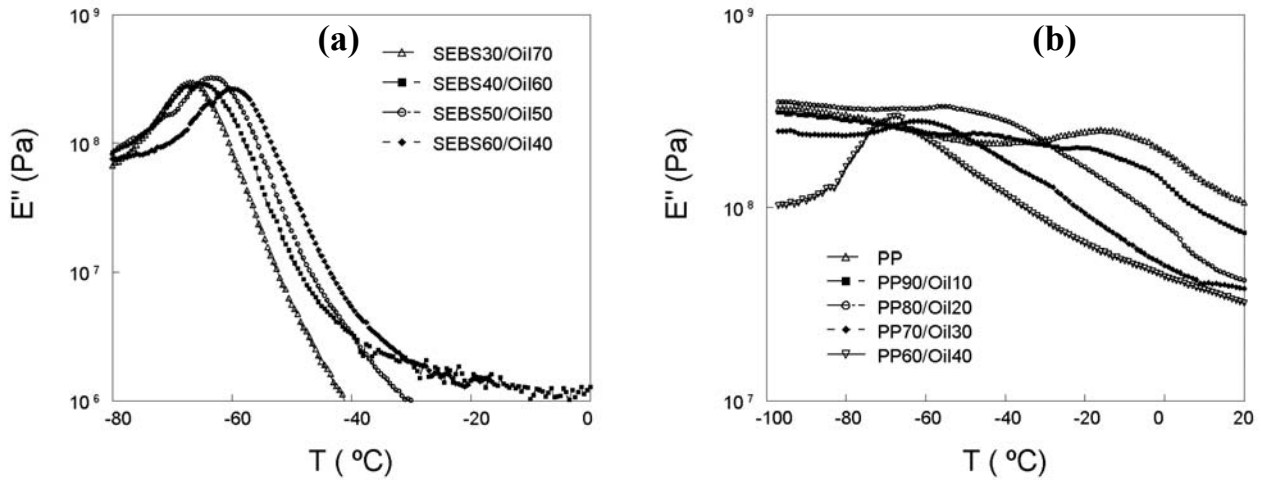


Figure 4.3: Temperature dependence of the dynamic moduli of the OTPE blends (a) PP/SEBS, different PP content (b) TPVs, different oil content.

The temperature dependent dynamic moduli of the OTPE blends with different composition are shown in Fig 4.3. The dependence of the dynamic moduli on composition is comparable for the two blend types. Between -70 and -40 °C only one peak in E'' is observed, where two peaks should be expected, corresponding to the PP and elastomer phases. Apparently, the glass transition dynamics of the two phases are so close to each other that they overlap.

Fig 4.3 shows the dynamic moduli of the OTPE blends. The behaviour of the two blends is comparable. Increasing the amount of PP in the TPVs results in a shift of the E'' peak to higher temperatures (Fig 4.3a), while the peak becomes broader at the high temperature side. Both E' and E'' increase with increasing PP content. The PP matrix phase is the stiffer phase and an increase of its volume fraction results in an increase of the blend modulus. Fig. 4.3b shows that an increasing oil content results in a shift of the single E'' peak to lower temperatures and a narrowing of the peak. E' decreases upon adding more oil because of the plasticizing effect. The extra amount of oil is distributed over the two phases and the T_g of both phases decreases.

Fig 4.4 shows the T_g 's (E'' maxima) of the PP-oil and SEBS-oil binary mixtures and of the PP/SEBS/oil blends as a function of the total oil content. The double points for the PP-oil mixtures correspond to the two local maxima in E'' shown in Fig 4.2b and are probably due to the presence of two phases: one oil-rich and one PP-rich. This ambiguity in the identification of the relaxations of the PP phases propagates into the difficulty to identify these transitions in the ternary blends. It has been mentioned that the higher temperature transition of the PP rich phase disappears above 30 wt% oil. The lower temperature transition is very close to the glass transition of the SEBS-oil mixture. As a result, the corresponding transition of the PP/SEBS/oil ternary blend falls also at the same temperature region and cannot be identified as either the transition of the PP-oil or the SEBS-oil phase. For the ternary blends, therefore, the E'' maxima of Fig. 4.3 are the weighted summations of the two peaks present due to the transitions of the two phases around the same temperature. To complicate matter further, the values of the dynamic moduli of immiscible blends may depend also on the morphology [16-18], which is not known a-priori.

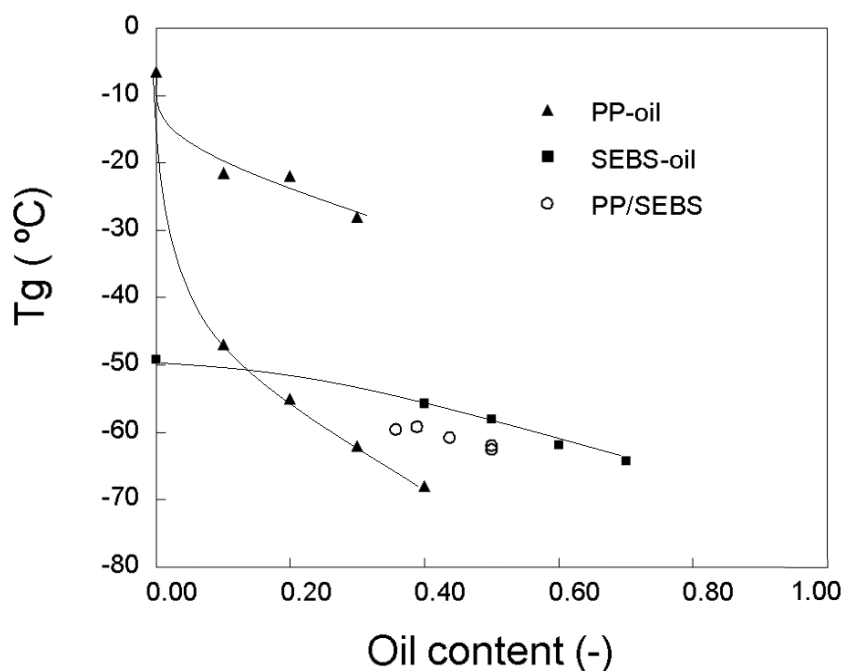


Figure 4.4: Glass transition temperature of the binary mixtures as a function of the total oil content measured with DMA of PP/SEBS blends, PP/oil and SEBS/oil. The lines are a guide to the eye.

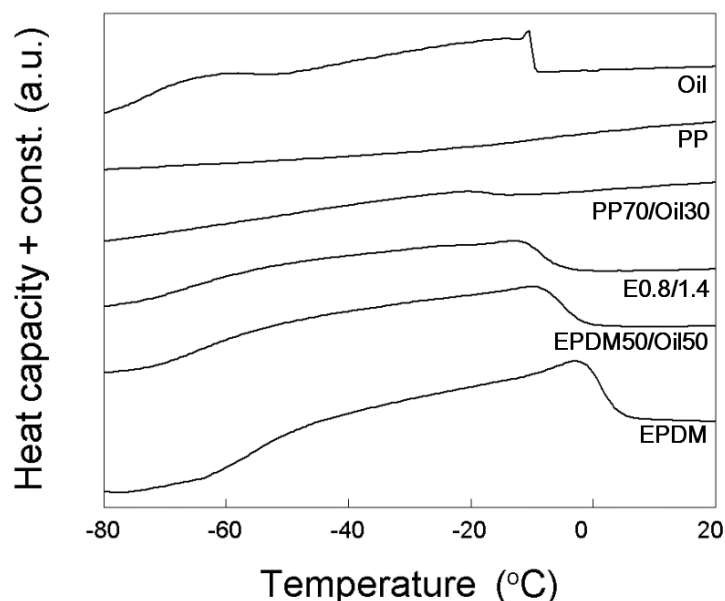


Figure 4.5: Heat capacity of TPV E0.8/1.4 and its two phases and its components measured by DSC (cooling at 10°C/min).

The determination of the T_g s of the OTPE blends by DSC proved to be inaccurate. Fig. 4.5 shows the heat capacity of TPV E0.8/1.4 and its components measured during cooling. The T_g of pure PP is difficult to discern at around -8 °C. The pure oil and elastomer components show a broad exothermic process at temperatures between -10 and -50 °C. This is probably due to the crystallisation of repeating ethylene units [19,20]. The PP-oil binary blends also show this transition, which overlaps with their T_g . The shifting of the T_g in these blends cannot be quantified as a function of the oil

content with sufficient reliability. Similarly, the same transition is present in the EPDM-oil blends. Because of this transition, the determination of the T_g s of the PP and the elastomer phases using DSC is inaccurate. The problem becomes worse in the OTPE blends, where the glass transition temperatures that are found cannot be directly related to each one of the two constituting phases (Fig. 4.6).

DSC could be used, however, to estimate the crystallinity of the PP in the blends. This was found to vary between 0.45 and 0.49 (Table 4.1). The crystallinity of PP was slightly higher in the PP/SEBS blends than in the TPVs.

Summarising the above, the distribution of oil in the TPVs and the PP/SEBS blends cannot be calculated from the determination of the glass transition temperatures measured by DMA or DSC. The glass transition dynamics overlap in the blends and only a single T_g is found, which cannot be related specifically to one of the phases. Therefore, a new method is introduced using dielectric spectroscopy, which enables the separation of these two relaxation processes and the determination of the oil distribution in the two phases of the blends.

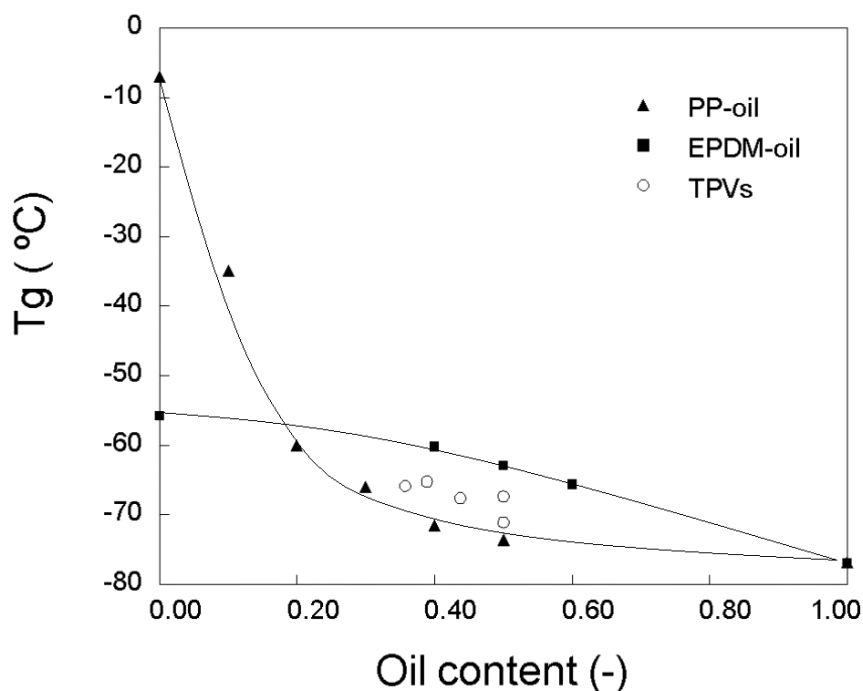


Figure 4.6: Glass transition temperature as a function of the total oil content measured with DSC of TPVs, PP/oil and EPDM/oil. The lines are a guide to the eye.

4.3.2 Dielectric Relaxation Spectroscopy

Dielectric Relaxation Spectroscopy (DRS) is a well-known technique to study polymer dynamics but is used mainly for polar polymers [21]. In [10] and [11], a method was proposed that allows to perform DRS also on apolar polymer systems, which have been sensitised by doping them with *4,4'-(N,N)-(dibutylamino)-(E)-nitrostilbene* (Fig 4.1). This probe molecule has a strong permanent dipole being almost in parallel to the molecular axis. The attached aliphatic tails enhance the solubility in olefinic media and prevent crystallisation of the probe. Because the

dipole moment is parallel to the molecular axis, the orientation dynamics of the dipole is directly coupled to the rotation dynamics of the molecule. The rotation dynamics, for its part, depends on the microviscosity of its direct surrounding. The dielectric response of the probe, therefore, is affected by changes in the viscosity of the host in the region of the glass transition.

When this method is applied to blends of two polyolefins, then the probe is present in both phases because the polarity difference of the two polymers is small [11]. In addition, the values of the relative permittivity, ϵ^* , of the two polymers are comparable. For this reason, the total dielectric loss of the blend, ϵ'' , can be described as the sum of the individual loss contributions from the two polymers weighted by their respective volume fractions.

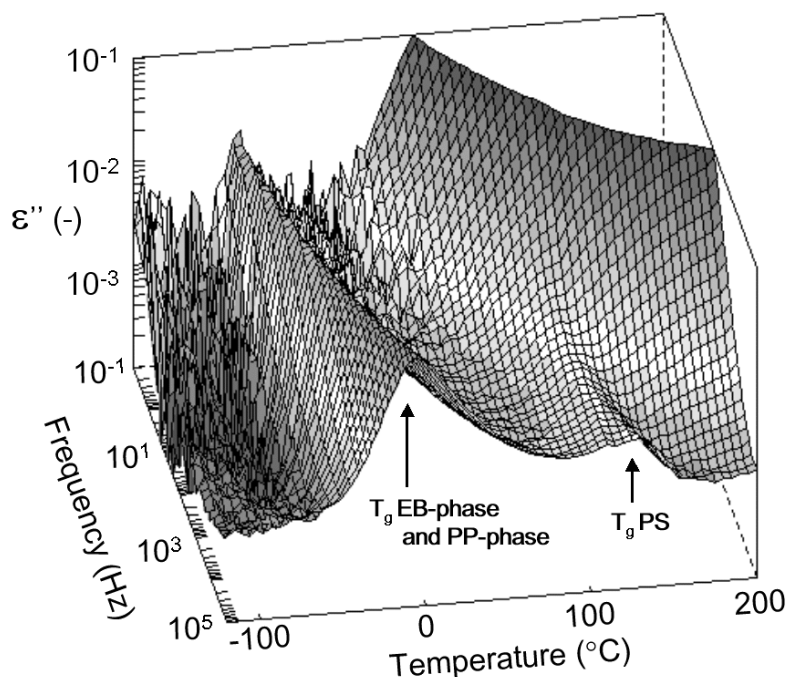


Figure 4.7: Dielectric loss, ϵ'' , as a function of frequency and temperature for S0.8/1.4.

When DBANS is added to the OTPE blends, a homogeneous distribution of the probe over the PP and the elastomer phases are expected. Fig 4.7 shows a typical result of the DRS measurements for the blend S0.8/1.4, where the dielectric loss, ϵ'' , is plotted as a function of frequency and temperature. The peaks in ϵ'' correspond to changes in the mobility of the surroundings of the probe. The increase of ϵ'' at high temperatures and low frequencies is due to Ohmic conduction. The peak of ϵ'' between 100 and 150 $^{\circ}\text{C}$ at high frequencies corresponds to the glass transition dynamics of the PS blocks within the SEBS. The probe molecules are also present in this phase and enhance its dynamics, so that the peaks are visible even though the total PS content in the PP/SEBS blend is only about 9 wt%. As shown by DMA and DSC, the glass transition dynamics of the PP and the elastomer phase overlap. This is also found in the DRS experiments. The overlapping glass transitions of the PP and elastomer phases appear as a single peak between -50 and 30 $^{\circ}\text{C}$, depending on the frequency.

The main advantage of the dielectric technique for the separation of the relaxation peaks and the eventually determination of the oil distribution, is that the samples can

be measured isothermally over a wide frequency range (7 decades). This enables the analysis of the dielectric losses also in the frequency domain, $\epsilon''(\omega)$.

The overlapping peaks in $\epsilon''(\omega)$ of the ternary blends can then be reconstructed from the peaks of the two phases.

To model the loss peaks in $\epsilon''(\omega)$ of the binary PP-oil and elastomer-oil mixtures we have used the imaginary part of the empirical Havriliak Negami (HN) function:

$$\epsilon'' = -\text{Im} \left\{ \frac{\Delta\epsilon}{\left(1 + (i\omega\tau)^a\right)^b} \right\} + \frac{\sigma}{\epsilon_0\omega} \quad (4.2)$$

where $\Delta\epsilon$ and τ are the relaxation strength and the mean relaxation time of the corresponding transition. The shape parameters a and b are the logarithmic slopes of the curve determined by the underlying distribution in relaxation times. The parameter a corresponds to the logarithmic slope at low frequencies and $-a \cdot b$ is the logarithmic slope at high frequencies. The second term in Eq. 4.2 accounts for possible Ohmic conduction.

The effect of the oil content in the binary mixtures on the shape and position of the $\epsilon''(\omega)$ peak can be described by the HN-parameters, $\Delta\epsilon$, τ , a and b , if they are considered as functions of the oil content. By interpolation of these parameters, the dielectric losses of the two phases can be predicted for any oil concentration. The dielectric response of the ternary blends is then reconstructed by a weighted addition of the losses of the two phases. The oil distribution coefficient is found for each temperature in the range of -40 to 10 °C by an optimal fit of the ternary blend.

4.3.2.1 Binary mixtures

Fig. 4.8 shows the loss permittivity for three binary polymer-oil mixtures as a function of the frequency at -20°C. The peak in $\epsilon''(\omega)$ corresponds to the dynamic glass transition process of pure oil and the plasticized polymer-oil phase, respectively. In Fig. 4.8a, the plasticizing effect of oil on the primary relaxation of PP is demonstrated, which expresses in the increase of the loss peak intensity and its shift to higher frequencies. Since pure PP has a glass transition temperature around -10°C, no corresponding loss peak is discernable for unplasticized PP. In addition, the peak shape becomes narrower as the oil content increases.

The change in relaxation behaviour of the SEBS-oil and the EPDM-oil mixtures is presented in Figs. 4.8b and 4.8c. Note that the pure elastomers ($c_{oil} = 0$) were too viscous and elastic for melt mixing and they were blended with PP to make them processable. The dielectric response arising from the glass transition dynamics of the elastomer phase is not affected by the addition of PP because the PP does not show any dielectric process at this temperature and frequency range. Fig. 4.8b shows the dependence of $\epsilon''(\omega)$ on oil content for the EPDM-oil mixtures. The behaviour is comparable to that of the PP-oil mixtures: increasing the oil content increases the value of the maximum in $\epsilon''(\omega)$ and shifts the peak to higher frequencies. The peak

narrows, especially on the low frequency side. Similarly to the SEBS-oil mixtures (Fig. 4.8c), the loss peaks shift to higher values and higher frequencies with increasing amount of oil. In these mixtures, the shape of the peaks does not change significantly with oil content. This is possibly due to the low polydispersity of the EB chains as compared to the high molecular weight PP and EPDM.

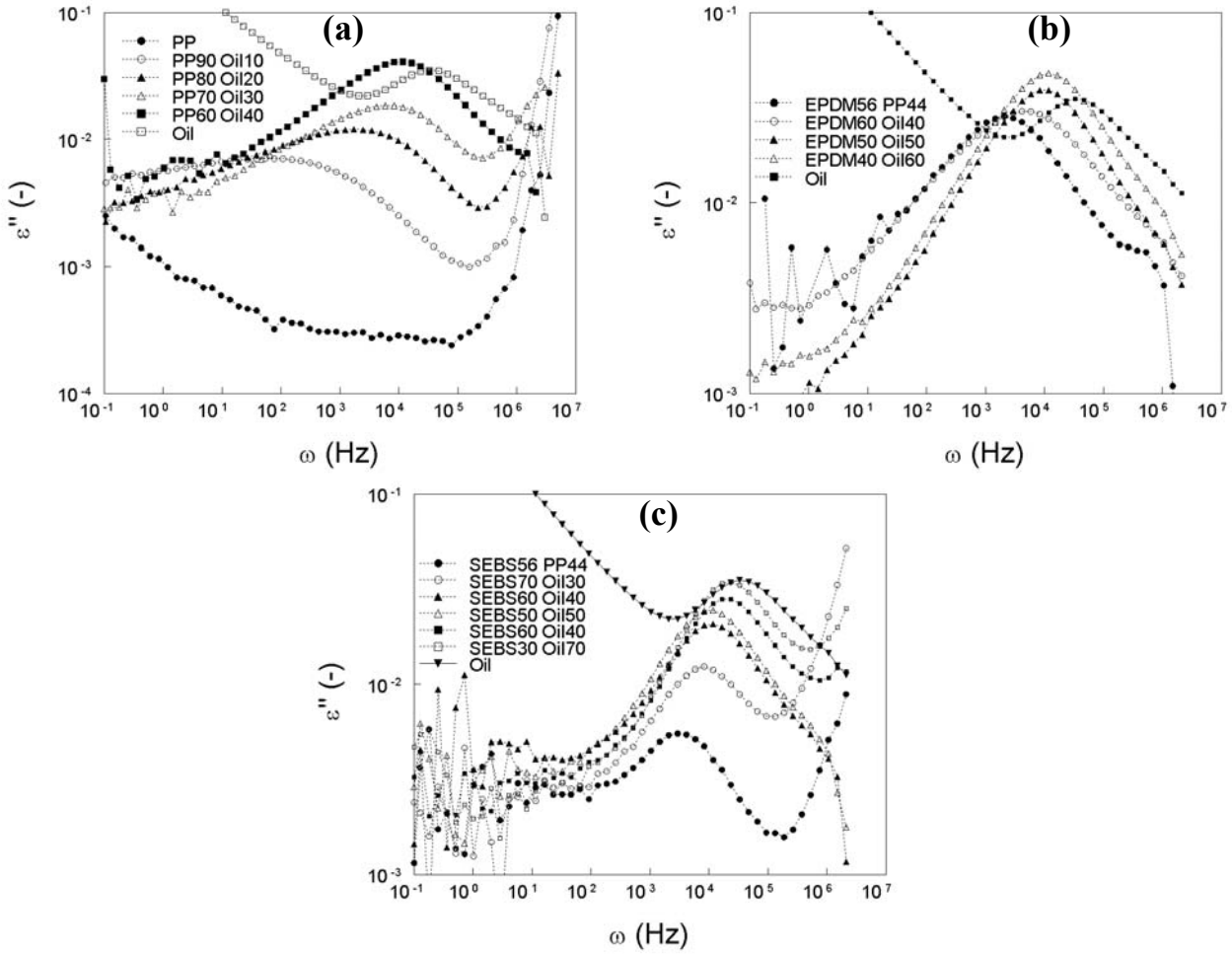


Figure 4.8: Dielectric loss, ϵ'' , of the binary mixtures as a function of frequency at -20°C . (a) PP/oil (b) EPDM/oil and (c) SEBS/oil.

To quantify the dielectric response of the binary mixtures, the relaxation peaks were fitted with the HN-function (Eq. 4.2). It was found that the shape parameter b of the mixtures did not change significantly with changing oil content and it has been kept constant for each temperature in the following analysis. As shown in Fig. 4.8, the peaks of PP-oil and EPDM-oil mixtures become steeper with increasing oil content. This results in an increase of the shape parameter a . For the SEBS-oil mixtures, the parameter a had a constant value of 0.77, independent of temperature and composition.

The values of the HN-parameters for the T_g dynamics of the binary mixtures at -20°C are summarised in Fig 4.9. The relaxation strength, $\Delta\epsilon$, increases linearly with the oil content (Fig 4.9a). This increase is faster for the PP-oil mixture because PP is semi-crystalline and the oil is only present in the amorphous part. The local oil concentration, and thus the relaxation strength, increases faster than the overall oil content in the total PP phase.

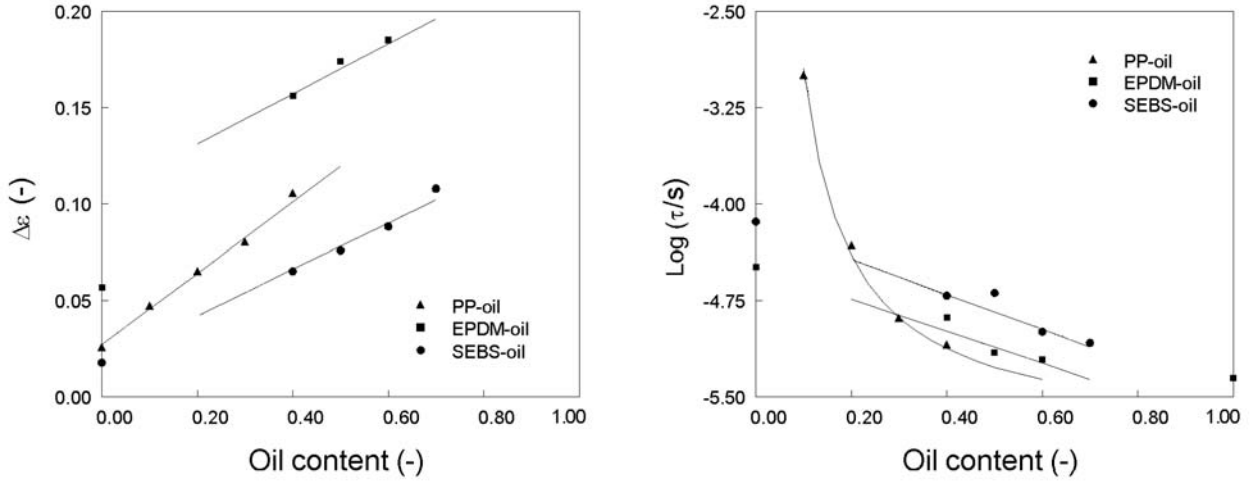


Figure 4.9: Dependence of the HN parameters of the binary mixtures on the oil content (a) relaxation strength and (b) relaxation time at -20 °C. See Table 2 for the drawn fitting curves.

The relaxation times, τ , (Fig. 4.9b) and the shape parameter a , (Table 4.2) of the PP-oil mixtures are different from the ones of the elastomer-oil. The two elastomer-oil mixtures show comparable behaviour of the relaxation times: they scale exponentially with the oil content. The relaxation times of the PP-oil mixtures decrease faster because of the faster increase of the local oil concentration in the amorphous parts of PP. The shape parameter, a , also increases with increasing oil content (Table 4.2).

Table 4.2: Dependence of HN fit parameters of binary mixtures on oil content at -20 °C

	HN parameter	Fit function
PP-oil	$\Delta\epsilon$	$\Delta\epsilon = 0.19 \cdot c_{oil,PP} + 0.027$
	τ	$\text{Log}(\tau) = 0.28 / c_{oil,PP} - 5.85$
	a	$a = 0.69 \cdot c_{oil,PP} + 0.27$
	b	$b = 1.5$
SEBS-oil	$\Delta\epsilon$	$\Delta\epsilon = 0.13 \cdot c_{oil,SEBS} + 0.011$
	τ	$\text{Log}(\tau) = -1.36 \cdot c_{oil,SEBS} - 4.16$
	a	$a = 0.77$
	b	$b = 0.8$
EPDM-oil	$\Delta\epsilon$	$\Delta\epsilon = 0.23 \cdot c_{oil,EPDM} + 0.056$
	τ	$\text{Log}(\tau) = -1.25 \cdot c_{oil,EPDM} - 4.49$
	a	$a = 0.076 \cdot c_{oil,EPDM} + 0.57$
	b	$b = 1.64$

4.3.2.2 OTPE blends

Fig. 4.10 shows the effect of the composition on $\epsilon''(\omega)$ for the OTPE blends at -20 °C. As also observed in the DMA results, the $\epsilon''(\omega)$ of the OTPE blends reveals a single peak that corresponds to the overlapping glass transition processes of the two phases. Fig. 4.10a shows the loss permittivity of PP/SEBS blends with different PP content. The spectra of the two binary mixtures, PP with 30 wt% oil and SEBS with 50 wt%

oil, are also included. The maximum of the relaxation peak of the blends is close to the one of the SEBS-oil binary mixture. The curve of the blend has a shoulder at the frequencies where the PP phase relaxation should be. The peak decreases in height and shifts to lower frequencies, while the low frequency shoulder increases with increasing PP content. The peak in $\epsilon''(\omega)$ changes, thus, from elastomer-like to PP-like behaviour.

Changing the oil content also affects the position of the relaxation peaks in the blends (Fig. 4.10b). The relaxation strength of the loss permittivity of the PP/EPDM blends increases and the maximum shifts to higher frequencies with increasing oil content. This is due to the plasticizing effect of the oil, as observed also in the binary mixtures. The reduction of the low frequency shoulder is due to the change in shape of the PP phase peak. Similar to the PP-oil binary mixtures, the relaxation time and the relaxation strength increase with increasing oil content. In addition, the peak of this phase becomes sharper.

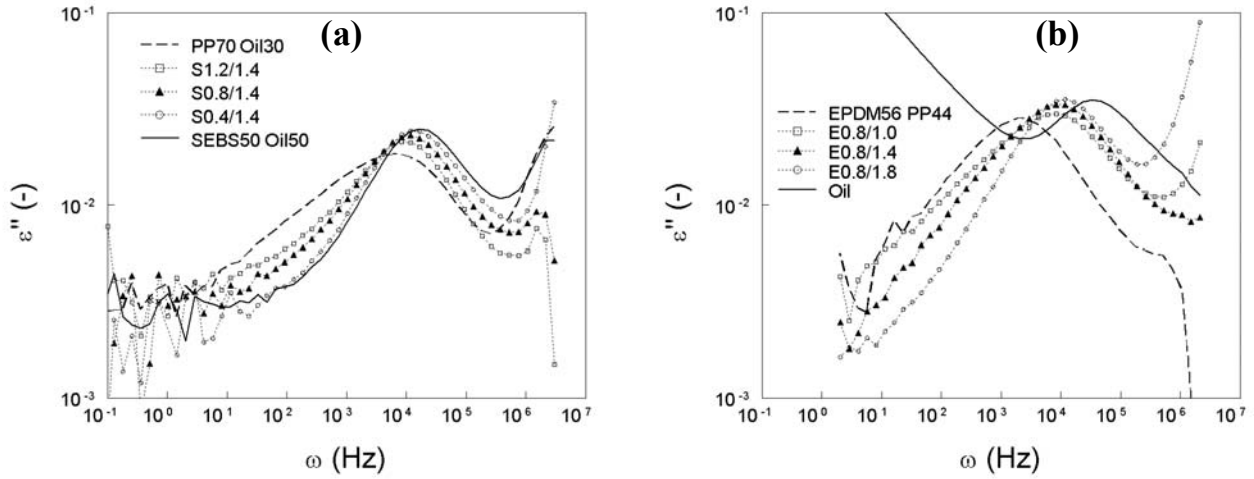


Figure 4.10: Frequency dependence of the dielectric loss, ϵ'' , of the OTPE blends at -20 °C. (a) PP/SEBS with different PP content (b) PP/EPDM with different oil content.

From the above we can conclude that the curves of $\epsilon''(\omega)$ of the OTPE blends consists of the peaks of the two phases that partially overlap. Increasing the PP content, the relaxation behaviour changes gradually from elastomer-like to PP-like. When the oil content is increased, both phases are plasticized and the peak in loss permittivity shifts to higher frequencies.

4.3.3 Determination of the oil distribution coefficient

The trends in the dielectric response of the OTPE blends can be correlated to the changes in the phase volume fractions and in the concentration levels of oil in the two phases. Therefore, the spectra of the OTPE blends can be reconstructed by adding the ones of the binary mixtures. The determination of the oil concentrations in the two phases can, thereby, be achieved.

To quantify the preference of the oil in one of the phases, the distribution coefficient, K , is used [3]. This is the ratio of the oil concentration of the PP phase, $c_{oil,PP}$, over the one of the elastomer phase, $c_{oil,El}$:

$$K = \frac{c_{oil,PP}}{c_{oil,El}} \quad (4.3)$$

These concentrations are interrelated via the mass balance of the system, where the oil is distributed over the two phases:

$$\begin{aligned} w_{PP} + w_{oil,PP} + w_{oil,El} + w_{El} &= I \\ \text{and} \\ w_{oil,PP} + w_{oil,El} &= w_{Oil} \end{aligned} \quad (4.4)$$

where w_i is the mass fraction of component i . The oil concentrations are related to the phase mass fractions of the components:

$$c_{oil,PP} = \frac{w_{oil,PP}}{w_{oil,PP} + w_{PP}} \quad \text{and} \quad c_{oil,El} = \frac{w_{oil,El}}{w_{oil,El} + w_{El}} \quad (4.5)$$

The dielectric losses of the ternary blends are calculated at a constant temperature by adding the losses of the PP and elastomer phases. This is done by an iterative technique. An initial value of K is chosen for the specific ternary blend and the oil concentrations are calculated using Eqs. 4.3-4.5. The parameters $\Delta\epsilon(c_{oil})$, $\tau(c_{oil})$, $a(c_{oil})$ and b for the two phases are calculated by the equations listed in Table 4.2 and the two peaks of the phases, $\epsilon''_{PP}(\omega, c_{oil,PP})$ and $\epsilon''_{El}(\omega, c_{oil,El})$ are calculated from Eq. 4.2. Finally, The dielectric loss of the ternary blend, $\epsilon''_{TPE}(\omega)$, is reconstructed by the addition of $\epsilon''_{PP}(\omega, c_{oil,PP})$ and $\epsilon''_{El}(\omega, c_{oil,El})$:

$$\epsilon''_{TPE}(\omega) = x_{PP}\epsilon''_{PP}(\omega, c_{oil,PP}) + x_{El}\epsilon''_{El}(\omega, c_{oil,El}) \quad (4.6)$$

with $x_{PP} = w_{PP} + w_{oil,PP}$ and $x_{El} = w_{El} + w_{oil,El}$ the phase mass fractions. The curve is compared to the measured one and the value of K is obtained by a least squares fit.

An example of this calculation is given in Fig. 4.11, which shows the loss permittivity curve for the blend S0.8/1.4 at -20 °C. The graph shows the measured peak, the calculated individual peaks of the two phases (dashed lines) and the reconstructed peak for the blend using the above procedure for an estimated value of $K = 0.62$.

The values of K for the two TPE blends do not change significantly with temperature in the range of -40 to 10 °C. The averaged values are listed in Table 4.3. Within experimental error, the oil distribution in the PP/SEBS blends is comparable to that in the PP/EPDM blends. The average value of K in all the blends is smaller than one, indicating that the oil concentration in the elastomer phase is higher than in the PP phase. The composition has a minor effect on the value of K : in both the OPTE blends K decreases slightly with increasing PP content. The total amount of oil does not affect the oil distribution coefficient significantly.

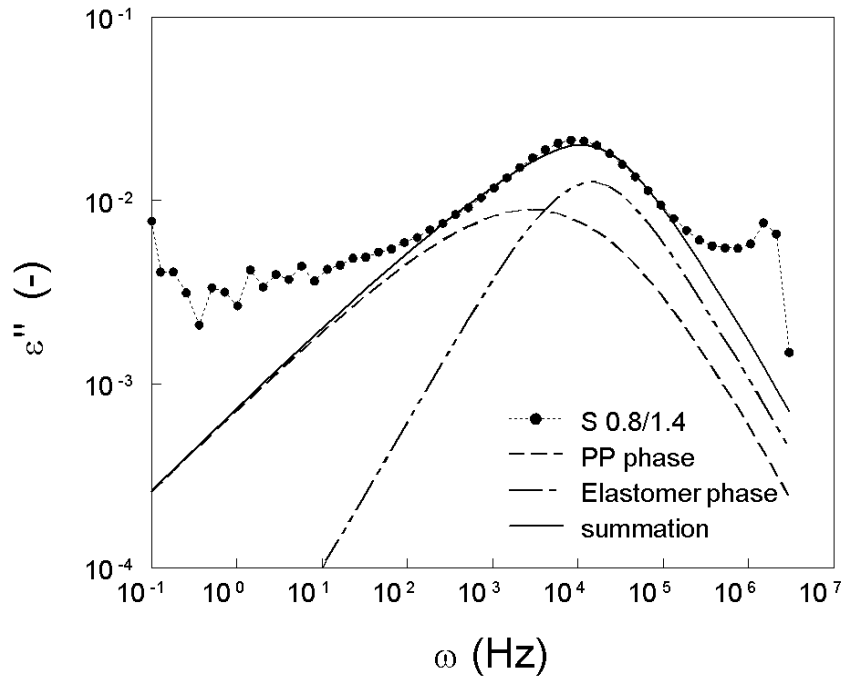


Figure 4.11: Fit of ε'' for the blend S0.8/1.4 at -20 °C.

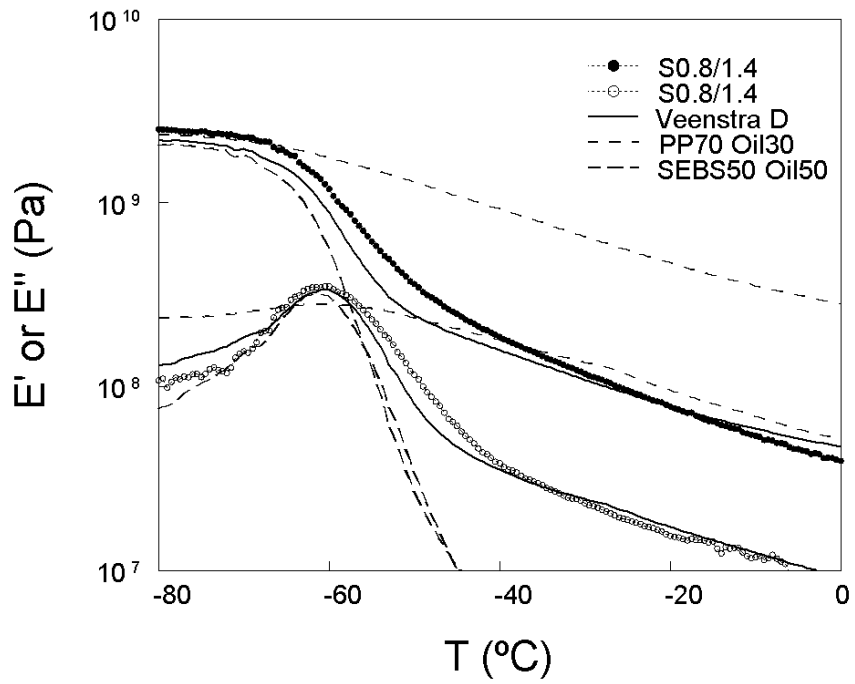


Figure 4.12: Calculated DMA response of the blend S0.8/1.4 using Veenstra model D, compared to the experimental results.

Table 4.3: Oil distribution coefficients in OTPE blends

Blend	DRS -40 to 10 °C	DRS -40 to 10 °C	Veenstra D 190°C	Veenstra D 190 °C
	K	$K_{corrected}^a$	K^b	$K_{corrected}^c$
S0.4/1.0	0.68 ± 0.04	0.84	0.54	0.44
S0.4/1.4	0.63 ± 0.02	0.79	0.91	0.82
S0.4/1.8	0.58 ± 0.03	0.75	1.08	0.93
S0.8/1.0	0.61 ± 0.02	0.78	0.36	0.30
S0.8/1.4	0.62 ± 0.03	0.77	0.63	0.53
S0.8/1.8	0.57 ± 0.03	0.73	0.72	0.56
S1.2/1.4	0.90 ± 0.05	1.02	0.20	0.20
S1.2/1.4	0.57 ± 0.03	0.74	0.48	0.40
S1.2/1.4	0.56 ± 0.02	0.72	0.58	0.50
E0.4/1.4	0.70 ± 0.04	1.04	0.10	0.10
E0.4/1.4	0.67 ± 0.03	0.96	1.14	1.14
E0.4/1.4	0.51 ± 0.04	0.75	1.67	1.67
E0.8/1.0	0.65 ± 0.04	0.86	0.04	0.04
E0.8/1.4	0.60 ± 0.06	0.85	0.60	0.60
E0.8/1.8	0.63 ± 0.03	0.88	0.94	0.94
E1.2/1.0	0.49 ± 0.03	0.69	0.03	0.03
E1.2/1.4	0.62 ± 0.04	0.90	0.34	0.34
E1.2/1.8	0.56 ± 0.04	0.82	0.60	0.60

a: $K_{corr} = c_{oil, amorphPP}/c_{oil,EB}$; $K_{corr} = c_{oil, amorphPP}/c_{oil,EPDM}$

b: Obtained from Chapter 5

c: $K_{corr} = c_{oil, PP}/c_{oil,EB}$; $K_{corr} = c_{oil, PP}/c_{oil,EPDM}$

To test the validity of the present results we fitted also the dynamic moduli using the Veenstra model D [8]. This model has been used successfully to describe the frequency dependence of the dynamic moduli in the melt state. We applied this model to the ternary blend S0.8/1.4, where the concentrations of oil in the phases (31 wt% oil in the PP phase and 53 wt% in the SEBS phase) are close to two of the binary mixtures in the series made here: 30 wt% oil in PP and 50 wt% oil in SEBS. The values of the dynamic moduli in the latter binary mixtures are used to calculate the dynamic moduli of the blend using the Veenstra-D model. Fig. 4.12 shows the temperature dependent dynamic moduli of blend S0.8/1.4 and the results of the model. The moduli of the PP and the elastomer phases are also included. The calculated E' underestimates the values of the blend in the glassy state slightly, but the calculated E'' values describe the blend values well. It is noted that the curve calculated using the Veenstra model D gives a remarkable agreement with the measured peak of the PP/SEBS blend at the glass transition. The model predicts that the E'' peak of the blend is indeed a weighted summation of two overlapping glass transition processes and that the maximum in E'' does not correspond to the T_g of only one of the individual phases. The peak height of the blend is broad at the low temperature side because of the contribution of the glass transition of the elastomer phase. At the high temperature side, it is broad because of the contribution of the T_g of the PP phase.

4.4 Discussion

There is a small difference in polarity between the PP and the elastomers that could affect the solubility parameters and the oil distribution. This difference is small and a value of K close to 1 should be expected. The oil, however, is paraffinic in nature and could be considered as an EP oligomer with an ethylene content of 70 % [7]. Since both elastomers contain ethylene as co-monomer, it is likely that a small preference of the oil for the elastomer phase exists, resulting in a value of K slightly less than 1. The distribution of the oil in the compounds was found in the present work to favour the elastomer phase: the average value of K was 0.60 for the PP/SEBS blends and 0.63 for the TPV, which is lower than the ones expected theoretically. The distribution coefficient seems to be relatively insensitive to the blend composition.

Non-uniform oil distribution has been previously observed in comparable PP/SEBS systems by Ohlsson et al. [3], who found a value of $K \approx 0.35$ in the solid state. This is lower than what was found here, indicating that the oil preferred the elastomer phase much stronger in their case. However, Ohlsson et al. used different oil and PP and it is expected that the chemical structure and the molecular weight of the components will affect their affinity.

The values of K for the PP/SEBS blends found for the melt state in [8] were around 0.36 and 0.97. These values are comparable to the values found here for the solid state, but depend on the composition. The values for K in the melt were obtained from modelling and not by direct measurements. Furthermore, increasing the PP content for these blends has a larger effect in the melt state than in the solid state.

The values of K for the TPVs were also found in general to be less than 1. Jayaraman et al. [6] reported values in the range of 0.65-0.68 for the solid state, the same as in the present work. The concentration of oil in the PP phase was found to decrease with increasing PP content in the blend. These results are similar to what was reported in [6] for the TPVs in the melt state and do not agree fully with what is found here for the solid state, where K depends on the PP/elastomer ratio. The oil distribution was evaluated in [6] by comparing the domain areas in the transmission electron micrographs. In the present DRS experiments, the elastomer phase in the blends was not cured. The swelling behaviour of a polymer network differs from a freely entangled polymer. Entropic contributions to the swelling due to constraints imposed by the cross-links may account for the greater composition dependence of the distribution of oil between the two phases in the TPVs.

A final point concerns the proportion of the mass in the phases that is available for the oil to diffuse. As outlined above, K was calculated based on the total mass fractions of the components. There is, however, 45 to 49 % crystallinity in the PP phase in the blends (Table 4.1). The oil cannot be present in the crystalline regions [5]. Further, the paraffinic nature of the oil will prevent it from diluting the aromatic PS domains of the SEBS phase. The crystalline parts of PP and the PS domains of the SEBS can, thus, be considered as hard fillers and are not available for the oil.

Therefore, they should be excluded from the calculation of the oil distribution coefficient and only the amorphous PP and the EB part of the SEBS should be considered.

New values of the oil distribution coefficient were, therefore, calculated from the data by considering only these amounts of PP and elastomer that were actually available for the oil. These “corrected” values of K are listed in Table 4.3. For the PP/SEBS blends, the average value of K is now 0.51 in the melt and 0.76 in the solid state. The average corrected value of K for the TPVs is 0.89 in the solid state. These values for K are closer to an equal distribution than the uncorrected values, but the oil has still a preference for the elastomer phase.

4.5 Conclusions

Three experimental techniques for the determination of the distribution of oil in the PP/SEBS and PP/EPDM blends were tested and evaluated. Although DMA and DSC results revealed the plasticizing effects on the glass transitions in the PP and the elastomer phase, there was no unambiguous way to determine the phase-specific oil concentration from the depression of the T_g s due to the strong overlap in the glass transition regions. The third approach, dielectric relaxation spectroscopy (DRS) using dielectric probes, turned out to be successful in analysing and separating the glass transition processes related to the two individual, oil-containing, phases. The oil distribution coefficient is determined by modelling the imaginary part of the permittivity of the blend from those of binary PP-oil and elastomer oil mixtures. Both in the TPVs and in PP/SEBS blends the values for K are lower than one, indicating that the oil prefers the elastomer phase. The composition has minor effect on the values of K . Based on the oil distribution calculated from the DRS experiments the mechanical properties of the blends can be modelled successfully.

4.6 References

- [1] Holden G, Legge NR. eds., New York: Hanser, 1996.
- [2] Abdou-Sabet S, Patel RP, Rubber Chemistry and Technology 1991; 64:769.
- [3] Ohlsson B, Hassander H, Tornell B, Polymer Engineering and Science 1996; 36:501.
- [4] Vennemann N, Hundorf J, Kummerlowe C, Schulz P, Kautschuk Gummi Kunststoffe 2001; 54:362.
- [5] Ellul MD, Rubber Chemistry and Technology 1998; 71:244.
- [6] Jayaraman K, Kolli VG, Kang SY, Kumar S, Ellul MD, Journal of Applied Polymer Science 2004; 93:113.
- [7] Winters R, Lugtenburg J, Litvinov VM, van Duin M, de Groot HJM, Polymer 2001; 42:9745.
- [8] Chapter 5, this thesis
- [9] Havriliak S, Negami S, J Polym Sci Part C: Polym Symp 1966; 14.:99.
- [10] van den Berg O, Sengers WGF, Jager WF, Picken SJ, Wübbenhorst M, Macromolecules 2004; 37:2460.
- [11] Chapter 3, this thesis

- [12] Brandrup J, Immergut EH, Grulke EA. Polymer Handbook, London: Wiley, 1999.
- [13] Wübbenhorst M, van Turnhout J, J. Non-Cryst. Solids 2002; 305:40.
- [14] van Turnhout J, Wübbenhorst M, J. Non-Cryst. Solids 2002; 305:50.
- [15] Sengupta P., PhD thesis, Twente University, Enschede, 2004.
- [16] Veenstra H, Verkooijen PCJ, van Lent BJJ, van Dam J, Posthuma de Boer A, Nijhof A, Polymer 2000; 41:1817.
- [17] Takayanagi M, Mem Fac Eng Kyushu U 1963; 23:41.
- [18] Kolarik J, Polymer Composites 1997; 18:433.
- [19] Sierra CA, Galan C, Fatou JG, Parellada MD, Barrio JA, Polymer 1997; 38:4325.
- [20] Pizzoli M, Righetti MC, Vitali M, Ferrari P, Polymer 1998; 39:1445.
- [21] Kremer F. editor. Broadband Dielectric Spectroscopy, Berlin: Springer-Verlag, 2002.

Chapter 5

Linear viscoelastic properties of olefinic thermoplastic elastomer blends

Mechanical modelling of dynamic moduli in the melt state and solid state

Abstract

The linear viscoelastic properties of two types of olefinic thermoplastic elastomer blends were studied using dynamic rheology. The first type consists of a blend of PP, SEBS and oil and has a co-continuous morphology. The second type consists of vulcanised EPDM particles dispersed in a PP matrix. The dynamic rheological behaviour of the blends is a weighted contribution of the properties of the two individual phases. In the melt state, the storage modulus at low frequencies can be correlated to the properties and morphology of the elastomer phase. With increasing PP or oil content in the blend the value of the modulus at low frequencies are reduced. In the solid state, the modulus increases with increasing hard/soft ratio. The mechanical models of Coran and Veenstra are able to describe the dynamic moduli both in the solid state as in the melt state. An additional parameter was included to determine the oil concentration in the two phases. The behaviour of the model parameters depend on the morphology a phase. They are a measure of effective continuity of the phase with the highest modulus.

Based on:

W.G.F.Sengers, P. Sengupta and J.W.M. Noordermeer, S.J. Picken and A.D. Gotsis, Polymer 45 (26) 8881-8891 (2004)

W. Sengers, A. Gotsis, P. Sengupta and J. Noordermeer, ANTEC 2004: Proceedings of the 62nd Annual Technical Conference & Exhibition, 3265-3269 (2004)

5.1 Introduction

Blending an elastomer with a thermoplastic polymer can result in blends called thermoplastic elastomers (TPE). They have rubber-like properties but can be processed like thermoplastic polymers [1]. The combination of these properties makes these blends good alternatives for cross-linked rubbers. The polymer matrix in most cases is semi-crystalline and acts as a physical cross-linker for the elastomer phase. This phase melts at elevated temperatures and the blend becomes processable with thermoplastic processing equipment. The linear viscoelastic properties of two of the most common olefinic TPE blends are studied in this article.

The first type are blends of polystyrene-block-poly-(ethylene-co-butylene)-block-polystyrene triblock copolymers (SEBS) with PP [2–4]. At blending conditions the SEBS has still some elasticity due to the presence of polystyrene domains that act as physical cross-links. This reduces phase break-up and stabilises the formed morphology. Depending on the SEBS type used and the processing conditions, the PP/SEBS blends can show co-continuous structures over a broad range of elastomer content. The second type of TPE blends used is thermoplastic vulcanisates (TPV). They consist of a blend of dynamically vulcanised ethylene–propylene–diene-terpolymer (EPDM) with isotactic polypropylene (PP) [5,6]. They are prepared in a dynamic vulcanisation process, in which the elastomer phase is cured during continuous mixing of the blend [6]. The EPDM phase changes from a viscous liquid into an elastic solid during the dynamic curing and is forced to break up. The resulting morphology consists of finely dispersed EPDM particles in a matrix of PP. This morphology does not change upon (re)processing of the blend. TPV blends can be prepared in this preparation process with very high elastomer content that still is dispersed [5].

Commercial blends often contain additives like carbon black, calcium carbonate or processing oil in order to tailor the properties [1]. In the present work we limited the additives to processing oil, which is added to lower the hardness and to improve the processability. The oil, paraffinic in nature, is distributed over the PP and the elastomer phases and plasticizes both of them [2,4,7]. The rheological properties of the co-continuous PP/SEBS blends have not been studied extensively. Ohlsson et al. [8] studied the processing characteristics of these blends. At high shear rates the flow properties were dominated by the PP phase, even at very high elastomer content. The Cox–Merz relation could be applied reasonably well to these systems. Polymer blends that show co-continuous structures are not in an equilibrium state and the morphology can change during the experiments due to the applied stresses. However, the presence of some elasticity in the SEBS phase stabilises the structure during the dynamic measurement. Since the TPVs consist of densely packed elastomer particles in a thermoplastic matrix their rheological behaviour can be compared with that of highly filled polymers [9–13]. They have pronounced shear-thinning behaviour; even at low deformation rates the viscosity shows power-law behaviour and a zero shear viscosity cannot be reached. Also the Cox–Merz relation does not hold. The dynamic melt properties differ from those of common polymer blends: the storage modulus is always higher than the loss modulus and the expected terminal flow behaviour at low frequencies is not observed. The value of the storage modulus at these frequencies

increases with decreasing hardness [13] and increasing cross-link density [14].

The linear viscoelastic properties of polymer blends in the solid state can be described by mixing rules based on micromechanical models [15-18]. The models take in account the blend morphology and are based on a combination of series and parallel connection of the two phases. The equivalent box model of Kolařik (Fig 5.1) is the general case of this summation [15]. Other models can be derived from this by simplification [16], or addition of restriction in the change of the volume elements [17-18].

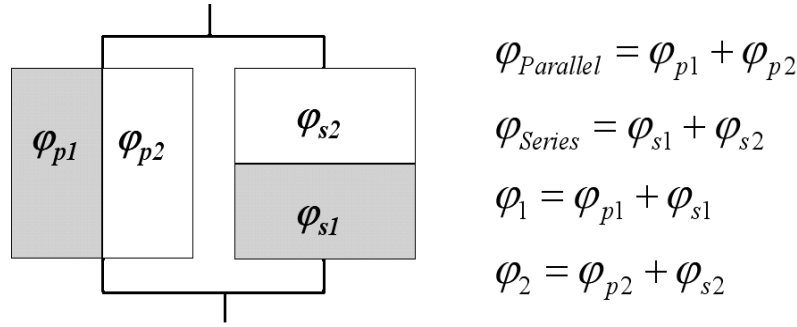


Figure 5.1: Schematic representation of the mechanical model of Kolařik.

In this study, we extend the application of these models to describe the behaviour of the dynamic moduli of PP/SEBS blends and TPVs in both the solid state as the melt state. If the morphology of these blends does not change then the models should hold for linear viscoelastic properties in general. The evaluation of the model parameters as a function of composition provides information about the present morphology.

5.2 Experimental

5.2.1 Materials

Two types of TPE blends were used in this chapter. To make a direct comparison, the two blend types contained the same PP matrix (PP homopolymer with a MFI of 0.3 dg/min at 230 8C and 2.16 kg, DSM Polypropylenes) and paraffinic oil (Sunpar 150, Sun Oil Company). The PP/SEBS blends contained SEBS (KRATON G 1651, KRATON Polymers) as elastomer and the TPVs contained EPDM (63 wt % C2, 4.5 wt% ENB, extended with 50 wt% of paraffinic oil, DSM Elastomers). The EPDM in the TPVs was dynamically vulcanised using 5 phr phenolic curing agent (SP 1045, Schenectady) in combination with 1 phr Stannous Chloride and Zinc Oxide (Merck). All materials contained antioxidants (0.5 wt% Irganox 1076 and 0.5 wt% Irgafos 168, Ciba Specialty Chemicals).

Table 5.1: Composition of OPTE blends.

Code	PP (wt%)	EPDM (wt%)	SEBS (wt%)	Oil (wt%)	Gel fraction in TPVs
S0.4/1.0	17		42	42	
S0.4/1.4	14		36	50	
S0.4/1.8	13		31	56	
S0.8/1.0	29		36	36	
S0.8/1.4	25		31	44	
S0.8/1.8	22		28	50	
S1.2/1.0	38		31	31	
S1.2/1.4	33		28	39	
S1.2/1.8	30		25	45	
E0.4/1.0	17	42		42	
E0.4/1.4	14	36		50	0.96
E0.4/1.8	13	31		56	
E0.8/1.0	29	36		36	0.95
E0.8/1.4	25	31		44	0.96
E0.8/1.8	22	28		50	0.97
E1.2/1.0	38	31		31	
E1.2/1.4	33	28		39	0.96
E1.2/1.8	30	25		45	

5.2.2 Sample preparation

The blends were prepared in an internal batch mixer (Brabender Plasticorder 390 cc with Banbury rotors) at 180 °C and 80 rpm. The blend composition has been varied in order to study the influence of the contents of PP and oil. Similar compositions were used for the PP/SEBS and TPV blends. They are shown in Table 5.1. The letter ‘S’ in the coding indicates the PP/SEBS blends and ‘E’ the TPV blends. The numbers x/y stand for the PP-elastomer and for the oil-elastomer ratio. Binary PP–oil mixtures were also made in an internal batch mixer at 180 °C (Table 5.2). The SEBS–oil mixtures were prepared by dry blending the SEBS pellets with oil. EPDM vulcanisates with different oil concentration were prepared by preblending the EPDM with curatives (same amount as in the TPVs) on a two-roll mill, followed by curing in compression moulding at 200 °C. An additional sample containing 60 wt% vulcanised EPDM was prepared by first extracting the oil from the EPDM–oil batch using n-hexane, precipitating the EPDM in acetone, and adding the appropriate amount of oil and curatives for the vulcanisation. All test samples were compression moulded into sheets of 2 mm at 200 °C.

5.2.3 Morphology

The morphology of the TPE blends was studied with transmission electron microscopy (TEM, Philips CM30). The samples were microtomed at -130 °C using a diamond knife followed by vapour staining with ruthenium tetroxide for 10 min. The co-continuity of the PP/SEBS blends was checked by selective extraction of the SEBS and oil with toluene for 24 h at room temperature [19]. The degree of continuity was given by the percentage of SEBS that could be recovered.

Table 5.2: Compositions, activation energies for time temperature superposition and concentration-frequency shift factors of binary mixtures at 190 °C.

	PP (wt%)	SEBS (wt%)	EPDM (wt%)	Oil (wt%)	E_{act} (kJ/mol)	a_C	b_C
PP100	1.00			0.00	-36.0	1.00	1.00
PO90	0.90			0.10	-43.8	0.55	0.90
PO80	0.80			0.20	-44.6	0.38	0.60
PO70	0.70			0.30	-46.6	0.26	0.52
PO60	0.60			0.40	-33.5	0.18	0.41
PO50	0.50			0.50	-32.8	0.15	0.31
SO70		0.70		0.30	-36.7	8.00	1.16
SO60		0.60		0.40	-65.1	5.50	1.15
SO50		0.50		0.50	-127.5	1.00	1.00
SO40		0.40		0.60	-165.5	0.15	0.70
SO30		0.30		0.70	-173.6	0.01	0.60
EO60			0.60	0.40	-85.7	1.2E+03	1.24
EO50			0.50	0.50	-154.5	1.0E+00	1.00
EO40			0.40	0.60	-116.6	6.0E-03	0.65
EO30			0.30	0.70	-95.7	2.0E-06	0.38

5.2.4 Rheological measurements

A Rheometric RMS 800 rheometer was used to determine the dynamic properties of the TPE blends and binary mixtures. The linear viscoelastic melt properties of the melt were measured in 25 mm parallel disk configuration with a fixed gap of 2 mm in a temperature range from 160 to 200 °C. The linear viscoelastic regime was established in the standard way by measuring the moduli at constant frequency (10 rad/s) and increasing strain magnitude. Because this regime extended for the present melts to 0.1 s.u., the value of 0.025 s.u. was used for the magnitude of strain oscillations in all measurements. Further, long time measurements (up to 3 h) confirmed the absence of major changes or degradation of the melt during the measurements. To see if the blends show wall slip, measurements were also performed using serrated disks. The spectra in the latter case were quantitatively the same as in the smooth disk configuration ruling out wall slip. It was found that time-temperature superposition could be applied to create mastercurves at 190 °C for all samples. The dynamic moduli in the solid state was determined in torsion setup with sample dimensions of 45 x 15 x 2 mm. Frequency sweeps were performed from $\omega = 0.01$ to 100 rad/s at 30 °C on the OTPE blends and on the binary mixtures.

5.2.5 Gel measurements on TPVs

In order to estimate the degree of cross-linking of the EPDM phase in the TPVs, the samples were subjected to a series of solvent extractions. About 1.5 g of TPV samples were extracted for 24 h through stainless steel pouches in boiling acetone to remove the oil and stabilizers, followed by extraction for 48 h with boiling xylene to remove the PP and the soluble rubber. The amount of gel content was calculated from the weight of the residue after xylene extraction.

5.3 Results and discussion

5.3.1 Morphology

In Figs. 5.2 and 5.3 TEM images are shown for the two TPE blends at different compositions. As can be seen the overall relation between morphology and composition is rather complex and the interpretation can only be done after studying multiple images and compare them with other methods, like low voltage SEM (LVSEM) and extraction experiments [20]. TEM images of PP/SEBS blends with different PP/elastomer ratios are shown in Fig 5.2. The SEBS appears as a dark grey phase, while the light grey corresponds to the PP phase. The magnification in the figure is suitable to observe the blend structure but it is too low to discern the 20 nm PS domains that are dispersed in the ethylene–butylene matrix of the SEBS block copolymer.

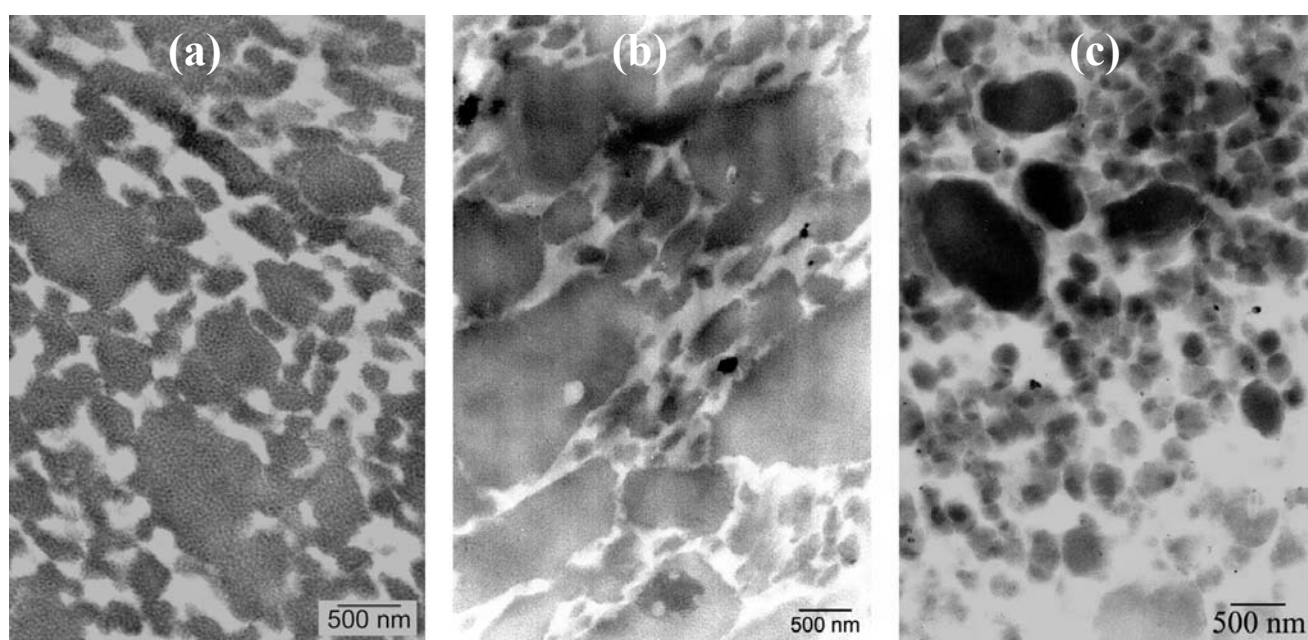


Figure 5.2: TEM images of PP/SEBS blends with different PP/Elastomer ratio (a) S0.4/1.4 (b) S0.8/1.4 (c) S1.2/1.4.

Both phases seem to be continuous, even though it is impossible to establish the continuity of the phases in the blends by microscopy alone. The co-continuous structure was confirmed in the present work by selective extraction of the SEBS and the oil [20]. In all these blends more than 95% of SEBS was recovered and the remaining PP phase was self-supporting. The average size (‘striation thickness’) of the SEBS phase was of 0.5–1 μm and decreased with increasing PP/elastomer or oil/elastomer ratio. This decrease resulted also in a reduction of the interconnectivity of the SEBS phase.

Fig. 5.3 shows TEM images of TPVs with different PP/ elastomer ratios. The EPDM phase is the darker areas. The morphology consists of elliptically shaped dispersed EPDM particles with lengths of 1–2 μm , even for the blend E0.4/1.4 (Fig 5.3a), despite its very high elastomer content. This morphology was confirmed using low-voltage SEM (LVSEM) [20]. Upon increasing the PP/elastomer ratio, the average

particle size decreases; increasing the oil/elastomer ratio results in a reduction of the inter-particle distance.

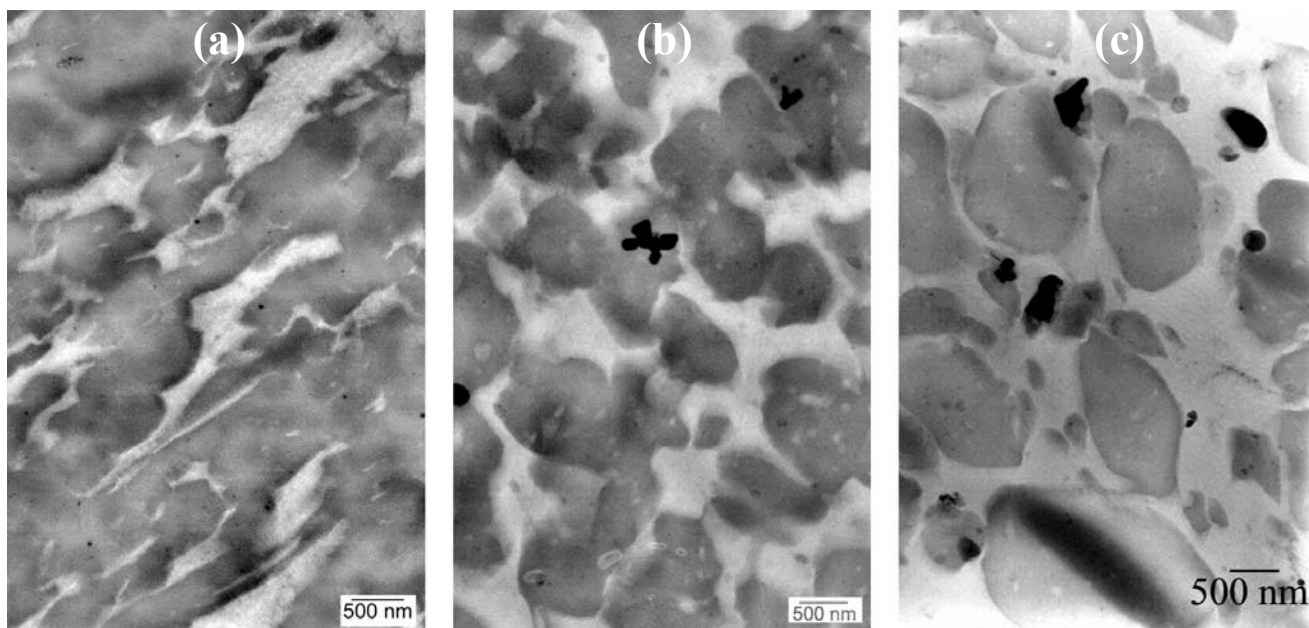


Figure 5.3: TEM images of TPVs with different PP/Elastomer ratio
(a) E0.4/1.4 (b) E0.8/1.4 (c) E1.2/1.4.

5.3.2 Melt state properties

The rheological properties of the blends appear to result from a weighted contribution of the properties of the individual phases. In these three-component systems, the paraffinic oil is present in both the PP and the elastomer phases and its concentration in the two separate phases is not known beforehand. To estimate the dynamic rheological properties of the two phases, binary mixtures are prepared at a range of compositions that correspond to the actual oil concentration in the two phases in the TPEs. In this way, the effect of the oil can be studied in the two phases of the blends separately.

5.3.2.1 Binary mixtures: concentration–time superposition

Fig. 5.4a shows the storage modulus of the binary PP–oil mixtures after time–temperature superposition at 190 °C. In general it is found that for all binary systems (including the elastomer–oil mixtures) the time–temperature superposition can be applied successfully. The Arrhenius activation energies for this shift are given in Table 5.2. The diluting effect of the oil is clearly visible in this figure: the storage modulus (G') decreases over the whole frequency range upon increasing the oil concentration. The curves of the dynamic moduli for the PP samples with different oil concentration can also be shifted around a reference value of the oil concentration to obtain a mastercurve. This concentration–time superposition has been suggested earlier by Nakajima [21] and is due to a simple diluting effect of the oil on the relaxation spectrum of the polymer.

The oil increases the available space between the chains, decreases the value of the moduli and shifts the relaxation times to lower values. This results in a shift of the curves in frequency and in modulus by factors a_c and b_c :

$$G_p = \frac{G_{T,c}}{b_c} \quad (5.1)$$

$$\omega_p = \omega_{T,c} a_T a_c \quad (5.2)$$

in which G_p is the modulus at frequency up of the reference sample. The vertical shift factor b_c is the correction for the diluting effect of the oil on the modulus. The factor a_c gives the effect of the oil on the relaxation times and a_T is the shift factor from the time–temperature superposition. $G_{T,c}$ represents the modulus at the frequency $\omega_{T,c}$ of a mixture at an oil concentration c and temperature T . In order to construct the mastercurve, the time temperature superposition should be performed first for all the samples. Then the curves at different oil concentration are shifted in frequency by a_c to obtain an overlap of the loss angle, $\tan d$, at the reference oil concentration. Finally, the reduction of the modulus values is compensated by dividing the modulus values by b_c . By using this method one can evaluate the moduli at any oil concentration. Fig 5.4b shows the mastercurves obtained as described above for the dynamic moduli of PP–oil mixtures at 190 °C, shifted to 0 wt% oil. The values for the two concentration–time shift factors are given in Table 5.2 and shown as an insert in Fig 5.4b. Both factors are expected to decrease with the oil content because the dilution by the oil increases the distances between entanglements or cross-links. The lines in these graphs are empirical fit lines used in the following section to interpolate the a_c and b_c data and evaluate the moduli of the phases in the ternary blends at any oil concentration.

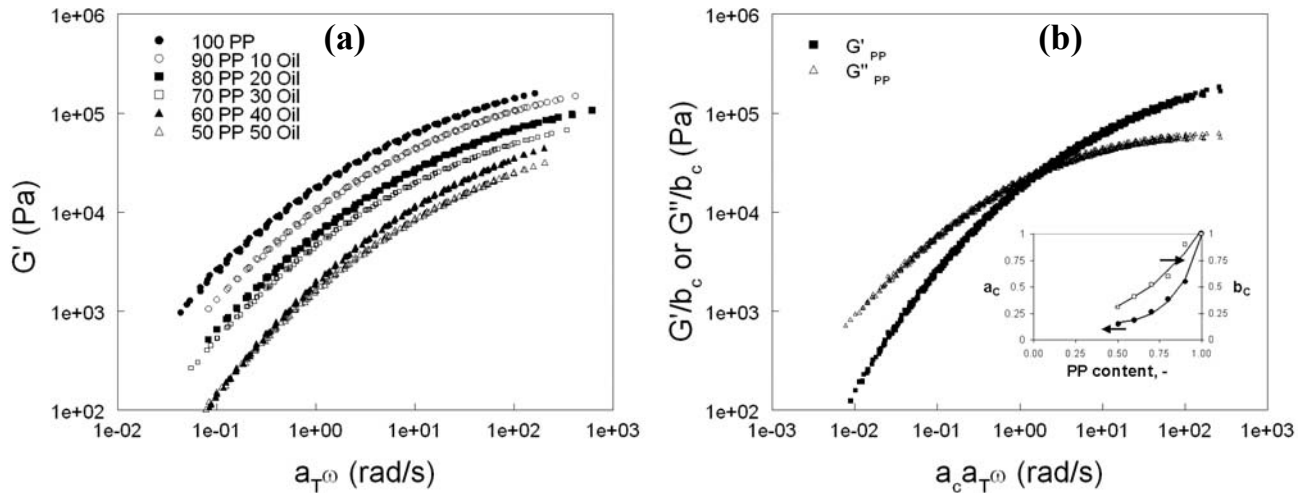


Figure 5.4: Dynamic modulus of PP-oil binary mixtures at 190 °C. (a) different oil content (b) after concentration-time superposition. In the insert of (b) are the values for the concentration-time shift factors and their empirical fits (lines).

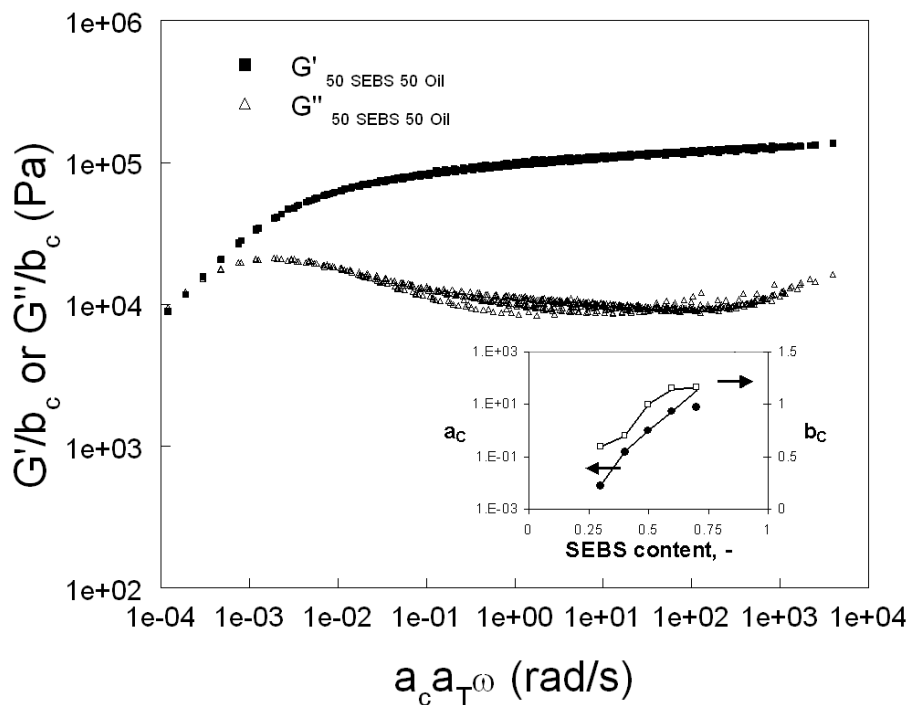


Figure 5.5: Dynamic modulus of SEBS-oil binary mixtures at 190 °C and 50 wt% oil after concentration-time superposition. In the insert are the values for the concentration-time shift factors and their empirical fits (lines).

The oil concentration–time superposition can also be applied to the elastomer–oil mixtures. The Arrhenius activation energies from the time–temperature superposition and the shift factors for the following oil-concentration superposition are given in Table 5.2. The mastercurves of SEBS–oil and EPDM–oil are given in Figs. 5.5 and 5.6, respectively. In both cases 50 wt% of elastomer is the chosen reference elastomer concentration, because measurements on pure SEBS and EPDM could not be performed. Their viscosity and elasticity are too high to process them.

Fig. 5.5 shows the mastercurve of SEBS containing 50 wt% oil. The mastercurve has a broad rubber plateau and shows a transition to flow at $\omega=10^{-3}$ rad/s. However, terminal flow is not observed down to the lowest frequency used, since molecular motions are still restricted due to the presence of physical cross-links. The time shift factor a_c decreases monotonically while the modulus shift factor b_c appears to show a transition. Apparently, the reduction in the modulus in the presence of physical cross-links of SEBS–oil differs from the reduction of the modulus by reduction of entanglements in PP–oil.

In Fig 5.6 the mastercurve of the 50 wt% EPDM vulcanisates is presented after the concentration–time superposition. For this elastomer the shift in G'' was not as successful as in G' . The effect of oil on the modulus is comparable to the SEBS–oil mixtures. Both a_c and b_c decrease monotonically with increasing oil content. In addition we note that the mastercurve covers a larger time span compared to the SEBS–oil system.

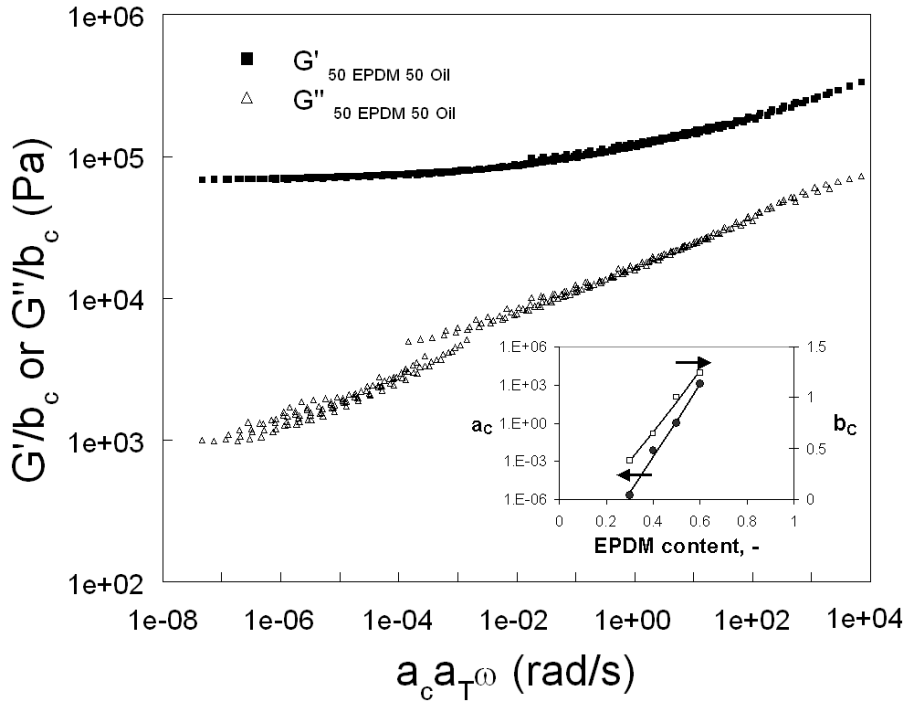


Figure 5.6: Dynamic moduli of EPDM-oil binary mixtures at 190 °C and 50 wt% oil after concentration-time superposition. In the insert are the values for the concentration-time shift factors and empirical fits (lines).

5.3.2.2 TPE blends

Time–temperature superposition of the dynamic moduli is in general observed for ‘simple’ viscoelastic fluids and is due to a shift of the relaxation time spectrum of the material with temperature. In an immiscible blend the phases retain their identity, including their distinct relaxation spectra. The time–temperature superposition, therefore, is not expected to apply in immiscible blends because the shift factors for the relaxation times for one component may be different from the shift factors of the other component. However, the superposition works reasonably for the elasticity modulus of most TPE blends in this work (e.g. Fig. 5.7). This is remarkable since there is also oil present in the two components, the distribution of which may change in the two phases with temperature. For the time–temperature superposition to work in these blends, one of the following conditions should apply:

1. The shift factors (or the Arrhenius activation energies) of the phases should be the same.

The phases themselves are mixtures of polymer and oil. From the activation energy of binary mixtures, listed in Table 5.2, it can be seen that the PP–oil values do not match the ones of elastomer–oil. This condition, therefore, cannot be the explanation for the successful superposition.

2. The superposition is possible when the PP phase is the continuous phase and the moduli of the elastomer have values that are independent of frequency.

The mastercurves of the modulus of these blends will result from the horizontal (frequency) shift of the contribution of the PP phase using the shift factor of PP and a constant contribution (independent of the value of the shift factor) of the elastomer phase. The dynamic moduli of the SEBS–oil mixtures are shown in Fig. 5.5. For 50 wt% SEBS or higher and for the EPDM

vulcanisates, the values of the G' indeed remain independent of frequency over a large frequency range. The morphology measurements have indicated that in the case of the PP/SEBS blends both phases are continuous. Indeed the values of the Arrhenius activation energies of PP/SEBS blends and TPVs shown in Tables 5.3 and 5.4 are very close to the ones of the binary PP–oil mixtures in Table 5.2. Apparently, this is the reason why the time–temperature superposition works for the present TPE blends.

Because time–temperature superposition works reasonably well, one can construct mastercurves for G' and G'' for the TPE blends. These curves are shown in Fig 5.7a for E0.8/1.4 and in Fig. 5.7b for S0.8/1.4, two blends that have similar composition. The storage moduli of the PP–oil and the elastomer–oil binary mixtures with the corresponding oil concentrations in the two phases are also shown to indicate the behaviour of the separate phases. The oil concentrations are obtained from the mechanical modelling part, as described later.

The only exceptions for achieving a successful time-temperature superposition are the blends with PP/Elastomer = 0.4, which is the lowest PP phase volume fractions. In these cases, the values of the activation energies exceed the ones of the PP–oil mixtures. Apparently, the fraction of PP is so low there that some of its continuity may have been lost (in the case of PP/SEBS blends) or the PP phase cannot dominate the behaviour of the blend.

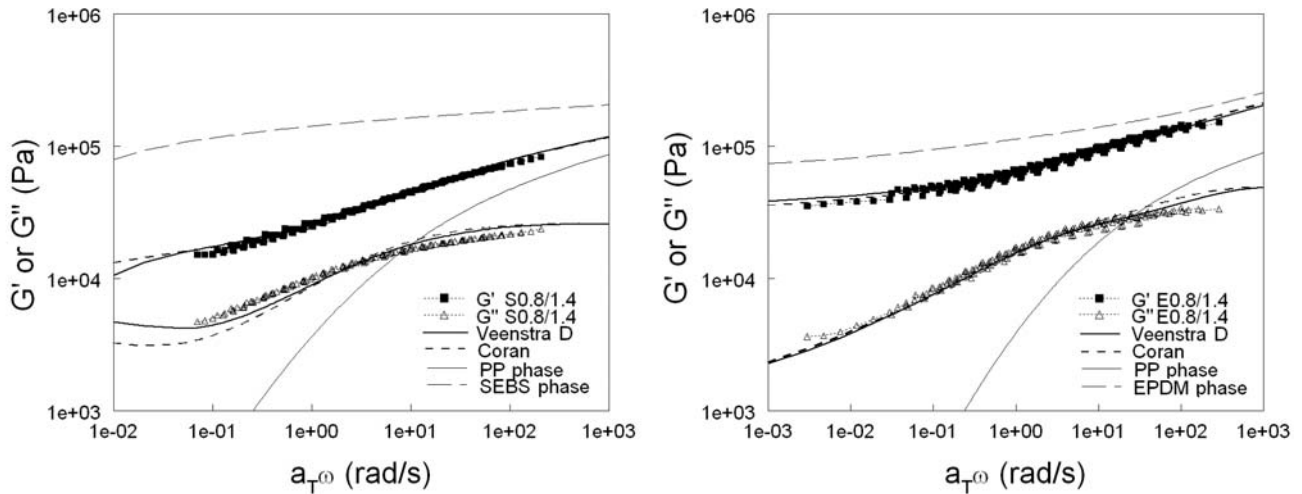


Figure 5.7: Dynamic moduli of two blends with the same composition at 190 °C. (a) PP/SEBS and (b) TPV. The thick lines represent the model results. The thin solid lines are the storage moduli of the two phases, with (a) $c_{oil,PP} = 0.27$; $c_{oil,EPDM} = 0.54$ and (b) $c_{oil,PP} = 0.31$; $c_{oil,SEBS} = 0.51$.

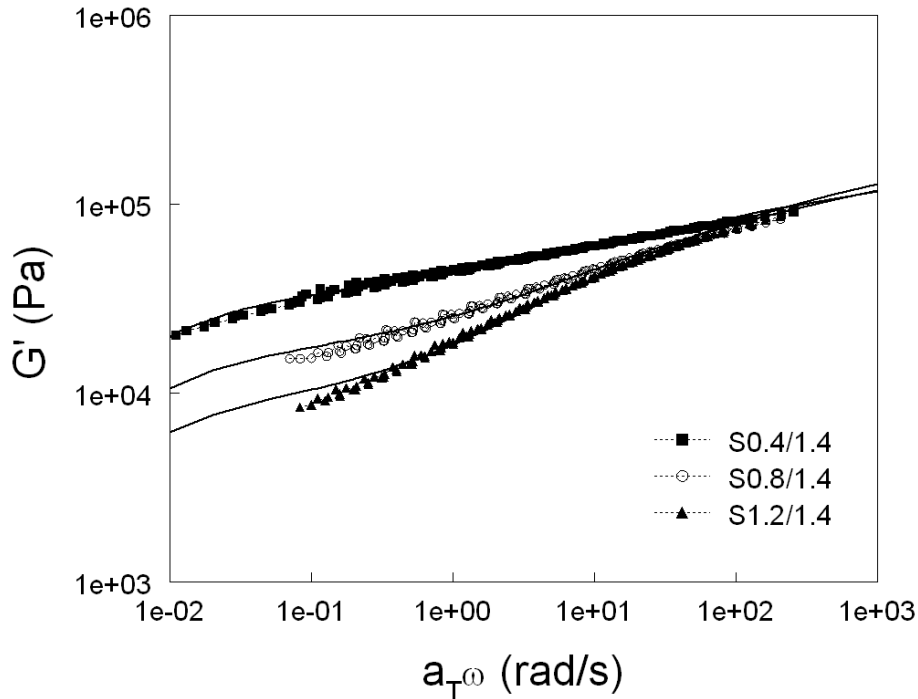


Figure 5.8: Storage modulus of PP/SEBS blends with different PP/elastomer ratio at 190°C. Lines represent results of Veenstra model D.

In general, the moduli of the TPVs are higher than the ones of their PP/SEBS analogues. This is due to the higher modulus of the EPDM phase. The storage modulus of the blends shows two characteristic regimes. At high frequency, the rubber plateau of the blend is present. It is the result from the additive contribution of the moduli of the PP and the elastomer phase. In the low frequency regime, the PP phase shows terminal flow behaviour and its contribution to the modulus of the blend becomes negligible. On the other hand, the modulus of the elastomer phase still persists as the frequency goes to zero. The values of G' of the blend at low frequencies are due to the elastomer phase only. Ordinary polymer blends do not show such behaviour at low frequencies. Disperse morphology blends show a shoulder in the curves of G' versus frequency corresponding to the relaxation of the interface [22]. The interfacial relaxation in blends with co-continuous morphology results in a curve of G' with a slope of less than two in the low frequency range [23-24]. In the case of the two TPE blends, the polarity difference between the PP and elastomer phase is low and the contribution of interface relaxation to the modulus is overshadowed by the large elasticity of the elastomer phase. To understand this behaviour of G' at low frequencies, we look at the effect of composition and morphology on G' .

Fig 5.8 shows the effect of the PP content on the storage modulus of PP/SEBS blends. The values of G' at low frequencies decrease with increasing PP content while the values at high frequencies remain unaffected. In these blends, both the PP and the elastomer phase are continuous and they contribute proportionally to the blend modulus. Increasing the PP content results in a gradual transition from SEBS-like to PP-like behaviour of the blends. The elastomer network becomes more disconnected and, thus, the values of G' at low frequencies decrease.

Table 5.3: Activation energies for the time-temperature superposition and fit parameters for Coran and Veenstra D models of the PP/SEBS blends.

	$E_{act} \text{ (kJ/mol)}$	Coran			Veenstra		
		$f_{30^\circ\text{C}}$	$f_{190^\circ\text{C}}$	$K_{190^\circ\text{C}}$	$a_{30^\circ\text{C}}$	$b_{190^\circ\text{C}}$	$K_{190^\circ\text{C}}$
S0.4/1.0	-61.8	0.14	0.48	0.77	0.20	0.63	0.54
S0.4/1.4	-70.3	0.06	0.36	1.11	0.13	0.54	0.91
S0.4/1.8	-45.0	0.04	0.34	1.05	0.09	0.53	1.08
S0.8/1.0	-37.2	0.22	0.21	0.68	0.28	0.39	0.36
S0.8/1.4	-32.5	0.16	0.21	0.93	0.22	0.39	0.63
S0.8/1.8	-31.8	0.11	0.22	0.90	0.18	0.40	0.72
S1.2/1.0	-38.7	0.33	0.13	0.48	0.37	0.30	0.20
S1.2/1.4	-34.1	0.28	0.14	0.78	0.35	0.29	0.48
S1.2/1.8	-41.0	0.18	0.15	0.83	0.29	0.30	0.58

Table 5.4: Activation energies for the time-temperature superposition and fit parameters for Coran and Veenstra D models of the TPVs.

	$E_{act} \text{ (kJ/mol)}$	Coran			Veenstra		
		$f_{30^\circ\text{C}}$	$f_{190^\circ\text{C}}$	$K_{190^\circ\text{C}}$	$a_{30^\circ\text{C}}$	$b_{190^\circ\text{C}}$	$K_{190^\circ\text{C}}$
E0.4/1.0	-32.8	0.07	0.70	0.04	0.12	0.80	0.10
E0.4/1.4	-59.6	0.06	1.00	0.98	0.12	0.86	1.14
E0.4/1.8	-81.8	0.06	0.96	1.45	0.13	0.80	1.67
E0.8/1.0	-39.6	0.24	0.53	0.04	0.30	0.62	0.04
E0.8/1.4	-48.8	0.13	0.78	0.50	0.20	0.72	0.60
E0.8/1.8	-38.0	0.19	0.84	0.90	0.23	0.64	0.94
E1.2/1.0	-35.0	0.42	0.66	0.04	0.41	0.41	0.03
E1.2/1.4	-33.9	0.30	0.64	0.37	0.39	0.50	0.34
E1.2/1.8	-27.0	0.26	0.75	0.74	0.32	0.43	0.60

The same trend can be seen in Fig 5.9, where the PP content in TPVs is varied. The G' curves overlap at high frequencies and the values of G' at low frequencies decrease with increasing PP content. Compared to the PP/SEBS blends, the reduction of these modulus values is larger. This is due to the dispersed morphology in the blends, shown in Fig. 5.3. However, the volume fractions of the elastomer phase are so high that the dispersed elastomer particles can touch each other without being truly connected to each other. This 'quasi-continuous' network-like structure remains intact in the linear viscoelastic regime and acts as a co-continuous structure, but it can be broken down at processing conditions [13]. As a result, G' at low frequencies reaches a constant value. Increasing the PP phase volume fraction results in a less agglomerated, and weaker, structure and the values of G' in the low frequency regime decrease. The dynamic moduli of PP/SEBS blends with different oil/elastomer ratio are shown in Fig. 5.10. Similar curves are observed for TPV blends. Increasing the oil/elastomer ratio results in a reduction of both the storage and the loss modulus over the whole frequency range. The extra oil is distributed over the PP and the elastomer phase; it reduces the modulus and shifts the relaxation times of the two phases to lower values.

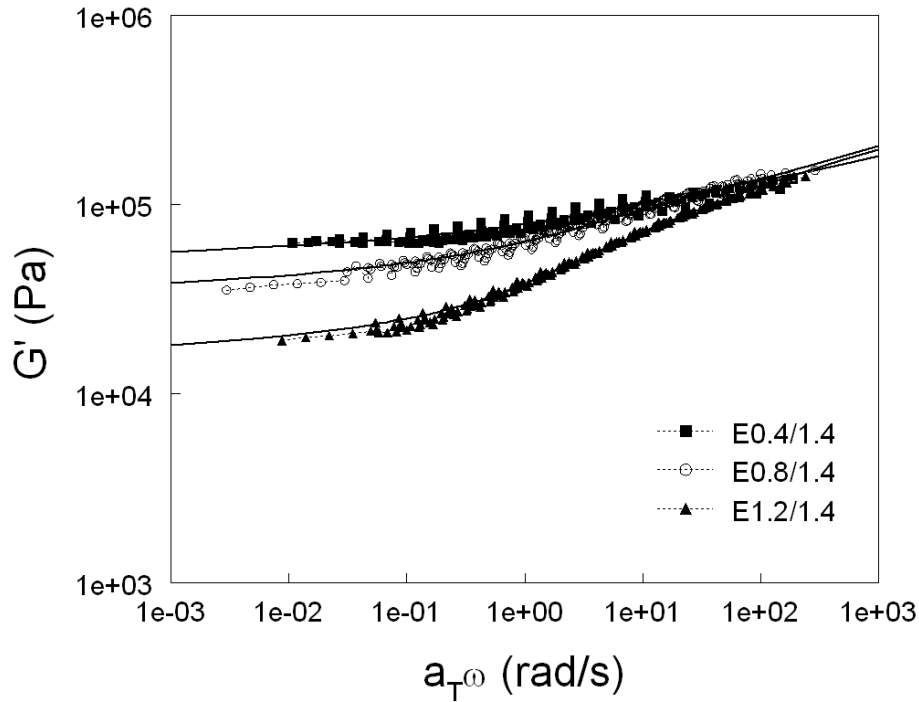


Figure 5.9: Storage modulus of TPV blends with different PP/elastomer ratio at 190°C. Lines represent results of Veenstra model D.

5.3.2.3 Summary

The linear viscoelastic behaviour of the TPE blends in the melt can be explained by changes in the composition. In both blend types, the increase of PP phase volume results in a reduction of the storage modulus at low frequencies and increasing the oil content in the blend results in a reduction of both storage and loss modulus. The values of the storage modulus at low frequencies depend on the amount and on the structure of the elastomer phase. This description, however, is only qualitative and does not include the effects of morphology. The change in composition not only affects the morphology but it can also affect the oil concentration in the PP and elastomer phase. To have a quantitative description of the dynamic mechanical behaviour, we use models based on mixing rules that reflect the morphology present in the blends. The properties of both the PP and the elastomer phase are estimated by interpolation of the dynamic moduli of the binary mixtures.

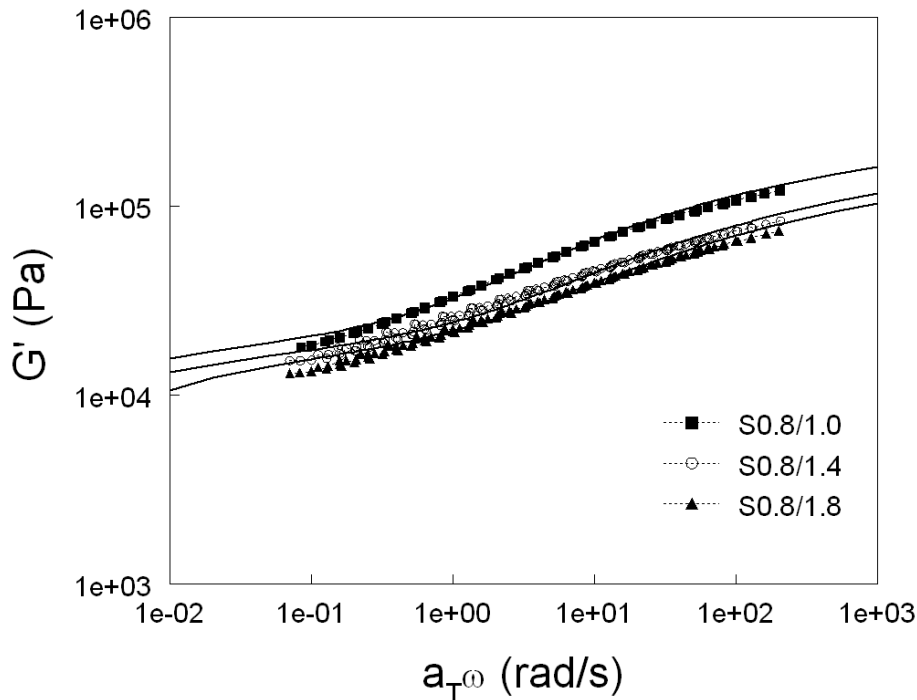


Figure 5.10: Storage modulus of PP/SEBS blends with different Oil/elastomer ratio at 190°C. Lines represent results of Coran model.

5.3.3 Solid-state properties

The dynamic moduli in the solid-state can be evaluated in a similar way. In both TPVs and PP/SEBS blends, this phase is continuous and is semi-crystalline, resulting in a large increase of the modulus. Therefore, this phase has the largest influence on the linear viscoelastic properties.

5.3.3.1 Binary mixtures

In the solid state, the dynamic moduli increase slightly with increasing frequency. Fig 5.11 shows the effect of oil on the dynamic moduli of PP-oil (Fig 5.11a) and elastomer-oil binary mixtures (Fig 5.11b) at $\omega = 1$ rad/s. For all binary mixtures, both the storage and the loss moduli decrease gradually with increasing oil content due to the diluting effect of the oil. Hence, the storage modulus of SEBS-oil mixtures is higher than that of the EPDM-oil vulcanisates at similar oil content (Fig 5.11b), but is still 2-3 decades lower than the PP-oil mixtures (Fig 5.11a). The decrease of the moduli can be described by an exponential decay function (PP-oil and EPDM-oil) or by power-law function (SEBS-oil). These functions will be used in section 5.3.4 to estimate the solid-state properties of the ternary blends.

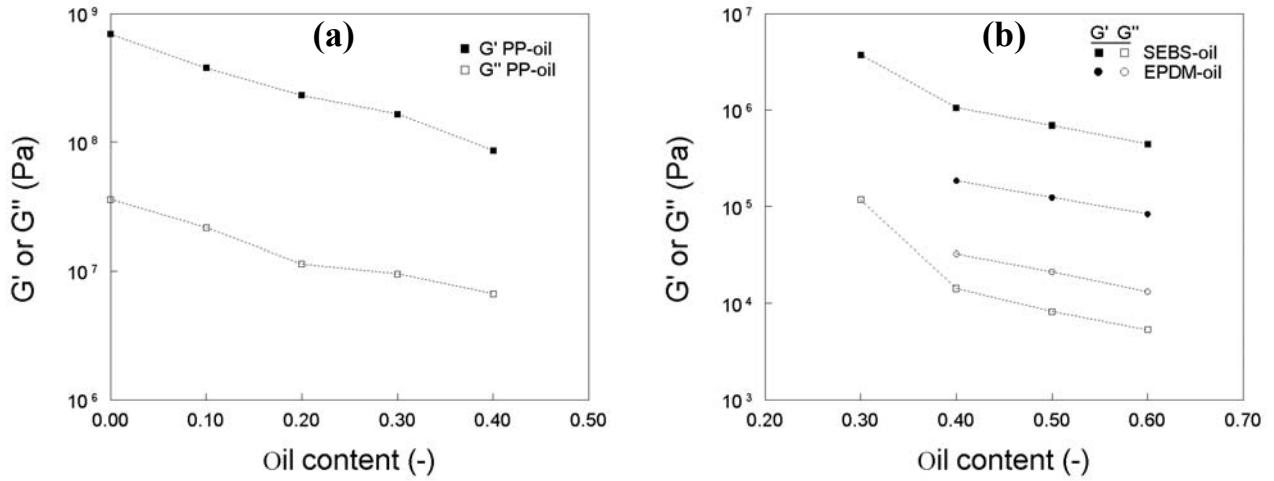


Figure 5.11: Dynamic moduli of binary mixtures as a function of oil content at 30 °C and 1 Hz. (a) PP-oil and (b) elastomer-oil

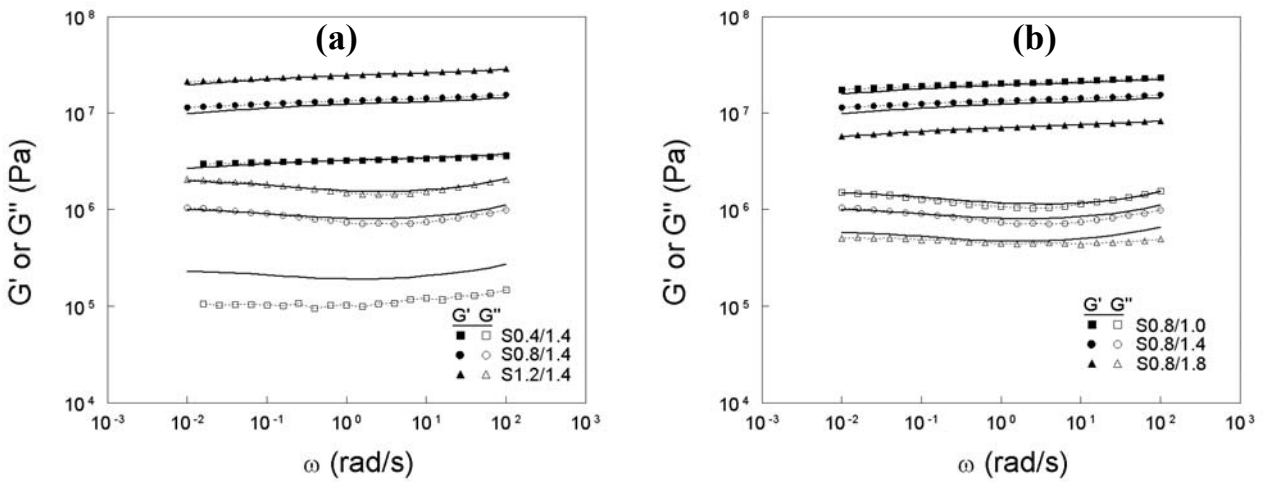


Figure 5.12: Dynamic moduli of PP/SEBS blends as a function of frequency at 30 °C . (a) different PP content, Oil/Elastomer = 1.4 and (b) different elastomer content, PP/Elastomer = 0.8. Lines represents fits for Coran-Patel model.

5.3.3.2 OTPE blends

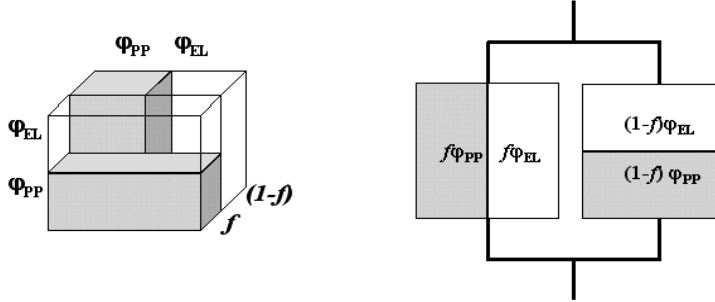
Fig 5.12 shows the dynamic moduli of the OTPE blends at 30 °C. Despite the difference in morphology, the TPVs and PP/SEBS blends show comparable values of the dynamic moduli at similar composition. For simplicity, only the data of PP/SEBS blends is shown. Increasing the PP content in the blend results in a large increase of both G' and G'' (Fig 5.12a). The PP phase has the highest modulus and the blend moduli increase with the increase of the volume fraction of this phase. The oil has a small diluting effect on the blend moduli (Fig 5.12b).

5.3.3.3 Summary

The dynamic moduli of the OTPE increase with increasing the hard/soft ratio i.e., with increasing PP content or decreasing oil content. The linear viscoelastic properties are dominated by the properties of the (continuous) PP phase. Because the moduli of the PP phase are 2-3 decades higher than those of both elastomer types the dynamic moduli of the two OTPE blends have comparable values. The above results

are only described qualitatively and do not include the effect of the morphology. In the next section the properties of the blends will be quantified by modelling of the properties based on the properties of the two phases.

Coran-Patel



Veenstra model D

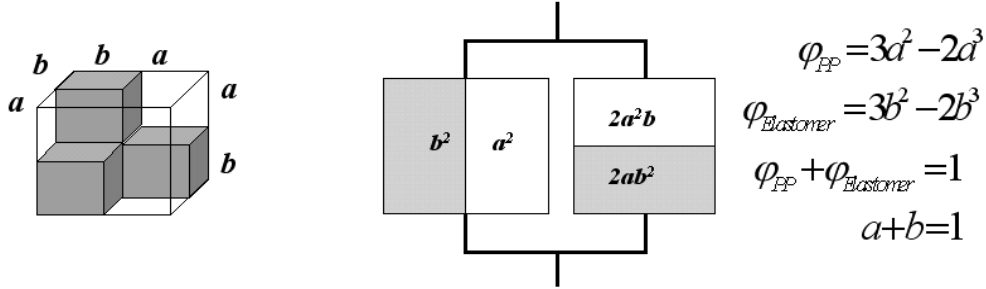


Figure 5.12: Schematic representation of the mechanical models of Coran-Patel and Veenstra model D.

5.3.4 Micromechanical model description

The relation between the morphology and the linear viscoelastic properties of these materials is studied by fitting the behaviour of the dynamic moduli with appropriate models. Rheological models based on the free energy of the deformation of the interface (e.g. Palierne [25] and Lee-Park [26]) could not be used in the melt state. The Palierne model is not applicable for blends with dispersed phase content larger than 15 wt% [27] and the Lee-Park model could not describe the characteristic behaviour of these materials at low frequencies. The main reasons for this failure are the large viscosity and elasticity differences and the low interfacial tension between the two phases. Due to the low interfacial tension, the elasticity caused by the deformation of the interface is overshadowed by the elasticity of the elastomer phase. On the other hand, mechanical models that reflect the morphology, together with the well-known series and parallel rule of mixture approaches, are found to be rather suitable to describe the observed rheological behaviour. These models were already applied successfully to describe the linear viscoelastic properties in the solid state [18,19]. Changes in morphology are not expected when the blend melts, because coalescence is restricted due to the presence of (physical) cross-links. The same models can then be used for both solid-state and melt-state properties. Both the storage and the loss components of the complex modulus are taken into account to allow a more rigorous test of the models. In the present study two different models are used that are based on partially parallel connection of the two phases. They are shown schematically in Fig. 12.

5.3.4.1 Micromechanical models

The model proposed by Coran and Patel [18] is a weighted addition of a series and a parallel model (Fig 5.12).

$$G_{coran}^* = f \cdot G_{par}^* + (1-f) \cdot G_{ser}^* \quad (5.3)$$

$$G_{ser}^* = \left[\frac{\varphi_1}{G_1^*} + \frac{\varphi_2}{G_2^*} \right]^{-1} \quad (5.4)$$

$$G_{par}^* = \varphi_1 G_1^* + \varphi_2 G_2^*$$

where 1 represents the PP phase, and 2 the elastomer phase. G_i^* and φ_i are the complex modulus and the volume fraction of phase i. The factor f is the degree of applicability of the parallel model and gives a measure for the continuity of the phase with the highest modulus.

The models of Veenstra [19] were originally developed for the Young's modulus of blends, but they are extended here via complex continuation to describe the complex shear modulus $G^* = G' + iG''$ of the TPE blends. The Veenstra D model has been used for co-continuous morphologies. It consists of an arrangement of the two phases within a unit cube so that the dual phase interconnectivity is incorporated in three dimensions as shown in Fig. 5.12. The expression resulting from this model for G^* is the following:

$$G_{Veenstra, D}^* = \frac{a^2 b G_1^{*2} + (a^3 + 2ab + b^3) G_1^* G_2^* + ab^2 G_2^{*2}}{b G_1^* + a G_2^*} \quad (5.5)$$

The factor a is related to the volume fraction of the first phase by:

$$\varphi_1 = 3a^2 - 2a^3 \quad (5.6)$$

The factor b is: $b=1-a$. Thus, b is related to the other phase, φ_2 , by an equivalent relation:

$$\varphi_2 = 3b^2 - 2b^3 \quad (5.7)$$

These two parameters are in essence weighted volume fractions, which emphasise the relative importance of the continuous phases: if a phase is continuous at a volume fraction φ_i of less than 0.5, then its effective contribution to the mechanical properties is larger than what its real volume fraction would suggest. On the other hand, if $\varphi_i > 0.5$ the reverse holds as $a+b=1$. This model can also be used when the co-continuity in the morphology is not perfect. However, in this case Eqs. 5.6 and 5.7 will not hold exactly. The weighted volume fraction a is then an adjustable parameter and its (negative) deviation from Eq. 5.6 will give an indication for the degree of disruption of continuity of this phase. In the following, a and φ_1 correspond to the PP phase and b and φ_2 correspond to the elastomer phase. The models give the moduli of the blends as a function of their composition, the morphology and the moduli of the individual

phases. The phases, however, also contain significant amounts of oil. If the oil concentration in each phase (c_i) is known, their moduli, $G^*_1(\omega, c_1)$ and $G^*_2(\omega, c_2)$, can be evaluated from the measurements of the binary mixtures (section 5.3.2.1) and the shift factors a_c and b_c in Table 5.2. However, while the total amount of oil in the blend is known, its distribution within the phases is not known at every temperature. This distribution is usually described by the distribution coefficient K , which is the ratio of the oil concentration in the PP phase (c_1) over its concentration in the elastomer phase (c_2) [2].

Attempts to measure the value of K directly by dielectric relaxation measurements [28] were successful at lower temperatures. These values were used for the solid-state properties. In the melt-state, the crystalline part of the PP phase has molten and becomes accessible for oil. The oil distribution, therefore, can differ from the solid-state values and is not known beforehand. To solve this, the distribution coefficient K has been incorporated in the mixing models for the melt measurements. Fortunately, this can be done without compromising the predictive ability of the models. In the present work this is achieved as described below. The two models described above are based on combinations of simple parallel and series models. Both models, however, give the same results when the properties of the two phases are equal. In the case of the melt-state properties of the present blends, this happens at high frequencies, where the plateaus of the dynamic moduli of the elastomer phases have close values to the ones of the PP phases over a broad range of oil contents. This indicates that the results of the models at these frequencies are independent of the parameters f and a . The oil distribution coefficient can be evaluated at this frequency range, independent from the other model parameters. The parameters f and a (or b) can then be evaluated at low frequencies, where the modulus is determined by the elastomer phase only. An iteration process is finally used to find the optimal values for K and the other parameters of the models to fit the whole curves of both the storage and the loss moduli.

The two models describe the dynamic moduli of the OPTE blends very well, both in the solid state and in the melt state (see lines in Figs 5.7-5.10 and Fig 5.12). The only exception is the loss modulus in the solid state of the blends with the lowest PP content (PP/elastomer=0.4) (Fig 5.10a). These blends behave more elastic than expected: the loss modulus is lower than the calculated values obtained from the two models. This could be another clue for the possibility that the PP phase, although it is continuous in both blend types, does not behave as a truly continuous phase. This was already mentioned for the time-temperature superposition (section 5.3.2.1). The results of the modelling are shown in the Tables 5.3 and 5.4. Since the two models are combinations of parallel and series connection of the two phases, the continuity of each phase can be related to the fraction of parallel behaviour. The continuity of this component, therefore, will dominate the properties of the blend. Further, the values of the parameters of both models will reflect the status of the continuity of this phase.

5.3.4.2 Evaluation of the Coran-Patel model

In the model of Coran and Patel, the parameter f is related to the fraction of parallel connection of the two phases and, therefore, it should correspond to the phase with the highest modulus. In the solid state, that is the PP phase and in the melt state that

should be the elastomer phase. The continuity of each phase can be evaluated by the behaviour of the model parameter.

In the solid state, the PP phase is continuous in both the TPVs and the PP/SEBS blends. As a result, the behaviour of f is comparable for the two blend types. Obviously, f increases with increasing PP content due to the higher volume fraction of the PP phase. In the PP/SEBS blends, f decreases with increasing oil content. No trend was found for the effect of oil content on the TPVs

In the melt state, the elastomer phase is the phase with the highest modulus and f is now related to this phase. f decreases with increasing PP content due to the decreasing volume fraction of the elastomer phase. No trends are found for changing oil content. The oil affects the domain sizes but this apparently does not affect the interconnectivity of the phases. The presence of parallel behaviour in the TPV in the melt state is remarkable since the elastomer phase is dispersed. In addition, the values of f are higher than the PP/SEBS analogues, in which the elastomer phase is continuous. This can be explained by the high volume fraction of elastomer particles in the TPVs. The particles can touch each other and form an agglomerated structure, entrapping some parts of the PP phase. Therefore, the elastomer phase behaves as if it is continuous and the two models can be applied successfully. For instance, the moduli of the blend with the lowest PP content (PP/elastomer = 0.4) follows the parallel model: i.e. $f \approx 1$. Even though the PP phase is the continuous phase, it does not dominate the properties of the blend. This behaviour was also observed in the time-temperature superposition of this blend. With increasing amount of matrix PP phase, the number of elastomer particles per volume decreases. This results in a less dense elastomeric network structure and, as a result, f decreases.

A possible source for a small error in the calculations for the melt state properties should be mentioned here. This is related to the value of the cross-link density used in the model for the EPDM in the TPVs. The cross-link density of the elastomer phase was assumed to be the same in all binary and ternary compositions. However, as the amount of oil in the blend was increased, it was found that the gel fraction increased from 0.95 to 0.97 as shown in Table 1. The moduli of the elastomer phase in the compounds, therefore, may differ somewhat from the ones in the binary EPDM-oil vulcanisates reflecting the differences in their cross-link densities. We expect the relation between cross-link density and the modulus to be linear in that level of gel fractions. The error in the modulus of the EPDM phase, then, should also be in the order of 5%. This may affect the calculated values of the parameters.

5.3.4.3 Evaluation of Veenstra model D

The parameters a (related to PP phase) and b (elastomer phase) can be calculated from the volume fractions of each phase by Eqs 5.6 and 5.7. It was found that the Veenstra model could describe the moduli best when these parameters are adjustable, as described in section 5.3.3.

In the solid state, the parameter a behaves in a similar way as f (Tables 5.3 and 5.4). In both blends, the PP phase is continuous and has the higher modulus. The increase of the PP content in the OTPEs results thus in an increase in the value of a due to the

higher volume fraction. For the PP/SEBS blends, a decreases with increasing oil content. No trend was found for the change of oil content in the TPVs. In the melt state, the elastomer phase has the highest modulus and the parameter b , just as f , decreases with increasing PP content.

The effect of morphology on the model results can be explained the best on the basis of the effective volume fraction of the elastomer phase, φ_{eff} . This volume fraction is calculated by Eq. 5.7 using the values of b from the modelling results. If φ_{eff} is equal to the real volume fraction of the elastomer phase, φ_{El} , then the morphology can be considered as assumed by the model. As shown in Figs 5.2 and 5.3, the blends have some inhomogeneities in the domain sizes of the two phases. Further there are some parts that may not contribute in a continuous way to the modulus, even when they are continuous. These parts can be considered as trapped. This leads to extra losses and the observed modulus differs from the values expected from the model. The *mechanical* volume fraction, φ_{eff} , can differ from the real volume fraction, φ_{El} .

The effective volume fraction of the elastomer phase is chosen because this phase has different morphologies in the two blend types. Fig 5.14 shows φ_{eff} as a function of the actual volume fraction of the elastomer phase, φ_{El} , for the PP/SEBS blends (Fig 5.14a) and TPVs (Fig 5.14b). The line represents the case of $\varphi_{eff} = \varphi_{El}$, where the net co-continuity of the blend can be considered as perfect.

In both blend types, the values of φ_{eff} are higher than φ_{El} in the solid state. Because φ_{eff} is related to the elastomer phase, this means that the effective volume fraction of the PP phase is lower than expected. In both blend types the PP phase has the highest modulus and is continuous. The mechanical properties are dominated by this phase but are lower than what is assumed by the model: a part of the PP phase behaves as if it is not connected in a continuous way. The deviation of φ_{eff} from the real volume fraction can be considered as a measure of this imperfection. Increasing the volume fraction of the elastomer phase results in a larger deviation: the PP phase loses more of its continuous character due to the increasing amount of inhomogeneties. At the lowest PP content, the contribution of this phase becomes very small and the blend behaves as a pure elastomer. Comparable values for φ_{eff} were found using the Young's modulus, obtained from tensile tests.

The TPVs and PP/SEBS blends have comparable values of φ_{eff} in the solid state. This means that, despite the difference in morphology, the PP behaves in a similar way in both blends. This can be a reason for the striking similarities between the two OPTE blends.

In the melt state, the behaviour of φ_{eff} differs for the two blend types. For PP/SEBS blends, the φ_{eff} is always lower than φ_{El} . At this temperature, the elastomer phase has the highest (average) modulus and the properties are dominated by this phase. Because this phase is continuous, the behaviour of φ_{eff} is similar to that of the PP in the solid state: Mechanically, the effective volume fraction of the SEBS phase is lower than its real volume fraction. The difference becomes smaller with increasing φ_{El} .

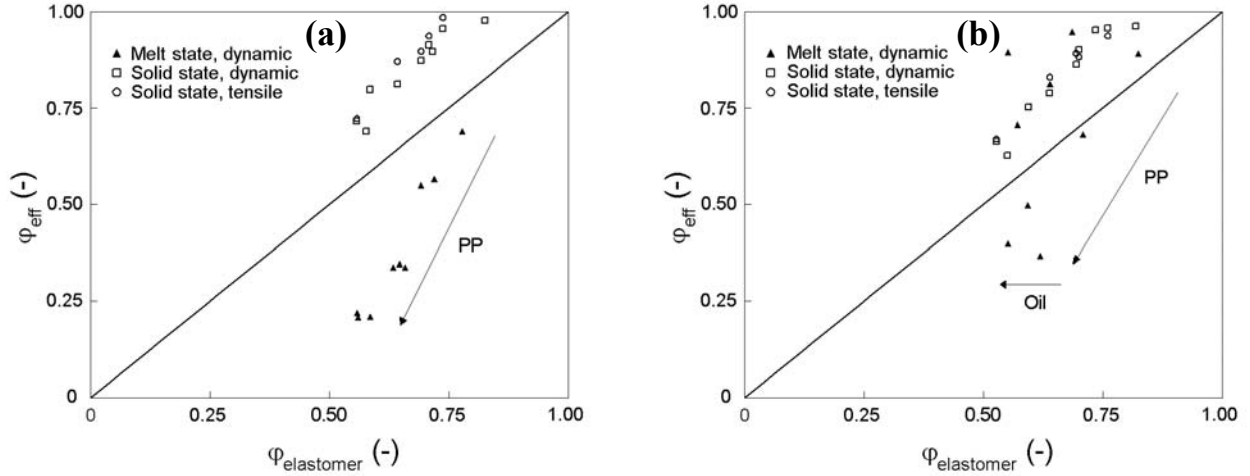


Figure 5.14: Effective volume fraction obtained from Eq. 7 versus the actual volume fraction of the elastomer phase (a) PP/SEBS blends and (b) TPVs.

In the TPVs, the elastomer phase is dispersed and the behaviour of ϕ_{eff} reflects this difference in morphology. Remarkably, the values of ϕ_{eff} are higher than the PP/SEBS ones and depend strongly on composition. The elastomer particles form an agglomerated network-like structure. At the lowest PP content, this network structure has values of ϕ_{eff} that are close to one. The elastomeric network is so dense that it dominates the properties. The PP phase can be considered as trapped between the elastomer particles, as explained in the solid state behaviour of ϕ_{eff} . Increasing the PP content results in a reduction of the number of elastomer particles per volume and the network becomes disrupted. As a result, the value of ϕ_{eff} decreases drastically and the elastomer network stops dominating the mechanical behaviour.

5.3.4.4 Distribution of oil

The oil distribution in the two phases of the compounds is given by the second model parameter, K . In general, the distribution of the oil in the compounds was found in the present work to favour the elastomer phase: $K < 1$ (Tables 5.3 and 5.4). The model indicates that K also depends on the blend composition. For both systems K decreases with increasing PP content in the melt. When the oil content is increased, the value of K increases in the TPVs but it remains unaffected in the PP/SEBS blends. These oil distributions, however, are the results of fitting a model to the data. Direct measurements are necessary in order to prove that the calculated values of K are accurate.

Non-uniform oil distribution has been previously observed in comparable PP/SEBS systems by Ohlsson et al. [2], who found a value of $K=0.35$ in the solid state. Jayaraman et al. [29] found that the concentration of oil in the PP phase of TPVs decreases with increasing PP content. Measurements of K using dielectric relaxation spectroscopy on the same compounds as in the present work also indicated that its values are $K < 1$ at room temperature [28]. There is a small difference in polarity between the PP and the elastomers that could affect the solubility parameters. This difference, however, is small and an almost uniform equilibrium oil distribution ($K=1$) should be expected, based on classical thermodynamic arguments.

Even though the low values of K predicted by the model are not yet clearly understood, the changes in K shown in Tables 5.3 and 5.4 when the composition is varied may be explained by considering the entropy of the systems. Conformational constraints exist for the chains in the elastomer phase due to the cross-links. These constraints are absent in the linear PP. With increasing oil content in the TPVs, one expects that these constraints will prevent the extra oil to enrich the elastomer phase, forcing it to concentrate in the PP phase, thus, increasing the value of K , as it can be seen in Table 5.4. In the case of PP/SEBS this effect is absent as there are only physical cross-links. This entropic effect, therefore, could be responsible for the skewed oil distribution.

5.4 Conclusions

The linear viscoelastic melt properties of TPVs and PP/SEBS blends can be described as a weighted contribution of the properties of the two individual phases. Both the storage and loss moduli can be described by micromechanical mixing models based on combinations of parallel and series contribution of the PP and elastomer phases. The model parameters are related to the composition and morphology of the blends.

The model of Veenstra describes the effect of morphology on the model parameters. In the PP/SEBS blends both phases are continuous but their morphology differs from the one represented by the Veenstra model. The effective volume fractions of the phase with the highest modulus are lower than those calculated for the fully co-continuous morphology and the difference becomes larger with decreasing the content of that phase. Some parts can be considered as trapped in the other phase and cannot contribute in a continuous way.

In TPVs the elastomer phase is dispersed, but its volume fraction is high enough so that the separate particles form a network-like structure. The effective volume fractions reduce strongly with increasing PP content in the blend due to the breakdown of this network structure.

5.5 References

- [1] Coran AY, Patel RP. In: Holden G., Thermoplastic elastomers. New York, 1996: Hanser; p. 153.
- [2] Ohlsson B, Hassander H, Tornell B. Polym Eng Sci 1996;36:501.
- [3] Veenstra H, van Lent BJJ, van Dam J, Posthuma de Boer AP, Polymer 1999;40:6661.
- [4] Vennemann N, Hundorf J, Kummerlowe C, Schulz P. Kautschuk Gummi Kunststoffe 2001;54:362.
- [5] Coran AY, Patel R. Rubber Chem Technol 1980;53:141.
- [6] Abdou-Sabet S, Patel RP. Rubber Chem Technol 1991;64:769.
- [7] Ellul MD. Rubber Chem Technol 1998;71:244.
- [8] Ohlsson B, Tornell B. Polymer Eng Sci 1998;38:108.
- [9] Goettler LA, Richwine FJ. Rubber Chem Technol 1981;55:1448.
- [10] Han PK, White JL. Rubber Chem Technol 1995;68:729.
- [11] Araki T, White JL. Polym Eng Sci 1998;38:590.

- [12] Marinovic T, Susteric Z, Dimitrievski I, Veksli Z. *Kautsch. Gummi Kunstst.* 1998;51:189.
- [13] Steeman P, Zoetelief W. *SPE Tech Papers* 2000;46:3297.
- [14] Ellul MD, Tsou AH, Hu WG. *Polymer* 2004;45:3351.
- [15] Kolařík J, *Pol Eng Sci*, 1996;36, 2518
- [16] Takayanagi M, Harima H and Iwata Y, *Mem. Fac Eng Kyushu Univ* 1963;23:41
- [17] Coran AY, Patel R. *J Appl Polym Sci* 1976;20:3005.
- [18] Veenstra H, Verkooijen PCJ, van Lent BJJ, van Dam J, Posthuma de Boer A, *Polymer* 2000;41:1817.
- [19] Willemse RC, Posthuma de Boer A, van Dam J, Gotsis AD. *Polymer* 1998;39:5879.
- [20] Sengupta P, PhD thesis, Twente University, Enschede, 2004.
- [21] Nakajima N, Harrell ER. *J Rheol* 1982;26:427.
- [22] Graebbling D, Muller R. *J Rheol* 1990;34:193.
- [23] Weis C, Leukel J, Borkenstein K, Maier D, Gronski W, Friedrich C, *Polym Bull* 1998;40:235.
- [24] Steinmann S, Gronski W, Friedrich C. *Polymer* 2001;42:6619.
- [25] Palierne JF. *Rheol Acta* 1990;29:204.
- [26] Lee HM, Park OO. *J Rheol* 1994;38:1405.
- [27] Bousmina M, Muller R. *J Rheol* 1993;37:663.
- [28] Chapter 4; This thesis
- [29] Jayaraman K, Kolli VG, Kang SY, Kumar S, Ellul MD. *J Appl Polym Sci* 2004;93:113.

Chapter 6

Melt creep behaviour of elastomer-polymer blends

Effect of morphology on the deformation mechanism in olefinic thermoplastic elastomer blends during the start-up phase of flow

Abstract

The transient rheological behaviour of two olefinic thermoplastic elastomer blends was studied by melt creep measurements and strain recovery after cessation of creep flow. Yield stresses for flow could be found in the creep measurements while the deformation mechanism in the start up phase of the flow was elucidated by the strain recovery behaviour. The morphology of the thermoplastic vulcanisates consists of a dispersion of cured elastomer particles in a PP matrix. The volume fraction of the elastomer phase is very high and the particles form steric obstruction for their neighbours, resulting in a yield stress for flow. The recovery behaviour indicates that the TPVs have a yield strain in addition to this yield stress. The morphology of the PP/SEBS blends in the absence of flow consists of co-continuous structures of the PP and the SEBS phase. No measurable yield stress was found for the PP/SEBS blends. Their recovery behaviour indicates that the co-continuous blends form steady state structures in the flow regime. These structures result from a dynamic equilibrium between break-up and coalescence.

Based on:

W.G.F. Sengers, A.D. Gotsis and S.J. Picken, submitted to the Journal of Rheology

6.1 Introduction

Blending a thermoplastic polymer with an elastomer can result in materials called thermoplastic elastomers (TPE) [1]. These materials combine the melt processability of thermoplastics with rubber-like mechanical properties. This combination is due to the two-phase structure of the blend: the hard phase (thermoplastic polymer) is continuous and acts as physical cross-linker for the soft phase (elastomer). At processing temperatures, the hard phase melts or is far above its glass transition and the TPE becomes processable with common thermoplastic processing equipment, like extrusion and injection moulding. The properties of the TPEs can be tailored by adjusting the hard/soft ratio and by the addition of fillers and processing oil.

Two types of olefinic TPE blends (OTPE) are the subject of the present study. They both contain polypropylene (PP) as the hard phase while the type of olefinic elastomer differs. The first type contains the triblock copolymer *polystyrene-block-poly(ethylene-co-butylene)-block-polystyrene* (SEBS). The polystyrene (PS) end-blocks form separate domains and act as physical cross-links for the EB matrix phase. The blends of PP with SEBS can show a broad range of co-continuous structures, depending on the properties of components used and the processing conditions [2,3,4]. Stable co-continuous structures are possible due to the physical cross-links in the SEBS and the low interfacial tension between the PP and the elastomer phase [3]. The second type of OTPE consists of PP blended with the random copolymer *ethylene-propylene-diene-terpolymer* (EPDM). These blends, called *Thermoplastic Vulcanisates* (TPV), are prepared by *dynamic vulcanisation* i.e.: the elastomer phase in these blends is cured simultaneously with the mixing of the components [5,6]. The elastomer phase changes rapidly from a viscous fluid into an elastic solid and is forced to break up. Phase inversion takes place and the elastomer phase becomes dispersed in the PP matrix, even when it is the majority components [6]. This particle-matrix morphology in TPVs is permanent and does not change upon (re)processing the TPV.

Commercial OTPE blends often contain additives like carbon black, calcium carbonate or processing oil in order to tailor the properties [1]. In the present work we limited the additives to processing oil, which is added to lower the hardness and to improve the processability. The oil, paraffinic in nature, is distributed over the PP and the elastomer phases and plasticizes both of them [2,7]

Despite the many rheological studies on TPE blends using capillary rheometry and oscillatory strain measurement [e.g. Ref 8-13], not much is known about the transient properties of these OTPE blends. Transient rheological measurements give insight in the blend morphology and can be used to study the deformation processes during processing [14-16].

Akari and White [17] studied the creep behaviour of TPVs at very low shear rates. The transient viscosity increases sharply at low shear rates, indicating that the TPV has a yield stress for flow. Steeman and Zoetelief [11] reported that the yield stress increases with increasing elastomer content in the TPV. The yield stress in the TPVs is caused by the high elastomer content. The elastomer particles form an

agglomerated network-like structure [8,11,17] that has to be broken to enable flow of the TPV. The rheological properties of the TPVs show striking similarities with highly filled fluids [8]. Based on the behaviour of the latter, the yield stress in TPVs should increase with increasing volume fraction of elastomer particles, decreasing particle size and increasing the irregularity of particle shape [e.g. Ref 18,19].

The open literature about the rheological properties of PP/SEBS blends is limited to capillary [10] and oscillatory strain measurements [10,20]. The physical cross-links are still present in the melt state in this system and the elastomer phase has the highest values for the dynamic moduli. The moduli of the blend can be related, then, to the continuity of the elastomer phase [20]. In capillary flow, on the other hand, the strains are high enough for the physical cross-links to break and the blend is able to flow. It is expected that the co-continuous structures are not stable in capillary flow and the blend morphology becomes a dynamic equilibrium of break-up and coalescence of the two phases [21, 22 and Chapter 7 of this thesis]. This has been confirmed by the presence of a PP-rich skin layer in the extrudates of the PP/SEBS [10].

Transient rheological experiments have proved to be successful in the study of the interrelationship between the morphology and the rheology of polymers. The presence of an interface between the two phases leads to additional resistance to deformation. In polymer blends with droplet-in-matrix morphology, the droplets become extended. The increase of the interfacial area requires additional energy results in peaks of the transient viscosity in creep and start-up experiments, which are not present in either one of the phases [14-16]. The time change of the morphology during shear flow can be studied by stress relaxation after cessation of shear flow [16,23], flow reversal [24] or recovery after cessation of creep flow [25-26]. In these experiments, an additional relaxation process can be seen that is caused by the retraction of the deformed droplets in order to minimise the total surface area. The relaxation modulus shows two regimes, indicating two relaxation processes: the relaxation of the blend components at short relaxation times and the relaxation due to the retraction of the interface at longer times. [16] The recovered strain after creep flow also proved to be sensitive for changes in morphology [27]. Initially, the ultimate recovery strain increases with increasing the applied strain due to shape recovery of the dispersed phase. At larger deformations, the ultimate recovery strain decreases because the elongated structures do not retract to their original shape but they break up.

Not much has been reported about the transient rheological properties of polymer blends with co-continuous morphology. Krishnan et al. [28] showed that the rheological properties of bi-continuous microemulsions show similarities with worm-like micelles [29,30] or 'living polymers'. In start-up flow, three regimes were identified. In the linear regime, at short deformation times, the emulsions showed high elastic response. At intermediate times, the shear stress peaked due to stretch and orientation of the two phases, and at longer times, the emulsions showed inhomogeneous flow. The percolation of the two phases decreased and thereby, the elasticity decreased.

The linear viscoelastic properties of the PP/SEBS blends are comparable to those of the TPVs: the storage modulus persists at a constant value when the frequency decreases to zero. Their non-linear flow properties, however, are different. The empirical Co-Merz relation for the shear and the dynamic viscosity holds well for the PP/SEBS blends [10], while for the TPVs the dynamic viscosity is always higher than the shear viscosity [9]. In this chapter, the transition from linear elastic behaviour to flow is studied by melt creep experiments. Using similar compositions for the two blends, a direct comparison can be made between the dispersed and the co-continuous morphologies. The recovery from creep flow can elucidate the differences in the deformation mechanism between co-continuous and dispersed morphologies.

6.2 Experimental

6.2.1 Materials

Two types of TPE blends are used in this article. To make a direct comparison, the two blend types contain the same PP matrix (PP homopolymer with a MFI of 0.3 dg/min at 230 °C and 2.16 kg, DSM Polypropylenes) and paraffinic oil (Sunpar 150, Sun Oil Company). The PP-SEBS blends contain SEBS (KRATON® G 1651, KRATON Polymers) as elastomer and the TPVs contain EPDM (63 wt % C2, 4.5 wt% ENB, extended with 50 wt% of paraffinic oil, DSM Elastomers). The EPDM in the TPVs is dynamically vulcanised using 5 phr phenolic curing agent (SP® 1045, Schenectady) in combination with 1 phr Stannous Chloride and Zinc Oxide (Merck). All materials contain antioxidants (0.5 wt% Irganox 1076 and 0.5 wt% Irgafos 168, Ciba Specialty Chemicals).

6.2.2 Sample preparation

The PP-SEBS blends were prepared with a ZSK 25 co-rotating twin screw extruder operated at 250 rpm; the TPVs were prepared with a ZSK-40 co-rotating twin screw extruder, operated at 350 rpm. The temperature in the extruder ranged from 180 °C at the hopper to 210 °C at the die. The blend composition was varied in order to study the influence of the content of PP and oil. Similar compositions were used for the PP-SEBS and TPV blends. These compositions are shown in Table 6.1. The letter ‘S’ in the coding indicates the PP-SEBS blends and ‘E’ the TPV blends. The numbers x/y stand for the PP-elastomer and for the oil-elastomer ratio.

Binary PP-oil mixtures were made in an internal batch mixer (Brabender Plasticorder 20 cc with Banbury rotors) at 180 °C and 100 rpm. The SEBS-oil mixtures were prepared by dry blending the SEBS pellets with oil. The binary mixtures were compression moulded into sheets of 2 mm at 200 °C. EPDM vulcanisates with different oil concentration were prepared by preblending the EPDM with curatives (same amount as in the TPVs) and oil on a two-roll mill, followed by curing during compression moulding at 200 °C to obtain 2 mm sheets. An additional sample containing 60 wt% vulcanised EPDM in oil was prepared by first extracting the oil from the original EPDM-oil batch using n-hexane, precipitating the EPDM in acetone, and adding the appropriate amount of oil and curatives for the vulcanisation

Table 6.1: Composition of blends

Code	PP (wt%)	EPDM (wt%)	SEBS (wt%)	Oil (wt%)	Yield stress (kPa)
S0.4/1.4	14.3		35.7	50.0	--
S0.8/1.0	28.6		35.7	35.7	1 - 2
S0.8/1.4	25.0		31.3	43.8	--
S0.8/1.8	22.2		27.8	50.0	--
S1.2/1.4	33.3		27.8	38.9	--
E0.4/1.4	14.3	35.7		50.0	12-13
E0.8/1.0	28.6	35.7		35.7	13-15
E0.8/1.4	25.0	31.3		43.8	6.5 - 8
E0.8/1.8	22.2	27.8		50.0	5 - 6
E1.2/1.4	33.3	27.8		38.9	5 - 7.5

6.2.3 Morphology

The morphology of the TPE blends was studied using transmission electron microscopy (TEM, Philips CM30). The samples were microtomed at $-130\text{ }^{\circ}\text{C}$ using a diamond knife and stained with ruthenium tetroxide vapour for 10 minutes.

6.2.4 Rheological measurements

A Rheometric RS 5000 controlled stress rheometer was used in a 25 mm parallel disk configuration with a fixed gap of 2 mm. An axial force of 1.5-3 N was used to prevent slip. The melt creep measurements were performed at $190\text{ }^{\circ}\text{C}$. In the creep experiments, a constant shear stress, σ , is applied on a sample and the resulting shear strain deformation, γ , is measured over time. The time dependent creep compliance, $J(t)$, is the ratio of the deformation $\gamma(t)$ over the applied constant stress :

$$J(t) = \frac{\gamma(t)}{\sigma} \quad (6.1)$$

The transient viscosity, $\eta^+(t)$, is the inverse of the slope of the curve of the creep compliance versus time.

$$\frac{1}{\eta^+(t)} = \frac{\partial J(t)}{\partial t} \quad (6.2)$$

The recoil of the sample after releasing the stress was monitored for 1000 s. The 'recovery strain', γ_r , was defined as the difference between the deformation just before the time of the stress release, $\gamma(t_0)$, and the deformation after 1000 s recoil, $\gamma(t_0+1000)$.

$$\gamma_r(\gamma_0, \sigma) = \gamma(t_0)|_{\sigma} - \gamma(t_0 + 1000)|_{\sigma=0} \quad (6.3)$$

The time of 1000 s appeared to be sufficient to reach equilibrium values for the recovery strain. An example of the sample deformation during creep experiment and recovery is given in Fig. 6.1.

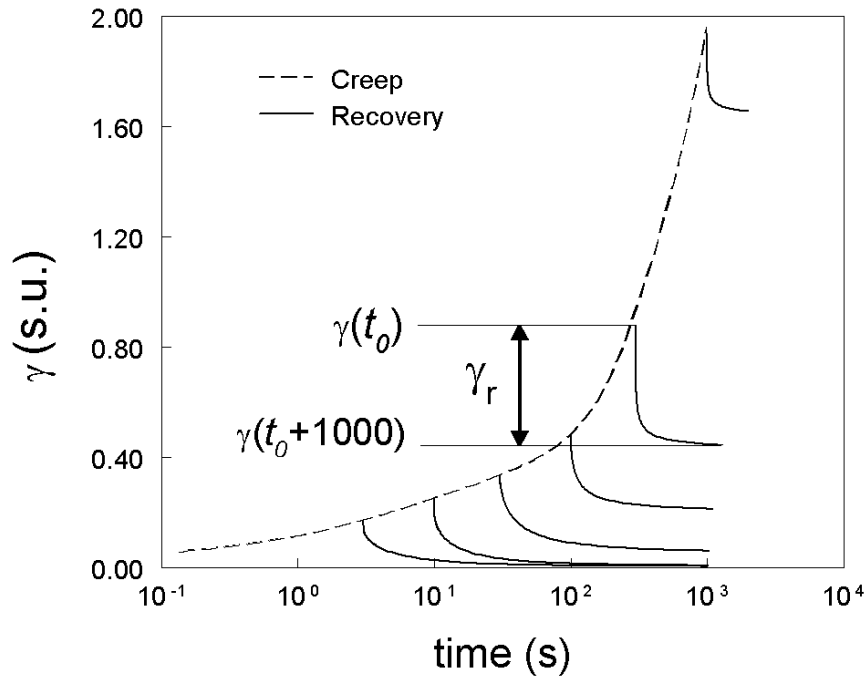


Figure 6.1: Deformation during creep-recovery experiment for E0.8/1.4 at a creep stress of 3 kPa.

6.3 Results

6.3.1 Morphology

Figs. 6.2 and 6.3 show TEM images for the two OTPE blends at different compositions. The overall relation between morphology and composition is rather complex and the interpretation can only be done after studying multiple images and comparing them with other methods, like Low Voltage SEM (LVSEM) and extraction experiments [31]. PP/SEBS blends with different PP/elastomer ratios are shown in Fig 6.2. The SEBS appears as a dark grey phase, while the light grey corresponds to the PP phase. The magnification in the figure is suitable to observe the blend structure but it is too low to discern the 20 nm PS domains that are dispersed in the ethylene-butylene matrix of the SEBS block co-polymer. Both phases seem to be continuous in Fig. 6.2. The co-continuous structure was confirmed by selective extraction of the SEBS and the oil [31]: In all these blends more than 95% of SEBS was recovered and the remaining PP phase appeared as a self-supporting porous, sponge-like structure. The average size ("striation thickness") of the SEBS phase is about 0.5 - 3 μm and decreases with increasing PP/elastomer or oil/elastomer ratio. The decrease of striation thickness also results in a reduction of the interconnectivity of the SEBS phase.

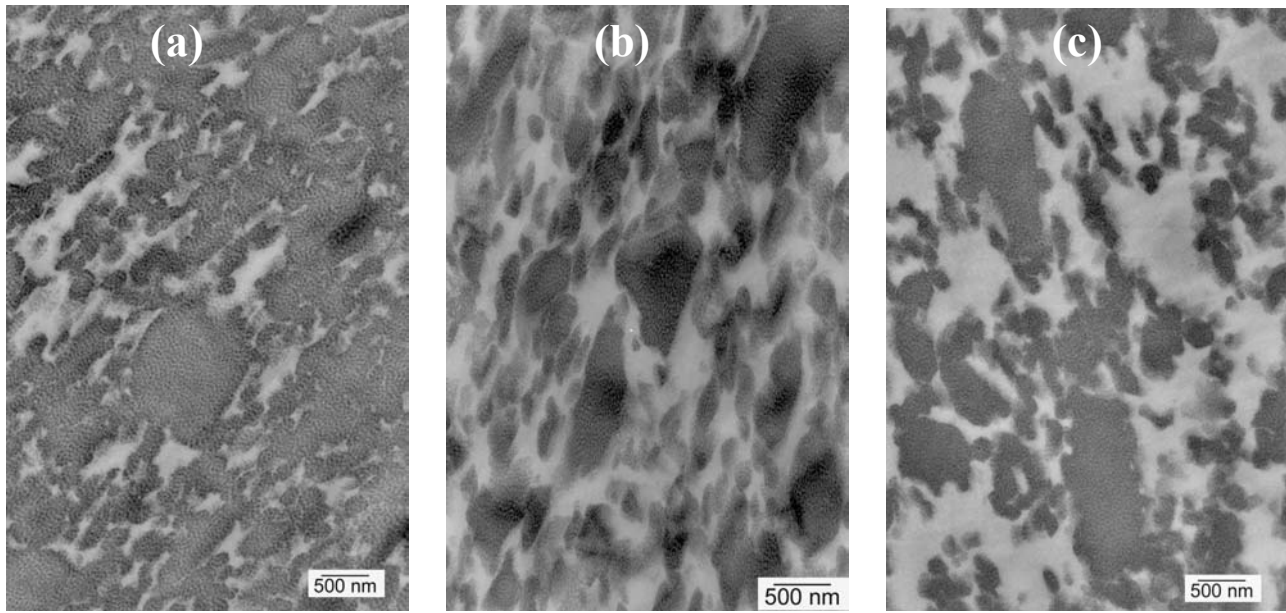


Figure 6.2: TEM images of PP/SEBS blends with different PP/Elastomer ratio (a) S0.4/1.4; (b) S0.8/1.4; (c) S1.2/1.4. For the codes see Table 6.1.

Fig 6.3 shows TEM images of TPVs with different PP/elastomer ratios. The EPDM phases are visible as the darker areas. The morphology consists of elliptically shaped dispersed EPDM particles with lengths of 1 - 3 μm , even for the blend E0.4/1.4 (Fig 6.3a), despite its very high elastomer content. This dispersed morphology was confirmed using low voltage SEM (LVSEM) [31]. Upon increasing the PP/elastomer ratio, the average particle size decreases; increasing the oil/elastomer ratio results in a reduction of the inter-particle distance but the sizes do not change.

6.3.2 Melt creep

The curve of the creep compliance, $J(t)$, gives a good picture of the deformation character of a material. If the material behaves elastically, $J(t)$ reaches a finite value. For fluid-like behaviour, the logarithmic slope of the $J(t)$ curve becomes 1. However, determining the point of the transition from elastic to fluid-like behaviour of the material is more difficult. The plot of the transient viscosity, $\eta^+(t)$ (Eq. 6.2), as a function of deformation, $\gamma(t)$, under constant shear stress has advantages in the determination of the yield point. If the material is a viscous fluid, the transient viscosity levels off and it reaches a constant value with increasing deformation. The curve of $\eta^+(\gamma)$ is then concave downwards. For an elastic solid the viscosity increases to infinity at an equilibrium deformation and $\eta^+(\gamma)$ has a convex shape, i.e. it is curved upwards. The stress at which the curve changes from elastic to viscous-like is the yield stress.

The OTPE blends contain considerable amount of paraffinic oil. This oil is distributed over the PP and the elastomer phases and it affects the properties of both phases [2,7,20]. The melt creep behaviour of these two binary phases is studied separately and this will be discussed first. The properties of the phases will be used later in the description of the effect of the composition and the morphology on the melt creep behaviour of the ternary blends.

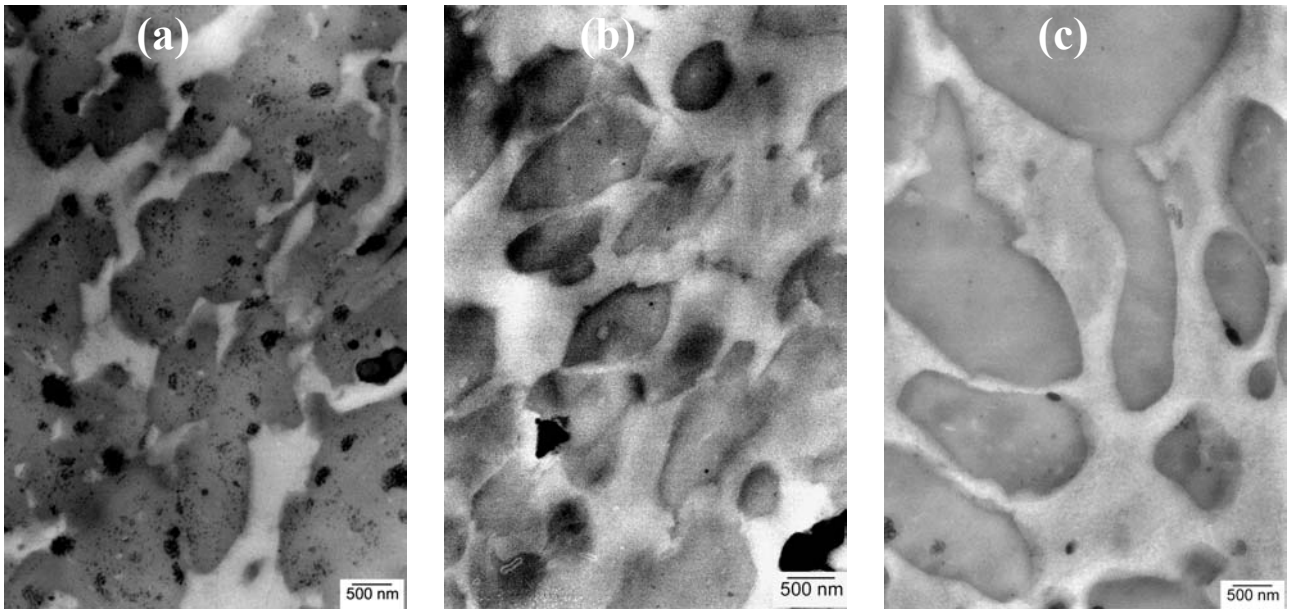


Figure 6.3: TEM images of TPVs with different PP/Elastomer ratio (a) E0.4/1.4; (b) E0.8/1.4; (c) E1.2/1.4. For the codes see Table 6.1.

6.3.2.1 Binary mixtures

The behaviour of each phase depends on both the polymer type and the amount of oil it contains. To study the effect of oil on the properties of the PP and the elastomer phases, creep measurements were performed on a series of PP-oil and elastomer-oil binary mixtures. Fig 6.4 shows the transient viscosity of these binary mixtures at 190 °C and 1 kPa.

The PP-oil mixtures behave as plasticized entangled linear polymers (Fig 6.4a). The transient viscosity, $\eta^+(\gamma)$, initially increases under a constant stress and it reaches a steady state value after 1 s.u.. The equilibrium viscosity decreases with increasing oil content due to the diluting effect of the oil.

The creep behaviour of the SEBS-oil mixtures is more complex due to the presence of physical cross-links (Fig 6.4b). Because the measurement temperature is above the T_g of PS but below the order-disorder temperature of the SEBS, the PS domains are still present as separate phases, and a yield stress for flow is expected. A transition from elastic to viscous behaviour in these mixtures is observed between 40 and 50 wt% oil for an applied stress of 1 kPa. At 40 wt% oil, $\eta^+(\gamma)$ increases to infinity at a finite deformation around 0.02 s.u.. In the binary mixture containing 50 wt% oil, the curve of $\eta^+(\gamma)$ is not concave upwards. This mixture does not show obvious yield behaviour at this stress, nor is a true flow regime reached within the time of the measurement. The transient viscosity curves of the mixtures containing 60 wt% oil or higher peak at around 0.5 s.u. and later they reach steady state. The SEBS is then able to flow by reorganising the position of the domains or by migration of the PS end blocks to other domains. This behaviour has also been observed in oil-SEBS gels [31,32]. The oil expands the elastomeric EB chains and the morphology becomes easier to break up at oil concentrations higher than 50 wt%. The steady state viscosity decreases with increasing oil content. A transition from elastic to viscous flow behaviour for this system has also been observed in dynamic rheological measurements [20]: Increasing

the oil content from 50 to 60 wt% the dynamic moduli at low frequencies (<0.1 rad/s) decrease drastically and become frequency-dependent.

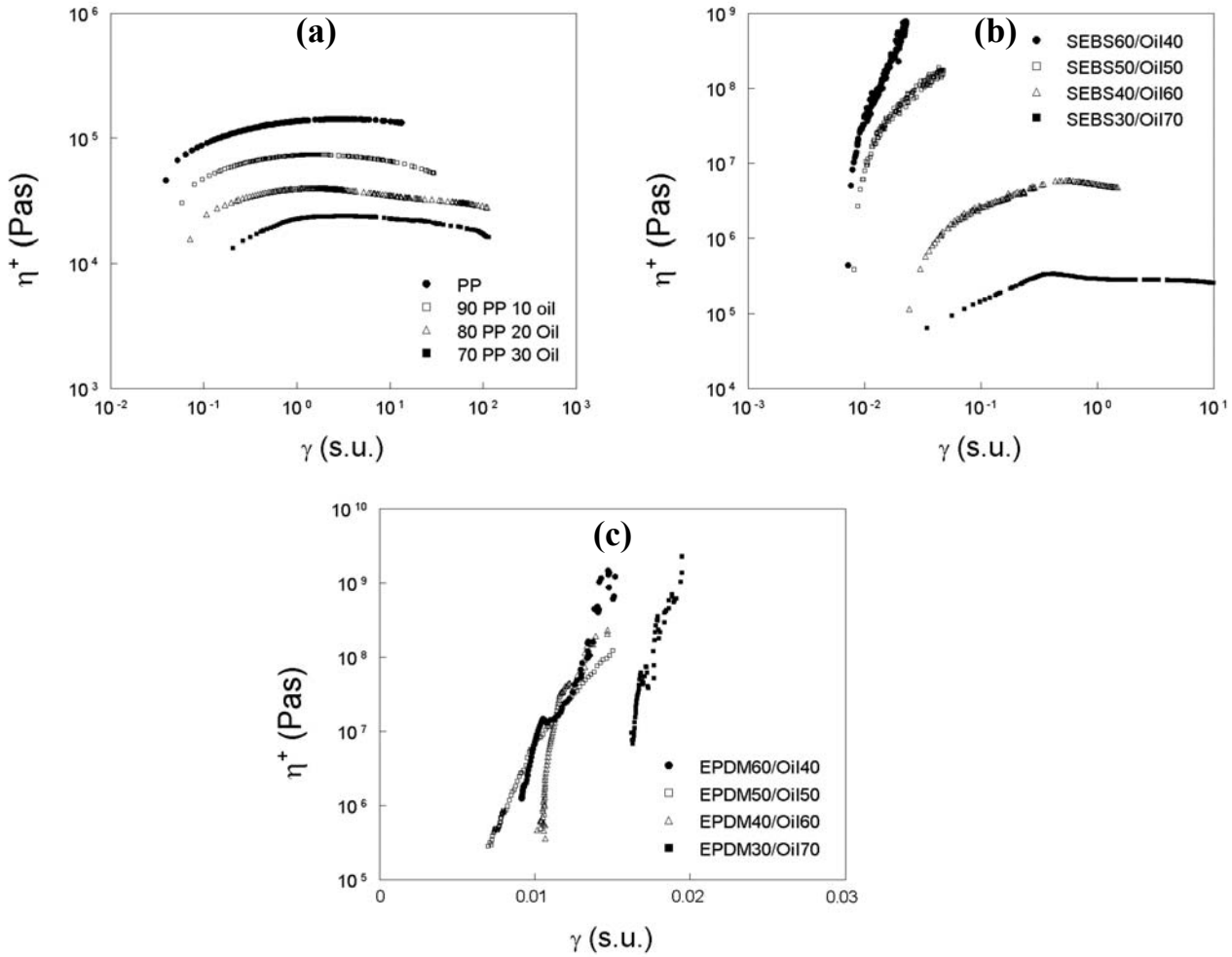


Figure 6.4: Transient viscosity of the binary mixtures as a function of the strain, at 190 °C and at a creep stress of 1 kPa. (a) PP-oil; (b) SEBS-oil; and (c) EPDM-oil.

The elastomer in the EPDM-oil vulcanisates is chemically cross-linked. This is shown in Fig 6.4c by the increase of $\eta^+(\gamma)$ to infinity at a finite deformation. With increasing oil content, this deformation increases from 0.015 to 0.02 s.u for a constant applied stress of 1 kPa. An elastic shear modulus can be determined based on these values. It ranges from 51 to 65 kPa for the different EPDM-oil binary mixtures. This is in reasonable agreement with the low frequency modulus measured in dynamic rheological experiments (69-103 kPa at 0.1 rad/s) [20].

6.3.2.2 PP-SEBS blends

When SEBS is blended with PP and oil, the blend morphology consists of co-continuous structures (Fig 6.2). The PS domains are still present within the elastomer phase in the melt. These physical cross-links have a stabilising effect on the blend morphology and prevent coarsening of the blend. As shown for the SEBS-oil binary mixtures, the elastomer phase is able to flow only when the applied stress is large enough and the PP-SEBS blends may show yield behaviour. On the other hand, the co-continuous morphology of the blends is an intermediate transient structure that depends on the processing history. Therefore, the morphology may change during the creep measurements. This has an effect on the creep behaviour. Further, the results will also depend on the initial deformation history.

Fig 6.5 shows the transient viscosity versus the deformation of blend S0.8/1.4 at different stresses. The PP-SEBS blends do not have a measurable yield stress. The curves of $\eta^+(\gamma)$ are not concave upwards for any of the applied stresses, even for the lowest stress of 0.1 kPa. The corresponding curves of the other Pp/SEBS blends are similar to those in Fig 6.5. The noticeable exception is the blend S0.8/1.0 that shows a transition to flow behaviour between 1 and 2 kPa. The oil content in the elastomer phase of this blend is estimated at 45 wt% [20]. As shown in Fig 6.4b, the viscosity of the elastomer phase at this oil concentration increases to infinity. For the other blends, the oil concentration in the elastomer phase varies between 50 and 57 wt%. These oil concentrations are sufficient for the elastomer phase to flow at all stresses.

Three regimes can be identified in the curve of the transient viscosity, $\eta^+(\gamma)$ (Fig. 6.5). At low strains, the slope of $\eta^+(\gamma)$ is constant in a logarithmic plot. This slope has a high value and it is independent of the stress. This linear regime has been estimated using dynamic oscillatory measurements to extend to 0.2 s.u. [20]. The blend morphology does not change in this regime. The elasticity of the blend at low shear rates/frequencies is dominated by the properties of the elastomer phase. Hence, in this regime, the curve of the creep compliance as a function of time, $J(t)$, is not affected by the applied stress.

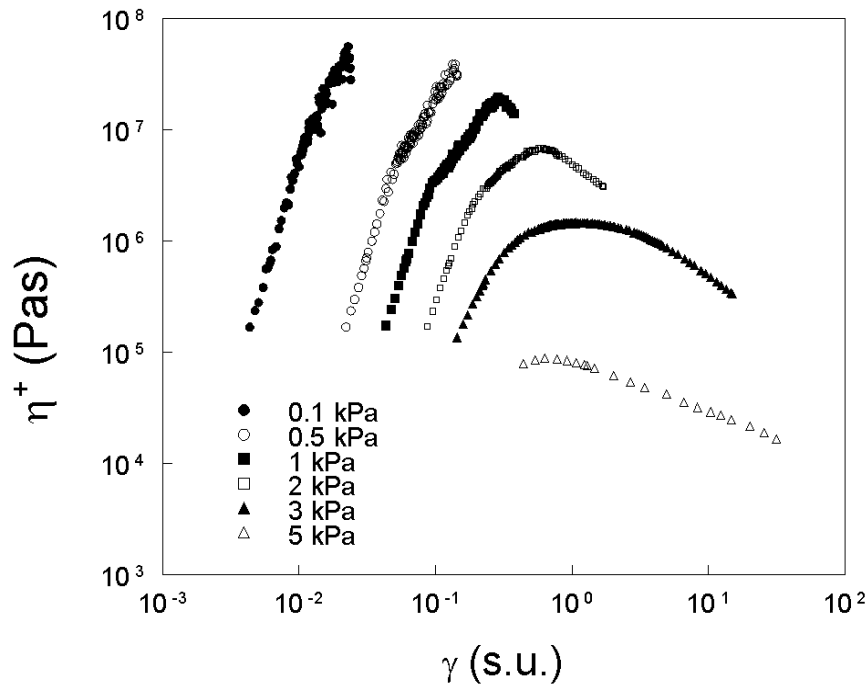


Figure 6.5: Transient viscosity of S0.8/14 blend as a function of the strain at 190 °C and at different stresses.

The beginning of the second transient regime can be identified by a reduction in the logarithmic slope of the curve. The blend morphology adapts to the applied stress by orientation and elongation of the two phases, leading to the slower evolution of the viscosity. This process continues until the viscosity shows an overshoot. The third regime starts after this peak in the viscosity, which is located between 0.1 and 1 s.u.. The physical cross-links in the elastomer phase are broken now and the material starts to flow.

Increasing the applied stress results in a larger initial deformation in the linear viscoelastic regime because of the constant value of the elasticity modulus (Fig. 6.5). The logarithmic slopes in $\eta^+(\gamma)$ are not affected and the transition regime begins at larger deformations and it becomes shorter. The flow regime, indicated by the peak of $\eta^+(\gamma)$, also shifts to larger deformations while the peak itself is lower. The initial regime is not present in creep experiments at stresses higher than 5 kPa. Apparently, the physical cross-links in the elastomer phase are broken down very fast then and the material is able to flow immediately.

The co-continuous morphology in these blends is a dynamic equilibrium morphology and it may change during deformation (or processing). The two continuous phases deform according to their resistance to flow. Since the PP phase has lower viscosity than the elastomer phase, this phase deforms easier and is mainly responsible for the flow. The curves of $\eta^+(\gamma)$ change gradually from SEBS-like to PP-like behaviour upon increasing the PP content in the blend (Fig 6.6a). The logarithmic slope of the transient viscosity decreases in the linear viscoelastic regime, while the viscosity decreases in the flow regime. A gradual change is also observed in the linear viscoelastic properties measured by dynamic oscillatory measurements [20]. In the flow regime, the value of $\eta^+(\gamma)$ decreases due to the increase of the volume fraction of the less viscous PP phase.

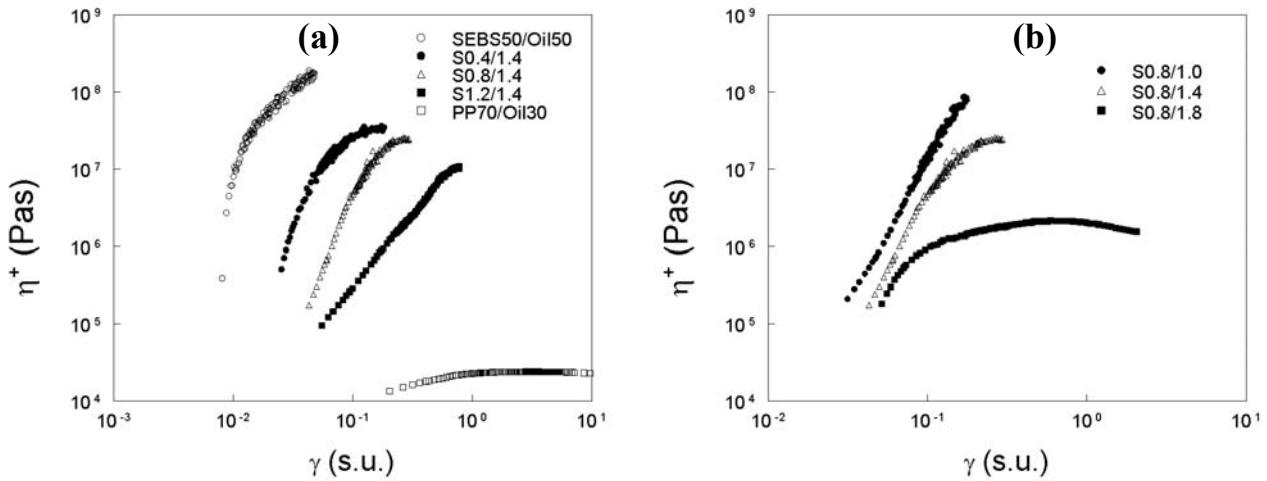


Figure 6.6: Transient viscosity of PP/SEBS blends as a function of the strain, at 190 °C and at a creep stress of 1 kPa. (a) different PP content; (b) different oil content.

The increase of the amount of oil in the blend results in dilution of both the PP and the elastomer phases. The blend morphology changes only slightly: The domain sizes in the two phases increase but the volume fractions are only affected by changes in the distribution of oil, which are small. With increasing oil content, therefore, the initial logarithmic slope of the viscosity does not change (Fig 6.6b). For the blend with the lowest oil content, the applied stress is below the yield stress and $\eta^+(\gamma)$ of this blend increases without bound with the deformation (or time). With increasing oil content, the blend viscosity decreases due to the lowering of the viscosities of both phases and the blends can be deformed to a larger extent.

6.3.2.3 Thermoplastic vulcanisates

The blend morphology of the TPVs consists of elastomer particles dispersed in a PP matrix phase. Due to the high volume fraction of the elastomer phase, the particles can touch each other and form a network-like structure. This structure has to be broken before the material is able to flow, resulting in yield behaviour [8,11,17]. The elastomer particles themselves are cured and are only deformed only up to a finite strain, depending on the applied stress (see Fig 6.4c). The flow properties of the TPVs, therefore, are mainly governed by the PP matrix phase. This can be seen in Fig 6.7 and 6.8.

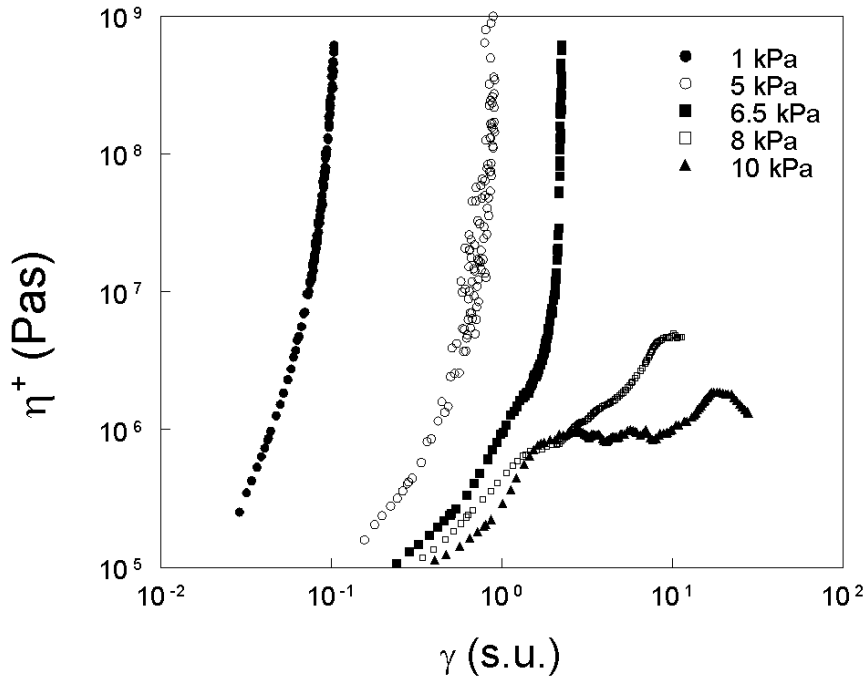


Figure 6.7: Transient viscosity of E0.8/1.4 blends as a function of the strain at 190 °C and at different stresses

Fig 6.7 shows the transient viscosity of TPV blend E0.8/1.4 for different applied stresses. This TPV shows a transition to flow at stresses between 6.5 and 8 kPa. The behaviour of the TPV can be divided into pre-yield and post-yield behaviour. At stresses below the yield stress, the viscosity, $\eta^+(\gamma)$, increases to infinity at a finite deformation. This deformation increases with increasing the applied stress. The initial agglomerated structure is still present below the yield stress and the elastomer particles form a steric obstruction for flow of the TPV. This structure can be broken at stresses higher than the yield stress. For these stresses, $\eta^+(\gamma)$ initially increases and peaks at 1-3 s.u. At larger deformations the curve of $\eta^+(\gamma)$ becomes unstable but the values remain bounded. The behaviour of $\eta^+(\gamma)$ for stresses higher than the yield stress can again be divided into three regimes of deformation, similar to the behaviour of the SEBS/PP blends. Initially the viscosity increases with a constant logarithmic slope. In the transition regime, $\eta^+(\gamma)$ goes over a peak at 1-3 s.u.. In the flow regime, the viscosity fluctuates but remains finite.

The other TPVs show comparable behaviour. The values of the yield stress, listed in Table 6.1, are depend on the composition and morphology. The increase of PP content in the TPVs results in reduction of the number of elastomer particles per volume (Fig 6.3) and the aggregated structure of the elastomer particles is diluted.

The resistance to flow decreases resulting in lower values of the yield stress. The addition of oil reduces the viscosity of the PP phase and, thereby, the stress needed to start the flow.

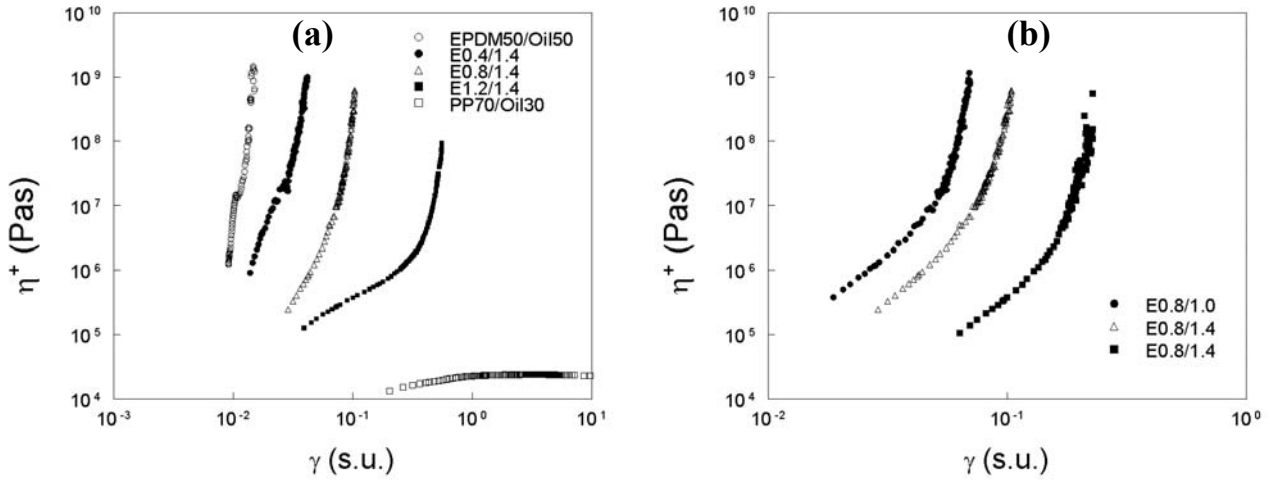


Figure 6.8: Transient viscosity of TPVs blends as a function of the strain, at 190 °C and at a creep stress of 1 kPa. (a) different PP content; (b) different oil content.

The morphology and composition affect the creep properties also at stresses below the yield stress. Fig 6.8 shows the transient viscosity of the TPVs, $\eta^+(\gamma)$, at 1 kPa. At this stress, the TPVs have not yielded and a final deformation is reached. Fig 6.8a shows the effect of PP content on $\eta^+(\gamma)$. The curves of a binary PP-oil mixture and an EPDM-oil vulcanisate are included. The increase of the PP content in the TPV results in a decrease of the initial logarithmic slope and an increase of the finite deformation. At low PP content, the agglomerated structure of the elastomer phase is closely packed and the macroscopic properties are dominated by the elastomer phase. The steric obstruction is too large for this stress to break the network structure and the TPV deforms elastically. The addition of more PP results in an increase of the interparticle distance (Fig. 6.3) and, thereby, a less dense elastomer network. Because of the lower number of particles per volume, the TPV can deform to a larger extent before it is obstructed. On the other hand, due to the increase of the volume fraction of the matrix phase, the TPV has a lower resistance to flow and the blend viscosity decreases.

The addition of oil affects the properties of the two phases but it has negligible effect on the type of the morphology and it does not affect the volume fractions of the phases. The particle size of the elastomer phase and the interparticle distance both increase. This results in a lower viscosity and a larger final deformation of the blend below its yield stress (Fig 6.8b). Hence the initial logarithmic slope does not change. The lower viscosity is due to the diluting effect of the oil on the viscosity of the PP matrix phase and the modulus of the elastomer particles (Fig 6.4c). The final deformation increases due to the lower modulus of the elastomer phase.

The deformation behaviour of the TPV melt is thus strongly affected by the content and the viscosity of the matrix phase. With increasing the volume fraction of the matrix phase by the addition of PP, the network of elastomer particles becomes less dense. The initial resistance to deformation decreases, resulting in a lower blend viscosity, and the particles are able to move to a larger extent before becoming an

obstruction to flow. Similarly, decreasing the matrix viscosity by the addition of processing oil, the total blend viscosity decreases and the blend can be deformed to a larger extend.

6.3.3 Recovery from creep

The peak in $\eta^+(\gamma)$ of the blends above the yield stress represents the transition from elastic-like to viscous-like behaviour. For both blend types, this maximum is located between 0.5 and 3 s.u. The presence of the peak indicates a change of the blend behaviour but it does not provide direct information on the changes in the blend morphology.

The origin of the yield behaviour differs in the two types of blend. In the case of PP-SEBS blends, the continuous SEBS phase is able to flow when the PS end-blocks are pulled out of the PS domains. As shown in Figs 6.5 and 6.7, the position of the maximum then depends on the applied stress and the blend composition. A TPV flows only when the elastomer particles are able to pass over each other. The peak in $\eta^+(\gamma)$ is located between 1 and 3 s.u. and hardly depends on the applied stress. This indicates that the TPVs show a *yield strain* in addition to a *yield stress*. That is, a deformation of the blend above a threshold is needed for the elastomer particles to pass over each other in addition to the application of enough stress to break the initial agglomerated structure. The presence of a *yield strain* in concentrated suspensions has been suggested earlier in Refs. [34,35,36]

This hypothesis is studied further by recovery measurements after cessation of creep flow (Fig 6.1). The recovery strain, γ_r , gives an indication of the remaining melt elasticity of the material after a certain deformation at a constant stress (Eq. 6.3). The elastic recovery consists of a structure-dependent contribution and a contribution from the time-dependent entanglement elasticity of the two phases. The elastic contribution from the individual phases becomes saturated with increasing creep time and deformation. The structure-dependent elasticity, on the other hand, mainly depends on the applied deformation. At small deformations, below a critical strain, the elastomer network structure remains intact and its recovery is almost complete. If the structure is broken or rearranged, the material does not go back to its original shape. The contribution of the structure to γ_r diminishes then and the total recovery decreases. Investigating this incomplete recovery after creep flow as a function of the applied strain gives information of the dissipation process due to changes in the blend structure.

6.3.3.1 PP-SEBS blends

Fig 6.9 shows the recovered strain after creep flow versus the applied strain, γ_0 , at the point where the stress was released for a PP-SEBS compound at different stresses. The transient viscosity (at 3 kPa) is also shown. The three regimes in deformation, indicated by changes in the form of $\eta^+(\gamma)$ curve are visible also in the recovered strain. The linear regime at low creep strains is characterised by complete elastic recovery. The recovered strain is close to the applied deformation then (solid line in Fig 6.9). In the transition regime, at applied strains around the point where $\eta^+(\gamma)$ would show a maximum, the recovered strain still increases but it starts to deviate

from the total elastic recovery curve. For γ_0 after the peak in $\eta^+(\gamma)$, the recovered strain reaches a constant value in the flow regime (steady state recoil) and most of the initial elasticity is saturated. At a constant value of γ_0 , the recovered strain increases with increasing the applied creep stress (Fig 6.9). This is due to the shorter creep times needed to reach that deformation and indicates that the (time-dependent) elasticity of the individual phases is the major contributing factor in the recovery.

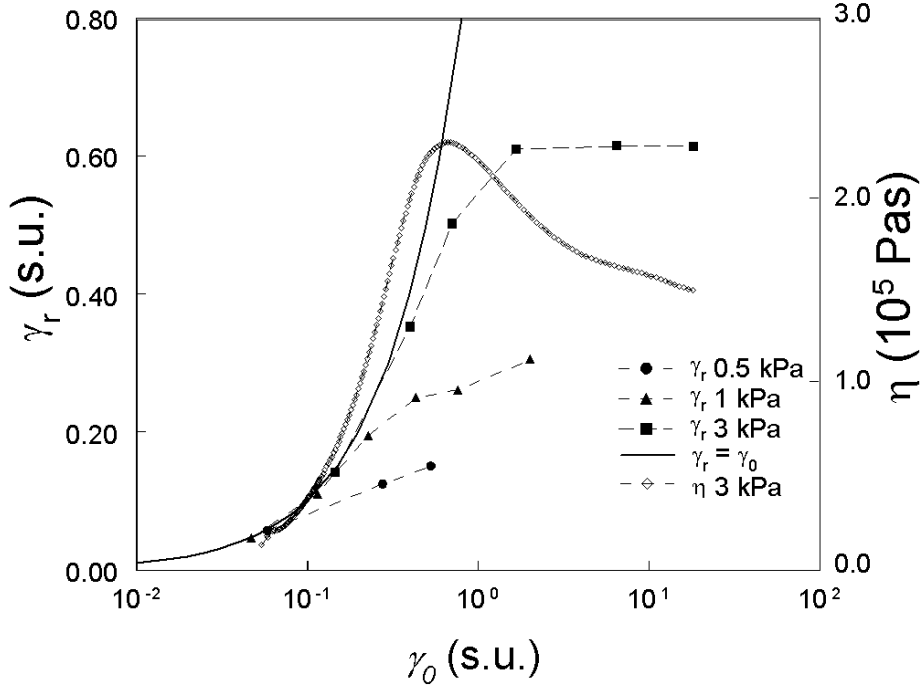


Figure 6.9: Recovered strain after cessation of creep flow at 190 °C and different stresses, as a function of the applied creep strain for the blend S1.2/1.4. The solid line represents ideal elastic behaviour (recoil=deformation). The open symbols show the curve of the transient viscosity, $\eta^+(\gamma)$ measured at a creep stress of 3 kPa (right axis). The dashed lines are to guide the eye.

The behaviour of γ_r in the flow regime is the result of the co-continuous blend morphology. This morphology is a dynamic equilibrium structure and it changes when the material is deformed. The contribution of the initial structure diminishes at larger strains and a new dynamic ‘steady state’ structure is formed. The morphology in the flow regime evolves continuously by break-up and rearrangement of the two phases. Its contribution to the elasticity of the blend is constant. The elasticity of the phases in this flow regime, therefore, depends on the applied stress and not on the deformation.

Fig 6.10 shows the effect of composition on γ_r at 3 kPa creep stress for a PP-oil and an SEBS-oil binary mixtures and the PP-SEBS blends. The 50-50 SEBS-oil binary mixture hardly deforms (0.2 s.u.) after creep at this stress for one hour. In quiescent state, the domains show *body centred cubic* (*bcc*) packing [32]. Higher ordered structures (e.g. twinned *bcc* textures) are formed in shear flow. The mixtures can relax within these long creep times by rearrangement of the PS domains. After removing the stress, the domains rearrange in a new *bcc* packing. The recovered strain thereby is low (ca 0.05 s.u.). On the other hand, the PP-oil binary mixture deforms faster under the same stress; since the material cannot relax during the creep time, the values of its recovery, γ_r , are higher.

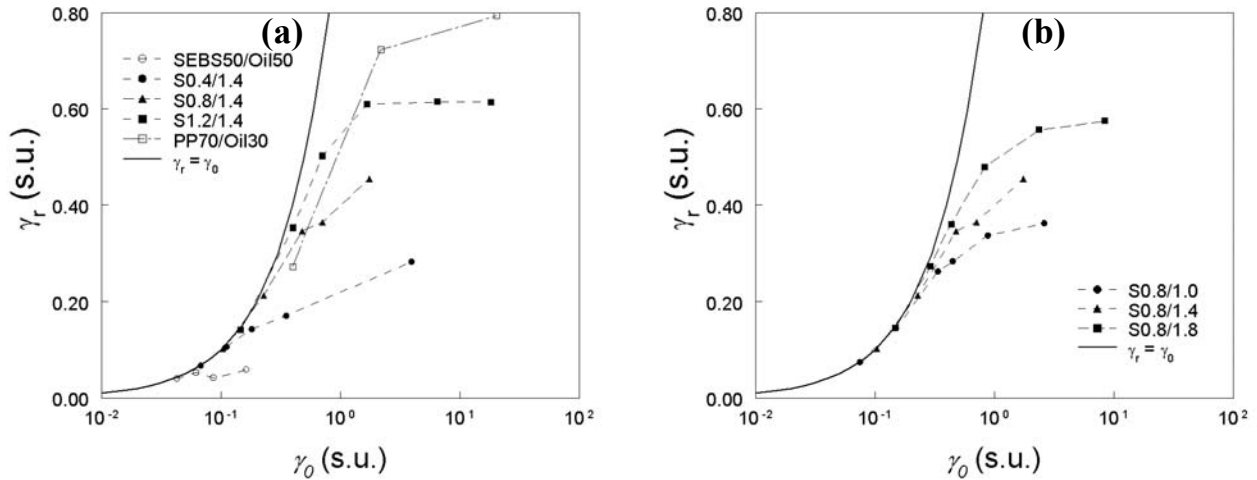


Figure 6.10: Recovered strain after cessation of creep flow at 190 °C and a stress of 3 kPa as a function of the applied creep strain for the PP/SEBS blends. (a) different PP content; (b) different oil content. The solid line represents ideal elastic behaviour (recoil=deformation). The dashed lines are to guide the eye.

The deformation and recovery behaviour in the ternary blends is determined by the weighted contribution of the two phases. By adding more PP the behaviour changes gradually from that of the SEBS-oil blend to the one of the PP-oil blend. The blend viscosity decreases and the final deformation is achieved in shorter times. This results in higher values of the recovery, γ_r , (Fig 6.10a) at constant applied strain. The transition from the linear to the transient regime is delayed.

Similar trend is seen in the series of blends with different oil content (Fig 6.10b). The transition from the linear to the transient regime in this case appears at 0.2 s.u. for all blends. The recovery increases with increasing oil content because of the shorter creep times to reach the same deformation. The effect is smaller than when varying the PP content because all three blends have similar morphologies and the volume fractions of their two phases are comparable.

By lowering the viscosity of the blends, either by adding PP or by adding oil, the PP-SEBS blends deform faster under the same stress. Shorter creep times are needed to obtain the same deformation, γ_0 , in Fig 6.10 and the material cannot relax during the creep. This results in larger recovery strain after removing the stress. The larger recovery strain indicates that the contribution of the (time-dependent) elasticity of the individual phases, and especially that of the continuous PP phase, is the major contributing factor in the recovery behaviour of these blends. This is supported also by the absence or very low values of the yield stress. Similar behaviour is also observed in the extrudate swell in capillary [37].

6.3.3.4 Thermoplastic Vulcanisates

The deformation behaviour of the TPVs is mainly governed by the PP phase properties and the steric interactions of the elastomer particles. At an applied stress of 8 kPa, and for a shear modulus of 60 kPa (Fig 6.4c), the deformation of the elastomer phase is just 0.13 s.u.. The rest of the deformation comes from the flow of the PP phase and the movement of the elastomer particles and is affected by the creep time and the stress dependent properties of the PP phase.

The yield behaviour of the TPVs originates from the agglomerated structure of the dispersed elastomer phase. The elastomer particles have to pass over each other to enable the material to flow. The break-up of this initial structure results in a reduction of the melt elasticity. This can be seen in Fig 6.11, which shows the recovery of a TPV at two stresses that are higher than the yield stress. The curve of $\eta^+(\gamma)$ at one of the two stresses (10 kPa) is included in Fig. 6.11a.

The network-like structure of the elastomer phase is still present in the linear regime. The recovery is complete there and does not depend on the applied stress. In the transient regime, where $\eta^+(\gamma)$ peaks at 0.5-1 s.u., the recovered strain of the TPVs deviates from the elastic curve. The initial agglomerated structure breaks at these strains and its contribution to the elastic recovery decreases. The recovered strain goes through a peak at the same applied strain as where the viscosity, $\eta^+(\gamma)$, also peaks. The abrupt reduction in γ_r at applied strains around 1 s.u. marks the end of the transient regime. The increase of $\eta(\gamma)$ is due to the steric obstruction of the elastomer particles. The particles have to move a certain strain (around 1 s.u.) to pass over each other in order for the TPV to start to flow. Once this has happened, the network structure is broken and the particles are able to retain their original shape. The structure dependent part of the initial melt elasticity is diminished and the recovery decreases. γ_r increases with increasing the applied stress because of the higher elastic deformation of the individual and the shorter creep times needed to obtain the same deformation. The representation of the relative recovery, γ_r/γ , as a function of γ , does not include this time effect (Fig 6.11b). The curves of the *relative recovery* remain similar, indicating that the elastomer particles follow the same deformation path (1-3 s.u.) in order to pass over each other.

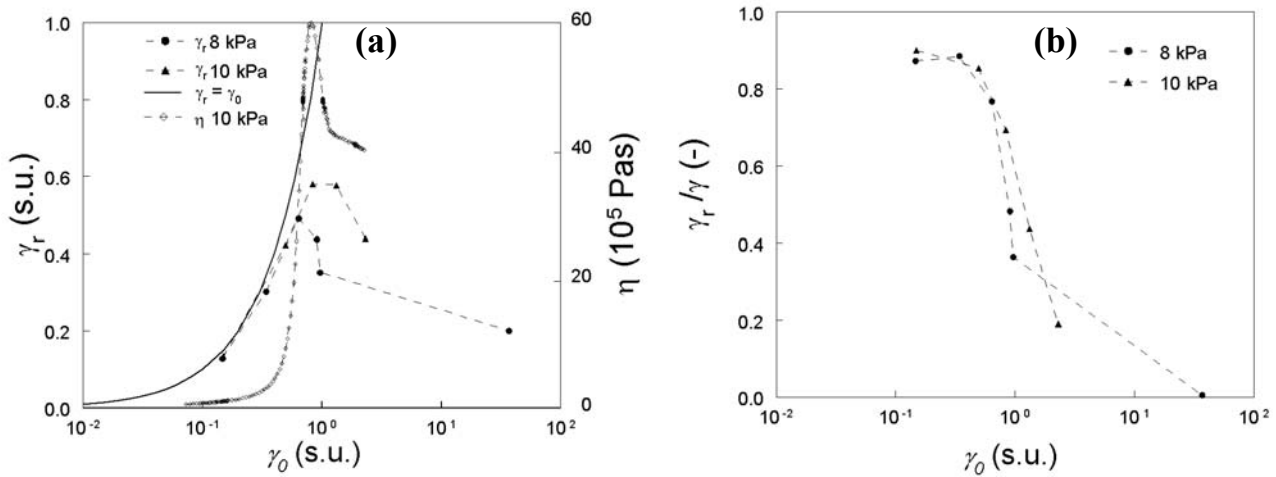


Figure 6.11: Recovered strain after cessation of creep flow at 190 °C and different stresses as a function of the applied creep strain for the TPV E1.2/1.4. The solid line represents ideal elastic behaviour (recoil=deformation). The open symbols show the curve of the transient viscosity, $\eta^+(\gamma)$ measured at 10 kPa (right axis). The dashed lines are to guide the eye.

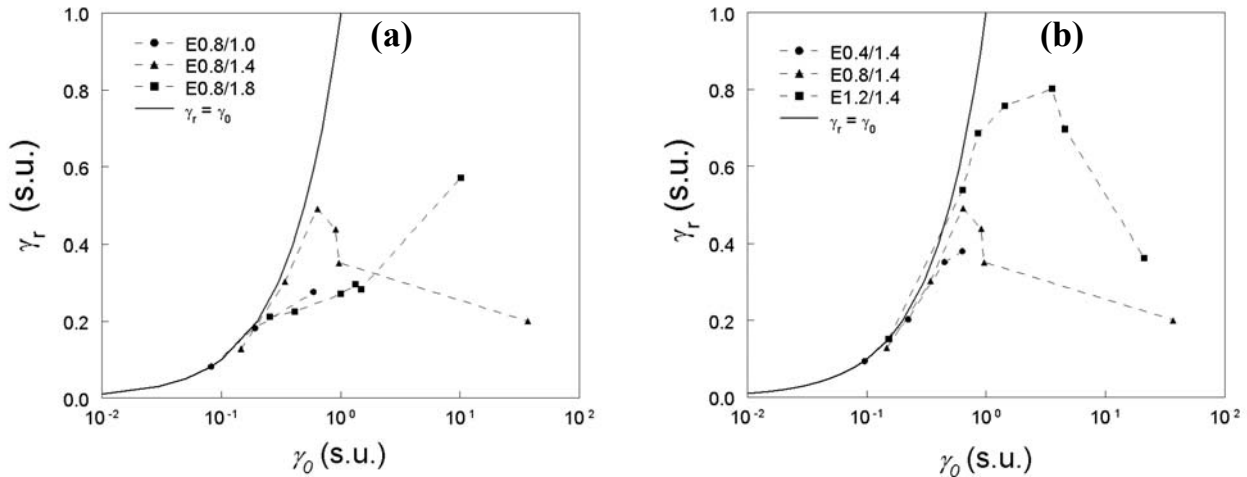


Figure 6.12: Recovered strain after cessation of creep flow at 190 °C and a stress of 8 kPa as a function of the applied creep strain for the TPVs. (a) different PP content; (b) different oil content. The solid line represents ideal elastic behaviour (recoil= deformation). The dashed lines are to guide the eye.

This deformation mechanism is also supported by the form of the dependence of γ_r on the PP content of the blend (Fig 6.12a). The main change in morphology is the number of elastomer particles per volume (Fig 6.3), which decreases with increasing PP content in the TPV. At low PP content the elastomer network is dense and the particles form steric obstructions for each other. The creep stress of 8 kPa in Fig 6.12 is lower than the yield stress of the TPV E0.4/1.4, the blend with the lowest PP content (Table 6.1), and this TPV does not reach the flow regime under these conditions. The elastomer network is diluted with increasing PP content and the particles are able to cover a larger distance before they are obstructed. The TPVs get softer and need a lower yield stress to break the agglomerated structure; they can flow now at a creep stress 8 kPa. Therefore, the melt reaches larger deformations and the values of γ_r in the transient regime increase. For the same reasons the recovery behaviour also depends strongly on the oil content in the TPVs (Fig 6.12b). The oil reduces the viscosity of the PP phase and the elasticity of the elastomer phase, and, thereby, the yield stress. The creep stress of 8 kPa in Fig 6.12b is below the yield stress of the TPV E0.8/1.0, the blend with the lowest oil content, while it is far above the yield of the TPV E0.8/1.8, the blend with the highest oil content (Table 6.1). The deformation of the latter starts to be non-linear already at short creep times, or 0.2 s.u..

6.4 Discussion

The type of elastomer is the only difference between the two OTPE blends that are compared here. This difference results in different blend morphologies and, hence, different continuity of the elastomer phase. The elastomer particles in the TPVs retain their form upon (re)processing of the blend. The yield stress in these blends originates from the destruction of the initial agglomerated structure of the elastomer particles and the need of the dispersed particles to pass over each other. The cross-links in the SEBS, on the other hand, are reversible during processing above the glass transition temperature of the PS blocks. These cross-links have to be broken in order to let the material flow but they can, then, reform.

In the melt creep experiments, both blends show similar behaviour of the transient viscosity as a function of the strain: an initial sharp increase, followed by a peak located at 0.5-3 s.u.. This indicates that the structure is broken at this strain and the melt can flow afterwards. The behaviour of the recovery strain after creep, on the other hand, shows the differences between the two materials and confirms the specific deformation mechanisms proposed for the blends.

6.4.1 PP-SEBS blends

The PP-SEBS blends consist of two continuous phases with different rheological properties. The PP phase is a viscoelastic fluid, while the SEBS phase shows a transition from elastic to viscous-like behaviour that depends on the amount of oil present in that phase. The two phases show strain relaxation during creep, resulting in a reduction of the recovered strain. The PP phase shows high elastic behaviour (complete recovery of the strain) at low applied creep strains, while at larger strains the recovery strain deviates from total because it reaches the steady state flow regime. For the SEBS phase, on the other hand, strain relaxation occurs already at low strains caused by the long creep times and the migration of the PS end-blocks to other PS domains.

In the ternary blend, the co-continuous structure can change upon deformation. Flow is possible in these blends when the physical cross-links, formed by the PS domains, are broken and rearranged. This occurs already at the lowest stresses measured (0.1 kPa). For these reasons the PP-SEBS blends do not reach a finite deformation at which the viscosity increases to infinity but they can flow with a high viscosity. In the initial (linear) strain regime the structure in the blend remains intact and the system shows elastic response (100% recoil). The strain at the peak in the transient viscosity, where the initial blend structure is broken, coincides with the deviation from the elastic behavior. This point is also the start of the continuous change in blend morphology in the flow regime. The two phases break and rearrange with steady state kinetics and the contribution of the initial structure to the recovery strain has diminished. The remaining melt elasticity in the flow regime is constant, characterized by a constant value of the recovery strain. This represents the contributions of the steady state elasticity of the two individual melt phases and mainly depends on the PP content in the blend.

6.4.2 Thermoplastic Vulcanisates

All the TPVs used have a yield stress for flow. The volume fraction of elastomer particles is so high that they form agglomerated (quasi continuous) structures. At creep stresses higher than the yield stress, this structure is broken and the material flows. The elastomer particles deform elastically by the applied stress and have to pass over each other in this process. The value of the yield stress depends strongly on the volume fraction of the elastomer phase and the viscosity of the PP matrix phase. At creep stresses higher than the yield stress the transient viscosity shows a maximum at 1-3 s.u., where the structure breaks and the flow starts. When the applied stress increases, the elastomer particles deform more and this peak shifts to higher strains.

The recovery behaviour of the TPV after melt creep confirms the hypothesis of positional rearrangement of elastomer particles after a critical deformation. The mechanism of deformation of the TPV melt can be divided into three regimes of strain. In the linear regime the initial blend structure is extended elastically and the strain recovery after removal of the stress is complete. In general, this regime lasts up to 0.2 s.u. If the creep stress is high enough, the network of elastomer particles starts to break in the transient regime. The transient viscosity increases and the melt elasticity decreases. The flow regime starts with a drop in the absolute recovery strain. The particles are able to pass over each other after around 1 s.u. and rearrange their positions. The contribution of the morphology to the melt elasticity is diminished then and the recovery comes mostly from the deformed PP matrix phase. This is opposite to the deformation mechanism in the solid state, where the contribution of the elastomer particles governs the elastic properties of the blend [38, 39]. The final flow regime starts at 1-3 s.u. After the first yield strain, the elastomer particle may be subjected to periodic stretching, hopping over other particles and retraction. This results in an irregular behaviour of the viscosity and the recovered strain at larger applied strains.

6.5 Conclusion

The melt creep and recovery measurements help to elucidate the transient rheological behaviour of the melts of olefinic thermoplastic elastomers and to determine their deformation and flow mechanisms. These mechanisms are governed by the changes of the morphology in the melts. The morphology of the PP/SEBS blends in the absence of flow consists of co-continuous structures of the PP and the SEBS phase with striation sizes in the order of 0.5-3 μm . The cured EPDM in the thermoplastic vulcanisates is present as particles of 1-3 μm dispersed in the PP matrix phase. These elastomer particles form an agglomerated network structure. In both blends the oil is distributed over the PP and the elastomer phase. No measurable yield stress can be found for the PP/SEBS blend, with the exception of the blend with the lowest oil content, where the elasticity of the SEBS phase was high enough to prevent the blends to flow at stresses lower than 2 kPa. Yield stresses were found for all the compositions of the TPVs. They depend strongly on composition and morphology, increasing with increasing number of elastomer particles per volume and decreasing with decreasing matrix viscosity.

When the olefinic thermoplastic elastomers are deformed in the melt, their blend structure changes. The deformation behaviour of the blends during creep flow is related to these changes and can be divided into three strain regimes: The linear regime at low strains, where the initial blend structure is still present and the recovery from creep is complete; the transient regime, where the changes in the morphology take place and where the viscosity shows a maximum; and the steady state flow. The deformation mechanisms in the last two regimes are different for each type of OTPE.

For the PP/SEBS blends the transient viscosity peaks at 0.1-1 s.u.. Both creep time and applied stress affect the viscosity and the strain recovered after stopping the creep flow in the transient regime. A dynamic 'steady state' morphology is formed in the flow regime, which is a balance between break-up and coalescence of the two phases. This results in a constant value of the recovery strain and the viscosity.

The transient viscosity and the recovered strain from creep confirm the yield behaviour of TPVs. After the break-up of the agglomerates, the particles in these blends have to pass over each other before the TPVs are able to flow. The lowest stress at which this is possible is the yield stress. Both transient viscosity and recovery strain have a maximum around 0.5-3 s.u., indicating that the materials also have a *yield strain*, which is the strain needed for an elastic particle to pass over its neighbour.

6.6 References

- [1] Holden G, Legge, N eds. Thermoplastic elastomers, New York, 1996; Hanser
- [2] Ohlsson B, Hassander H, Tornell B, Polym Eng Sci 1996;36:501.
- [3] Veenstra H, van Lent BJJ, van Dam J, Posthuma de Boer A., Polymer 1999;40: 6661.
- [4] Setz S, Stricker F, Kressler J, Duschek T, Mulhaupt R, J. Appl. Pol. Sci 1996;59:1117
- [5] Coran AY, in Holden G, Legge, N eds. Thermoplastic elastomers, New York, 1996;Hanser:p153.
- [6] Abdou-Sabet S, Patel RP, Rubber Chem Technol 1991;64:769.
- [7] Ellul MD, Rubber Chem Technol 1998;71:244.
- [8] Goettler LA, Richwine FJ, Rubber Chem Technol 1981;55:1448.
- [9] Han PK, White JL, Rubber Chem Technol 1995;68:729.
- [10] Ohlsson B, Tornell B, Polymer Eng Sci 1998;38:108
- [11] Steeman P, Zoetelief W, ANTEC SPE Tech Papers 2000;46:3297.
- [12] Jayaraman K, Kolli VG, Kang SY, Kumar S, Ellul MD, J. Appl. Pol. Sci 2004;93:113
- [13] Fritz, HG Bolz U, Cai Q, Pol. Eng. Sci 1999;39:1087
- [14] Lacroix C, Grmela M, Carreau PJ, J.Rheol 1998;42: 41
- [15] Vinckier I, Moldenaers P, Mewis J, J.Rheol 1997;41:705
- [16] Martin P, Carreau PJ, Favis BD, Jerome R, J. Rheol 2000;44: 569
- [17] Araki T, White JL, Polym Eng Sci 1998;38:590.
- [18] Zhou ZW, Solomon MJ, Scales PJ, Boger DV, J. Rheol 1999;43:651
- [19] Watanabe H, Yao ML, Osaki K, Shikata T, Niwa H, Morishima Y, Rheol. Acta 1999; 38:2
- [20] Chapter 5; this thesis
- [21] Veenstra H, van Lent BJJ, van Dam J, Posthuma de Boer A, Polymer 1999;40:5223
- [22] Kishnar, K, Burghardt WR, Lodge TP, Bates FS, J. Rheol. 2002;46:529
- [23] Jansseune T, Moldenaers P, Mewis J, T Rheol. Acta 2004;43:592
- [24] Hayashi R, Takahashi M, Kajihara T, Yamane H, J. Rheol 2001;45:627
- [25] Gramespacher H, Meissner J, J. Rheol 1995;39:151
- [26] Vinckier I, Mewis J, Moldenaers P, Rheol Acta 1999;38:65

- [27] Vinckier I, Mewis J, Moldenaers P, Rheol Acta 1999;38:198
- [28] Krishnan K, Burghardt WR, Lodge TP, Bates FS, Langmuir 2002;18:9676
- [29] Berret JF, Langmuir 1997;13:2227
- [30] Lerouge S, Decruppe JP, Berret JF, Langmuir 2000;16:6464
- [31] Sengupta P, PhD thesis, Twente University, Enschede, 2004.
- [32] Mortensen K, Theunissen E, Kleppinger R, Almdal K, Reynaers H, Macromolecules 2002;35:7773
- [33] Hotta A, Clarke SM, Terentjev EM, Macromolecules 2001;35:271
- [34] Berry GC, Hager BL, Wong CP, Macromolecules 1977;10:367
- [35] Paulin SE, Ackerson BJ, Wolfe MS, Phys Rev Lett E 1997;55:5812
- [36] Uhlherr PHT, Gou J, Tiu C, Zhang XM, Zhou JZQ, Fang TN, J Non-Newton Fluid Mech 2005;125:101
- [37] Chapter 7; this thesis
- [38] Soliman M, van Dijk M, van Es M, Shulmeister V, ANTEC 1999:1051
- [39] Boyce MC, Yeh O, Socrates S, Kear K, Shaw K, J. Mech Phys Sol 2001; 49:1343

Chapter 7

Capillary rheology of Olefinic Thermoplastic Elastomer blends

*Comparing viscosity and processability of blend
with co-continuous or dispersed structures*

Abstract

The viscosity and processability of two olefinic thermoplastic elastomer blends is studied by capillary rheometry. The blend properties are related to the morphology and composition of the blend. The first blend type consists of PP, the triblock copolymer SEBS and paraffinic oil. These blends show co-continuous structures of a PP-rich phase and an SEBS-rich phase at all compositions used. The oil is distributed over the two phases. The blend viscosity can be approached by the logarithmic addition of the viscosities of the two phases according to their weight fractions. The extrudates show smooth surfaces and low swell, indicating that flow instabilities are absent or suppressed. This behaviour can be addressed to the continuing change in the blend morphology and the reversibility of the physical cross-links in the SEBS phase. The second blend type, the thermoplastic vulcanisates (TPV) consist of cured elastomer particles dispersed in a PP matrix. These blends also contain paraffinic oil that is distributed over the PP and the elastomer phase. Due to the high volume fraction of elastomer particles, the TPV have a yield stress for flow. To include this in the rheological evaluation and the Herschel-Bulkley equation has to be used for the shear stress in the capillary. The power-law index of the TPVs is close to the one of the PP phase, indicating that the flow properties at high shear rates are dominated by the PP phase. The yield stress increases with decreasing PP or oil content. Their values however, are lower than the ones determined by melt creep measurements. The strands of the TPVs with high elastic behaviour (low PP or oil content) show melt fracture. The extrudate swell is low, but larger than the PP/SEBS blends, and it increases with increasing PP content.

Based on:

W.G.F. Sengers, A.D. Gotsis and S.J. Picken: submitted to the Journal of Applied Polymer Science

7.1 Introduction

Blending an elastomer with a thermoplastic polymer can result in materials called thermoplastic elastomers (TPE) [1]. They have rubber-like properties but can be processed with common thermoplastic processing equipment, such as extrusion and injection moulding. These properties are due to the two-phase structure of the blend. The soft phase (elastomer) gives the material the rubber-like properties, while the hard phase (thermoplastic polymer) acts as physical cross-linker and gives strength to the blend. At elevated temperatures the latter phase melts and the material can be processed with thermoplastic processing equipment. TPEs based on blends of polypropylene (PP) with an olefinic elastomer are an important class because they can be good alternatives for vulcanised EPDM rubber. Two types of olefinic TPE blends (OTPE) are the subject of the present study. They both contain PP as the hard phase and only the type of olefinic elastomer is different.

The first type of OTPE used here contains the random copolymer ethylene-propylene-diene terpolymer (EPDM) and the second type contains the triblock copolymer polystyrene-block-poly(ethylene-co-butylene)-block-polystyrene (SEBS). These two elastomers differ in the type of cross-links (chemical and physical respectively) and, as a result, the morphology is either particle in matrix in the PP/EPDM blends [2,3] or co-continuous in the PP/SEBS blends [4-6]. Both blends also contain considerable amounts of oil paraffinic oil. This oil is added to improve the processability and to make softer TPE compounds. It is present in both the elastomer and the PP phase and has a large effect on the phase properties.

In the blends of PP with EPDM, called thermoplastic vulcanisates (TPV), the elastomer phase is cured during continuing mixing with PP [2]. The elastomer phase changes from a viscous fluid into an elastic solid and, thereby, it breaks up. The blend morphology consists of cured, micron-sized elastomer particles dispersed in a PP matrix [3]. This morphology is permanent and does not change upon (re)processing of the TPV. The SEBS is a triblock copolymer with an elastomeric middle-block of poly(ethylene-butylene) (EB) between two polystyrene (PS) end-blocks. The PS end-blocks form separate domains and act as physical cross-links for the EB phase [7]. Above the glass transition temperature of the PS blocks, they are able to break and rearrange and the material becomes processable; SEBS itself is already a TPE. SEBS is blended with PP to improve the processability and to make a compound with a higher modulus. Depending on the SEBS and PP type used and the processing conditions, the PP/SEBS blends show co-continuous structures over a broad concentration range [4,5]. The PS domains have a stabilising effect on the formation of these structures.

The rheological properties of TPVs were first studied by Goettler [8]. These blends show many similarities with highly filled polymers, including possible yield stress for flow. Due to the high volume fraction of the elastomer phase, the elastomer particles form an agglomerated network-like structure that has to be broken in order for TPV to start to flow. Akari and White [9] and Steeman and Zoetelief [10] confirmed the existence of a yield stress by melt creep experiments. Sengers [11] studied the effect of composition on the yield stress. He found that the yield stress increases with

increasing the content of the elastomer (by the decrease of PP content) or increasing the matrix viscosity (by the decrease of oil content).

Most rheological studies performed on TPVs are based on capillary rheometry [8,10,12-14]. The materials studied include also other polymer-elastomer combinations [15-17]. In general, it has been found that the viscosity of the TPVs does not reach zero shear plateau viscosity values and the regime of power-law like shear rate thinning is extended to very low shear rates. In most studies until now, however, the yield behaviour is not included in the quantification of the shear viscosity.

Goettler [8] studied the processability of TPVs. The extrudate swell of the TPVs with cured elastomer phase is lower than the uncured analogues, because of the limited possible deformation of the elastomer phase, and the extrudate swell increases with increasing hardness of the TPV, i.e. increasing PP content.

Ohlsson et al. [18] studied the rheological properties of PP/SEBS/Oil blends. In capillary rheometry, the rheological properties appeared to be controlled by the PP phase. The viscosity shows power-law like shear-rate thinning behaviour with an index close to the one of the PP phase. Because the viscosity of the PP phase is lower than the one of the SEBS, phase segregation occurs. The extrudates from capillary rheometry have a PP rich skin layer. Injection moulded parts show flow induced surface heterogeneities.

The co-continuous morphology, such as the one of the PP/SEBS blends, in general is a dynamic equilibrium structure and is subjected to changes when deformation is applied on the material. Veenstra et al. [19] showed that this is the case for polymer blends and Krishnan [20] for bi-continuous microemulsions.

In this chapter, the viscosities of the two OTPE blend types are quantified by taking into account the blend morphology. The processability of the materials is studied by examining the extrudate swell and the appearance of the extrudates surface texture. The effect of morphology is studied by comparing the two OTPE blends at similar compositions. The processability can be understood by the nature and the changes in the blend morphology and the properties of the PP and elastomer phases.

7.2 Experimental

7.2.1 Materials

Two types of TPE blends are used in this article. To make a direct comparison, the two blend types contain the same PP matrix (PP homopolymer with a MFI of 0.3 dg/min at 230 °C and 2.16 kg, DSM Polypropylenes) and paraffinic oil (Sunpar 150, Sun Oil Company). The PP-SEBS blends contain SEBS (KRATON® G 1651, KRATON Polymers) as elastomer and the TPVs contain EPDM (63 wt % C2, 4.5 wt% ENB, extended with 50 wt% of paraffinic oil, DSM Elastomers). The EPDM in the TPVs is dynamically vulcanised using 5 phr phenolic curing agent (SP® 1045, Schenectady) in combination with 1 phr Stannous Chloride and Zinc Oxide (Merck).

All materials contain antioxidants (0.5 wt% Irganox 1076 and 0.5 wt% Irgafos 168, Ciba Specialty Chemicals).

Table 7.1: Composition of blends

Code	PP (wt%)	EPDM (wt%)	SEBS (wt%)	Oil (wt%)
S0.4/1.4	14.3		35.7	50.0
S0.8/1.0	28.6		35.7	35.7
S0.8/1.4	25.0		31.3	43.8
S0.8/1.8	22.2		27.8	50.0
S1.2/1.4	33.3		27.8	38.9
E0.4/1.4	14.3	35.7		50.0
E0.8/1.0	28.6	35.7		35.7
E0.8/1.4	25.0	31.3		43.8
E0.8/1.8	22.2	27.8		50.0
E1.2/1.4	33.3	27.8		38.9

7.2.2 Sample preparation

The PP-SEBS blends were prepared with a ZSK-25 co-rotating twin screw extruder operated at 250 rpm; the TPVs were prepared with a ZSK-40 co-rotating twin screw extruder, operated at 350 rpm. The temperature in the extruder ranged from 180 at the hopper to 210 °C at the die. The blend composition was varied in order to study the influence of the content of PP and oil. Similar compositions were used for the PP-SEBS and TPV blends. These compositions are shown in Table 7.1. The letter ‘S’ in the coding indicates the PP-SEBS blends and ‘E’ the TPV blends. The numbers x/y stand for the PP-elastomer and for the oil-elastomer ratio.

Binary PP-oil mixtures were made in an internal batch mixer (Brabender Plasticorder 20 cc with Banbury rotors) at 180 °C and 100 rpm. The SEBS-oil mixtures were prepared by dry blending the SEBS pellets with oil.

7.2.3 Morphology

The morphology of the TPE blends was studied by transmission electron microscopy (TEM, Philips CM30). The samples were microtomed at –130 °C using a diamond knife followed by vapour staining with ruthenium tetroxide for 10 minutes.

7.2.4 Rheology

The rheological measurements were performed at 190 °C in a Rosand Precision Capillary Rheometer. Two sets of capillary dies were used: $l/d = 4/1, 16/1, 30/1$ and $4/2, 20/2$ mm/mm. All capillaries have entrance angled of 90°. The Bagley correction was applied to correct the data for capillary entrance and exit effects. The apparent shear rate, $\dot{\gamma}_{app}$, and the shear stress at the wall, σ_w , were calculated from the volume flow rate, Q_V , and the pressure drop over the capillary, ΔP , by:

$$\dot{\gamma}_{app} = \frac{4Q_V}{\pi R^3} \quad (7.1)$$

and

$$\sigma_w = \frac{R \cdot \Delta P}{4L} \quad (7.2)$$

where R and L are the capillary radius and length respectively. The apparent viscosity, η_{app} , is calculated by:

$$\eta_{app} = \frac{\sigma_w}{\dot{\gamma}_{app}} \quad (7.3)$$

The data of the TPVs are analysed using the Hershel-Bulkley expression for the shear stress (Eq 7.7 in section 7.3.3.2).

7.2.5 Extrudate swell and surface appearance

The extrudate strands of the 1 mm capillary were used to study the processability of the OPTE blends. The extrudate swell, D , was determined from the diameter of the strands at room temperature, d_{25} , and corrected for the change in density:

$$D = \frac{d_{RT}}{d_{cap}} \sqrt[3]{\frac{\rho_{RT}}{\rho_{190}}} - 1 \quad (7.4)$$

where d_{cap} is the capillary diameter (= 1 mm), and ρ_{RT} and ρ_{190} are the densities at room temperature and at 190 °C. The blend densities were calculated by the weight fractions in the blend. The values of the densities of each component are listed in Table 7.2. The surface appearance was studied by optical examination of the extrudates. Three surface types were defined to indicate flow instabilities during extrusion: smooth, sharkskin and gross melt fracture. A sharkskin structure indicates melt fracture. The periodic curling of the extrudates is caused by flow instabilities in the capillary entrance.

Table 7.2: Densities of the blend components at 25 and 190 °C

	PP	Oil	EPDM	SEBS
ρ_{25} (kg/m ³)	0.91	0.88	0.75	0.91
ρ_{190} (kg/m ³)	0.77	0.79	0.73	0.87

7.3 Results and discussion

The only differences between the two OTPE are the type of elastomer and the blend morphology. The SEBS contains physical cross-links that can break and rearrange and the blends of PP with SEBS show co-continuous structures over a broad concentration range. The EPDM in the TPVs is present as chemically cross-linked particles dispersed in the PP matrix phase. The PP and the elastomer phases are not pure but they contain paraffinic oil in both blend types. In the next paragraph, the rheological properties of these two phases are studied by series of PP-oil and SEBS-oil binary mixtures. They are used to estimate the properties of the two phases in the blends.

7.3.1 Binary mixtures

Figs 7.1 and 7.2 show the apparent viscosity, η_{app} , of the series PP-oil and SEBS-oil binary mixtures respectively. Capillary rheology tests on EPDM-oil vulcanisates could not be performed, because the elastomer phase in the TPVs is cured; their elasticity modulus was estimated at 60-100 kPa [21]. The oil has a diluting effect on PP and on SEBS. The viscosity at a constant shear rate decreases gradually with increasing oil content. The PP-oil mixtures show the characteristic viscosity curve of entangled polymer melts: a zero shear viscosity and shear thinning at high shear rates (Fig 7.1). The viscosity of pure SEBS could not be measured accurately because it was too viscous and too elastic at this temperature. The SEBS contains physical cross-links and, therefore, a yield stress for flow is expected. The stresses in the capillary are high enough to enable flow for all SEBS-oil mixtures with 30 wt% oil or more. These mixtures behave as linear polymers (Fig 7.2).

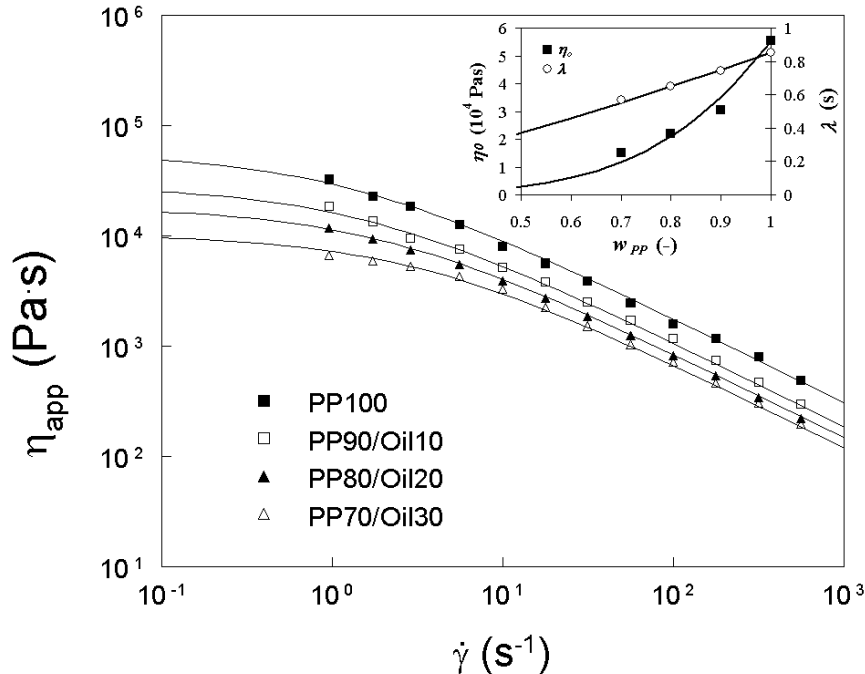


Figure 7.1: Viscosity of PP-oil binary mixtures at 190 °C. The lines are the fits with Eq. 7.5. The insert shows the dependence of the Cross parameters η_0 and λ on the PP content.

The viscosity curves of both types of binary mixtures can be fitted with the Cross equation:

$$\eta_{app}(\dot{\gamma}) = \frac{\eta_0}{1 + (\lambda\dot{\gamma})^m} \quad (7.5)$$

The power-law index, m , is related to the shear thinning behaviour of the viscosity at high shear rates: $\eta = k\dot{\gamma}^{n-1}$. Thus $m = 1 - n$. The inserts in Figs 7.1 and 7.2 show the values of η_0 and λ as a function of the polymer content in the binary mixture. Increasing the oil content in the binary mixture, c_{oil} , results in a gradual decrease of the values of the Cross parameters, η_0 and λ , indicating that the viscosity becomes lower and the shear thinning starts later. This behaviour was also observed in dynamic oscillatory measurements of these materials [21]. The time constant $1/\lambda$, which give the onset of shear thinning, increases due to the time shift of the relaxation spectrum by the plasticizing effect of the oil. The decrease in η_0 is due to the lower number of entanglements per volume in the diluted binary mixtures. The values of η_0 and λ can be fitted with power-law function of the polymer or elastomer concentration, which are listed in Table 7.3. These functions will be used to estimate $\eta_{app}(\dot{\gamma})$ of both the PP and the elastomer phase in the following sections. The power-law indices of the SEBS-oil mixtures are lower than the ones of the PP-oil mixtures, indicating a stronger shear thinning in the former case. The shear rate where shear thinning starts (at $\dot{\gamma} = 1/\lambda$) is lower in the SEBS-oil mixture than in the PP-oil.

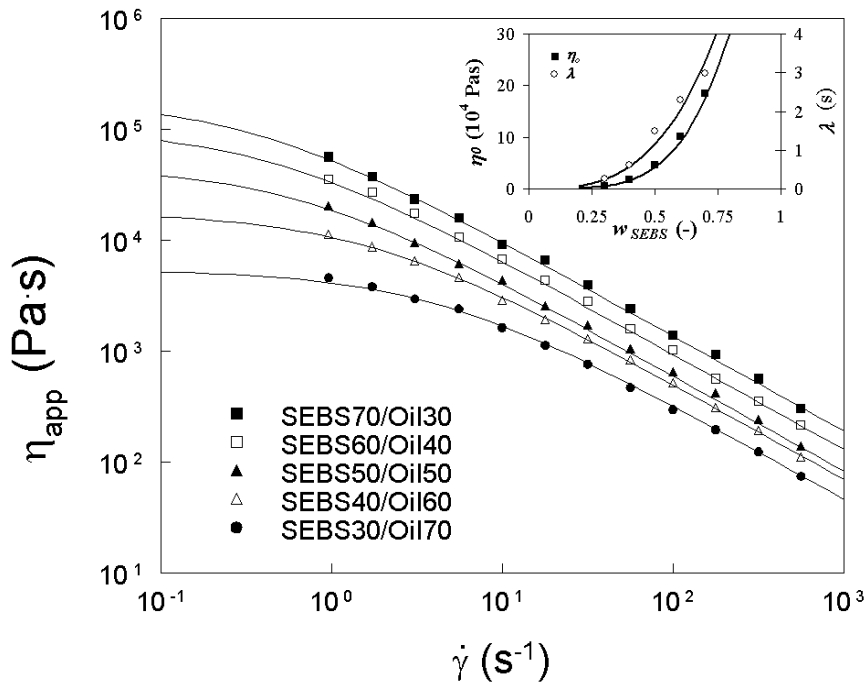


Figure 7.2: Viscosity of SEBS-oil binary mixtures at 190 °C. The lines are the fits of Eq. 7.5. The insert shows the dependence of the Cross parameters η_0 and λ on the SEBS content.

Table 7.3: Dependence of Cross parameters on the polymer content in binary mixtures

	PP-oil	SEBS-oil
η_0 (10^4 Pas)	$\eta_0 = 5.5 \cdot C_{PP}^{3.6}$	$\eta_0 = 78 \cdot C_{SEBS}^{4.2}$
λ (s)	$\lambda = 0.85 \cdot C_{PP}^{1.2}$	$\lambda = 10.1 \cdot C_{SEBS}^{3.1}$
m (-)	$m = 0.77$	$m = 0.86$

7.3.2 PP/SEBS blends

7.3.2.1 Morphology

Fig 7.3 shows TEM images of PP/SEBS blends with different PP content. The SEBS appears as a dark grey phase, while the light grey corresponds to the PP phase. The magnification in the figure is suitable to observe the blend structure but it is too low to discern the 20 nm PS domains that are dispersed in the ethylene–butylene matrix of the SEBS block copolymer. Both phases seem to be continuous, even though it is impossible to establish the continuity of the phases in the blends by microscopy alone. The co-continuous structure was confirmed in the present work by selective extraction of the SEBS and the oil [22]. In all these blends more than 95% of SEBS was recovered and the remaining PP phase was self-supporting. The size (*‘striation thickness’*) of the SEBS phase is 0.5–1 μm and decreases with increasing PP/elastomer or oil/elastomer ratio. This decrease results also in a reduction of the interconnectivity of the SEBS phase.

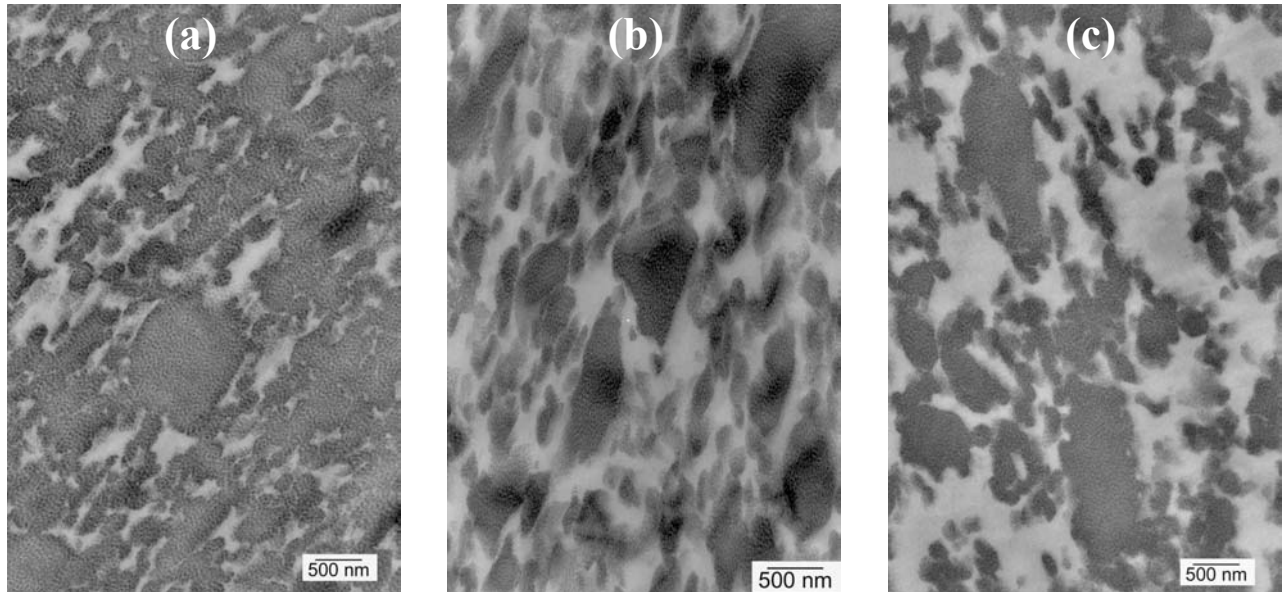


Figure 7.3: TEM Images of PP/SEBS blends with different PP content
(a) S0.4/1.4 (b) S0.8/1.4 and (c) S1.2/1.4

7.3.2.2 Viscosity

The formation and existence of co-continuous structures, in general, depend on the applied stress, the flow history and the properties of both phases [23-26]. The blends are able to adapt to the applied stress by break-up and rearrangement of the two phases.

Fig 7.4 shows the curves of $\eta_{app}(\dot{\gamma})$ with the composition of PP/SEBS blends as a parameter. The curves of PP-oil and SEBS-oil binary mixtures corresponding to the blend S0.8/1.4 are included in Fig. 4a. The blend viscosities from the two different capillary diameters show good agreement with each other. The viscosity of the SEBS phase is higher at low shear rates than the one of the blends. Because of the different slopes the curves of the blends cross each other, at around $\dot{\gamma}_{app} = 100 \text{ s}^{-1}$. The blend viscosities measured in the different capillary diameters show good agreement with each other, which indicates that wall slip is negligible.

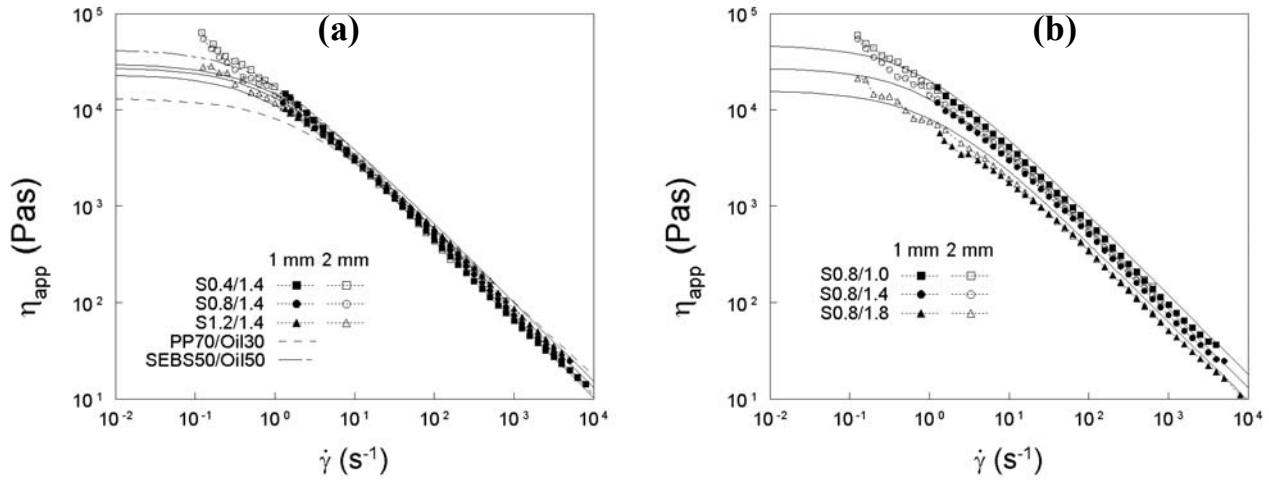


Figure 7.4: Viscosity of PP/SEBS blends at 190 °C. (a) different PP content (b) different Oil content. The solid lines are the fits of Eq. 7.6; The dashed lines are the PP-oil and elastomer-oil binary mixtures.

Fig 7.4a shows the effect of the PP content on the blend viscosity. Increasing the PP content in the blend results in a gradual change from SEBS-like to PP-like behaviour as the slope of this curve decreases. $\eta_{app}(\dot{\gamma})$ increases with increasing PP content at shear rates higher than 20 s^{-1} , while the opposite behaviour occurs at lower shear rates. Because the two phases are, or can be, continuous, they both have a weighted contribution to the blend viscosity. A higher mass fraction of the PP phase results in a more PP-like behaviour. Fig 7.4b shows the effect of oil on $\eta_{app}(\dot{\gamma})$. The extra amount of oil is distributed over the two phases and, as shown for the binary mixtures, the oil dilutes both phases. The increasing of oil content results thus in a lower blend viscosity but the shape of the curve is not affected. From morphological observation and from modelling the dynamic shear moduli [21] of these blends it has been concluded that the volume fractions do not change significantly with increasing oil content. Only the dimensions (striation size) of the two phases increase.

The gradual change in $\eta_{app}(\dot{\gamma})$ of the blends from SEBS-like to PP-like behaviour can be described by the logarithmic addition rule (Eq. 7.6) of the two phases.

$$\eta_{TPE} = \eta_{PP}^{w_{pp}} \cdot \eta_{SEBS}^{1-w_{pp}} \quad (7.6)$$

where w_i and η_i are the phase weight fraction and the viscosity of phase i. The

viscosities of the two phases are calculated from the functions listed in Table 7.3 and the actual polymer/oil concentrations are estimated from modelling the dynamic shear moduli of these OTPE blends [21]. Negative deviation of the blend viscosity from Eq. 7.6 can be caused by miscibility of the two polymers [27] or interfacial slip between the phases [28], while positive deviation indicates good interaction between the phases [29]. The viscosities of the two phases of the PP/SEBS blends are comparable (at least at high shear rates) and the interfacial tension between the two phases is low. Both phases are deformed affinely and the viscosity of the blends fit the logarithmic additivity rule well.

The calculated values of $\eta_{app}(\dot{\gamma})$ (solid lines in Fig 7.4) are in good agreement with the experimental data. At the lowest shear rates the calculated values show a negative deviation from the experimental ones. This deviation becomes larger with increasing mass fraction of the elastomer phase. In this regime, the viscosity of the elastomer phase is much higher than the PP phase. Due to this larger viscosity difference and due to the presence of physical cross-links, the kinematics of break-up and coalescence change there. The low viscous PP phase tends to encapsulate the elastomer phase and the blend behaves more like a highly filled polymer.

7.3.2.3 Extrudate swell and surface appearance

The processability of the two OTPE blends was studied by observation of the extrudates. The extrudate swell, D , as defined by Eq. 7.4, is a measure of the remaining melt elasticity after the flow in the capillary. In the capillary, the polymer chains are extended in the direction of the shear flow. When the material leaves the capillary, there is no external force working on it and the polymer chains tend to go back to their unstretched shape, resulting in an increase of the extrudate diameter. The elasticity of polymers decreases in time due to disentanglement. The increase of the residence time in the capillary results in lower swell of the extrudates because the melt forgets the intensive extensional flow at the entrance region. On the other hand, the surface texture and shape of the extrudates is an indication for the occurrence of flow instabilities and melt fracture in the capillary.

Fig 7.5 shows the extrudate swell of the PP/SEBS blends as a function of shear stress. The values for PP-oil and SEBS-oil binary mixtures are included in Fig 7.5a to show the behaviour of the two phases in the blend S0.8/1.4. With increasing the stress, the PP phase shows a large increase in extrudate swell. The PP shows normal behaviour for an entangled, high molecular weight linear polymer with a broad molecular weight distribution. The increase in shear rate results in higher stresses in the capillary and shorter residence times. With increasing the shear stress, the PP is thus more extended for a shorter time. This results in a high elastic recovery and an increase for D . On the other hand, the extrudate swell of the SEBS phase is almost negligibly small. The physical cross-links of the SEBS are broken and the elastomer is able to flow, as shown in Fig 7.2. Restructuring of the physical cross-links takes place during flow and, thereby, the SEBS-oil binary mixture does not show high elasticity. This observation is interesting as it shows that a TPE, which is associated with high melt elasticity in the solid state, does not behave always also as an elastic solid.

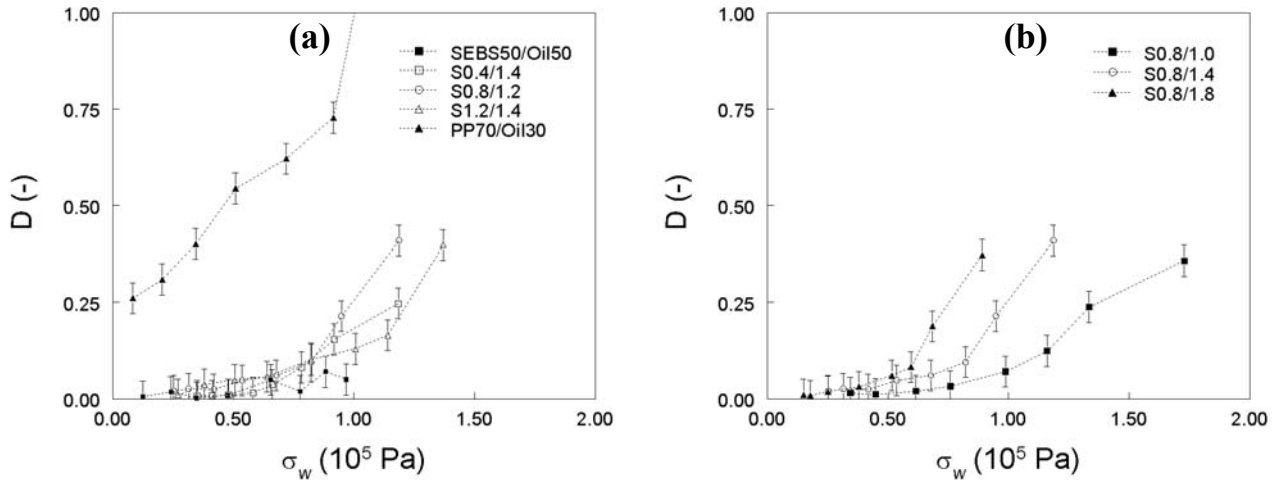


Figure 7.5: Effect of composition on extrudate swell of PP/SEBS blends at 190 °C.
(a) different PP content (b) different Oil content.

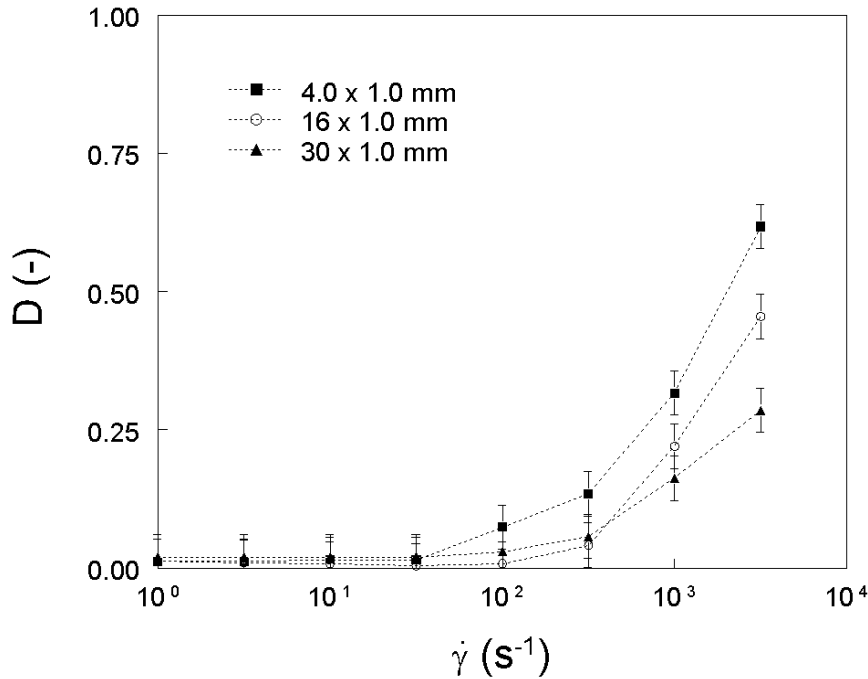


Figure 7.6: Effect of capillary length on extrudate swell of PP/SEBS blend S1.2/1.4 at 190 °C

In the capillary, the morphology of the blend changes continuously. In this process, the extended PP phase is able to relax from strain through adjustment of the phase morphology. The initial melt elasticity that is mainly caused by the PP phase, decreases rapidly and D is low. Comparable behaviour of the remaining melt elasticity was observed in melt creep experiment [11]. No trends were found when changing the PP content in the blend (Fig 7.5a). Fig 7.5b indicated that D increases with increasing oil content. This is due to the lowering of the viscosity of the phases, which accelerates the restructuring of the morphology and increases the shear rates at a constant stress. The residence time increases and the remaining melt elasticity is, therefore, higher. Hence, D of all the blends has comparable values at the same shear rates.

The effect of the capillary length on D is shown in Fig 7.6 for the sample S1.2/1.4 as a function of the shear rate. This blend has the highest PP content and the effect of the residence time should, therefore, be the most pronounced. At a constant shear rate D decreases with increasing the capillary length, as expected. The blend has a longer residence time in the capillary. The curves of $D(\dot{\gamma})$ remain comparable in shape and are shifted on the time scale.

Table 7.4: Surface appearance of PP/SEBS blends as they emerge from the capillary 16 x 1 mm at 190 °C.

shear rate (s ⁻¹)	1	3.2	10	31.6	100	316	1000	3162
SEBS50/Oil50	shark skin							
S0.4/1.4	smooth							
S0.8/1.0	smooth							
S0.8/1.4	smooth							
S0.8/1.8	smooth							
S0.4/1.4	smooth							
PP70/Oil30	smooth		sharks kin		sharkskin, gross fracture		gross fracture	

Table 7.4 shows the surface appearance of the extrudates of the ternary blends. It also shows the surface appearance of the two phases in the blend S0.8/1.4 when extruded apart. The two phases show melt fracture. This starts already at low shear rates for the SEBS-oil binary mixture and it becomes more pronounced at shear rates higher than $\dot{\gamma}_{app} = 100 \text{ s}^{-1}$. The instability in the PP-oil extrudates starts at $\dot{\gamma}_{app} = 10 \text{ s}^{-1}$ and at $\dot{\gamma}_{app} = 100 \text{ s}^{-1}$, the onset of the increase of extrudate swell, the strands curl into a spiral shaped strand. The ternary blends all have smooth surfaces, independent of composition or shear rate. One possible reason is that the flow instabilities are absorbed by the continuing evolution in blend morphology. On the other hand, Ohlsson et al. [18] found that the surface of the extrudates consists of a low-viscous PP rich layer. This layer lowers the blend viscosity and prevents stick slip behaviour.

7.3.3 Thermoplastic Vulcanisates

7.3.3.1 Morphology

In the preparation process of the TPVs (*dynamic vulcanisation*) the elastomer phase is cured during continuous mixing of the blend and it changes from a viscoelastic liquid into an elastic solid. This phase breaks up into microns-sized elastomer particles and its coalescence is restricted. TPVs can be prepared with very high (80 wt%) content of dispersed elastomer phase using this process.

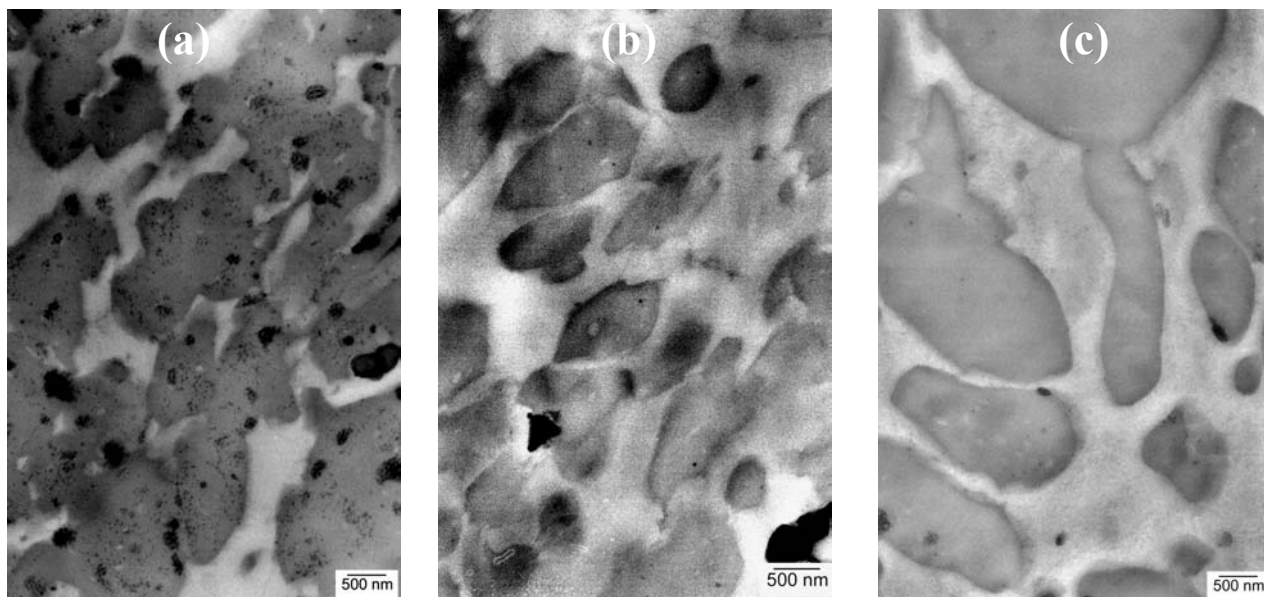


Figure 7.7: TEM Images of TPVs with different PP content.
(a) E0.4/1.4 (b) E0.8/1.4 and (c) E1.2/1.4

Fig 7.7 shows TEM images of TPVs with different PP/elastomer ratios. The EPDM phase is the darker areas. The morphology consists of elliptically shaped dispersed EPDM particles with lengths of 1–2 μm , even for the blend E0.4/1.4 (Fig 7.7a), despite its very high elastomer content (>70 wt%). This morphology was confirmed using low-voltage SEM (LVSEM) [22]. Upon increasing the PP/elastomer ratio, the average particle size decreases and the inter-particle distance increases; increasing the oil/elastomer ratio results in larger particles and a reduction of the inter-particle distance.

7.3.3.2 Viscosity

Due to the high volume fraction, the elastomer phase form an agglomerated network of elastomer particles that has to be broken to enable flow of the TPV. This results in a yield stress for flow [8-11]. To quantify the flow behaviour of the TPVs from the capillary measurements, an expression for the volumetric flow rate, Q_v , as a function of the pressure drop over the capillary, $\Delta P/L$, has to be used that includes the yield behaviour, instead of Eqs. 7.1-7.3.

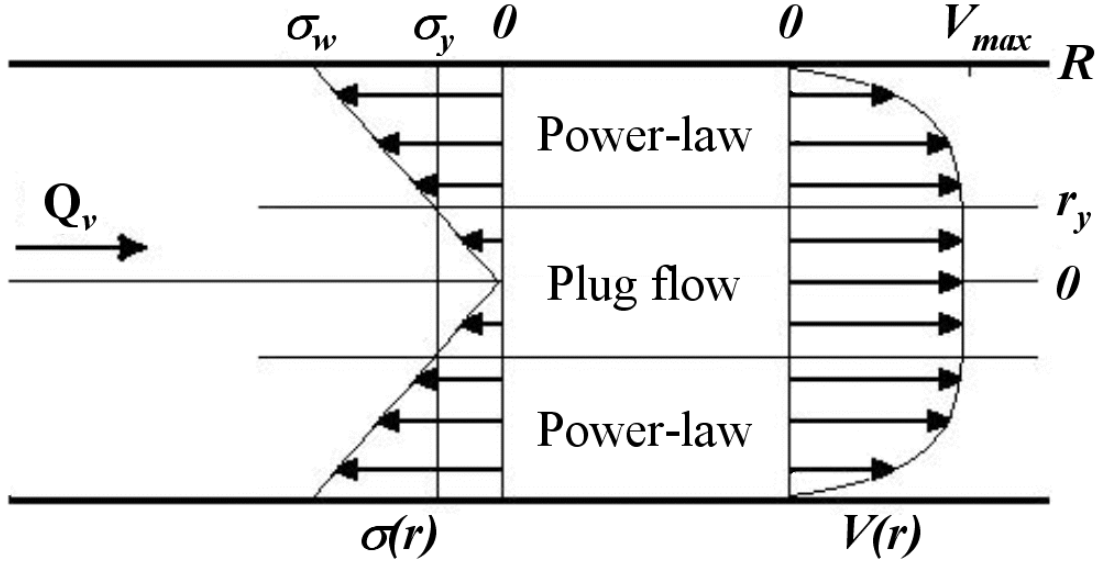


Figure 7.8: Velocity profile in a cylindrical capillary for a Herschel-Bulkley fluid.

The Heschel-Bulkley expression is chosen for the shear stress, σ . It consists of addition of a yield stress, σ_y to the power law behaviour of the viscosity:

$$\sigma = \sigma_y + k\dot{\gamma}^n \quad (7.7)$$

in which k and n are the stress constant and the exponent of the power law. The velocity profile in the capillary (Fig 7.8) can be derived using Eq 7.7 . This derivation is shown in the Appendix. The local stress in the capillary is a linear function of the pressure drop and the radius (Eq. 7.8a).

$$\sigma = \frac{\Delta P r}{2L} \quad (7.8a)$$

$$r_y = \frac{2L\sigma_y}{\Delta P} \quad (7.8b)$$

At stresses below the yield stress, the agglomerated structure is still present and the elastomer phase is only deformed partially. The material is transported as a plug with a constant velocity and the shear rate is zero (Eq. 7.9a). This regime lasts up to r_y , the radius at with the local stress is equal to the yield stress (Eq. 7.8b). At higher stresses, or from r_y to R , the velocity profile corresponds to power-law viscosity behaviour and the shear rate can be calculated from Eq. 7.9b.

$$\dot{\gamma} = 0 \quad \text{for } 0 \leq r < r_y \quad (7.9a)$$

$$\dot{\gamma} = \left[\frac{\sigma - \sigma_y}{k} \right]^{1/n} \quad \text{for } r_y \leq r \leq R \quad (7.9b)$$

The velocity profile in the capillary consists thus of a combination of plug flow behaviour in the core and a shell of power-law behaviour. The flow rate is the integral of this velocity profile and can be related to $\Delta P/L$:

$$Q_v = 2\pi R^{\frac{3n+1}{n}} \frac{n}{n+1} \cdot \left[\frac{-\Delta P}{2kL} \right]^{\frac{1}{n}} \cdot \left[\begin{aligned} &\frac{1}{2} \left[1 - \frac{2L\sigma_y}{\Delta PR} \right]^{\frac{n+1}{n}} \\ &- \frac{n}{2n+1} \left[1 - \frac{2L\sigma_y}{\Delta PR} \right]^{\frac{2n+1}{n}} \\ &+ \frac{n}{2n+1} \cdot \frac{n}{3n+1} \left[1 - \frac{2L\sigma_y}{\Delta PR} \right]^{\frac{3n+1}{n}} \end{aligned} \right] \quad (7.10)$$

where σ_y , k and n , the material parameters, can be found by fitting the experimental data to this equation. The viscosity can be calculated then by:

$$\eta_{app}(\dot{\gamma}) = \frac{\sigma_y}{\dot{\gamma}} + k\dot{\gamma}^{n-1} \quad (7.11)$$

Fig 7.9 shows the flow rate as a function of the pressure drop for two capillary diameters after the Bagley correction. The experimental data can be fitted well with Eq. 7.10 for the 1 mm capillary (lines in Fig 7.9). The pressure drop over the 2 mm capillary was low and inaccurate for a successful fit. The pressure drop, $\Delta P/L$, at which Q_v asymptotically decreases to zero is a measure for the yield stress. The values of the σ_y , k and n evaluated from the fitting the curves in Fig 7.9 for the TPVs are listed in Table 7.5. The yield stresses obtained from creep measurements [11] are also included. The power law indices, n , of the TPVs are close to the values of the PP-oil binary mixtures ($n_{PP}=0.23$, Table 7.3), indicating that the flow behaviour at high shear rates is dominated by the PP phase. The index increases with increasing PP content and remains constant with changing oil content. The yield stress decreases with increasing PP or oil content. These trends were also observed in the melt creep experiments. The decrease of the yield stress with increasing PP content is due to the decrease of the density of the elastomer network. The oil reduces the matrix viscosity and, thereby, the stress needed to break the elastomeric network. The yield stresses from the capillary measurements are lower than those observed in melt creep experiments. Apparently, a network of elastomer particles in extended state (capillary flow) is easier to break than from a quiescent state (melt creep).

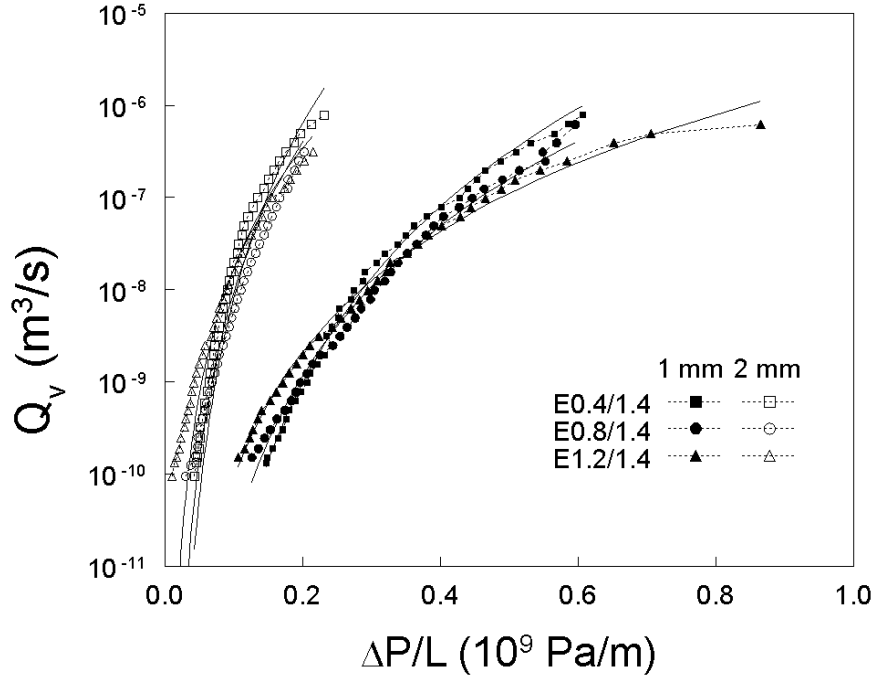


Figure 7.9: Flow rate as a function of the pressure drop for TPVs with different PP content at 190 °C. Lines are fits for Eq 7.10.

Table 7.5: Power law parameters and yield stress for TPVs at 190 °C

Code	n (-)	k (kPas ⁿ)	σ_y (kPa)	σ_y^a (kPa)
E0.4/1.4	0.18	24.9	6.4	12-13
E0.8/1.0	0.21	31.4	7.2	13-15
E0.8/1.4	0.20	23.3	5.2	6.5 - 8
E0.8/1.8	0.19	19.0	1.4	5 - 6
E1.2/1.4	0.24	19.2	3.0	5 - 7.5

a: from Chapter 6

Fig 7.10 shows the apparent viscosity of the TPVs, calculated by the Eqs. 7.1-7.3. The solid lines are the fits of Eq. 7.11 and show good agreement with the experimental data. The viscosity of the TPVs at low shear rates still shows power-law behaviour as a result of the yield stress. The amount of PP in the TPV does not affect the viscosity much (Fig 7.10a). The curve of a PP-oil binary mixture is included in this figure to show the behaviour of the PP phase of the blend E0.8/1.4. At high shear rates, the viscosity is comparable to that of the PP phase and increases slightly with increasing PP content. This increase is due to the change in oil distribution [21]. With increasing PP content, the oil concentration in the PP phase decreases and the viscosity of this phase increases. The PP-like behaviour of the TPVs at these shear rates are due to the high stresses. The stress at the wall is very high and the relative contribution of the yield stress of the TPVs to the flow behaviour decreases. At $\dot{\gamma}=100 \text{ s}^{-1}$ an inversion of the trend occurs and the viscosity now decreases with increasing PP content. At these shear rates the unyielded region of the flow becomes small and the agglomerated network structure of the elastomer may start to break even there. For the TPVs with low PP content, the power-law like behaviour continuous even at low shear rates. Increasing the PP content results in a negative

deviation from the above behaviour. The yield stress decreases and more material has yielded. Fig 7.10b shows the effect of oil on the viscosity. The oil dilutes both phases and, as a result, both the viscosity of the PP matrix phase and the yield stress of the TPV decrease. The viscosity of the TPVs decreases over the whole range because of the lower resistance to flow.

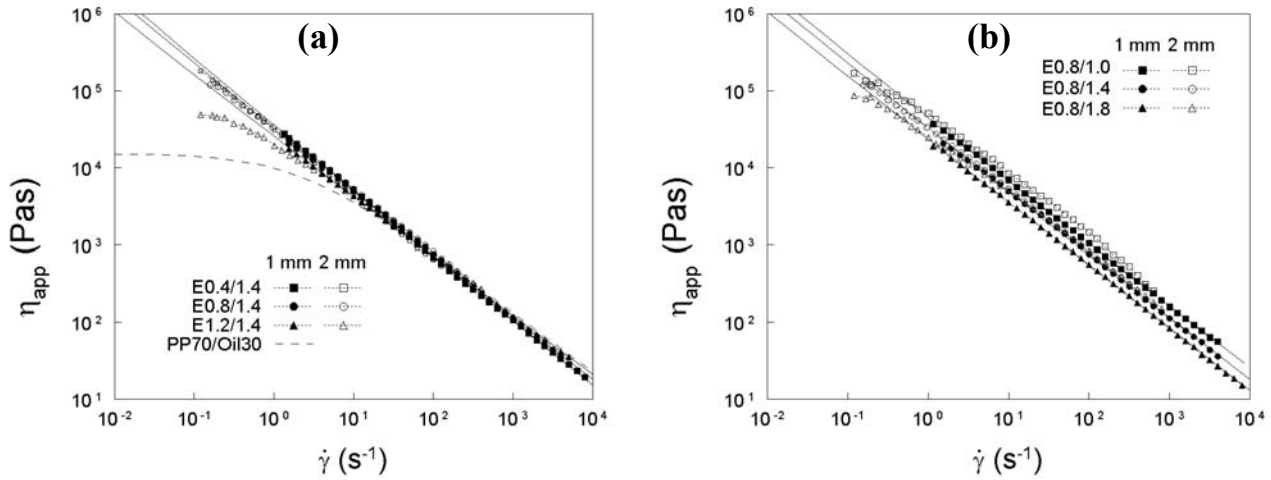


Figure 7.10: Effect of composition on viscosity of TPVs at 190 °C. (a) different PP content (b) different Oil. The solid lines are fits of Eq 7.10 and the dashed line is the PP-oil binary mixture.

7.3.3.3 Extrudate swell and surface appearance

Fig. 7.11 shows the extrudate swell of the TPVs. Compared to the PP phase, the extrudate swell decreases by the presence of elastomer particles. This behaviour was already observed by Goettler [8]. The PP content has the largest effect on D (Fig 7.11a). Increasing the PP content results in an increase of D. This is due to a two-fold effect of the PP phase volume fraction. Firstly, the yield stress and the viscosity of the TPV decrease. More material has yielded and, thereby, more PP is deformed. The lower viscosity results in shorter residence times in the capillary and thus the time-dependent elasticity of this phase is larger. The second effect is simply due to the volumetric change: More PP in the TPV results in more PP-like behaviour. The effect of the increase of oil content in the TPVs is similar to that of changing the PP content. More oil also results in an increase of extrudate swell at a constant stress (Fig 7.11b). The oil mainly affects the viscoelastic properties of the PP phase. It lowers the viscosity and elasticity of this phase. At a constant shear stress, the shear rates increases with oil content and the residence time of the TPV in the capillary becomes shorter. This results in a larger contribution of the time dependent elasticity of the PP phase. In addition, more material has yielded because of the lower yield stress.

Fig 7.12 shows the effect of capillary length on the extrudate swell of blend E1.2/1.4 for different shear rates. The smaller capillary length results in an increase of the extrudate swell at high shear rates due to the shorter residence times. The surface appearance depends on the composition of the TPVs (Table 7.6). At low PP and low oil content, the surfaces of the extrudates were not smooth. Due to the high elastic behaviour and the high yield stresses of these blends they show melt fracture. At high shear rates the extrudates curl into spiral shaped strands. The start of this behaviour shifts to higher shear rates with increasing PP or oil content.

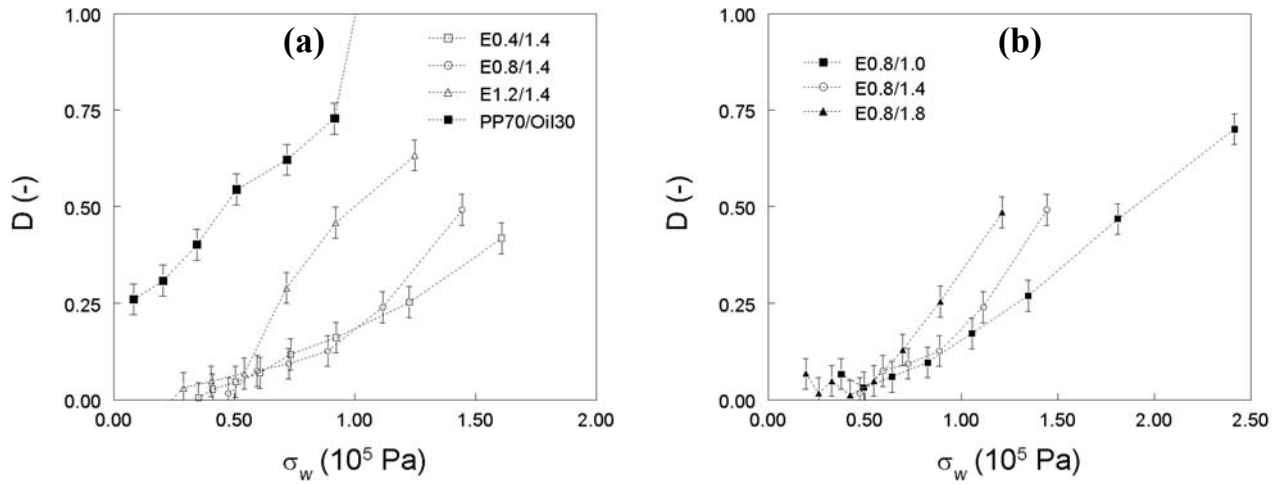


Figure 7.11: Effect of composition on extrudate swell of TPVs at 190 °C.
(a) different PP content (b) different Oil content

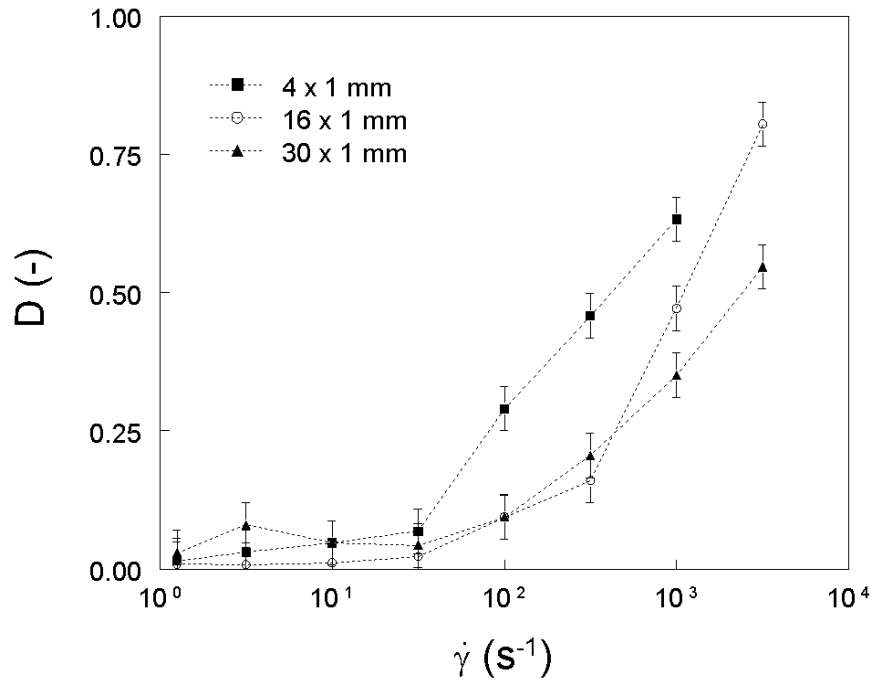


Figure 7.12: Effect of capillary length on extrudate swell of TPV E1.2/1.4 at 190 °C.

Table 7.6: Surface appearance of TPVs as they emerge from the capillary 16 x 1 mm at 190 °C

shear rate (s ⁻¹)	1	3.2	10	31.6	100	316	1000	3162
E0.4/1.4			sharkskin				sharkskin, gross fracture	
E0.8/1.0			sharkskin				sharkskin gross fracture	
E0.8/1.4			smooth					gross fracture
E0.8/1.8				smooth				
E1.2/1.4				smooth				
PP70/Oil30		smooth		Shark skin		sharkskin, gross fracture		gross fracture

7.4 Discussion

7.4.1 Summary of the rheological behaviour of the OTPE blends at high strains/rates

7.4.1.1 PP/SEBS blends

The PP/SEBS blends consist of co-continuous structures of the PP-oil and the SEBS-oil phase. This equilibrium structure is sensitive for changes during the experiment. The steady state structure is a dynamic equilibrium between break-up and coalescence of the two phases. This process is enhanced by the low value for the interfacial tension between the two phases and the matching shear viscosities at high shear rates. These features ensure good processability of these materials. The extrudates have smooth surfaces and the swell is low. The extrudate swell is mainly caused by the time-dependent melt elasticity of the PP phase. During the morphological evolution in the capillary, the extended PP chain is able to relax and the memory effect diminishes.

The apparent viscosity is the results of the weighted contribution of the two phases. The blend viscosity can be estimated by the logarithmic addition of the viscosity of the two phases. This behaviour can also be contributed to the ‘steady-state’ morphology. The changing in composition confirms this picture. By increasing the PP content the phase volume fraction of the PP phase increases. The apparent viscosity changes gradually from SEBS-like to PP –like behaviour. The increase of the oil content does not affect the phase volume fractions of the blends. The shape of the curves remains the same and the viscosity decreases due to the diluting effect of the oil on each phase.

7.3.3.4 TPVs

In the melt state, the TPVs exhibit yield behaviour for flow. The velocity profile in the capillary can be described using the Herschel-Bulkley expression for the shear stress. The yield stress increases with increasing the viscosity of the matrix (by decreasing the oil content in the TPV) and increasing the number of elastomer particles per volume (by decreasing the amount of PP). At high shear rates, at stresses far above the yield stress, the viscosity is dominated by PP phase. This can be

concluded from the comparable power-law indices and the comparable viscosity of the TPVs with different PP content.

The processability of the TPVs depends strongly on the composition. This is caused by the dispersed blend morphology. When the TPV leaves the capillary, the deformed elastomer particles retract to their original shape. At high elastomer content or high elasticity of the blend, this leads to melt fracture. The extrudate swell increases with increasing the PP or the oil content. With increasing PP content, the volume fraction of the PP matrix phase increases and the yield stress of the TPV decreases. The PP concentration in the PP phase being higher, the number density of entanglements in this phase increases, resulting in larger extrudate swell. The increase of oil in the TPV lowers the viscosity and, thereby, the residence time in the capillary. The time-dependent elasticity of the PP phase is still high and the PP chain are larger extended due to higher shear rates.

7.4.1 The viscosity

The type of elastomer, blend composition and morphology have a significant effect on the rheological properties of these OTPE blends. In PP/SEBS blends, both the PP and the elastomer phase are continuous and the elastomer phase contains physical cross-links. These blends can be considered as a continuous elastomer network that is interrupted by the PP phase. The TPVs consist of cured elastomer particles that are dispersed in the PP matrix phase. Due to the high volume fraction, the particles form an agglomerated network structure and the elastomer phase can be considered as a 'quasi'-continuous phase.

The presence of a (quasi) continuous elastomeric network in these blends should indicate yield behaviour: the elastomer phase has to break in order to let the material flow. Yield stresses were observed neither in the PP/SEBS blends nor in the SEBS-oil binary mixtures. Apparently, the stress needed to pull the PS end-blocks out of the PS domains is too low to be measured. The co-continuous morphology changes during the deformation in the capillary. A 'steady state' structure is obtained that is an kinematic equilibrium between break-up and coalescence of the two phases.

The elastomer particles in the TPVs do not break. They are stretched during flow and regain their initial shape when they come out of the capillary. However, the particles have to pass over each other for the TPVs to flow, resulting in a yield stress for flow. This yield stress increases with increasing the number of elastomer particles or increasing the blend viscosity (by respectively decreasing the amount of PP or oil in the blend).

The effects of the change in composition elucidate the shear rate dependence of the viscosity of both blends types. The values of the viscosity of the PP/SEBS blends can be considered as weighted averages of the properties of the PP and the elastomer phase. The increase of the volume fraction of the PP phase results in a gradual change from elastomer-like to PP-like behaviour and the addition of oil reduces the viscosity. The shape of the viscosity curves in the latter case is not affected since the volume fractions do not change significantly.

The viscosity of the TPV is dominated by the PP matrix phase. The values of the power-law index are close to the ones of the PP phase and the values of the blend viscosity at high shear rates are comparable to the viscosity of the PP phase. At low shear rates, where the yield stress becomes more important, the power-law behaviour continues. Here, the viscosity increases with increasing number of elastomer particles per volume.

7.4.2 Processability

Even though the extrudate swell of the blends is caused mainly by the swell of the PP phase, the properties of the elastomer phase also play an important role. In both blend types, the extrudate swell at a constant *shear stress* increases with increasing PP or oil content. The increase of oil content results in higher deformation rates and shorter residence time, caused by the lower blend viscosity at the same stress. The PP phase is deformed to a larger extent for a shorter time. The elastic recovery at the exit of the capillary is higher, resulting in larger swell of the extrudates.

The effect of PP content on the extrudate swell is more complex. It consists of both the effect of the volume fraction of the PP phase and the effect of elastomer properties. The PP phase is the only phase that can deform to a large extent and is able then to recover. Therefore, this phase shows high extrudate swell. At a constant shear stress, the extrudate swell of the blends increases with increasing PP content due to the volumetric effect, but the values differ for the two blend types. For similar composition, the swell of a PP/SEBS blend is less than the swell of a TPV.

In the case of the co-continuous PP/SEBS blend, the initial elasticity of the molten elastomer phase diminishes quickly when it starts to flow. The PS domains break and rearrange during flow in the capillary and enable the elastomer phase to flow. Due to the continuous change of the blend morphology, the elasticity of the PP phase is able to relax if the residence time is enough. This results in a reduction of extrudate swell.

The elastomer particles in the TPVs can only deform to a limited extent determined by their modulus and local stress. Because of the high volume fraction of this phase, the PP matrix phase is deformed to a larger strain and thereby, the recovery is higher.

In general, the two types of OTPE blend have smooth surfaces, except for the two TPVs with high elastic behaviour, i.e. with the lowest PP or oil content. These two show melt fracture at all shear rates. The melt fracture can be caused by the high values of the yield stress of the TPVs. This results in a larger extended elastomeric network. If the stress becomes too high, the elastomer phase breaks and retracts, resulting in irregular surface texture. Some TPVs also show some periodic curling of the strands, indicating stagnation effects in the capillary entrance.

The PP/SEBS blends all have smooth surfaces independent of the shear rate. The PP-oil and SEBS-oil binary mixtures both show melt fracture. By mixing the two phases together, the surface quality improves and the flow instabilities that are present in the PP-oil binary mixture are absent. It seems that the continuing changes in the blend morphology and phase segregation during the capillary flow have a damping effect on the flow instabilities. This prevents the sudden strain relaxation of the PP phase that

causes melt fracture.

7.5 Conclusions

The viscosity and processability of two OTPE blends types has been studied and related to the present blend morphology. In PP/SEBS blends both the PP phase and the elastomer phase are continuous. During capillary flow, the blend morphology changes continuously due to break-up and coalescence of the two phases. The blend viscosity can be estimated by the logarithmic addition of the viscosity of the two phases according to their mass fractions. The processability of the blends is good. The extrudates of all blends have smooth surfaces and the swell is low. Probably, this is due to the changes of the morphology during flow.

The elastomer in the TPVs is present as cross-linked particles, dispersed in the PP matrix phase. Due to the high volume fraction of the non deformable elastomer particles, these blends have yield stress for flow. The viscosity of the TPV can be described using the Herschel-Bulkley equation for the shear stress. In general, the extrudate appearance of the TPVs is good and the swell is low. Exceptions are the blends with high elastomer content and highly elastic behaviour, which show melt fracture even at mild extrusion conditions.

7.6 Appendix

The assumed velocity profile of the TPVs in a cylindrical capillary consists of an unyielded region in the centre of the capillary surrounded by yielded material that show power-law like behaviour. This is described in the Herschel-Bulkley equation. The parameters can be obtained directly from the integration of the local velocity in the capillary. This results in an expression of the volumetric flow rate, Q_v , as a function of the pressure drop, ΔP (Eq 7.10) This expression was not found in the literature and will be derived here.

The expression of the shear stress of a Herschel-Bulkley fluid is:

$$\sigma = \sigma_y + k\dot{\gamma}^n \quad (\text{A1})$$

The shear stress in a capillary with cylindrical shape is a linear function of the pressure, ΔP and the radius, r :

$$\sigma = \frac{r\Delta P}{2L} \quad (\text{A2})$$

The velocity in the capillary can be divided into two regimes. At stresses below the yield stress the velocity is constant and at stresses higher than the yield stress the velocity shows power-law dependence on the radius. The transition occurs at the radius at which the local stress is equal to the yield stress:

$$r_y = \frac{2L\sigma_y}{\Delta P} \quad (\text{A3})$$

where L is the capillary length. The stress balance over the capillary becomes:

$$\frac{-r\Delta P}{2L} = \sigma_y + k\dot{\gamma}^n \quad (\text{A4})$$

The shear rate as a function of the radius can be divided into two parts. For stresses higher than the yield stress the shear rate becomes:

$$\dot{\gamma}(r) = \left[\frac{-r\Delta P}{2kL} - \frac{\sigma_y}{k} \right]^{\frac{1}{n}} = \frac{dV_z(r)}{dr} \quad \text{for } r_y < r \leq R, \quad (\text{A5a})$$

and for stresses lower than the yield stress the shear rate becomes:

$$\dot{\gamma}(r) = 0 \quad \text{for } 0 \leq r \leq r_y \quad (\text{A5b})$$

The velocity as a function of the radius becomes:

$$\int_r^R dV_z = \left[\frac{-\Delta P}{2kL} \right]^{\frac{1}{n}} \cdot \int_r^R [r - r_y]^{\frac{1}{n}} dr \quad (\text{A6})$$

Making the assumption that wall slip is absent, i.e. $V_z(R)=0$, the solution of the integral becomes:

$$V_z(r) = \left[\frac{-\Delta P}{2kL} \right]^{\frac{1}{n}} \cdot \frac{n}{n+1} \left([R - r_y]^{\frac{n+1}{n}} - [r - r_y]^{\frac{n+1}{n}} \right) \quad \text{for } r_y < r \leq R, \quad (\text{A7a})$$

At stresses below the yield stress, the material flows with a constant velocity of

$$V_z(r) = \left[\frac{-\Delta P}{2kL} \right]^{\frac{1}{n}} \cdot \frac{n}{n+1} [R - r_y]^{\frac{n+1}{n}} \quad \text{for } 0 \leq r \leq r_y \quad (\text{A7b})$$

These equations are made dimensionless by dividing the radii by the capillary radius, R :

$$V_z(r) = R^{\frac{n+1}{n}} \frac{n}{n+1} \cdot \left[\frac{-\Delta P}{2kL} \right]^{\frac{1}{n}} \left(\left[1 - \frac{r_y}{R} \right]^{\frac{n+1}{n}} - \left[\frac{r}{R} - \frac{r_y}{R} \right]^{\frac{n+1}{n}} \right) \text{ for } r_y < r \leq R, \text{ and} \quad (\text{A8a})$$

$$V_z(r) = R^{\frac{n+1}{n}} \frac{n}{n+1} \cdot \left[\frac{-\Delta P}{2kL} \right]^{\frac{1}{n}} \left[1 - \frac{r_y}{R} \right]^{\frac{n+1}{n}} \text{ for } 0 \leq r \leq r_y \quad (\text{A8b})$$

This velocity profile is shown in Fig 7.8. The volumetric flow rate, Q_v , is the integral of this velocity profile:

$$Q_v = \int_0^R V(r) 2\pi r dr = \int_0^{r_y} 2\pi r V(r) dr + \int_{r_y}^R 2\pi r V(r) dr \quad (\text{A9})$$

using Eqs. A8a and A8b the volumetric flow rate becomes:

$$Q_v = \frac{2\pi n R^{\frac{n+1}{n}}}{n+1} \cdot \left[\frac{-\Delta P}{2kL} \right]^{\frac{1}{n}} \cdot \left[\int_0^{r_y} r \left[1 - \frac{r_y}{R} \right]^{\frac{n+1}{n}} dr + \int_{r_y}^R r \left[1 - \frac{r_y}{R} \right]^{\frac{n+1}{n}} dr - \int_{r_y}^R r \left[\frac{r}{R} - \frac{r_y}{R} \right]^{\frac{n+1}{n}} dr \right] \quad (\text{A10})$$

Integration of Eq A9 yields the expression for the flow rate:

$$Q_v = 2\pi R^{\frac{3n+1}{n}} \frac{n}{n+1} \cdot \left[\frac{-\Delta P}{2kL} \right]^{\frac{1}{n}} \cdot \left[\frac{1}{2} \left[1 - \frac{r_y}{R} \right]^{\frac{n+1}{n}} - \frac{n}{2n+1} \left[1 - \frac{r_y}{R} \right]^{\frac{2n+1}{n}} + \frac{n}{2n+1} \cdot \frac{n}{3n+1} \left[1 - \frac{r_y}{R} \right]^{\frac{3n+1}{n}} \right] \quad (\text{A11})$$

The yield radius can be replaced by Eq. A3 to include the yield stress of the material

and the pressure drop over the capillary. The final expression of $Q_v(\Delta P)$ becomes is Eq 7.10:

$$Q_v = 2\pi R^{\frac{3n+1}{n}} \frac{n}{n+1} \cdot \left[\frac{-\Delta P}{2kL} \right]^{\frac{1}{n}} \cdot \left[\begin{aligned} &\frac{1}{2} \left[1 - \frac{2L\sigma_y}{\Delta PR} \right]^{\frac{n+1}{n}} \\ &- \frac{n}{2n+1} \left[1 - \frac{2L\sigma_y}{\Delta PR} \right]^{\frac{2n+1}{n}} \\ &+ \frac{n}{2n+1} \cdot \frac{n}{3n+1} \left[1 - \frac{2L\sigma_y}{\Delta PR} \right]^{\frac{3n+1}{n}} \end{aligned} \right] \quad (A12)$$

where n , k and σ_y are the material parameters. This expression is still relative simple and enables to determine the material parameters directly from the data of capillary rheometry. The well-known models for capillary flow are obtained by simplification of the parameters:

Limiting cases:

1) a Bingham fluid: $n=1$ and $k=\eta$

$$Q_v = \left[\frac{-\Delta P \pi R^4}{8\eta L} \right] \cdot \left[1 - \frac{4r_y}{3R} + \frac{1}{3} \left[\frac{r_y}{R} \right]^4 \right] \quad (A13)$$

2) a Power-law fluid: $\sigma_y=0$

$$Q_v = \pi R^{\frac{3n+1}{n}} \frac{n}{3n+1} \cdot \left[\frac{-\Delta P}{2kL} \right]^{\frac{1}{n}} \quad (A14)$$

3) a Newtonian fluid: $\sigma_y=0$ and $n=1$; $k=\eta$

$$Q_v = \left[\frac{-\Delta P \pi R^4}{8\eta L} \right] \quad (A15)$$

7.7 References

- [1] Holden G, Legge N (eds) Thermoplastic elastomers. New York: Hanser; 1996
- [2] Coran AY, Patel R, Rubber Chem Technol 1980;53:141.
- [3] Abdou-Sabet S, Patel RP, Rubber Chem Technol 1991;64:769.
- [4] Ohlsson B, Hassander H, Tornell B, Polym Eng Sci 1996;36:501.
- [5] Veenstra H, van Lent BJJ, van Dam J, Posthuma de Boer AP, Polymer 1999;40:6661.
- [6] Vennemann N, Hundorf J, Kummerlowe C, Schulz P, Kautschuk Gummi Kunststoffe 2001;54:362.
- [7] Holden G, Milkovich R, US Patent 3.265.765, 1962
- [8] Goettler LA, Richwine FJ, Rubber Chem Technol 1981;55:1448.

- [9] Araki T, White JL, Polym Eng Sci 1998;38:590.
- [10] Steeman P, Zoetelief W, SPE Tech Papers 2000;46:3297.
- [11] Chapter 6; This thesis
- [12] Han PK, White JL, Rubber Chem Technol 1995;68:729.
- [13] Jayaraman K, Kolli VG, Kang SY, Kumar S, Ellul MD, J Appl Polym Sci 2004;93:113.
- [14] Xiao HW, Huang SQ, Jian T, J Appl. Pol. Sci 2004;92:357
- [15] Oommen Z, Zachariah SR, Thomas S, Groeninckx G, Moldenaers P, Mewis J, J. Appl. Pol. Sci. 2004;92: 252
- [16] Kumar CR, Nair SV, George KE, Oommen Z, Thomas S, Pol. Eng. Sci. 2003;43:1555
- [17] George S, Ramamoorthy K, Anand JS, Groeninckx G, Varughese KS, Thomas S, Polymer 1999;40:4325.
- [18] Ohlsson B, Tornell B, Polymer Eng Sci 1998;38:108.
- [19] Veenstra H, van Lent BJJ, van Dam J, Posthuma de Boer A, Polymer 1999;40:5223
- [20] Krishnan K, Burghardt WR, Lodge TP, Bates FS, Langmuir 2002;18:9676
- [21] Chapter 5; This thesis
- [22] Sengupta P, PhD thesis, Twente University, Enschede, 2004.
- [23] Willemse RC, Posthuma de Boer A, van Dam J, Gotsis AD. Polymer 1998;39:5879.
- [24] Scott CE, Macosko CW, Polymer 1995;36:461
- [25] Potschke P, Paul DR, J Macromolec Sci-C 2003;C43:87
- [26] Utracki LA, Sammut P, Pol Eng. Sci 1990;30:1027
- [27] Kim BK, Jeong HM, Lee YH, J. Appl Pol Sci 1990;40:1805.
- [28] Thomas S, Groeninckx G, Polymer 1999;40:5799
- [29] Koshy AT, Kuriakose B, Thomas S, J. Appl Pol Sci 1993;49:901

Chapter 8

General overview

Despite the different morphology, comparable values and trends for hardness and modulus were found in a direct comparison of the two OTPE blends [1]. Differences can be observed in the non-linear mechanical properties, such as the ultimate tensile properties and the permanent set. The differences in the rheological properties were more visible and are caused by the structure and properties of the elastomer phase.

First, the rheological properties of each phase and the distribution of oil will be discussed separately. These finding can be used further in the discussion of the rheological properties of the two OPTE blends.

8.1 Rheological properties of PP-oil and elastomer-oil binary mixtures

8.1.1 *PP-oil*

The PP is an entangled linear polymer and shows the normal viscoelastic behaviour. The paraffinic oil has a diluting effect on the PP. Above the melting temperature of the crystals, the PP-oil mixtures can be considered as homogeneous systems. At crystallisation, the oil is pushed out of the crystals, resulting in an increase of the local oil concentration in the amorphous parts of PP. There, it plasticizes this phase and the glass-rubber transition temperature (T_g) decreases.

The linear viscoelastic properties in the melt state can be described by a relaxation spectrum consisting of a summation of Maxwell elements. In steady state shear flow, the shear rate dependent viscosity can be described with the Cross equation. This includes a constant value for the viscosity, as the shear rate goes to zero, and power-law like shear thinning behaviour at high shear rates.

With increasing the oil content, the polymer concentration and the entanglement density decrease, resulting in a decrease of the shear modulus and the viscosity. The oil also affects the time scale of the relaxation processes: The relaxation spectrum shifts to shorter times with increasing the oil content. As proposed by Nakajima [2], the relaxation times and the reduction of the modulus can be scaled by a set of shift factors. This concentration-time superposition allows the estimation of the viscoelastic properties at any oil concentration and shear rate or frequency.

8.1.2 *SEBS-oil*

The PS end-blocks of the SEBS are still present as separate domains at the processing temperatures of the PP/SEBS blend. Because the PS phase is above its T_g , the end-blocks are able to migrate between the domains when an external stress is applied. Due to these physical cross-links, the rheological behaviour depends on the applied deformation.

At small deformations, in the linear viscoelastic regime, the presence of the PS domains causes an elastomer-like behaviour in the SEBS-oil mixtures. In melt creep measurements, the transient viscosity peaks around 0.5-1 s.u. indicating a change in morphology. The positional order of the PS domains changes from a *bcc* packing into higher ordered structures (like twinned *bcc* packing) and PS end-blocks are able to migrate to other domains. Due to these changes, the melt elasticity of the mixtures decreases drastically. In steady shear flow, the mixtures behave as entangled polymers. The Cross equation can be used again as an expression for the shear rate dependent viscosity.

The paraffinic oil is a selective solvent for the elastomeric EB part. The amount of oil present in the PS domains is negligible. Increasing the oil content results in a reduction of the number of physical cross-links per volume and dilution of the EB blocks. As seen for the PP-oil mixtures, the dynamic moduli and the steady state shear viscosity can be scaled by the oil content via the oil concentration-time superposition.

8.1.3 EPDM-oil

By vulcanisation, the EPDM changes from a highly entangled polymeric viscoelastic fluid into an elastic solid. From the dynamic and transient rheological measurements, it was found that terminal flow behaviour is not present. The storage modulus persists to a constant value with decreasing the frequency to zero and a finite equilibrium value for the deformation is observed in creep measurements. The frequency dependent moduli of vulcanisates with different oil content can be scaled by the concentration-time superposition idea discussed previously.

8.2 Distribution of oil in OTPE blends.

The paraffinic oil is present in both the elastomer and the PP phases. The blend properties come from the combined properties of the two phases and the blend morphology. In order to estimate the properties of the two phases, the oil concentration in each phase should be known. If this is not possible, the conclusions are limited to composition effects.

The oil has a plasticizing effect on both the PP and the elastomer phases. The concentration of oil in each phase can be obtained from the reduction of the T_g of that phase. Dielectric spectroscopy using a dielectric probe molecule proved to be the most suitable technique to study the glass transition dynamics of these OTPE blends. The glass transition regions of the two phases partially overlap, however, and the determination of the oil distributions becomes complex. The oil distribution coefficient could be estimated from the modelling the loss part of the dielectric permittivity.

The oil distribution coefficient, K , is defined as the ratio of the oil concentration in the PP phase over the oil concentration in the elastomer phase. K depends slightly on composition and its averaged value is 0.63 for the TPVs and 0.60 for the PP/SEBS blends. In both blend types K increases slightly with decreasing PP content. No clear trend was found for the oil content.

If the oil concentrations are corrected for the presence of the hard domains (PS domains and crystalline PP phase), the averaged values of K become 0.88 for the TPVs and 0.76 for the PP/SEBS blends. These values indicate that the oil has a small preference for the elastomer phase.

A remark has to be made about the oil concentration in the PP phase, which varies from 26 to 37 wt%. The oil is only present in the amorphous parts of the PP. The local oil concentration becomes then 30 to 53 wt%. This is so high that the oil could be present as a separate phase. A separate oil phase was not observed in image analysis (SEM, TEM) of either the PP-oil binary mixtures or the ternary elastomer/PP/oil blends. In DMTA measurements, however, two maxima in the loss modulus were observed at (overall) oil concentrations of 30 wt% or higher, indicating that a possible PP-rich and an oil-rich phase can be present.

In the melt state, the oil distribution coefficient could be introduced in the mechanical models as an additional parameter. The values of K in the melt state increase with decreasing PP content or increasing oil content. The averaged value for both blend types is 0.60. The large change of K with composition can explain the difference in swelling behaviour of the entangled linear PP and the (physically) cross-linked elastomer.

From these results it can be assumed that the oil does not migrate from the PP to the elastomer phase upon crystallisation of the PP phase. It is more likely that the oil is trapped between the PP crystals in the form of an oil-rich and a PP rich phase.

The present, newly developed dielectric method enables the analysis of complex systems of apolar polymers. The effect of the molecular weight and the polarity of the oil on the distribution coefficient can be studied in order to make OPTe blends in which one of the phases is diluted selectively. The dielectric method can be improved by grafting of the probe to one of the polymers. This way, the T_g dynamics of a specific phase can be studied selectively.

8.3 Effect of morphology on rheology

8.3.1 Linear viscoelastic properties

The two OPTe blends have similar behaviour of the linear viscoelastic properties. At first sight, no direct distinction can be made between the PP/SEBS blends and the TPVs. The effect of the morphology could be quantified using mechanical models in which both phases are considered to be partially continuous.

In the solid state, the linear viscoelastic properties are dominated by the PP phase. This phase has the highest modulus and is continuous in both blend types. From the modelling, it can be concluded that the PP phase is mechanically less continuous than assumed: There are parts of the PP phase that can be considered as trapped in the elastomer phase. As a result, the modulus is lower. This works in a similar way for the PP/SEBS blends and the TPVs and can explain the comparable properties of the two blend types. The PP phase in the PP/SEBS phase is mechanically as discontinuous as in the TPVs.

In the melt state, the elastomer phase has the higher modulus but its continuity depends on the blend type. The elastomer phase is continuous in the PP/SEBS blends and their behaviour can be explained in the opposite way as from their solid-state properties: due to morphological inhomogeneities the elastomer is mechanically less continuous than assumed. Although the elastomer phase in the TPVs is dispersed, the elastomer particles form an agglomerated network structure. This results in a high melt elasticity and a yield stress for flow. At very low PP content, this elastomer network is mechanically more continuous than assumed by the model. The strength of the elastomer network decreases rapidly as the network becomes less dense (e.g. by the addition of PP).

These mechanical models have some limitations. Although the PP is continuous in both blend types, the solid state and melt state properties are dominated by the elastomer phase at the lowest PP content used (13-17 wt%). For instance, the mechanical models overpredict the loss modulus in solid state, indicating that the OPTEs behave more elastic than the models assume. To describe this in a correct way, new or other models are needed.

8.3.2 *Transient properties*

The difference between co-continuous structures and dispersed morphology can be examined by transient rheological measurements. The initial blend structure is broken under controlled conditions (in this case: at a constant stress). The transient viscosity and the remaining melt elasticity as functions of the shear strain indicate morphological changes.

The PP/SEBS did not show a measurable yield stress under flow. At the lowest stresses, the transient viscosity did not diverge and the blend flows with a very high viscosity. The physical cross-links in the form of the PS domains are able to break and rearrange under an applied deformation and, as a result, the domains can orient in the direction of the applied stress.

The TPVs have a yield stress for flow due to the high volume fraction of the dispersed elastomer phase. This affects the creep behaviour. At stresses below the yield stress, the TPV is only deformed partially and reaches an equilibrium deformation at which the viscosity increases asymptotically. At applied stresses higher than the yield stress, the behaviour of the transient viscosity is comparable to that of the PP/SEBS blends. The behaviour of the recovery strain, a measure for the remaining melt elasticity, differs.

In the linear regime, at small deformations, the blend structure is deformed partially but the morphology does not change much. The transient viscosity increases with increasing the deformation due to the increasing resistance to flow of the two phases and the elastic recovery is high. This regime lasts up to 0.2 strain units.

From 0.2 up to 3 strain units is the transient regime. The viscosity peaks and the recovery is lower than total recovery. The initial blend structure starts to break and this change is irreversible. In this regime, the behaviour of the PP/SEBS blends

differs from that of the TPVs. For the PP/SEBS blends, the recovery strain levels off to a constant value. The co-continuous morphology is an equilibrium morphology and it changes when deformation is applied.

The recovery strain in the TPVs reaches a maximum value at the same deformation at which the viscosity peaks and decreases suddenly after that. At this strain, the elastomer particles are able to pass over each other and the TPV is able to flow. The reduction in the recovery strain is caused by the retraction of the elastomer particles to their equilibrium shape. This indicates that the TPVs have a *yield strain* in addition to a *yield stress*. This yield strain is a measure for the steric obstruction of the surrounding particles.

The flow regime is present at larger deformations. In the PP/SEBS blends this is characterised by the formation of a 'steady state' morphology, which is an equilibrium between break-up and rearrangement of the two phases. Both the viscosity and elastic recovery reach constant values. The flow behaviour of the TPVs becomes irregular in the flow regime. The viscosity and the elastic recovery fluctuate due to the periodic elongation, hopping and retraction of the elastomer particles.

8.3.4 Capillary rheology

At first sight, the plots of the viscosity as a function of shear rate are comparable for the two blend types. The comparison of the blend viscosity with the properties of the two phases and the morphology clarifies the processing behaviour of the blends.

The viscosity of the PP/SEBS blends changes gradually from SEBS-like to PP-like behaviour. This means that the blend viscosity decreases with increasing fraction of the PP phase at low shear rates but it increases at high shear rates. The PP phase at high shear rates is slightly more viscous than the SEBS phase. The blend viscosity can be described using the logarithmic additive rule of the viscosities of the two phases.

The viscosity curves of the TPVs show persisting power-law behaviour at decreasing shear rates due to the yield behaviour. This makes the comparison with the properties of the two phases complex. To solve this, the capillary data were analysed using the Herschel-Bulkley model for the local stress in the capillary. This equation consists of a yield stress in addition of power-law shear thinning behaviour of the viscosity. The parameters of the model can be obtained from the relation of the volumetric flow rate and the pressure drop over the capillary (Eq 7.10). The values of the power law exponent are close to the one of the PP phase, indicating that the flow properties are dominated by this phase. The yield stress for flow is lower than the ones obtained from the creep measurements. It can be stated that the network structure is easier to get broken in the elongational flow in the capillary entrance than in quiescent state (as in creep flow).

The processability of PP/SEBS is very good, as shown from the absence of severe melt fracture instabilities. The extrudate surfaces are smooth and the swell is low. The viscosities of the two phases are comparable, while the SEBS phase does not contribute to the extrudate swell. The continuing change in the blend morphology enables the stresses to relax in the capillary and flow instabilities are suppressed.

The processability of the TPVs is also good, except for the blends with the highest elasticity. The blends with the lowest PP and the lowest oil content show melt fracture over the whole range of shear rates. The high volume fraction of elastomer phase and the highly elastic behaviour promotes the increase of the local shear rates between the particles. The PP phase is deformed there to a larger extent, resulting in melt fracture.

8.3.5 Summary

From the above description of the rheological behaviour of the two OTPE blends it can be concluded that the main differences in processability are caused by the differences in the properties of the elastomers. The main results of this study are listed in Table 8.1. The effects of the PP content and the oil content are comparable. Both components lower the viscosity and, thereby, enhance the processability. The effect of the morphology in combination with the properties of the elastomer can explain the processability.

The cured elastomer particles in the TPVs are deformed partially during processing but they do not break. They have to pass over each other for the melt to flow and form physical obstructions for other particles. Most deformation is realised by the PP phase and this phase controls the processing properties.

The physical cross-links in the PP/SEBS blends break when the applied stress is high enough. This enables the TPE to flow and the morphology changes continuously. The blend properties can be considered as a weighted average of the properties of the two phases.

Table 8.1: Summary of rheological properties of the PP/SEBS blends and TPVs.

	PP/SEBS blends	TPV
cross-links	physical	chemical
morphology	co-continuous depends on stress and flow history	elastomer dispersed in PP stable
yield stress for flow	no ^a	yes
steady state flow	logarithmic additive rule	Herschel-Bulkley fluid
extrudate swell	low	Increases with PP content
surface texture	smooth	improves with PP content

a: only observed at lowest oil content

The similar properties of the two different OTPE types at temperature of application come from the PP phase. In the PP/SEBS blends the PP is *mechanically* as discontinuous as in the TPVs.

8.4 Rheology of PP/SEBS blends

All the PP/SEBS blends used in this work showed co-continuous structures. Sengupta [1] showed that the change in composition affects the domain sizes of the two phases and the processing conditions affect the interconnectivity of the two phases. The elastomer domains are 0.5-2 μm in sizes and they increase with decreasing PP content

or increasing oil content. These co-continuous structures are obtained because of the low interfacial tension between the PP and SEBS phase and the matching viscosities at processing conditions. The physical cross-links have a stabilising effect on the morphology.

The two phases in the PP/SEBS blends have different rheological properties. The PP is a linear polymer with 'normal' viscoelastic behaviour. The SEBS, on the other hand, has physical cross-links that have to be broken in order to enable flow of the material.

The presence of physical cross-links affects the rheological properties and the processability of the blends:

- There is no coarsening of the morphology; the shape of the sample is stable in quiescent state
- There is no or very low yield stress
- The melt elasticity is low at high shear strains / rates
- The mechanical history is wiped out sooner during processing (low extrudate swell, caused by strain recovery of the PP phase during flow in the capillary)

The rheological properties of the PP/SEBS blends appear to be controlled by the properties of the two phases. The effect of the co-continuous morphology is that the properties of the blend change gradually according to the weight fractions of the two phases. The behaviour of the blends can be explained by the deformation mechanism, schematically shown in Fig 8.1, as it was discussed for the melt creep measurements in Chapter 6.

The linear regime in creep flow lasts up to 0.2 s.u.. The blend is deformed elastically and the PS domains remain intact. The physical cross-links stabilise the morphology and alter the blend modulus at low frequencies. The moduli can be described with mechanical models that reflect the co-continuous morphology.

At larger deformations the two phases and the blend interface orient in the direction of the applied stress (Fig 8.1b). The elastomer chains are deformed to a large extent and the physical cross-links break. Thereby, the elastomer phase loses most of its melt elasticity and the blend does not recover to its original state. At larger deformation, the two phases can break up in order to allow strain relaxation of the polymer chains.

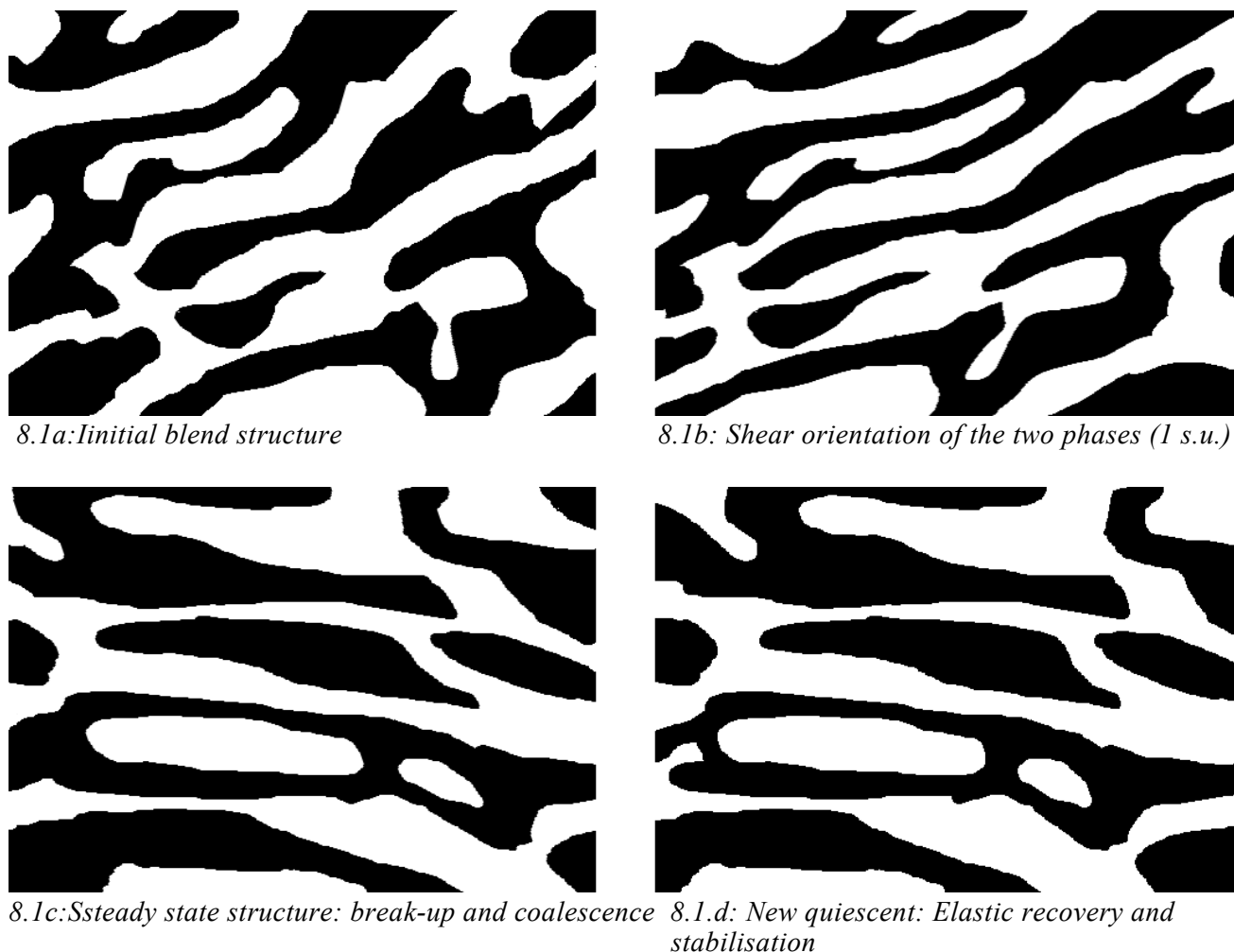


Figure 8.1: Schematic representation of the deformation mechanism of PP/SEBS blends

Upon increasing the shear strain, a new steady state is formed (Fig 8.1c) that consists of a dynamic equilibrium between break-up and coalescence of the two phases. Due to the matching viscosity and the low interfacial tension, the kinetics of this process can be fast and the two polymers are able to recover from strain by reshaping the blend structure. In this process, the initial elasticity of the PP phase decreases. The SEBS loses its initial elasticity by migration of the PS end blocks to other domains. This results in a decrease of the extrudate swell of the blend. When the flow is stopped, the extended phases retract to recover from strain and to minimise the surface area (Fig 8.1d). The PS end-blocks rearrange into new domains and new physical cross-links are formed.

This picture consists only of a qualitative description of the possible mechanism of blend deformation. To confirm the observed properties, rheological models have to be developed. This can be done by the introduction of (high) melt elasticity in models that describe the properties of co-continuous blends, like the model of Lee and Park [3] or diffuse interfacial models, e.g. [4].

8.5 Rheology of TPVs

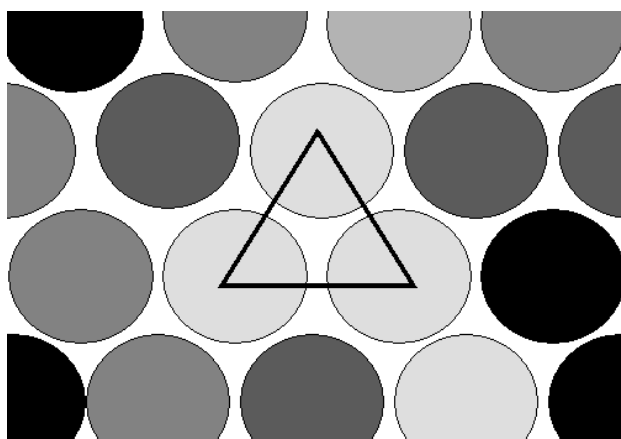
In the TPVs, the elastomer phase is present as a network of agglomerated particles [1]. This morphology does not change upon melting, cooling or processing of this material. The rheological properties of the TPVs depend on the number of particles per volume (particle density) and the properties of the matrix phase. Because the volume fraction of the elastomer phase is high, the particles form steric obstacles for each other. The particles have to pass over each other to let the TPV flow. From the met creep measurements, it was shown that these materials have *yield strain* in addition to a *yield stress*. The deformation process is schematically shown in Fig 8.2.

In the linear viscoelastic regime, the TPV is deformed below its yield strain. The network-like structure of the elastomer phase is still intact. Due to this structure, there are parts of the PP phase that can be considered as trapped between the elastomer particles and cannot contribute to the overall blend properties. The elastomer phase, even though it is dispersed, still dominates the rheological properties.

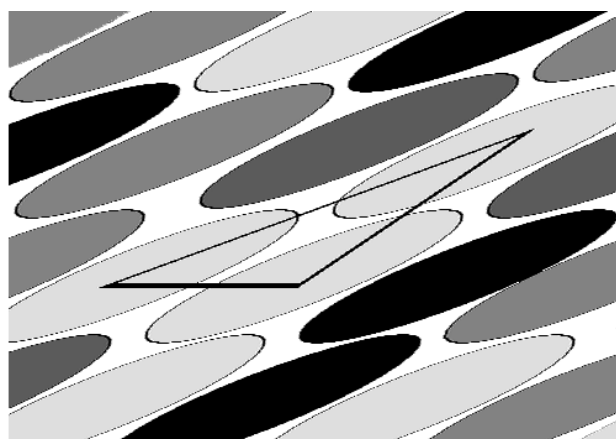
In the transient regime (between 0.2 and 3 s.u.), the extended elastomer particles pass their yield point (from Fig 8.2b to Fig 8.2c) and are able to regain their original shape (Fig8.2d). This results in a temporary decrease of the melt elasticity. For larger deformations, the viscosity keeps fluctuating, due to periodic stretch, hopping and retraction of the elastomer particles.

The processing of the TPVs with high elasticity (low PP or low oil content) show melt fracture. The origin of this behaviour can be the high yield stress in or increase of local shear rate between the particles, as stated in [5]. This topic has to be investigated in more detail.

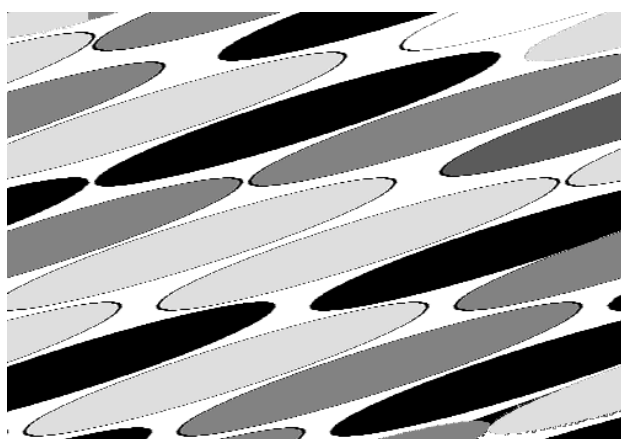
If the origin of melt fracture lies in the yield behaviour, the processability of TPVs with high elastomer content can be improved by making TPVs with a lower yield stress. This can be done by adjusting the PP matrix viscosity. Another possible method can be the preparation of TPVs using spherical particles with a bimodal distribution of sizes. In general, the yield stress in a suspension of solid particles increases with increasing volume fraction, decreasing particle size and increasing surface irregularity. The presence of bimodal distribution of sizes ensures high volume fraction of elastomer and lower values for the yield strain, thereby lowering the yield stress.



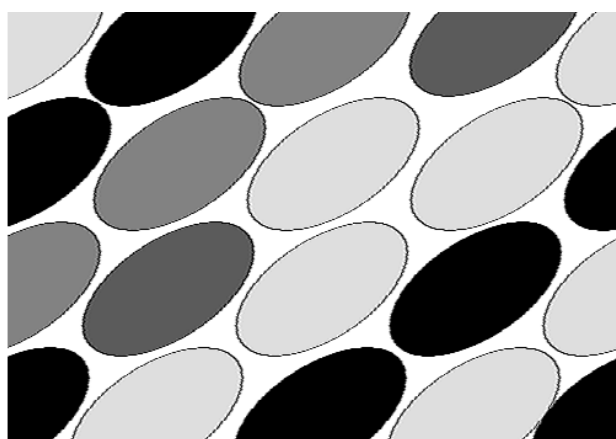
8.2.a: Initial blend structure



8.2.b: strain = 3 s.u.; Deformation of particles



8.2.c: strain = 3 s.u.; Reordering position



8.2.d: Shape recovery particles

Figure 8.2: Schematic representation of the yielding mechanism of TPVs

8.6 References

- [1] Sengupta P, PhD thesis, Twente University, Enschede, 2004
- [2] Nakajima N, Harrell ER, J Rheol 1982;26:427
- [3] Lee HM and Park OO, J. Rheol 1994;38:1405
- [4] Anderson DM, McFadden GB, Wheeler AA, Annual Rev Fluid Mech 1998;30:139
- [5] Cakmak M, Cronin SW, Rub. Chem. Techn. 2000;73:753

List of Symbols

Symbol	Description	Unit	Chapter
α	1 st relaxation process in polymers upon cooling	-	3,4
β	2 nd relaxation process in polymers upon cooling	-	3,4
ε^*	Complex dielectric permittivity	-	3
ε'	Real part of dielectric permittivity	-	3
ε''	Imaginary part of dielectric permittivity	-	3,4
$\Delta\varepsilon$	Change in dielectric permittivity	-	3,4
γ	3 rd relaxation process in polymers upon cooling	-	3
γ	Shear strain	s.u.	6
γ_r	Recovered strain after creep flow	s.u.	6
$\gamma(t_0)$ or γ_0	Strain at moment of stress release	s.u.	6
$\gamma(t_0+1000)$	Strain after 1000 s recoil	s.u.	6
$\dot{\gamma}_{app}$	Apparent shear rate	s ⁻¹	7
η	Viscosity	Pa·s	6,7
η^+	Transient shear viscosity	Pa·s	6
η_0	Zero-shear viscosity	Pa·s	7
η_{app}	Apparent shear viscosity	Pa·s	7
φ	Volume fraction	-	5
φ_{eff}	Effective volume fraction	-	5
λ	Time constant in the Cross equation	s	7
μ	Dipole momentum	C·m	3,4
ρ_T	Density at temperature T	kg/m ³	7
σ	Shear stress	Pa	6,7
σ_w	Shear stress at the wall	Pa	7
σ_y	Yield stress	Pa	6,7
τ	Relaxation time	s	3,4
ω	Frequency	rad/s	4,5
a	Shape factor in HN equation	-	3,4
a	Parameter in Veenstra model D	-	5
a_c	Concentration-time shift factor	-	5
a_T	Time-temperature shift factor	-	5
b	Shape factor in HN equation	-	3,4
b	Concentration-modulus shift factor	-	5
b_c	Parameter in Veenstra model D	-	5
$c_{i,j}$	Concentration of component i in phase j	-	4,5
ΔC_p	Change in heat capacity	J/g·K	3,4
D	Extrudate swell	-	7
d	Diameter	m	7
d_{25}	Extrudate diameter at 25 °C	m	7
d_{cap}	Capillary diameter	m	7

Symbol	Description	Unit	Chapter
E^*	Dynamic tensile modulus	Pa	3,4
E'	Real part of tensile modulus	Pa	3,4
E''	Imaginary part of tensile modulus	Pa	3,4
E_a	Activation energy in Arrhenius equation	kJ/mol	3
E_v	(Vogel) Activation energy in VFT equation	kJ/mol	3
f	Frequency	Hz	3,4
f	Amount of parallel behaviour in Coran model	-	5
G^*	Dynamic shear modulus	Pa	5
G'	Real part of shear modulus	Pa	5
G''	Imaginary part of shear modulus	Pa	5
ΔH	Heat of crystallisation	J/g	3,4
J	Creep compliance	Pa ⁻¹	6
K	Oil distribution coefficient	-	4,5
k	Viscosity constant in power law equation	Pa·s ^{1/n}	7
L	Capillary length	m	7
m	Power-law index in Cross equation	-	7
n	Index in power law equation	-	7
ΔP	Pressure drop over the capillary	Pa	7
Q_v	Volumetric flow rate	m ³ /s	7
R	Gas constant	J/mol·K	3
R	Capillary radius	m	7
r	Radius	m	7
r_y	Radius at which the local stress is equal to the yield stress	m	7
T	Temperature	°C or K	3,4,5,6,7
T_c	Crystallisation temperature	°C	3,4
T_v	Reference temperature in VFT equation	K	3
T_g	Glass transition temperature	°C	3,4
t	Time	s	6
$\tan \delta$	Tangent of loss angle	-	5
w_i	Mass fraction of component i	-	3,4,5
X	Crystallinity	-	3,4
x_i	Mass fraction of phase i	-	4

List of Abbreviations

Abbreviation	Description
AFM	Atomic Force Microscopy
a.u.	Arbitrary units
bcc	Body centred cubic packing
DBANS	<i>4,4'-(N,N-dibutylamino)-(E)-nitrostilbene</i>
DMA	Dynamic Mechanical Analysis
DMTA	Dynamic Mechanical Thermal Analysis
DRS	Dielectric Relaxation Spectroscopy
DSC	Differential Scanning Calorimetry
EB	<i>ethylene-co-butylene</i> copolymer
EPDM	<i>ethylene propylene diene</i> termer copolymer
HN	Havriliak-Negami
LDPE	Low density <i>polyethylene</i>
LVSEM	Low voltage scanning electron microscopy
NMR	Nuclear magnetic resonance
ODT	Order-disorder temperature
OTPE	olefinic thermoplastic elastomer
PB	<i>Polybutadiene</i>
PE	<i>Polyethylene</i>
PP	<i>Polypropylene</i>
PS.	<i>Polystyrene</i>
rpm	revolutions per minute
SBS	<i>polystyrene-block-polybutadiene-block-polystyrene</i>
SEBS	<i>polystyrene-block-polyethylene-co-butylene-block-polystyrene</i>
SEM	Scanning electron microscopy
SIS	<i>polystyrene-block-polyisoprene-block-polystyrene</i>
s.u.	stain unit
TEM	Transmitting electron microscopy
TiO ₂	<i>Titanium dioxide</i>
TPE	Thermoplastic elastomer
TPE-G	Thermoplastic elastomer gel
TPV	Thermoplastic vulcanisate
VFT	Vogel-Fulcher-Tammann

Summary

Rheological properties of olefinic thermoplastic elastomer blends

The aim of this thesis is to understand the relations between the morphology and the rheological properties in olefinic thermoplastic elastomer (OTPE) blends. To do this, two types of OTPE blends are used that differ in morphology:

- Thermoplastic vulcanisates (TPV)

The TPVs consists of cured elastomer particles dispersed in a polypropylene (PP) matrix. The number density of particles is high and the particles form an agglomerated network. This morphology does not change upon (re) processing of the blend.

- PP/SEBS blends

The elastomer and the PP phase in the PP/SEBS blends are both continuous. The elastomer phase contains physical cross-links that have a stabilising effect on the morphology. The co-continuous morphology is a dynamic equilibrium morphology that is sensitive to changes when the blend is deformed.

Chapter 2 gives a general introduction about the OTPE blends. The morphology formation in the two blend types, some mechanical properties and the rheological properties are discussed. The two blend types used in this thesis have the same type of PP and oil and are similar in composition. In this way, the effect of morphology (dispersed vs. co-continuous) can be determined by direct comparison of the two blends.

Chapter 3 describes a new method to study glass transition dynamics in blends of apolar polymers (PS, PP and PE) using dielectric spectroscopy. The dielectric permittivity in the glass transition region is selectively amplified by the addition of a rod-like *probe molecule* with a strong permanent dipole directed parallel to the molecular longitudinal axis. The relaxation times of the two phases in the blend correspond to those of the pure polymers and they are not affected by the blend composition and the morphology. From the relaxation strength of the permittivity, it can be concluded that the *dielectric probe* is distributed equally over the two phases.

Chapter 4 discusses the distribution of paraffinic oil over the PP and the elastomer phase in the OTPE blends. Common techniques, like DMTA and DSC, proved to be inaccurate for the detection of the glass transition temperatures of the two phases: the glass transition dynamics of the two phases overlap. Using the method described in Chapter 3, the blends were made accessible to dielectric spectroscopy. The oil distribution was determined by modelling the dielectric loss of the blends in the glass transition region using the values of binary PP-oil and elastomer-oil mixtures. In general, the oil prefers the elastomer phase and the composition has a minor influence on the values of the oil distribution coefficient.

In **Chapter 5** the linear viscoelastic properties of the OTPE blends are discussed. In the solid state, the PP phase has the higher modulus. The value of the blend modulus increases with increasing the hard/soft ratio of the blends i.e., increasing the PP content or

decreasing the oil content. In the melt state, the elastomer phase has the higher modulus and the value of the blend modulus increases with decreasing PP or oil content. The dynamic moduli of the blends are described with mechanical models that reflect the blend morphology. The models of Veenstra and Coran can be used to estimate the frequency dependent moduli both in the solid state and in the melt state. In the Veenstra model D, the model parameter can be related to an effective volume fraction. This is a measure for the *mechanical* continuity of the phase with the highest modulus.

Chapter 6 discusses the transient rheological properties of the two OTPE blends. Melt creep measurements were performed to determine the yield stress for flow. The yield stress in the TPV increases with increasing the number of elastomer particles per volume or by increasing the matrix viscosity. The PP/SEBS blends did not show yield behaviour, except the blend with the lowest oil content. The deformation mechanism of in the start-up phase of flow was investigated using strain recovery after cessation of the creep flow. The destruction of the initial morphology results in a peak of the transient viscosity and in a reduction of recovered strain. In TPVs, The recovered strain decreases drastically after a certain strain due to reordering and retraction of the deformed elastomer particles. The TPVs have a *yield strain* in addition of a yield stress. In PP/SEBS blends, the recovered strain reaches a constant value with increasing the deformation. This indicates the formation of a dynamic '*steady state*' morphology that is an equilibrium between breaking and coalescence of the two phases.

Chapter 7 discusses the rheological properties in steady shear flow, measured by capillary rheometry. In the PP/SEBS blends, the blend viscosity can be estimated by the logarithmic mean of the viscosity of the two phases. Due to the ongoing change of the morphology of these blends in the capillary, possible flow instabilities are suppressed and the extrudate swell is low. The steady shear viscosity of the TPVs can be described with the Hershel-Bulkley expression for the shear stress. At low shear rates, the yield behaviour alters the blend viscosity and at high shear rates the viscosity is dominated by the matrix PP phase. The TPVs show melt fracture at compositions that show high elastic behaviour. The extrudate swell is low, but larger than the PP/SEBS analogues, and it increases with increasing the content of the matrix PP phase.

Chapter 8 gives a general overview of the findings in this thesis. In the PP/SEBS blends, the morphology has a minor effect on the rheological properties. The moduli and viscosity are found to be described by taking the appropriate average of the properties of the two phases. The change in morphology during shear flow suppresses the occurrence of flow instabilities. The agglomerated structure of the elastomer particles in the TPVs results in yield behaviour. The particles have to pass over each other to allow the TPV to flow. The similar properties of the two OTPE blend types come from the PP phase. The similarity in properties of the two OPTPE blends in the solid state can be explained by the fact that in both cases the PP matrix phase from a mechanical point of view can be considered to be partially discontinuous.

Wilco Sengers

Samenvatting

Rheologische eigenschappen van olefine thermoplastische elastomeer blends

In dit proefschrift wordt de correlatie gelegd tussen de morfologie en rheologische eigenschappen van olefine thermoplastische elastomeer (OTPE) blends. Twee soorten polymeer/elastomeer blends werden gebruikt die vergelijkbare mechanische eigenschappen hebben maar ze verschillen in de morfologie.

- Thermoplastische Vulcanisaten (TPV)

Deze blends bestaan uit gevulcaniseerde EPDM rubber deeltjes gedispergeerd in een polypropyleen (PP) matrix. Het aantal deeltjes per volume is zo hoog dat de deeltjes een vrijwel continue netwerk vormen. Deze structuur verandert niet tijdens (her)verwerking van deze materialen.

- PP/SEBS blends

Het elastomeer en de PP fasen in de PP/SEBS blends zijn beide continue. De crosslinks in het elastomeer zijn fysisch van aard en ze hebben een stabiliserend effect op de morfologie. De co-continue morfologie is een evenwichtsstructuur die onderhevig is aan verandering als de blend wordt vervormd.

Hoofdstuk 2 geeft een algemene introductie over de OTPE blends. De vorming van de morfologie in de twee typen blends, de mechanische eigenschappen en de rheologische eigenschappen worden besproken. De twee typen blends die in dit proefschrift worden gebruikt bestaan uit hetzelfde PP en olie en hebben dezelfde samenstelling. Op deze wijze kan het verschil in blend eigenschappen direct gecorreleerd worden met de morfologie (dispers versus co-continue).

Hoofdstuk 3 beschrijft een nieuwe methode om de dynamica van de glas-rubber overgang in blends van twee apolaire polymeren (PS, PP of PE) te bestuderen met behulp van dielectrische spectroscopie. De dielectrische permitiviteit in de glas-rubber overgang wordt selectief versterkt door toevoeging van een *probe molecuul* aan de polymere blend. Dit molecuul is staafvormig en heeft een hoog, permanent dipool moment dat parallel ligt aan de lange as van het molecuul. De relaxatie tijden van de twee fasen in de blend komen overeen met die van de pure polymeren en zijn niet afhankelijk van de samenstelling of de morfologie. Uit de relaxatie sterkte blijkt dat de *dielectrische probe* gelijk verdeeld is over beide fasen.

Hoofdstuk 4 behandelt de verdeling van paraffine olie over de PP en de elastomeer fase in de OTPE blends. De bepaling van de glas-rubber overgangstemperatuur met behulp van de meest gebruikelijke methoden, zoals DMTA en DSC, bleken in dit geval niet toereikend: de dynamica van de glas-rubber overgang van de twee fasen overlappen. Met de methode die beschreven wordt in Hoofdstuk 3 werden de blends dielectrisch actief gemaakt. De verdeling van de olie werd bepaald door modellering van het dielectrisch verlies van de blends in het regime van de glas-rubber overgang met behulp van de waarden van binaire PP-olie en elastomeer-olie mengsels. Voor alle samenstellingen is de olie concentratie in de elastomeer fase hoger dan in de PP fase en de samenstelling van de blend heeft een klein effect op de waarden.

In **Hoofdstuk 5** worden de lineaire viscoelastische eigenschappen van de OTPE blends besproken. De waarde van de modulus in de vaste toestand neemt toe met de hard/zacht verhouding van de blends (door toename van hoeveelheid PP of door afname van hoeveelheid olie in de blend). In de smelt heeft de elastomeer fase de hoogste modulus. De blend modulus neemt dan toe met afnemende hoeveelheid PP en/of olie. De dynamische moduli van de blends kunnen beschreven worden met mechanische modellen die de morfologie van de blends in acht nemen. De modellen van Veenstra en Coran werden gebruikt om de frequentie afhankelijke moduli te beschrijven in zowel de vaste toestand als in de smelt. De waarde van de modelparameter in het Veenstra model D kan gerelateerd worden aan een effectieve volumefractie. Deze volumefractie is een maat voor de *mechanische continuïteit* van de fase met de hoogste modulus.

Hoofdstuk 6 beschrijft de rheologische eigenschappen van de twee OTPE blends in het overgangsbereik. Kruip metingen werden uitgevoerd om de zwichtspanning voor stroming te bepalen. De TPVs hebben een zwichtspanning die toeneemt met toenemend aantal rubberdeeltjes per volume en toenemende viscositeit van de PP matrix fase. De PP/SEBS blends vertonen geen zwichtgedrag, behalve bij de blend met de laagste hoeveelheid olie. Het deformatie mechanisme in de opstartfase werd opgehelderd door het bepalen van de teruggewonnen deformatie na het stoppen van de kruip stroming (elastisch herstel). De afbraak van de initiële morfologie resulteert in een piek van de overgangsviscositeit en in een afname van het elastisch herstel. Het elastisch herstel van de TPVs neemt sterk af na een bepaalde deformatie door herordening en retractie van de elastomeer deeltjes. De TPVs hebben een *zwicht deformatie* boven op een zwichtspanning. Het elastisch herstel van de PP/SEBS blends bereiken een constante waarde bij toenemende deformatie. Dit duidt op de vorming van een nieuwe structuur van de blend, die een dynamisch evenwicht is tussen het opbreken en coalescentie van de twee fasen.

Hoofdstuk 7 beschrijft de rheologische eigenschappen tijdens stroming door een capillair. De viscositeit van de PP/SEBS blends kan benaderd worden door het logaritmisch gemiddelde van de viscositeit van de twee fasen. Door de continue verandering van de morfologie van de blend in het capillair worden stromingsinstabiliteiten onderdrukt en is de zwelling van het extrudaat laag. De viscositeit van de TPVs kan beschreven worden met de Herschel-Bulkley uitdrukking voor de afschuifspanning. Bij lage afschuifsnelheden neemt de viscositeit toe door het zwichtgedrag van de elastomeer deeltjes en bij hoge afschuifsnelheden wordt de viscositeit gedomineerd door de PP fase. Smelt breuk komt voor bij de TPVs die sterk elastisch gedrag vertonen. De zwelling van het extrudaat is laag, maar hoger dan bij de vergelijkbare PP/SEBS blends, en neemt toe met toenemende hoeveelheid PP in de blend.

Hoofdstuk 8 geeft een algemeen overzicht van de resultaten van dit proefschrift. In de PP/SEBS blends heeft de morfologie een ondergeschikte rol in de rheologische eigenschappen. De moduli en viscositeit kunnen worden beschreven met de juiste middeling van de eigenschappen van de twee fasen. De verandering van de morfologie tijdens afschuifstroming onderdrukken mogelijke stromingsinstabiliteiten. De agglomeraatstructuur van de elastomeer deeltjes in de TPVs resulteert in zwicht gedrag. De deeltjes moeten over elkaar heen bewegen om stroming van de TPV mogelijk te maken. De vergelijkbare eigenschappen van de twee OPTE blend typen in de vaste toestand worden veroorzaakt door de structuur van de PP matrix fase: mechanisch gezien kan deze fase beschouwd worden als gedeeltelijk discontinue.

Wilco Sengers

Curriculum Vitae

Wilco Sengers werd geboren op 31 december 1975 te Nijmegen en groeide op in Wijchen. Nadat hij in 1993 zijn HAVO diploma behaalde op het Maas Waal College te Wijchen, ging hij naar het Hoger Laboratorium Onderwijs op de Hogeschool van Arnhem en Nijmegen. Daar studeerde hij af in 1997 in de Polymeerchemie na een stage en afstudeeropdracht bij Akzo Nobel Central Research Center te Arnhem. Hij vervolgde zijn studie aan de Rijksuniversiteit Groningen, waar hij in 2000 zijn doctoraal haalde in Scheikundige Technologie. Het afstudeerwerk werd uitgevoerd onder begeleiding van Prof. dr. ir. Leon Janssen en Mario Cioffi .

In Oktober 2000 begon hij aan het promotieonderzoek aan de faculteit Technische Natuurwetenschappen van de Technische Universiteit Delft. Onder begeleiding van Prof. dr. Stephen Picken en dr. Alexandros Gotsis bestudeerde hij de relatie tussen de morfologie en de rheologische eigenschappen van olefine thermoplastische elastomeer blends. Het onderzoek werd uitgevoerd in samenwerking met Pratip Sengupta en Prof. dr. ir. Jacques Noordermeer van de Universiteit Twente. De resultaten van dit onderzoek zijn gepubliceerd in verschillende wetenschappelijke tijdschriften en gepresenteerd op (inter)nationale congressen. In 2002 behaalde hij het diploma 'geregistreerd polymeerkundige' (RPK) bij de onderzoeksschool Polymeer Technologie Nederland (PTN).

List of Publications

- *'Melt Creep Behavior of Elastomer-Polymer Blends'*

W.G.F. Sengers, S.J. Picken and A.D. Gotsis, submitted to the Journal of Rheologie

- *'Capillary rheology of elastomer-polypropylene blends'*

W.G.F. Sengers, S.J. Picken and A.D. Gotsis, submitted to the Journal of Applied Polymer Science

- *'Distribution of oil in olefinic thermoplastic elastomer blends'*

W.G.F. Sengers, M. Wübbenhorst, S.J. Picken and A.D. Gotsis, Polymer 46 (17) 6391-6401 (2005)

- *'Dielectric spectroscopy using dielectric probes: A new approach to study glass transition dynamics in immiscible apolar polymer blends'*

W.G.F. Sengers, O. van den Berg, M. Wübbenhorst, A.D. Gotsis and S.J. Picken, Polymer 46 (16) 6064-6074 (2005)

- *'Linear viscoelastic properties of olefinic thermoplastic elastomer blends'*

W.G.F. Sengers, P. Sengupta, J.W.M. Noordermeer, S.J. Picken and A.D. Gotsis, Polymer 45 (26) 8881-8891 (2004)

- *'Distribution of processing oil in TPE blends'*

W.G.F. Sengers, M. Wübbenhorst, S.J. Picken and A.D. Gotsis, poster at the International Dielectric Conference, Delft, 23-26 Aug 2004

- *'Dynamic rheological properties of PP containing TPE blends'*

W.G.F. Sengers, P. Sengupta, J.W.M. Noordermeer, S.J. Picken and A.D. Gotsis, proceedings and poster at the ANTEC, Chicago (USA), 16-24 May 2004

- *'Dielectric and fluorescent probes to investigate glass transition, melt, and crystallization in polyolefins'*

van den Berg O., Sengers W.G.F., Jager W.F., Picken S.J., Wübbenhorst M., Macromolecules 37 (7), 2460-2470 (2004)

- *'Dynamic rheological properties of TPE blends'*

W.G.F. Sengers, P. Sengupta, J.W.M. Noordermeer, S.J. Picken and A.D. Gotsis, presentation at the Polymer Days, Lunteren

- *'Distribution of processing oil in TPE blends'*

W.G.F. Sengers, S.J. Picken and A.D. Gotsis, presentation at the Europa-Africa meeting of the Polymer Processing Society, Athens (Greece), 14-17 Sept 2003

- *'Rheological properties of TPE compounds'*

W.G.F. Sengers, P. Sengupta, J.W.M. Noordermeer and A.D. Gotsis, proceeding and presentation at the Annual meeting of the Polymer Processing Society, Guimarães (Portugal), 16-20 June 2002

Dankwoord

Een proefschrift schrijf je nooit alleen. Vele mensen leveren direct en indirect een bijdrage aan het werk en aan een goede sfeer. Dit resulteerde in de aangename omgeving waarin ik het onderzoek gedaan heb. Ik ben veel dank verschuldigd aan mijn promotor Stephen Picken en mijn dagelijkse begeleider Alexandros Gotsis (die nu goed vertoefd op Kreta). Zij gaven mij veel vrijheid in het onderzoek en hebben mij veel geleerd over interpretatie van de resultaten en over het schrijven in het Engels. Ook wil ik Pratip Sengupta (UTwente) bedanken voor de goede en fijne samenwerking. Geen enkel communicatiemiddel hebben we onbenut gelaten om de resultaten door te spreken en te discussiëren over hoe deze materialen in elkaar zitten.

Dit onderzoek was een onderdeel van een DPI project. Voor hun steun en advies wil ik de mensen van de Industrial User Committee bedanken: Jacques Noordermeer (UT), Xavier Muyldermans (Kraton), Martin van Duin (DSM), Alberto Dozeman (DSM) Jernej Jelenic (Akzo Nobel) Ans van de Bovenkamp (Akzo Nobel), Wim Zoetelief (DSM), Ben van Baarle (TNO), Ruud Sturme (Océ) en Wilma Dierkes (UT). En ook de andere 'rubber'-AIO's, uit Twente: Kinsuk Naskar en Francesca de Risi.

Natuurlijk mag ik mijn kamergenoten Daniel, Otto en Telma niet vergeten. En verder alle anderen uit de PME groep: De 'oude' AIO's Paul, Marcel en Seb, en de 'nieuwe' AIO's Plamen, Massimiliano, Zeynep, Arek, Ceren, Chris en Louise; de postdocs Daniele Cangialosi, Hayley Every, Jan Groenewold en Liang Bin Li; het wetenschappelijke personeel Sjaak Elmendorp, Wolter Jager, Eduardo Mendes, Jan van Turnhout en Michael Wübbenhorst; en de secretaresses Fem Brenk, Tonny Verheul en Karin Wilhelm. Ook ben ik veel dan verschuldigd aan Ben Norder, Piet Droppert en Gerard de Vos, de technici van de groep. Zonder de goede sfeer in de groep is het moeilijk vol te houden.

De leden van Yoroshi moesten het ontgelden tijdens karate trainingen om mijn fysieke frustraties op te vangen, maar het was vooral erg gezellig. Ook wil ik Niels, Plamen, Daniel en Sonia, Massimiliano en Cristiana, Akardiusz (Arek) en Aleksandra (Ola), Zeynep en Ceren bedanken voor de vele gezellige dagen/avonden.

Als laatste wil ik natuurlijk mijn familie bedanken: broer Arno, zus Mariëlle, en mijn ouders. Zij stonden en staan altijd voor mij klaar met advies, steun en toeverlaat.

Wilco

